Combatting Bacterial Infections Through Polymer-Bacteria Interactions

by

Leanna Lauren Foster

A dissertation submitted in partial fulfillment
of the requirements for the degree of
Doctor of Philosophy
(Macromolecular Science and Engineering)
in the University of Michigan
2019

Doctoral Committee:

Professor Kenichi Kuroda, Chair
Professor Brian Love
Professor Timothy Scott
Assistant Professor Scott Van Epps

Leanna Lauren Foster

llfoster@umich.edu

ORCID iD: 0000-0002-1921-5277

Acknowledgements

I would like to acknowledge the support of the many people who made this accomplishment possible. I would like to thank my parents, Larry and Nancy Cooper, who have always encouraged, guided, and allowed me the freedom to become the person I am today. I would also like to thank my husband, Donyphn Ryan Foster, for his constant support and comfort throughout this journey- the house was not always clean, but it was always full of love. To my many friends who have been with me throughout this graduate school roller coaster, thank you for the coffee dates that kept me sane, and the words that grounded me when things were good and when things got hard.

I appreciate the time, thoughtful discussion and encouragement from my committee, especially Dr. Kenichi Kuroda. When I joined your lab, you said we would kill bacteria together. Over these years, we have killed many bacteria, and I hope our work goes on to kill many more. I also want to thank all of those in the Kuroda lab that helped shape me into the scientist I am today through their support in research and life, including Dr. Haruko Takahashi, Dr. Hamid Mortazavian, Dr. Rajani Bhat, Ms. Maggie Priebe, and Ms. Shyrie Patel.

The research presented in this dissertation was supported through the generosity of many within the scientific community. Dr. Shin-ichi Yusa generously provided the polymers used in biofilm studies. Dr. Robert Davenport and the university of Michigan Hospital kindly

supplied red blood cells for this work. Dr. Jianfeng Wu and Dr. Chuanwu Xi with the School of Public Health provided *Pseudomonas aeruginosa* (*P. aeruginosa*) PAO1 and aided with florescence imaging of bacteria and additional biofilm experiments not described here. Joanne Beckwith and Dr. Michael Solomon provided support for biofilm confocal imaging. This research was supported by Department of Biologic and Materials Sciences, Rackham Graduate School, University of Michigan School of Dentistry, MCube (Cost-effective novel antibiotics to combat multidrug-resistant bacteria), the National Institute of Health (No. U01DE023771) and the National Science Graduate Research Fellowship (No. DGE-1315231)

Table of Contents

List of Tables

List of Figures

List of Appendices

Abstract

In this dissertation, new antimicrobial functions stemming from synthetic polymer structures and properties were explored to address antibiotic resistance and tolerance in bacterial infections. Amphiphilic antimicrobial polymers that mimic host defense peptides have been explored as alternative antibiotics which could bypass existing antibiotic resistance and have a low risk of resistance development. However, their antimicrobial activity and selectivity need to be improved toward clinical use. This dissertation explored the use of macromolecules with multiple polymer chains, while the previous studies have been limited primarily to tuning monomer compositions. Since antimicrobial peptides act by collective action of multiple peptide chains, it was hypothesized that macromolecules presenting multiple antimicrobial polymer chains will show improved antimicrobial activity and selectivity towards bacteria as compared to the previously studied linear structures. Initially, we attempted to synthesize hyperbranched amphiphilic methacrylate copolymers through free radical polymerization with a crosslinking monomer (Chapter 2). However, these structures resulted in only lightly crosslinked polymers with high molecular weight, having comparable antimicrobial activity to linear polymers and increased hemolytic activity. To address the lack of target architecture, we also synthesized 4-armed star-shaped copolymers by atom transfer radical polymerization (Chapter 3). 4-armed star-shaped copolymers did not show any improved antimicrobial activity as compared to linear polymers, while they significantly increased the hemolytic activity,

resulting in low selectivity. We propose future work explore architecture with additional polymer arms, which may better mimic the membrane disruptive behavior of multiple polymers on bacterial membranes.

The challenge of bacterial biofilm stem from both the difficulty to prevent their formation and the difficulty to treat by traditional antibiotics, as summarized in Chapter 1. Previous anti-biofilm coatings suffer from short lifetimes, and their applications are limited to surfaces. In this dissertation, we explored a new approach to biofilm prevention based on the hypothesis that changing planktonic bacteria behavior to result in sub-optimal biofilm formation (Chapter 4). Incubation of *Pseudomonas aeruginosa* planktonic bacteria with a cationic polymer resulted in the aggregation of planktonic bacteria, and a reduction in biofilm development. We propose that cationic polymers may sequester planktonic bacteria away from surfaces, thereby preventing their attachment and suppressing biofilm formation. In attempts to address the antibiotic tolerance in biofilms due to low metabolic activity in bacteria, we hypothesized treatment of cationic polymers may increase the antibiotic susceptibility of embedded bacteria while the polymers are not killing bacteria by disrupting the bacterial membrane (Chapter 5). The polymer increased the metabolic activity of bacteria in biofilm and membrane potential of planktonic bacteria. These suggest that the bacteria are awaken, and antibiotic tobramycin uptake might be enhanced due to increased membrane potential. However, treatment with a cationic polymer did not increase the sensitivity of *P. aeruginosa* biofilms to tobramycin. While this approach does not increase biofilm sensitivity to antibiotics, it may provide the foundation for future approaches with adjuvant materials for combination therapies.

Chapter 1 Introduction and Background

Motivation

Infectious diseases accounts for over 25% of worldwide mortality, cause primarily by bacteria and viruses.[1-2] In order to combat future bacterial infections, it is necessary to develop new strategies for antimicrobial treatment, including improvements to efficacy of current antibiotics and the development of new antimicrobial materials. Since the discovery of penicillin in 1928[3], antibiotics have been a potent tool to combat bacterial infections. Over 270 antibiotic drugs were introduced between then and the 1970s, but between 1987 and 2000, no new classes of antibiotics had been developed, despite the increasing rate of antibiotic resistance development to existing antibiotics. Antibiotic classes are distinguished by the mechanisms in which the agent acts against bacteria, such as the specific site it targets within the cell. The number of new antibiotics coming to market has been decreasing each year, and new antibiotics are modifications of previously used antibiotics[4], as in the new antibiotics were defined as antibiotic classes with the same mechanisms which bacteria were developing resistances to. The high cost of antibiotic development is economically unattractive to pharmaceutical companies, despite a new growing need, as the time they have to recover investment is significantly reduced with new antibiotic resistance development.[5] Over prescription of existing antibiotics has led to the recent surge in number of antibiotic resistant bacteria, especially multidrug resistant (MDR) species. Since 2000, two new classes of

antibiotics have been approved by the FDA (oxazolidinoes[6] in 2000 and cyclic lipopeptides[7] in 2003), introducing two new mechanisms of antibiotic activity which had previously not been targeted, and should therefore be effective against multi-drug resistant bacteria. However, the development of new traditional antibiotics for the market is not a viable long-term solution to the antibiotic resistance problem, as antibiotic lifetimes are only 5-15 years.[8-11]

Objectives

With growing concerns over the increase in the number of antibiotic resistant infections, the objective of this dissertation is to find materials that can subvert antibiotic resistance mechanisms. This could help to improve a drug's market longevity and economically incentivize new drug development. One objective of this study is to develop new antimicrobial compounds that won't contribute to antibiotic resistance development, which have low toxicity to human cells and ideally low manufacturing cost. These materials could theoretically also be able to overcome existing mechanisms of resistance, given they should subvert traditional antimicrobial pathways that lead to the development of antibiotic resistance. Secondly, it is ideal to address the antibiotic challenge of tolerant bacterial biofilms, which are associated with chronic infections. Development of new synthetic compounds that are able to effectively kill biofilm bacteria and/or modulate biofilm behavior such as slower biofilm formation, easier removal or enhanced susceptibility to existing antibiotics, would significantly contribute to the challenge of antibiotic tolerance, as biofilms contribute to the likelihood of antibiotic resistant mutation. These two objectives are not mutually exclusive; the convergence of these two strategies could allow for an enhanced bacterial infection treatment of a broad range of bacteria, including current antibiotic resistant strains.

Background: Antibiotic Resistance/Tolerance in Bacteria

Bacteria have existed for 3.5 billion years[12], and have accomplished this by the ability to respond to environmental threats. One of these survival responses is the development of antibiotic resistance, which can be imparted by genetic mutation (genotype) and/or bacteria characteristics and behavior (phenotype).

Mutations in the bacteria's DNA can imparts antibiotic resistance, termed acquired resistance, and consequently the division and propagation of the mutated bacteria imparts resistance to the subsequent generations. This survival response allows specific bacteria to survive antibiotic exposure when others have died, and thus leads to exclusively selection of antibiotic resistant populations rather than resistance development in all population. There are three major resistance mechanisms: modification of antibiotic molecule, change in the antibiotic target site, and drug uptake/efflux.[13] In an example of enzymatic degradation of antibacterial agents, bacteria resistant to β-lactam antibiotics (such as amoxicillin) mutated to produce an enzyme (β-lactamase) that to breaks open the 4-atom β-lactam ring structure, which renders the antibiotic ineffective.[14] Quinolone drugs are prone to resistance development by bacteria alterations to their antimicrobial target sites, where normally bacterial enzyme DNA gyrase is responsible for replication and repair of bacterial DNA, but can be trapped as a part of a quinoline-enzyme-DNA complex, leading to cell death. Amino acid substitutions in DNA gyrase result in poor quinolone-enzyme binding by reducing drug affinity, causing the antibiotic resistance.[15] Mutations can also affect the permeability of the bacterial membrane. For example, porin are protein channels that act as pores in the bacterial membrane, allowing the passive diffusion of molecules into the cell, such as nutrients and

antibiotics.[16] Mutations such as reducing the number or size of porins can effectively restrict antibiotic access into the bacteria.[17] Mutations which cause porins smaller than antibiotics size prevent access to inner cell targets, while decreasing the number of porins reduces the overall diffusion of antibiotics into the cell.[17] The specific mutation is related to the antibiotic mode of action, as surviving bacteria are those that can best prevent antibiotic exposure. However, it has also been noted that the presence of antibiotics at low concentrations can act as a trigger for the development of adaptive antibiotic resistance in some bacteria, affecting signaling pathways typically used in cell-cell communication.[18-20] MDR develops when bacteria have multiple resistance mechanisms encoded on their chromosomes.[21] The genetic codes of a bacteria populations are continually changing to subvert conventional antibiotics.

An important bacteria behavior is the formation of biofilms, three-dimensional structures of bacteria encased in self-produced extracellular polymeric substance (EPS).[22] Biofilms protect the encased bacteria from the surrounding environment, including antibiotics, making them difficult to treat and consequently account for 65-80% of bacterial infections.[23-24] Biofilms are intrinsically antibiotic tolerance, conveying inherent properties to the bacteria that helps limit antimicrobial effectiveness. While antibiotic resistance is exclusively conferred by genetics, antibiotic tolerance in biofilms is a due to a combination of protective mechanisms provided by the biofilm structure. As in, a dispersal of the biofilm structure would restore antibiotic sensitivity to planktonic bacteria. The exact mechanisms of biofilm antibiotic tolerance are still being explored, but several factors have been widely discussed including high cell density[25], slower growth rate[26], and low antibiotic penetration[27]. Many antibiotics target cell division and replication, such as preventing DNA separation or the formation of cell walls,

and thus have significantly reduced efficacy against non-dividing cells present in biofilms.[26] Even those antibiotics that do possess activity against dormant cells have reduced efficacy due to slow metabolic processes.[28-29] Antibiotics must also penetrate through the EPS in order to access embedded bacteria, and the limited diffusion of antibiotics may result in concentrations lower than effective concentrations. The biofilm matrix is composed of proteins, extracellular DNA, and polysaccharides, which combined are known as the extracellular polymeric substance (EPS).[30] Components of the EPS matrix can restrict the penetration of oppositely charged antibiotics, such as matrix eDNA blocking cationic tobramycin.[31-32] The exposure of bacteria to antibiotics at sub-lethal concentrations may result in resistance development in bacteria, known as adaptive resistance. As such, the tolerant nature of the biofilm itself contribute to its antibiotic resistance and antibiotic resistance development. Different bacteria within the biofilm may be resistant by different mechanisms[33], including enzymatic degradation of antibacterial agents, alteration of antimicrobial targets, or changes in membrane permeability.[34-35] The collective consequence is antibiotic tolerance 100 to 1000-fold larger than exponential planktonic (individual) bacteria.[36-39]

While all antibiotic resistance/tolerance mechanisms are survival responses, the manner in which the bacteria behave as antibiotic resistant have different sources but are intrinsically entangled. For example, bacteria within biofilms may be exposed to sub-lethal antibiotic concentrations due to diffusion[40], which contributes to the likelihood of mutation, especially because biofilm bacteria exhibit hypermutability[26]. Therefore, it is optimal to combat both sources of antibiotic resistance/tolerance (planktonic mutations and biofilms).

Antimicrobial Macromolecules as Alternative Antibiotics

Antimicrobials that don't contribute to traditional antibiotic resistance development are highly desirable targets for future drug development. Intrinsically antimicrobial macromolecules are a class of materials that are promising for such an application. A natural part of the innate immune system consists of these antimicrobial macromolecules (host defense peptides), and synthetic polymer mimics of these compounds can be designed to maintain excellent biological performance at a lower cost.

Host Defense Peptides and Synthetic Antimicrobial Peptides

Innate immune systems are found in all classes of plants and animals and are able to recognize and attack pathogens based on generic characteristics, such as differences in cell membrane charge. Host-defense antimicrobial peptides (AMPs) are a class of small proteins (10-50 amino residues) in the innate immune system that have broad spectrum bacterial activity, including against antibiotic resistant bacteria.[41] In literature, "HDPs" have been used when the function of peptides in the immune system, and "AMPs" have been used when the antimicrobial activity of peptides is the primary focus of study. AMPs are found in all known species of life[42], with over 2600 natural peptides known.[43] No common sequence has been found to exists between the diversity of HDPs, but all contain the same essential features that allow for antibacterial behavior. HDPs are characterized by cationic and hydrophobic amino acid residues, and the segregation of these functions by the formation of a secondary structure (i.e. α-helix, β-sheet) upon binding to cell membranes.[41, 44] These antimicrobial peptides have been identified in as a part of human saliva, sweat, seminal plasma, amniotic fluid, white blood cells, and skin.[43]

The antimicrobial mechanism of HDPs has been the topic of significant research.[44-48] Magainin-2 (Figure 1.1) was one of the first purified HDP derived from the skin of the African clawed frog *Xenopus laevis*[49], and the magainin class of antimicrobial peptides were the subject of early mechanism research.[50] While previous research had established the affinity of α-helical antimicrobial peptides to bind with lipid bilayers membranes[51], Matsuzki et al. observed magainin-1 would form amphiphilic α -helix structures in the presence of acidic lipid bilayer vesicles, and would induced concentration dependent leakage, indicating membrane disruption.[50] Due to the concentration dependent behavior, they suggested membrane disruption was linked to peptide-membrane binding.[50] As bacterial cell membranes are rich in anionic lipids, AMPs bind to bacterial cell membranes by electrostatic interactions between the cationic groups of AMPs and the anionic membrane surface of bacteria. On the other hand, mammalian cell membranes are comprised mostly of zwitterionic lipids and cholesterols and are comparatively less anionic as compared to the bacterial cell membrane (Figure 1.2). Therefore, AMPs preferentially bind to bacterial cell membranes over human cell membranes, resulting in selective activity against bacteria over human cells.

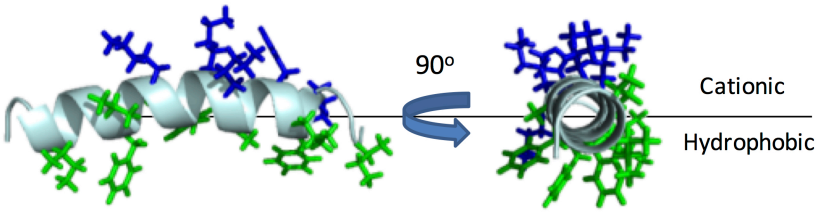

Figure 1.1. Structure of Magainin-2, depicted in the characteristic α-helix secondary structure. The α-helix structure is facially amphiphilic, where hydrophobic groups (green) are segregated to one side and cationic groups (blue) are located on the opposite.[52] Magainin-2 sequence: GIGKFLHSAKKFGKAFVGEIMNS. Reprinted with permission; Copyright 2013 American Chemical Society.[52]

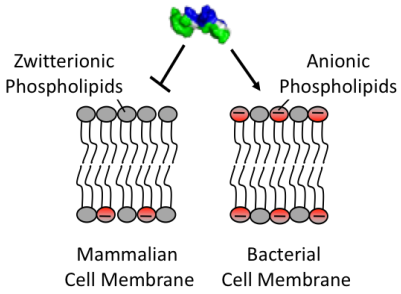

Figure 1.2. Schematic of bacterial and mammalian cell membranes that govern bacteria-selective membrane binding of HDPs (Magainin shown).[52] Cationic, amphiphilic HDPs bind to bacterial membranes by electrostatic and hydrophobic interactions, as compared to only hydrophobic binding to mammalian membranes.

Since then, several models of membrane disruption have been proposed to explain AMP's antimicrobial mode of action, where the mechanism can vary between the multitude of AMPs (Figure 1.3). Regardless of the mechanism of AMP-membrane incorporation, the end result is compromising the barrier function of cell membranes and increasing the membrane permeability, allowing the outflow of cellular components, and ultimately cell death. In the "barrel-stave" a critical density of HDPs causes self-aggregation within the membrane, resulting in the formation of ion channel-like transmembrane pores lined by HDPs, without any re-orientation of the lipid bilayer. [46, 53-56] In the "toroidal pore" model, the insertion of HDPs in the membrane induces induced curvature strain along the lipid monolayers, resulting in of the reorientation of the lipids into pores lined by HDPs.[46, 55] Lastly, the "carpet" model describes the accumulation of HDPs along the membrane surface, disrupt lipid bilayer structures non-specifically.[46, 53-55] Because the bacterial membranes are an essential component of the cells and common structures to all bacteria, the mode of action of AMPs can result in broad-spectrum antimicrobial activity and decreased potential for resistance.

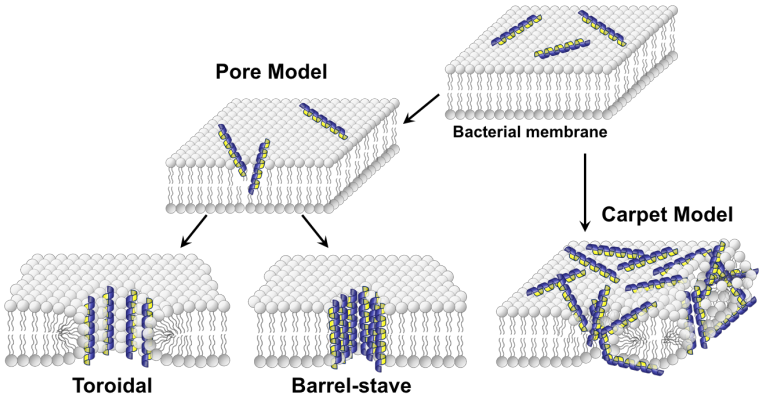

Figure 1.3. Proposed mechanisms of membrane disruption by antimicrobial peptides: (1) Barrel-stave, (2) Toroidal pore, and (3) Carpet models. Reprinted with permission; Copyright 2013 American Chemical Society.[52]

During the study of HDPs as potential therapeutics, researchers uncovered that the sequence of amino acids was not critical for antimicrobial behavior, but rather the physiochemical properties that provided the antimicrobial mode of action. This was supported by the results using AMP enantiomers; D-enantiomers of magainin exhibited comparable behavior to natural magainin. In addition, no common sequences had been discovered in natural HDPs. These results reveal that AMP mode of action was not dependent on specific protein-protein interactions, which require specific peptide configurations and sequences.[57] These results also suggested that the cationic amphiphilic structure of α-helices which were responsible for the mode of action were key to antimicrobial behavior. This discovery led to further studies that utilized synthetic peptides and peptidomimetics including beta-peptides[58] and peptoids[59] that mimic the facially amphiphilic helical structure. These synthetic peptides mimic both the charge distribution and secondary structure of known HDPs, with alterations to amino acid sequences and/or length to improve antimicrobial efficacy and reduce toxicity to mammalian cells.[60-62] Many synthetic AMPs have demonstrated promising antibiotic candidates, with several in clinical-efficacy trials, but to date no AMPs have achieved FDA

approval.[63-64] A common issue is that AMPs often fail to meet the requirement to provide superior behavior to traditional antibiotics for the intended use. The implementation of AMPs has been hampered in clinical application primarily due to the susceptibility to proteolytic degradation in physiological fluids. Practically, the high cost of design and manufacturing results in AMPs being a prohibitively expensive pharmaceutical therapeutic.[63-65]

Synthetic Antimicrobial Polymers as AMP Mimetics

The discovery that AMP activity does not necessarily require peptide structures prompted research into synthetic antimicrobial polymers as AMP mimetics. It has been postulated that by replacing amino acids with randomly distributed cationic and hydrophobic segments and enabling the segregation of cationic and hydrophobic charge when interacting with a bacterial membrane, synthetic antimicrobial polymers maintain the same mode of action as AMPs, without the need for any ordered sequences necessary to generate secondary structures. Therefore, the essential minimum requirements for synthetic antimicrobial polymers is a distribution of hydrophobic and cationic functionality, whereas AMP also require amino acid chemistry and the specific ordering of amino acids to generate secondary structures. Synthetic polymers are cost-effective, as the peptide synthesis is labor and cost-intensive. Synthetic polymers also resist enzymatic degradation. These properties of polymers meet the major challenges to clinical translation of AMPs.[66-68] Additionally, polymers can be designed with a diversity of chemistries and structural properties, which can be tailored to the desired application. In chapters 2 and 3 we design a star-shaped polymer architecture to improve antimicrobial functions, which are not readily accessible by peptides. A large body of antimicrobial polymers have since been designed using a diversity of strategies to explore the

AMP mimetic ability of varying polymer designs, some of which will be discussed in the following sections.

Polymethacrylate: Polymer Design and Design Rules

One research area of focus has been the design of antimicrobial polymethacrylate copolymers composed of a statistical or random distribution of hydrophobic and cationic ammonium side chains as the representative polymer is depicted in Figure 1.4. Upon bacterial membrane binding, these copolymers can spontaneously adopt an amphiphilic conformation capable of membrane disruption (Figure 1.4), and ultimately bacterial cell death.[69-79] The advantage to antimicrobial polymethacrylates is that the chemistries for preparation, modifications, and manufacture of methacrylate polymers have been well-established. This is advantageous for the exploration of tunable polymer parameters including polymer size, hydrophobic/cationic balance, chemical functionalities of cationic and hydrophobic groups, and polymer shapes and architectures.[68] Previous work has explored many of these properties, with a focus on modification of polymer chemistry to achieve desirable biological properties (high antimicrobial activity, low toxicity).

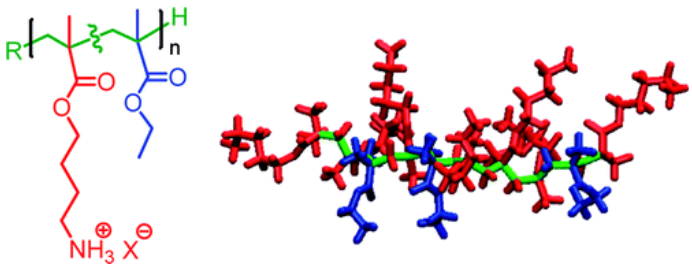

Figure 1.4. Representative Structure of antimicrobial polymethacrylate with random distribution of cationic (red) and hydrophobic (blue) monomer segments to result in a flexible amphiphilic structure. Cationic and hydrophobic groups segregate to opposite sides upon binding to bacterial membranes.[80]

In order to most closely mimic natural AMPs, polymers with low molecular weights were desired (2,500 —10,000 g/mol). This design was supported by findings that higher molecular weight amphiphilic polymethacrylate exhibited greater hemolytic activity against human red blood cells in addition to greater antimicrobial activity.[69, 81] Therefore, low molecular weight polymers offer the platform with the greatest opportunity to minimize mammalian cell toxicity, and therefore to improve selective activity towards bacterial cells while maintaining sufficient antimicrobial behavior. Free radical polymerization is a cost-effective, facile method for synthesis of polymers, a desirable approach when considering scalability for mass production of alternative antibiotic. By targeting low molecular weight polymers, free radical polymerization with chain transfer agents can be utilized without significant concern for characteristically broad molecular weight distributions ($Đ$>1.5). This is because low molecular weight polymers give a small range of molecular weight variations (a few hundreds to thousands), resulting in $Đ$= 1.3-1.5 when sufficiently high concentrations of CTA (10-15 mol%) are used.

Polymer optimization is primarily governed by controlling amphiphilic balance between cationic and hydrophobic group, and therefore the main stream strategy has been optimization in monomer compositions and chemical identities of these groups [73]. Learning from the antimicrobial mechanism of AMPs, we hypothesized that the cationic functionality and hydrophobicity are the minimal, but essential requirements for potent antimicrobial activity and selectivity. Therefore, a library of polymethacrylate derivatives with cationic and hydrophobic side chains have been previously explored to identify the structural properties optimal for high antimicrobial activity and low toxicity.

Previously, the effect of cationic and hydrophobic balance of copolymers on their antimicrobial and hemolytic activities has been examined using copolymers with different binary compositions of monomers with cationic and hydrophobic side chains. The result indicated that random copolymers with many cationic side chains showed low antimicrobial activity and low hemolytic activity. Increasing the hydrophobic monomers increased both the antimicrobial and hemolytic activities of copolymers, indicating that the hydrophobicity of polymers is a driving force for their activities. However, highly hydrophobic polymers showed high hemolytic activity. The result suggested that the cationic and hydrophobic functionalities should be balanced to maximize the antimicrobial activity and minimize the hemolytic activity. The cationic charge of copolymers promotes the selective binding of polymers to anionic bacterial cell membranes through electrostatic attractions over human cell membranes, but without hydrophobic groups, the copolymers cannot disrupt bacterial cell membranes, thus resulting in low antimicrobial activity. However, excess hydrophobicity of polymers in turn results in non-specific hydrophobic interaction with human cell membranes, causing high hemolytic activity.[69-70, 81] Therefore, the design rule here is that the cationic functionality of copolymers needs to be maximized for selectivity, and the hydrophobicity should be maximized to achieve high antimicrobial activity. The main challenge of the field has been to identify the balance of cationic functionality and hydrophobicity for potent antimicrobial activity and low hemolytic activity.

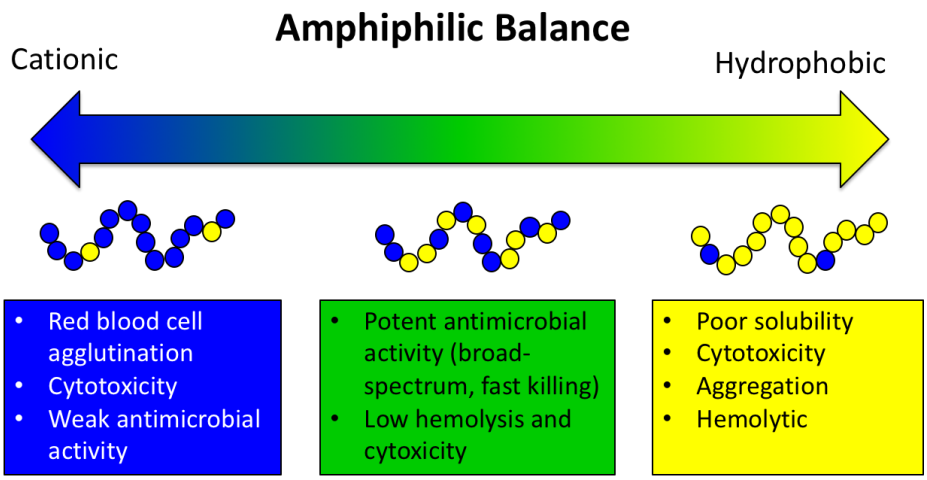

Figure 1.5. Amphiphilic balance of copolymers and biological activities. Optimized ratio of cationic and hydrophobic groups is critical for potent antimicrobial, non-hemolytic polymers. Copyright © 2010 by Springer. Adapted by permission of Springer [73].

In addition to monomer composition, tuning the hydrophobicity of monomers by alkyl length is another strategy previously to control the amphiphilic balance of copolymers. Copolymers with methyl, ethyl, butyl, or hexyl side chains have been prepared. In general, the antimicrobial activity increased (the MIC values decreased) as the mole percentage of alkyl monomers and reached the maximum activity (MIC values leveled off) at high mole percentages of alkyl monomers (Figure 1.6). The copolymers with shorter hydrophobic alkyl chain lengths required higher mole percentages to reach the maximum antimicrobial activity,[68-69, 81] while the MIC values at high mole percentages of alkyl monomers are same for all polymers with different alkyl monomers (Figure 1.6). However, the copolymers with shorter hydrophobic alkyl chain lengths were much less hemolytic, resulting in higher selectivity (Figure 1.6).[68-69, 81] Therefore, the chemical identity of hydrophobic side chains is also effective in tuning the antimicrobial activity and selectivity.

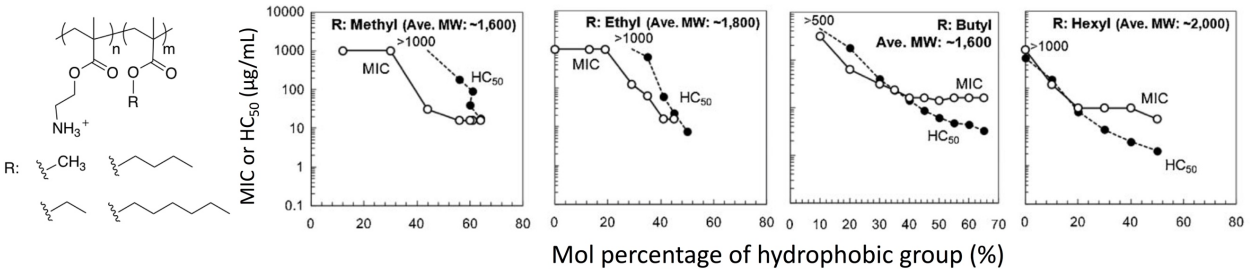

Figure 1.6. Antimicrobial and hemolytic activities of cationic amphiphilic methacrylate copolymers. Chemical structure of methacrylate copolymers with R= methyl, ethyl, butyl, or hexyl as hydrophobic side chains. Hydrophobic composition dependence. The average molecular weights of copolymers are in the range of 1,600-2,000. The data are adapted from references.[68]

Polymer length, or molecular weight, is one tunable parameter beyond amphiphilic balance that has been explored. Controlling polymer length controls the average number of biologically active groups per chain. As the molecular weight of random methacrylate copolymers containing butyl side chains increases, the MIC values against *E. coli* decrease (Figure 6C) when compared for the copolymers with the same mole percentage of butyl side chains.[69, 81] On the other hand, with increasing molecular weight, the HC_{50} values decreases, indicating the copolymers became hemolytic (Figure 6C).[69, 81] The increased antimicrobial and hemolytic activities are likely because a longer polymer chain provides more contact points with the bacteria and human cells. Accordingly, the molecular weight of polymers should be small to minimize the hemolytic activity, but large enough to warrant the antimicrobial action by the amphiphilic polymer structures. As the copolymers with 2,000-3,000 have been investigated, these copolymers showed potent antimicrobial activity and selectivity. These MWs are comparable to those of natural AMPs, which may suggest that such MW range may be optimal for membrane disruption mechanisms.

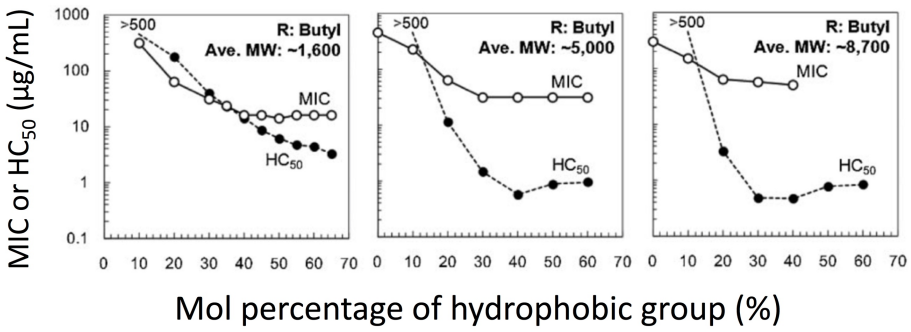

Figure 1.7. Molecular weight dependence for the copolymers with butyl side chains (R = C4). The data are adapted from references.[69, 81]

The chemical identity of the ammonium group is another parameter to control antimicrobial polymer activity. The primary ammonium groups have been selected for intimal study to mimic the lysine amino acid of AMPs. The copolymers with primary, tertiary, or quaternary ammonium groups have been prepared and their antimicrobial and hemolytic activities have been investigated [71, 74]. As the electrostatic interaction between the cationic charge of polymers and anionic bacterial membranes is responsible for polymer binding to bacteria for antimicrobial activity and selectivity, it was hypothesized that a permanent cationic charge such as found on quaternary ammonium would result in greater bacteria binding affinity and higher selectivity, resulting in the potent, selective antimicrobial activity. Primary and tertiary ammonium groups are pH-dependent owing to the equilibrium between deprotonated (neutral) and protonated (cationic). On the other hand, quaternary ammonium groups provide cationic charge regardless of the environmental pH. The copolymers with primary ammonium groups showed the higher antimicrobial activity against *E. coli* (MIC = 16 μg/mL) compared to counterpart polymers with either tertiary (MIC = 260 μg/mL) or quaternary ammonium (MIC >1,300 μg/mL) groups.[71] The copolymer with primary ammonium groups also showed stronger binding to a lipid bilayer that those with ternary or quaternary ammonium groups.[74] It has been

proposed that the primary ammonium groups are capable of forming a complex with the phosphate groups by electrostatic binding coupled with hydrogen bounding, increasing the affinity of polymers to bacterial lipid membranes [74], while the quaternary ammonium groups cannot form hydrogen bonds with lipid heads. Therefore, primary ammonium groups offer an advantage in polymer design based on improved membrane disrupting ability at physiological pH.

Polymer Architectures and Macromolecules

While we have been focused on linear polymers, which are intended to mimic AMPs, but other shapes and structures of macromolecules have also been explored by other laboratories, such as dendrimers and branched polymers. Synthetic antimicrobial peptides with short sequence (4-8 amino acids) dendrimer structures showed an increase in antimicrobial activity and lower toxicity to mammalian cells when branched to 4 arms, but only a marginal increase when the number of arms was further increased to 8, thought the authors fail to provide discussion on the mechanism of structure-property relationships.[82] Further exploration of star-shaped structures with multiple α -helical peptide arms by Wiradharma et al. also show an increase in antimicrobial activity and reduced hemolysis as compared to linear structures, leading to greater cell selectivity, which is hypothesized to be due to an increase in structure flexibility at the branching point.[83] The branched architectural design has been applied to synthetic antimicrobial polymers as well, though few studies have examined the comparative membrane activity of branched versus linear structures to provide a foundation for branching as a tunable factor. When utilized as coatings, Tiller and co-workers observed poly(4-vinyl-N-alkylpyridinium) 3-arm star polymers exhibited similar antimicrobial activity to linear

counterparts.[84] A study of 4-arm methacrylate-based star polymers showed good antimicrobial activity and low cytotoxicity when quaternized, but a lack of linear comparative provide no knowledge of structure-property relationship.[85] A study of branched polyethyleneimines examined the dependence of membrane disruption on amphiphilic balance, arm length, hydrophobic group identity and cationic group identity, but challenges with high polymer dispersity in branched polymer synthesis prevented conclusions regarding the role of architecture.[86] Based on the state of the field, there is a need for further studies on branched antimicrobial polymer architectures to determine foundational knowledge necessary to apply architecture as a tunable parameter for antimicrobial efficacy and cell selectivity.

Anti-Biofilm Approaches

Biofilms are a major concern in the healthcare industry, as they are often the cause of chronic infection. The development of biofilms is natural bacterial behavior, imparting antibiotic tolerance to the bacteria within, thus making treatment of biofilm associated infections very difficult. Due to their difficulty to treat, both methods that prevent of biofilm formation (prevention) and increase antibiotic effectiveness against existing biofilms (treatment) have been explored. For example of prevention, because medical devices are common biofilm colonization sites, researchers developed surfaces with hydrophilic coatings for physical repulsion or antimicrobial-releasing coatings which kill bacteria being attached.[87-88] In addition to surface coatings, another example is small molecules or polymers which can block adhesin or receptors to interfere with the adherence of bacteria to a surface. Examples of these will be discussed in detail later in this section. Approaches to improving biofilm treatment efficiency include targeting signaling pathways involved in biofilm tolerance.[89] For example,

quorum sensing signaling pathways involved in antibiotic tolerance can be interpreted by inhibitor molecules.[90-91] Because the biofilm matrix is known to block the antibiotic penetration into biofilms, enzymes have been used to degrade the biofilm matrix similar to biofilm dispersal. have been shown to enhance antibiotic efficacy by improving antibiotic penetration.[92-95] The challenge to these current approaches are three-fold: 1) coating chemistries may not be compatible to all abiotic surfaces; (2) many coatings suffer accumulation of cells and proteins when exposed to physiological conditions, reducing their activities; 3) biological agents such as adhesin are bacteria specific, but not effective in biofilm prevention against a diversity of bacteria.

Biofilm Formation Process and Properties

Bacterial biofilms form in several steps, beginning with the preparation of a surface for bacterial attachment through the adsorption of a conditioning film (or layer) of proteins and carbohydrates.[96] The conditioning layer creates hydrophobic surface which is favorable for bacteria attachment[97], increase surface roughness which promotes bacteria adhesion[98], and provides new functional groups at the surface which promote cell adhesion.[99] These changes to the materials surface enable initial attachment of planktonic bacteria to a surface, first by reversible, physical attachment caused by Brownian motion, and then by irreversible biological attachment, caused by the binding of cellular appendages called adhesin with complimentary receptors in the conditioning layer.[100] The subsequent proliferation of the attached bacteria and the production of extracellular polymeric substances (EPS) results in the formation of a three-dimensional community of bacteria (Figure 1.8). Medical implants are especially susceptible to biofilm colonization. Opportunistic bacteria can be introduced at the surgical site,

and damage to epithelial and mucosal barriers impairs host defense mechanisms which would otherwise defend against such bacteria.[101] Protein adsorption occurs quickly (seconds) on both hydrophilic and hydrophobic implant surfaces, which promotes cell adhesion but also consequentially bacteria attachment and subsequent biofilm fouling.[88, 102-103] Signals used in cell-cell communication, such as quorum sensing, indicate to the cells when critical density has occurred at a surface, at which point specific sets of gene expression are promote, enabling cells to develop into mature biofilms.[104] Mature biofilms are characterized by bacterial cells encased in self-produced extracellular polymeric substance, consisting of polysaccharides, extracellular DNA, and proteins.[105] The EPS matrix has multiple functions, including structurally maintaining cells in close proximity necessary for cell-cell communication, retaining components from dead cells which assists in conferring mutated antibiotic resistances, and protecting the cells from hostile environments. Once biofilms are established, they are difficult to remove by medicinal treatments or mechanical removal. The EPS matrix provides biofilms with viscoelastic properties, including elastic tension and viscous damping[106], and grow more tightly adhered and stronger under shear stress.[107] Treatment by medicinal means are challenged by features such as high cell density[25], slower growth rate[26], and low antibiotic penetration[27]. Once a biofilm has reached maturation, the cycle begins again as pieces of the biofilm structure disperse, attach to new surfaces, and result in secondary colonization sites. The seeding of new biofilms by existing dispersing biofilms promotes biological diversity and bacterial survival and can contribute to infection recurrence.[108]

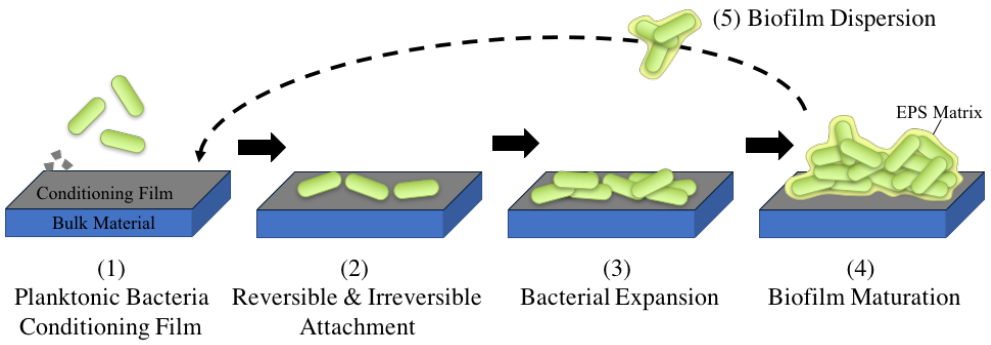

Figure 1.8. Biofilm formation occurs when planktonic bacteria produce a conditioning layer on a material surface (1), and subsequently attach to the surface (2). The attached bacteria grow and divide to form thick layers of bacteria (3). When sufficient bacteria are present, bacteria produce an extracellular polymeric substance (EPS) (4) that helps protect them against the surrounding environment. Portions of the biofilm can detach from the biofilm (5) and consequently form subsequent biofilms.

Approaches to Biofilm Mitigation

Engineered Surfaces

Difficulty in eradicating established biofilms has resulted in research strategies that aim to modify material surfaces to prevent initial reversible bacteria attachment before biofilm formation can occur. Polymer coatings make up a significant amount of this work in three main categories of functions: (1) non-bacterial adhesion, (2) antimicrobial releasing, and (3) contact-killing .[109-110] In all cases, polymers are physically adsorbed or chemically (covalently)-bound onto surfaces. Non-bacterial adhesion surfaces repel bacteria by manipulating the physicochemical interactions of bacteria with surfaces. As bacteria prefer to bind on hydrophobic and charged surfaces, coatings composed of hydrophilic nonionic or charge-neutral polymers can prevent bacterial attachment effectively, such as polyethylene glycol and zwitterionic polymers.[111-113] In addition to the physicochemical properties of polymers, high-density polymer brushes are also proven effective in preventing bacterial attachment. Antimicrobial-releasing surfaces contain antimicrobial agents such as metal ions or antibiotics,

which diffuse into the surrounding area, killing planktonic bacteria prior to surface contact or adherent bacteria.[114-116] As the objective is to kill bacteria near the implant surface that threaten to attach, the greatest killing potential is near the materials surface, and becomes diluted as it diffuses into the surrounding area. Contact-killing surfaces do not release any agent into the surrounding solution, but rather have antimicrobial agents immobilized at the materials surface. One example is surfaces coated with cationic antimicrobial polymers which compromise the bacteria membrane on contact.[117-118] Surfaces may be utilize multiple approaches for best effect, such as creating a surface that both releases antimicrobial agents and is anti-adhesion, such as through topological nano-patterning which disrupts bacteria surface recognitions.[119-121] However, while some recent approaches show promising results, in practice all modified surfaces suffer from a short lifetime due to protein and cell accumulations once exposed to physiological conditions.[122-123] Polymer regenerative surfaces for non-bacterial adhesion are of recent interest in the field, however most are only capable of one-time surface regeneration, and the efficacy of the renewed surface is low compared to the original surface for those that can achieve multiple cycles.[124-127]

Anti-adhesion Agents (interrupt biological attachment)

Non-surface approaches have relied on the interruption of the irreversible biological attachment mechanisms, such as the interaction of specific bacteria proteins (adhesins) with complementary surface receptors found on host cells or the conditioning layer on material surfaces. Several strategies have been employed to prevent adhesin-receptor binding, either by targeting the adhesin (bacteria) or receptor (biological surface). Inhibition of adhesin biosynthesis[128-130] in bacteria or receptor glycoslation[131] target the formation of the

adhesin/receptor. The use of adhesin[128, 132-133] or receptor analogs [134-136] block the adhesin/receptor site, preventing the complimentary interaction from occurring. Dendrimers have been of particular interest for use as scaffolds to present receptor analogs due to their multivalent nature, and have been used to inhibit bacterial cellular uptake to host cells by preventing binding of virulence factors AB_5 toxins.[137-138] However, bacteria can subvert these agents through mutation/adaptation, such as expressing a variety of adhesins that bind to different receptors, and a single adhesin variety capable of binding to multiple receptors.[128, 139] The prevention of biofilms continues to be a major scientific challenge: a single attached bacteria can theoretically result in a bacterial biofilm.

Increasing Biofilm Susceptibility

Given the challenges in the prevention of biofilm formation, several studies have instead focused on the development of approaches to improve treatment methods for bacterial biofilms, specifically through increasing biofilm antibiotic susceptibility. Biofilms are resistant to antibiotics for a multitude of reasons, including high cell density[26], low antibiotic penetration[27], and slower growth rate[26]. The dormancy of biofilm bacteria is a major challenge, as it restricts antibiotic uptake and the availability of antibiotic target sites.[140] Research has often targeted persisters, a sub-population of the dormant bacteria phenotype that are able to survive antibiotic threats that would otherwise kill the bacteria population, but whose tolerance is not due to resistant mutation.[141-142] By making biofilms more susceptible, conventional antibiotic treatment will be able to effectively eradicate biofilms, preventing resistance development in bacteria [143-144] and improving the treatment outcomes, reducing hospitalization time[145-147].

Many efforts have been made to understand antibiotic tolerance in biofilms, and a variety of different approaches have been studied to increase their antibiotic susceptibility. Quorum sensing inhibitors increased the efficacy of tobramycin against in *P. aeruginosa* in biofilms, but had no effect on planktonic cells, suggesting blocking quorum sensing may interrupt the regulation of characteristic biofilm gene expression involved in antibiotic tolerance.[90] Harrison et al. noted that *E. coli* lacking a nonessential protein transport pathway resulted in disorganized biofilms, and had increased sensitivity to antimicrobials when grown in nutrient-limited conditions.[148] Alginate in mucoid strains of *P. aeruginosa* biofilms have been suggested to impart antibiotic tolerance, and the co-administration of aminoglycosides with alginate lyase helped degrade alginate the biofilm, and enhanced the antibiotics effectiveness.[92] Approaches used to targeted persisters, a metabolically inactive sub-population (<1%) of dormant cells in biofilms[142, 149], may also be applicable to sensitize the slow-growing dormant cell majority through activity stimulation. Choudhary et al. found that exposure to host defense factors increases the sensitivity of persister cells in *P. aeruginosa* biofilms to antibiotics by upregulating genes associated with motility consequentially increasing bacterial activity as cells move away from host cytokines.[150] Biofilms grown in the presence of mannitol had increased susceptibility to tobramycin, reverting persister cells in biofilms to antibiotic susceptible phenotype by inducing a metabolic pathways and generating a PMF (proton motive force).[151] It is important to note that while studies that utilize mutant bacteria, such as those lacking specific signaling pathways, are useful in understanding the nature of the biofilm tolerance, they do not offer a tangible approach to treatment of clinical infections. Instead, it is

best understood that these approaches rely on modulating the natural behavior of bacteria in order to generate sub-optimal biofilms.

Thesis Objectives

The purpose of this dissertation is to develop new antimicrobial functions stemmed from synthetic polymer structures and properties that can be used for directly treat bacterial infections (antimicrobial) or indirectly act as biofilm suppressants and antibiotic adjuvant. This dissertation will introduce a new polymer architecture, specifically macromolecules with multiple polymer chains, designed to control the antimicrobial activity and hemolytic behavior. The findings of this dissertation will contribute fundamental knowledge necessary to develop high efficacy, low toxicity amphiphilic polymers to treat bacterial infections. This dissertation also introduces a new materials approach to modulate bacteria activity to prevent biofilm formation and potentially improve antibiotic efficacy. The findings of these studies provide new insight into the interaction of synthetic polymers with bacterial membranes, and the knowledge can be used to develop new antimicrobial and anti-biofilm strategies.

Approach 1: Multi-Armed Amphiphilic Polymers for Direct Bacteria Killing

In chapters 2 and 3, amphiphilic polymethacrylate derivates will be explored for their antimicrobial and hemolytic activities. The central hypothesis is that branched and multi-armed macromolecules presenting multiple antimicrobial polymer chains will show improved antimicrobial activity and selectivity towards bacteria as compared to the previously studied linear structures. In chapter 2, hyperbranched copolymers will be synthesized to examine the effect of branched structures and sizes on their antimicrobial and hemolytic activities. In

chapter 3, 4-armed star polymers will be synthesized, and the effect of star structure on antimicrobial and hemolytic activities will be examined. The goal of these chapters is to identify if macromolecules presenting multiple polymer chains can effectively be used to improve antimicrobial activity and improve selectivity compared to linear polymers, which could be used as a new tunable parameter for future polymer designs.

Approach 2: Biofilm Formation and Treatment Modulating Polymers

In chapters 4 and 5, cationic polymers will be explored for their ability to target bacteria behavior to modify biofilm formation and antibiotic susceptibility. In chapter 4, interactions between cationic poly[(3-methacryloylamino)propyl] trimethylammonium chloride and planktonic bacteria are investigated to change planktonic bacteria behavior during biofilm formation, which may result in downstream sub-optimal biofilm formation. In chapter 5, cationic poly[(3-methacryloylamino)propyl] trimethylammonium chloride was used to treat existing biofilms to determine if the polymer could increase antibiotic susceptibility of bacteria. The goal of these chapters is to identify new routes in which synthetic polymers can modify the behavior of bacteria to prevent biofilm formation and to improve biofilm treatments.

Chapter 2 Antimicrobial and Hemolytic Activities of Crosslinked Amphiphilic Methacrylate Polymers

Introduction

The number of antibiotic-resistance bacterial infections, including multidrug resistant infections, has been rapidly increasing over the past several decades. Conventional antibiotic treatment may no longer be a viable option. However, the number of new synthetic antibiotics entering the market decreased.[4] There is an urgent need for new antimicrobials that are effective in eradicating drug-resistant bacteria. To that end, the therapeutic potential of membrane-active antimicrobial polymers has been explored as new antimicrobial agents, which mimic the behavior of host-defense antimicrobial peptides (AMPs) found in the innate immune system.[66-68] The major barrier to antimicrobial polymers as antibiotic therapeutics is insufficient antimicrobial activity and poor selectivity.[152-153] Antimicrobial peptides typically require higher concentrations (μM) than traditional antibiotics (nM) in laboratory tests.[74-75, 78] The MIC values of antimicrobial peptide magainin-2, bee venom lytic peptide melittin, antibiotic ciprofloxacin and norfloxacin are listed in Table 2.1, which were determined in our laboratory for references. Many antibiotics are enzyme and DNA inhibitors, which act by binding a specific active site of proteins within the bacteria. Antibiotic resistance requires large quantities of antibiotics beyond

clinically useful concentrations to eliminate resistant bacteria. For example, our laboratory previously demonstrated that MIC of norfloxacin against *E. coli* increased 500 time greater than the initial MIC as the bacteria were passaged 21 times.[75] Such large doses of antibiotics may cause systemic toxicity, and it would be difficult to solubilize for clinical use. On the other hand, AMPs act by disrupting the bacterial cell membrane. While AMPs have reduced potency (lower MIC) as compared to antibiotics, they have a higher killing rate, broad-spectrum activity and a reduced likelihood of resistance development, which is highly desirable.[154]

Table 2.1. Antimicrobial activity of antimicrobial peptides (magainin-2, melittin) as compared to traditional antibiotics (ciprofloxacin, norfloxacin).[74-75, 78]

		MIC against *E. coli*	
		μg/mL	μM
Antimicrobial Peptides	Magainin-2	125	51
	Melittin	12.5	4.4
Traditional Antibiotics	Ciprofloxacin	0.01	0.02
	Norfloxacin	0.06	0.2

Cationic random amphiphilic polymers have been one design platform to explore structural factors to mimic AMPs, including monomer compositions and molecular sizes.[155-165] Traditionally, cationic and hydrophobic balance of polymers has been the major tunable factor to control their antimicrobial activity and cell selectivity to bacteria over mammalian cells, as the cationic functionality imparts the binding to anionic bacterial cell membranes and the insertion of hydrophobicity cause membrane disruption, resulting in bacterial cell death. The optimal balance has been achieved by tuning the composition of cationic and hydrophobic monomers during polymerization. This strategy has been extensively studied to improve the activities of polymers; however, it appears that there is a limit in the improvement. While the previous work has been focused on the monomer composition of polymer chains to mimic the

amphiphilic properties of AMPs, there may be the clue to improve the polymer activity in the mechanism of AMPs. When AMPs are bound to bacterial cell membranes, multiple AMPs are assembled to form pores in cell membranes or accumulated to non-specifically disrupt membrane structures. It has been reported that 4-11 peptide chains are necessary for pore formation, depending on AMPs.[166-167] Therefore, AMP activity should be thought of as the collective action of the peptides. Here we hypothesize that macromolecules presenting multiple antimicrobial polymer chains will show improved antimicrobial activity and selectivity. Because no need for assembly or accumulation of polymer chains for pore formation or membrane disruption, the low concertation of macromolecules would effectively kill bacteria.

Antimicrobial macromolecules with multiple polymer chains have not been extensively studied. A study conducted by Tiller and co-workers found that poly(4-vinyl-N-alkylpyridinium) 3-arm star polymers (10,000-85,000 g/mol) exhibited similar antimicrobial activity to linear counterparts when used as coatings[84], but the solution conformation of polymers prior to binding is proposed to affect antimicrobial properties and cell selectivity.[168] Liu and co-workers studied methacrylate-based 4-arm star polymers (16,000-28,000 g/mol) with good antimicrobial activity and low cytotoxicity when quaternized[85], but this does not provide essential knowledge of the advantages or disadvantages of branched or star-shaped architecture as compared to traditional linear antimicrobial polymer architecture.

To test the hypothesis, we investigated a synthetic approach to macromolecules which can present multiple antimicrobial polymer chains, and their antimicrobial and hemolytic activities. In this study, we further hypothesize that a hyperbranched polymer structure will provide a simple model scaffold to present multiple polymer chains in one (macro)molecule.

The purpose of this study is to study the synthesis of hyper-branched crosslinked polymers using free-radical polymerization with a chain transfer agent and examine the effect of structures and monomer compositions on their antimicrobial and hemolytic activities. In this study, we attempted to prepare hyper-branched polymers with different molecular sizes, degree of branching, and polymer densities by altering the concentrations of di-functional monomer (crosslinker) and chain transfer agent. The composition of cationic and hydrophobic monomers was also altered to tune the inherent antimicrobial activity of polymer chains.

Methods

Materials

Azobisisobutyronitrile (AIBN, Sigma Aldrich), methyl 3-mercaptopropionate (MMP, Acros Organic), dimethylformamide (DMF, Fisher Chemicals), acetonitrile (MeCN, Fisher Chemicals), dichloromethane (Fisher Chemicals), hexane (Fisher Chemicals), trifluoracetic acid (TFA, Fisher Chemicals), methanol (MeOH, Fisher Chemicals), ethanolamine (Acros Organic), tetrahydrofuran (THF, Fisher Chemicals), di-tert-butyldicarbonate (Acros Organic), ethyl acetate (Fisher Chemicals), and ethyl ether (Fisher Chemicals) were used as received. Methacryloyl chloride was purchased from Acros Organic and distilled prior to each use. Sodium hydroxide pellets (NaOH, Fisher Chemicals) was used to prepare solutions of desired molar concentrations. Sodium bicarbonate (Fisher Chemicals) and sodium chloride (NaCl, Fisher Chemicals) were used to prepare saturated solutions. Ethylene glycol dimethacrylate (EGDMA, Electron Microscopy Sciences) and ethylmethacrylate (EMA, Aldrich) were passed through a column of aluminum oxide (50-200 μm) to remove inhibitors prior to polymer synthesis.

Escherichia coli (ATCC 25922) and *Staphylococcus aureus* (ATCC 25923) were used as model bacteria evaluate antimicrobial activity. Human red blood cells (RBCs) (leukocytes reduced adenine saline added) were obtained from the American Red Cross Blood Services Southeastern Michigan Region and used prior to the out date indicated on each unit. Mueller Hinton Broth (MHB, BD and Company ©) and phosphate buffered saline (PBS, pH=7.4, Gibco®) were prepared according to manufacturer instructions and sterilized prior to use.

Synthesis of N-boc-protected aminoethyl methacrylate (boc-AEMA)

A solution of ethanolamine (255 mmol, 15.8 mL) in a biphasic mixture of THF (180 mL) and NaOH (aq) (1 M, 300 mL) was added dropwise to a solution of di-tert-butyldicarbonate (255 mmol, 55.7 g) in 120 mL THF. The solution was stirred at room temperature overnight. The solution was evaporated under reduced pressure, and the resulting solid dissolved in ethyl acetate. The desired N-boc-protected alcohol was extracted in ethyl acetate by washing with water (3x), followed by saturated NaCO3H (aq) and saturated NaCl (aq) to remove residual monomer. Residual water was removed by magnesium sulfate, and ethyl acetate removed by evaporation under reduced pressure. The resulting oily product was dried under vacuum. A solution of N-boc-protected alcohol (67.1 mmol, 10.8 g) and trimethylamine (162 mmol, 16.4 mL) in dichloromethane (150 mL) was bubbled with nitrogen for 10 minutes in a 0 °C ice bath. Freshly distilled methacryloyl chloride (67 mmol, 6.60 mL) was diluted with dichloromethane (15.0 mL), bubbled with nitrogen for 5 minutes, and added dropwise to the solution of N-boc-protected alcohol. The solution was stirred 16h in a 0 °C ice bath. The solution was filtered, and the filtrate concentrated by evaporated under reduced pressure. The resulting product was extracted in ethyl acetate by washing with water (3x), followed by saturated NaCO3H (aq) and

saturated NaCl (aq). Ethyl acetate was evaporated under reduced pressure, and the solid dissolved in minimal dichloromethane (~2 mL). Hexane was added to the solution (~10 mL), and the product recrystallized at room temperature, followed by 0 °C and -18 °C to maximize recovery of N-boc-protected aminoethyl methacrylate (boc-AEMA). The solid was isolated at each temperature, crushed and dried under vacuum overnight before confirmed high purity by 1H NMR.

Preparation of methacrylate polymers (20% monomer (wt) /solvent (v)) : Series a, b, c

Boc-AEMA (0.10 g, 0.44 mmol), ethyl methacrylate (EMA, varied), ethylene glycol dimethacrylate (EGDMA, varied), AIBN (14.5 mg, 0.09 mmol) and MMP (varied) were dissolved in a DMF/MeCN solution (1/4, v/v, 5 mL). Series b and c were designed with 30 or 50 mol% of EMA, relative to total monomer concentration (Boc-AEMA+EMA). The length and density of polymer arms were controlled by the amount of EGDMA and MMP, which was varied 0, 1, 5, or 10% relative to monomer concentration. The solutions were sealed by rubber septum, bubbled with nitrogen for 10 minutes, and reacted overnight at 60 °C with stirring. Having observed challenges synthesizing polymers with high EGDMA content without the formation of gels, a series of polymers was also generated at 5% monomer (w)/solvent (v), termed Series d.

^{1}H-NMR (CDCl3) was taken of crude solution to determine the conversion rates from monomer to polymer. The solutions were concentrated by evaporated under reduced pressure and re-dissolved in dichloromethane (~0.5 mL). The solution was then precipitated twice in hexanes to remove unreacted monomers and reagents, resulting in fine white particulates which were dried under high vacuum.

Removal of the boc protecting group to achieve a primary amine was achieved by reacting polymers with trifluoracetic acid (TFA) for 20 minutes. A small amount of MMP was included to quench the formation of the carbo cation. TFA is harmful, and exposure to TFA should be limited. TFA was removed by blowing with nitrogen gas. The polymer residue was dissolved in methanol (~0.5 mL) and the solution precipitated twice in diethyl ether, resulting in white particulates. The precipitate was dried under high vacuum and subsequently dissolved in water and lyophilized. The degree of polymerization and molar composition of monomers were determined by ^{1}H-NMR (D_2O), through comparing integration of peaks from side chains to that of the end group (MMP) of polymer chain (see Supporting Information for ^{1}H NMR spectra).

Series a was designed as MA homopolymer (100% cationic monomers). Series b was designed as 70% MA-30% EMA (70% cationic-30% hydrophobic monomers), and Series c as 50% MA-50% EMA (50% cationic-50% hydrophobic monomers). Series d revisited a 70% MA-30% EMA polymer design.

Characterization of methacrylate polymers

Gel permeation chromatography (GPC) analysis was performed using a Waters 1515 HPLC instrument equipped with Waters Styragel (7.8 × 300 mm) HR 0.5, HR 1, and HR 4 columns in sequence and detected by a differential refractometer (RI). Calibration curves were based on narrow dispersity polystyrene standards between 1,050-1,000,000 g/mol (Polymer Laboratories Ltd. And Polysciences, Inc.). Boc-protected polymers were characterized by gel permeation chromatography (GPC) to determine number average molecular weight (M_n) and weight-average molecular weight (M_w), and calculated dispersity ($Đ$).

Antimicrobial Activity

The minimum inhibitory concentration (MIC) of polymers against *E. coli* (ATCC 25922) and *S. aureus* (ATCC 25923) was determined in a standard microbroth dilution assay according to the Clinical and Laboratory Standards Institute guidelines with suggested modifications by R. E.W Hancock Laboratory (University of British Columbia, British Columbia, Canada)[169] and Giacometti et al.[170] Bacteria was grown overnight (~18 hours) in MHB at 37 °C with orbital shaking (180 rpm), and used as an inoculum by diluting overnight culture in MHB to a concentration of OD_{600}=0.1. The inoculated solution was then grown at 37 °C to the exponential phase (OD_{600}= 0.5-0.7, 2 hours). Final dilution to OD_{600}= 0.001, ~2 x 10^5 CFU/mL, was made with MHB. Bacterial suspension (OD_{600}= 0.001, 90 µL/well) was transferred to a 96-well sterile round-bottom polypropylene plate. Polymers were dissolved in 0.01% acetic acid to achieve stock concentrations of 20 mg/mL. Serial 2-fold dilutions of polymers were prepared from stock solutions in PBS and transferred to the 96-well sterile round-bottom polypropylene plate for a final concentration of 7.8-1,000 µg/mL (10 µL/well). PBS was used as a solvent control in place of polymer. Plates were sealed with parafilm and incubated for 18 hours at 37 °C without shaking. MIC was defined as the lowest concentration of polymers to completely inhibit bacterial growth, as indicated by lack visual of turbidity. Assays were repeated a minimum of three times in triplicate on different days.

Hemolytic Activity

Hemolysis, the lysis of human red blood cells (RBCs), was used to assess the toxicity of polymers to human cells. A 10% solution of human RBCs in PBS was centrifuged at 2000 rpm for 5 minutes and washed with PBS x2 to remove initial hemoglobin. The number of RBCs in the

resulting solution was determined by counting chamber, and the solution diluted in PBS to give a final concentration go 3.33 x 10^8 cells/mL. After serial dilutions, polymers (10 µL) were transferred to a 96-well sterile round-bottom polypropylene plate, followed by the RBC suspension (90 µL). Plates were incubated 37 °C with orbital shaking (180 rpm) for 1 hour. Triton X-100 (0.1% v/v in water) was used as the positive lysis control and PBS used as a negative control. Following incubation, the plate was centrifuged at 2000 rpm for 5 minutes. The supernatant (5 µL) from each well diluted in PBS (100 µL) with thorough mixing in a 96-well flat-bottomed polystyrene plate. The absorbance of released hemoglobin (415 nm) was measured using a Varioskan Flash microplate reader (Thermo Fisher). The percentage hemolysis was determined relative to Triton X-100 (100%) and PBS negative control (0%). The polymer concentration causing 50% hemoglobin release (HC_{50}) was determined, and the hemolysis (%) at the highest concentration of polymer (1000 µg/mL) was reported if below 50%. Assays were repeated a minimum of three times in triplicate.

Results and Discussion

Polymer Design and Synthesis

In our polymer design, we attempted to synthesize hyperbranched polymers by free radical polymerization to form a branched macromolecular structure of antimicrobial polymer chains through the incorporation of crosslinker. We built on a previously well-explored platform of methacrylate random copolymers with cationic primary ammonium side chains and hydrophobic ethyl side chains. The polymer chain length was controlled by thiol chain transfer agent 3-MMP. We polymerized boc-protected aminoethyl methacrylate (boc-AEMA), ethyl

methacrylate (EMA), and ethylene glycol dimethacrylate (EGDMA) using AIBN as an initiator and MMP as a chain transfer agent, followed by deprotection of the boc-group using TFA to yield polymers with primary ammonium groups (Figure 2.1).

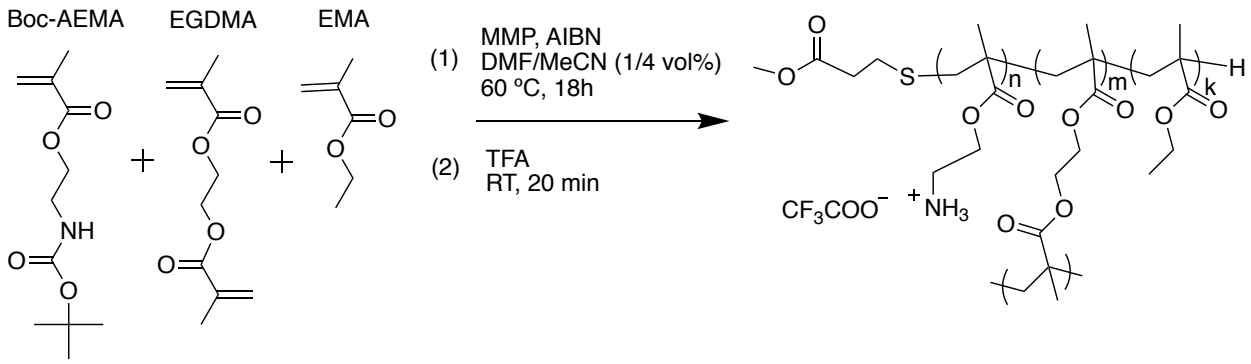

Figure 2.1. Synthesis of amphiphilic methacrylate-based copolymers containing crosslinking agent EGDMA. Feed stock compositions were varied as described in methods, where the ratio of EGDMA (m) was proportional to Boc-AEMA and EMA (n+k), and ratio CTA was relative to total monomer concentration (n+m+k).

Composition

We synthesized hyperbranched polymers and related linear polymers with three monomer compositions: 100% boc-AEMA homopolymer (Series a), 70% boc-AEMA -30%EMA copolymer (Series b and d) and 50% boc-AEMA -50%EMA copolymer (Series c). Previously, the balance of cationic and hydrophobic properties had been used to control antimicrobial and hemolytic activities. The ultimate goal of this project is to exploit the macromolecular presentation of polymer chains to improve their antimicrobial activity. Therefore, it is important we examine the activity of linear polymers and how the activity of individual polymer chains reflected the activity of macromolecular (branched) structures. Polymer composition was controlled by varying the feed composition of boc-AEMA and EMA. EGDMA was not factored into the calculation of monomer compositions due to an attempt to separate factors

controlling polymer architecture from factors controlling amphiphilic balance. The amount of EGDMA was 0, 1.0, 5.0, and 10 mol% of the total amount of boc-AEMA and EMA, and the amount of MMP was 0, 1.0, 5.0, and 10 mol% of the total amount of boc-AEMA and EMA and EGMDA.

The final monomer compositions were calculated by comparing the integrated areas in the ^{1}H-NMR spectra as shown in the Appendix A as percent AEMA, EMA, and EGDMA relative to total monomer amount. For example, series B polymers contained 63-75% AEMA, 24-32% EMA, and 0-11% EGDMA (Table 2.2). The final polymer composition, determined by ^{1}H-NMR analysis, was in good agreement with the feed monomer compositions, Series a, c, and d can be found in Appendix A.

Table 2.2. Comparison of monomer feed composition to polymer composition calculated by ^{1}H-NMR for Series b.

		Monomer Feed Composition (mol%)			Polymer Composition, ^{1}H-NMR (mol%)		
		Boc-AEMA	**EMA**	**EGDMA**	**AEMA**	**EMA**	**EGDMA**
Series b	**P_b17**	70.0	30.0	0.0	68	32	0
	P_b18	69.3	29.7	1.0	Gel	Gel	Gel
	P_b19	66.7	28.6	4.8	Gel	Gel	Gel
	P_b20	63.6	27.3	9.1	Gel	Gel	Gel
	P_b21	70.0	30.0	0.0	70	30	0
	P_b22	69.3	29.7	1.0	70	30	0.01
	P_b23	66.7	28.6	4.8	Gel	Gel	Gel
	P_b24	63.6	27.3	9.1	Gel	Gel	Gel
	P_b25	70.0	30.0	0.0	72	28	0
	P_b26	69.3	29.7	1.0	70	29	1
	P_b27	66.7	28.6	4.8	69	29	2
	P_b28	63.6	27.3	9.1	69	27	4
	P_b29	70.0	30.0	0.0	75	25	0
	P_b30	69.3	29.7	1.0	73	26	1
	P_b31	66.7	28.6	4.8	68	24	8
	P_b32	63.6	27.3	9.1	63	26	11

Conversion/Yield

Following polymerization, the conversion of monomers to boc-protected polymers was determined by comparing the integrated area of the methylene groups on monomer side chains signal (~4 ppm) to integrated area from the methylene on the monomer double bond signal (~6 ppm) in the ^{1}H-NMR spectra. Monomer conversion was between 85-99% for all series of polymers (

Table 2.3, Appendix A). Boc-protected polymers were collected by precipitation with good yield (78-100%), though some polymers retained trace amounts of DMF (<5 mol%) which were calculated to not affect polymer yields (<0.2 wt.%). Deprotected polymers were recovered

with excellent yield based on the theoretical weight of the resultant polymers (89-100%), and contained no solvent traces following lyophilization.

Table 2.3. Polymerization conversion and yield of Series b copolymer.

						Boc-Protected	Deprotected
				State	% Conversion	% Yield	% Yield
Series b	P_b17	0% MMP	0% EGDMA	Liquid	98	100	100
	P_b18		1% EGDMA	Gel	Gel	Gel	Gel
	P_b19		5% EGDMA	Gel	Gel	Gel	Gel
	P_b20		10% EGDMA	Gel	Gel	Gel	Gel
	P_b21	1% MMP	0% EGDMA	Liquid	98	78	100
	P_b22		1% EGDMA	Liquid	97	100	89
	P_b23		5% EGDMA	Gel	Gel	Gel	Gel
	P_b24		10% EGDMA	Gel	Gel	Gel	Gel
	P_b25	5% MMP	0% EGDMA	Liquid	98	100	100
	P_b26		1% EGDMA	Liquid	97	100	92
	P_b27		5% EGDMA	Liquid	97	100	89
	P_b28		10% EGDMA	Liquid	98	100	95
	P_b29	10 %MMP	0% EGDMA	Liquid	98	86	100
	P_b30		1% EGDMA	Liquid	99	91	100
	P_b31		5% EGDMA	Liquid	98	90	100
	P_b32		10% EGDMA	Liquid	99	89	100

Gelation

Due to the presence of crosslinking monomers, the polymerization mixtures resulted in either a solution or solid gel. Gelation occurred in some polymers when MMP ≥1 mol% and EGDMA ≤1 mol% (Figure 2.2). Monomer composition effected the critical ratios EGDMA/MMP for gelation. While the total monomer concentration in solvent remained constant across these series, the increasing percentage of EMA resulted in increase of gelation EGDMA/MMP ratios, which may reflect the solubility of monomers and resultant polymers to solvent; EMA may be more soluble (miscible) as compared to boc-AEMA.

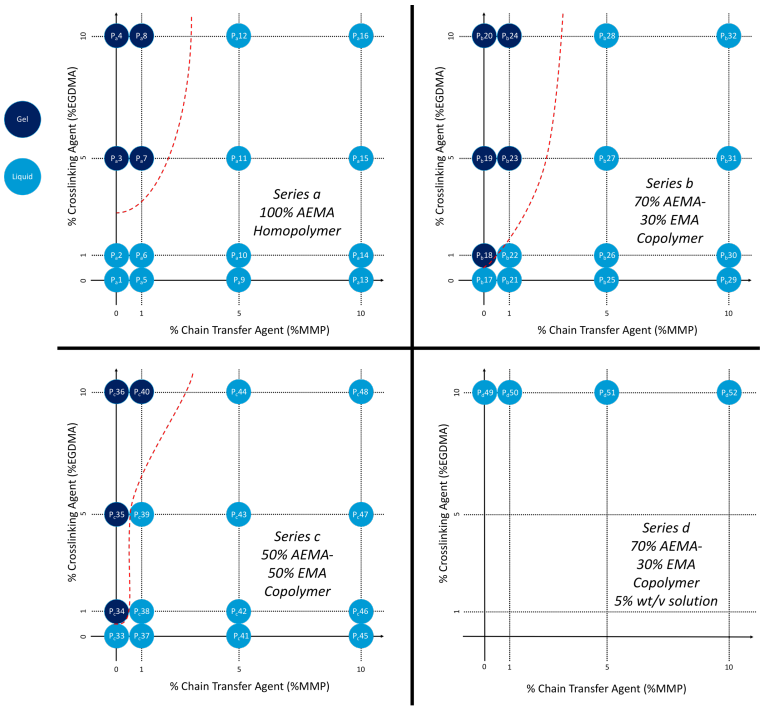

Figure 2.2. Phase diagrams of homo and copolymer series a, b, c, and d. Solution-gelation behavior is based on ratio of chain transfer agent (MMP) to crosslinking agent (EGDMA).

Polymer Characterization

Degree of Polymerization: Effect of CTA and Arm Length

MMP, a chain transfer agent, was used to control the length of polymer chains by chain termination and re-initiation of polymerization.[171] The degree of polymerization (DP) of the resultant polymer chains was determined by ^{1}H-NMR analysis by comparing the integrated area of signals from the polymer side chain units to that from the end-group CTA (described in Appendix A). The DP of the polymers synthesized without MMP was not able to be determined from the ^{1}H NMR spectra due to lack of the signal from the end groups. The degree of polymerization of polymers ranged from 12-80 repeat units (Table 2.4, Appendix A). The DPs of linear polymers without EGDMA was decreased as the mole percentage of MMP was increased from 1% to 10% as seen in P_b21 (DP= 82, 1% MMP), P_b25 (DP=33, 5% MMP) and P_b29 (DP=17,

10% MMP) (Figure 2.3). These results are consistent with the results from the previous reports.[69, 81] For the polymers containing EGDMA, the apparent DP was calculated as the number of monomers (AEMA, EMA, and EGDMA) per one MMP. The calculated DP is apparent, as opposed to that for the linear polymers, because the polymer chains are cross-linked. The apparent DP provides the measure of polymer chains cross-linked in the branched structures. Increasing the amount of MMP from 1% to 10% resulted in a decrease in apparent DP, as can be seen in the examples with 1 mol% EGDMA feedstock P_b22 (DP=80, 1% MMP), P_b26 (DP=33, 5% MMP) and P_b30 (DP=18, 10% MMP) (Figure 2.3). In branched polymers, the apparent DP is equal to the average length of polymer arms. However, we cannot determine the number of chains incorporated into the crosslinked macromolecule (true DP).

Table 2.4. Calculation of absolute degree of polymerization (linear) and apparent degree of polymerization (crosslinked) by ^{1}H NMR.

		Absolute DP	***Apparent DP***
Series b	**P_b17**	No CTA	No CTA
	P_b21	82.465	Linear
	P_b22	Crosslinked	80.075
	P_b25	26.39	Linear
	P_b26	Crosslinked	33.28
	P_b27	Crosslinked	31.475
	P_b28	Crosslinked	18.72
	P_b29	17.265	Linear
	P_b30	Crosslinked	18.16
	P_b31	Crosslinked	17.015
	P_b32	Crosslinked	13.995

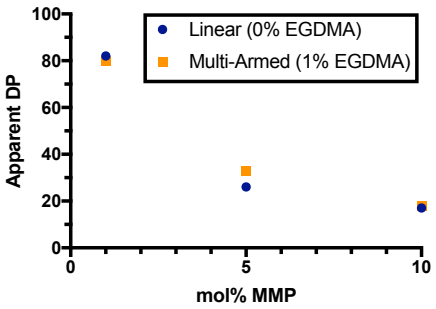

Figure 2.3. Effect of chain transfer agent (mol% MMP) on apparent DP.

Molecular weight and Dispersity

Apparent molecular weights of polymers were calculated based on apparent degree of polymerization (Table 2.4) and composition which are determined by ^{1}H NMR analysis using the molecular weights of monomers (AEMA, EMA, and EGDMA), and MMP (Table 2.2). A sample calculation can be found in the Appendix A. Apparent molecular weight of polymers ranged from 2,000-16,000 g/mol (Table 2.5). However, these calculations are based on apparent DP, and it is not possible to determine the number of polymer chains incorporated into the crosslinked macromolecule.

M_n, M_w and dispersity ($Đ$) of the boc-protected polymers were determined by GPC as relative to polystyrene standards. The M_n of boc-protected polymers ranged from 2,300-16,000 g/mol (polystyrene standard), but M_w were significantly higher and ranged from 3,400-49,000 g/mol (Table 2.5, Appendix A). For linear polymers, the highest M_n (15,872 g/mol) and M_w (49,002 g/mol) occurred in P_b17, which was synthesized in the absence of CTA. Additionally, P_b17 was also the linear polymer the highest $Đ$ (3.09) (Table 2.5). Comparatively, polymers synthesized with MMP, such as P_b29 (10 mol% MMP), had reduced M_n (2,530 g/mol), M_w (3,461 g/mol) and $Đ$ (1.37). This suggests that the chain termination by CTA helps control molecular

weight and molecular weight dispersity, where increasing the mol% of CTA decreases Mn and decreases *Đ* (Figure 2.4a). This effect was also seen in crosslinked monomers. A comparison of P_b22 (1 mol% MMP), P_b26 (5 mol% MMP), and P_b30 (10 mol% MMP) showed decreasing M_n at 11,662 g/mol, 4,922 g/mol and 2,925 g/mol respectively (Figure 2.4b). Increasing EGDMA content from 0 to 10 mol% shows both an increase in M_n and increase in *Đ*, seen in the case of P_b29 (0 mol%), P_b30 (1 mol%), P_b31 (5 mol%) and P_b32 (10 mol%) (Figure 2.4c). Evidence of greater dispersity can be observed by broadening of GPC column retention time (Figure 2.4d). Crosslinking polymer *Đ* was dependent on crosslinking monomer/CTA ratio, where the highest *Đ* occurred where crosslinking monomer content (mol%) was greater than CTA content (mol%). For example, P_b28 had the highest *Đ* (8.3) of Series b, which occurred at 10 mol% EGMDA and 5 mol%. This behavior is also evident in trend Series a and c (P_a12, P_c39, P_c44).

Table 2.5. Molecular weight and dispersity characterization by ^{1}H NMR and GPC of Series b copolymers.

		MW (g/mol) (^{1}H NMR)	***M_n* (g/mol) (GPC)**	***M_w* (g/mol) (GPC)**	***Đ* (GPC)**
Series b	**P_b17**	No DP	15872	49002	3.09
	P_b21	16174	8064	17804	2.21
	P_b22	15616	11662	33749	2.89
	P_b25	5238	3499	5238	1.50
	P_b26	6555	4922	9141	1.86
	P_b27	6046	8191	33631	4.11
	P_b28	3584	9415	78411	8.33
	P_b29	3487	2530	3461	1.37
	P_b30	3641	2925	4325	1.48
	P_b31	3470	3706	7040	1.90
	P_b32	2776	5649	19599	3.47

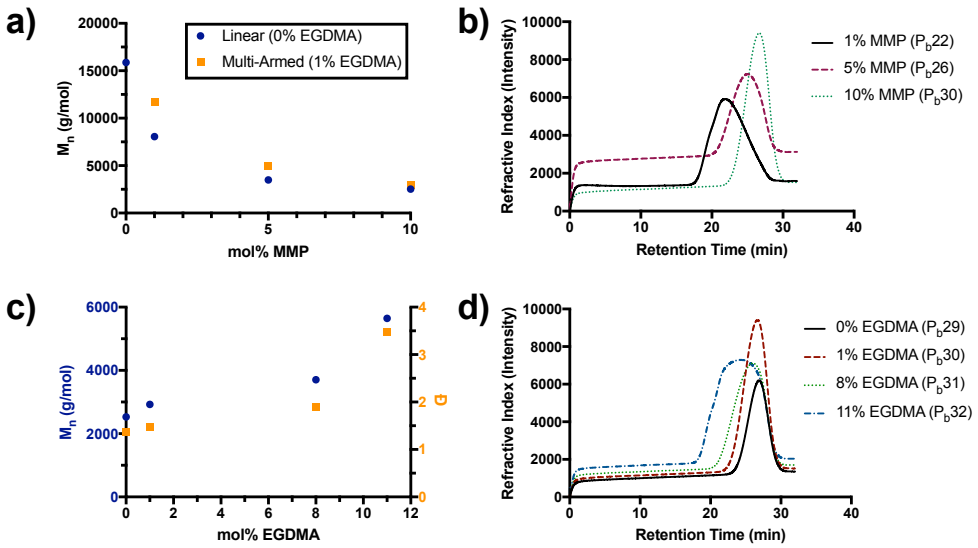

Figure 2.4. Polymer molecular weight and dispersity dependence on CTA and crosslinker content: (a) molecular weight dependence on MMP, (b) representative GPC spectrum of retention time variation by MMP content, (c) molecular weight and dispersity dependence on EGDMA, and (d) representative GPC spectrum of retention time variation by EGDMA content.

Probing Polymer Architecture by EGDMA/Chain Ratio

In order to gain insight on the polymer architecture in crosslinked polymers, a calculation of the number of crosslinkers per polymer chain (CTA end group). The number of EGDMA per polymer is indicative of the number of chains that are linked together through crosslinking (branches), and how structurally restricted the polymer is through multiple crosslinks between the same chains. The apparent DP was determined by ^{1}H-NMR relative to the MMP end group, and mol% EGDMA was used to determine the number of EGDMA monomers per polymer chain (terminated in MMP). The average number of crosslinks per CTA in the polymers synthesized at 20 wt% monomer/ v% solvent was typically between 0.2-1.7 (Table 2.6, Appendix A). The low degree of branching suggests a structure that is not multi-armed, but linear containing some crosslinking monomer. For gelled polymers, a theoretical calculation of crosslinks/CTA was carried out based on the EGDMA feed composition and degree of polymerization of comparable linear polymers. Gelled polymers P_b23 and P_b24 were

calculated to have crosslinker/CTA ratios of 4.1 and 8.2 respectively, indicating that polymers crosslinked into insoluble networks. The reduction of monomer content to 5 wt% in solvent (v) resolved the gelation and allowed a polymer to be synthesized with a crosslinker/CTA ratio of >2 (P_d50, 3.61).

Table 2.6. Degree of polymerization and average crosslink density as determined by ^{1}H-NMR for Series b copolymers. Average crosslink/CTA ratio denoted by * are theoretical calculations of gelled polymers based on linear comparable compositions. Denotations of N/A are indications of

		Apparent DP	Average #Crosslinks/CTA Ratio
Series b	**P_b17**	No CTA	No CTA
	P_b18	Gel	No CTA
	P_b19	Gel	No CTA
	P_b20	Gel	No CTA
	P_b21	82	No EGDMA
	P_b22	80	0
	P_b23	Gel	4.1*
	P_b24	Gel	8.2*
	P_b25	26	No EGDMA
	P_b26	33	0.3
	P_b27	31	0.6
	P_b28	19	0.8
	P_b29	17	No EGDMA
	P_b30	18	0.2
	P_b31	17	0.4
	P_b32	14	1.5

Antimicrobial Activity

We next investigated the relationship between polymer structure and antimicrobial activity of polymers. The antimicrobial activity of the polymers was quantified as the lowest polymer concentration that completely inhibit bacterial growth, or the minimal inhibitory concentration (MIC), as the bacterial growth was determined by turbidity. The activity of

polymers against Gram-negative *E. coli* and Gram-positive *S. aureus* were used as model bacterium. Gram-positive bacteria possess a thicker peptidoglycan cell wall as compared to Gram-negative bacteria, while Gram-negative bacteria possess two (cytoplasmic and outer) membranes. These differences in the membrane structure can give rise to different behavior of membrane-active membranes, because the polymers need to penetrate these cell wall and membranes to reach the cytoplasmic membranes to exert antimicrobial effects. A list of MICs can be found in Table 2.7 and Appendix A.

Effect of Polymer Composition

Previous designs of amphiphilic random copolymers have utilized cationic/hydrophobic ratio to control antimicrobial behavior. Specifically, increased hydrophobic content has been linked to increased antimicrobial activity, though a saturation of hydrophobic groups can be reached. [70, 172-173] The insertion of hydrophobic polymer segments into the bacterial cell membrane causes membrane disruption and ultimately death, and thus greater hydrophobic composition imparts greater antimicrobial efficacy. Against *E. coli*, crosslinked and linear polymers had decreased MICs as mol% EMA increased. Linear polymer P_a1 (0% EMA) had an MIC of 208 (±72), which decreased to 63 μg/mL in P_b17 (32% EMA) and 31 μg/mL in P_c33 (47% EMA) (Figure 2.5a). Crosslinked polymers with 10% EGDMA showed a decrease from >1000 μg/mL in P_a16 (0% EMA) to 63 μg/mL in P_b32 (26% EMA) and 12 μg/mL in P_c48 (42% EMA) (Figure 2.5a). Decreasing MIC values indicating increased antimicrobial efficacy with increasing hydrophobic content. However, MIC did not change significantly with hydrophobic content against *S. aureus*, as can be seen in P_a1 at 83 (±36) to P_c33 at 167 (±72), or P_a16 at 104 (±36) to P_c48 at 125 μg/mL (Figure 2.5b). Lack of MIC change indicates hydrophobic compositional

changes did not affect antimicrobial efficacy against *S. aureus*. Previously *S. aureus* has been reported to be sensitive to the cationic charge density in copolymers, as opposed to hydrophobic density, due to differences in the outer bacterial membrane.[72, 76] The lack of change in *S. aureus* antimicrobial activity with polymer composition suggests that cationic charge saturation occurs at 50 mol% MA.

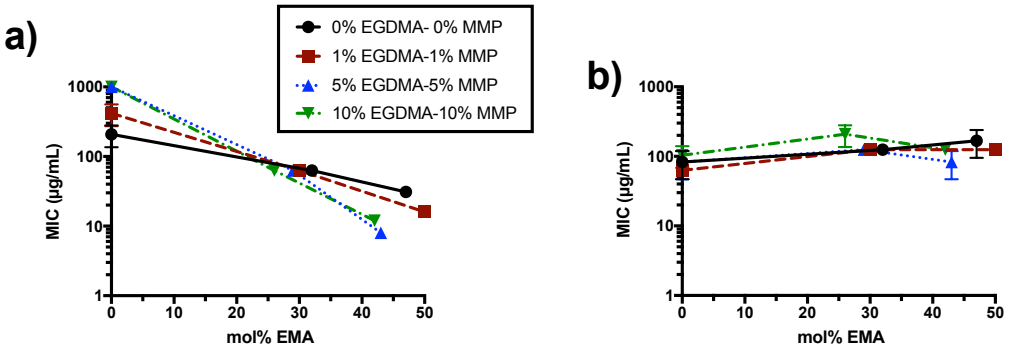

Figure 2.5. Hydrophobic content effect on antimicrobial activity of methacrylate random copolymers against (a) *E. coli* and b) *S. aureus*. Data points and error bars represent the average and s.d. from data in three independent experiments (n=3).

Effect of EGDMA

Crosslinked copolymers were designed with the intent to assess the effect of branched architecture on their antimicrobial activity as compared to linear architecture. While it is unlikely that crosslinked architecture was achieved by the incorporation of EGDMA due crosslink/chain ratios <2 (Table 2.6), EGDMA incorporation affected the antimicrobial behavior of the amphiphilic polymers, as seen as an example in Series b. Against *E.coli*, P_b29 (0% EGMDA)had an MIC of 417 (±144), which decreased to 250 µg/mL (P_b30, 1% EGDMA), 125 (P_b32, 8% EGDMA) and 63 µg/mL in P_b32 (11 mol% EGDMA) (Figure 2.6a). However, MICs did not decrease with increasing EGDMA against *S. aureus*, as seen in the cases of P_b25-28 (125

µg/mL) (Figure 2.6b). There is therefore an apparent increase in antimicrobial activity against *E. coli*, but not *S. aureus*, due to EGDMA crosslinking. EGDMA incorporation may contribute to antimicrobial activity in several ways, such as increasing hydrophobic content, changes to molecular weight or dispersity, which will both be later discussed in detail. Series a lacked sufficient antimicrobial behavior to observe any such change, while the high hydrophobic content of Series c obscured any effect of EGDMA.

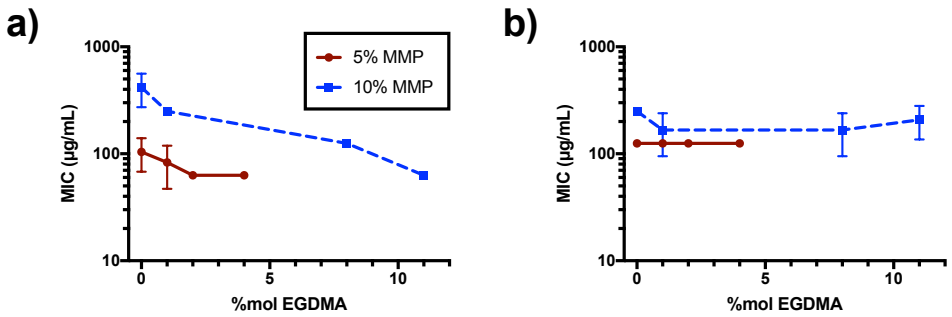

Figure 2.6. EGDMA content effect on antimicrobial activity of methacrylate random copolymers against (a) *E. coli* and b) *S. aureus*. Data points and error bars represent the average and s.d. from data in three independent experiments (n=3).

Effect of CTA, Molecular Weight and Dispersity

Chain transfer agents were included in the polymer design to control the length of polymer arms, or the total degree of polymerization of the chain. Length of polymer chains has previously been shown to be an important factor for antimicrobial behavior, specifically that increasing molecular weight in amphiphilic methacrylate copolymers enhances antimicrobial activity due to a total increase in the number of biologically active groups.[69] In the case of linear and EGDMA containing copolymers, increasing MMP content decreased the MIC against *E.coli* (Figure 2.7). For example, the P_b30 (10 mol% MMP) showed an MIC of 250 µg/mL, but $_{Pb22}$ showed an MIC of 63 µg/mL (Figure 2.7a). Polymers synthesized with increasing amounts of

MMP resulted in shorter polymer chains with lower molecular weights. Note in this discussion, M_n determined by GPC will be used as comparative molecular weights, as absolute molecular weights cannot be determined by ^{1}H NMR. MIC against *E. coli* decreased with increasing M_n for linear polymers, such as in P_b29 (2,530 g/mol) with an MIC of 417 (±144) μg/mL compared to P_b21 (8,064 g/mol) with an MIC of 63 μg/mL (Figure 2.7b). The same trend occurred for crosslinked polymers, where P_b30 (2,925 g/mol) with an MIC of 250 μg/mL decreases to 63 μg/mL in P_b22 (11,662 g/mol) (Figure 2.7b). The MIC of P_b30 at $Đ$ = 1.48 was 250 μg/mL, compared to P_b32 with $Đ$ = 3.5 with an MIC of 63 μg/mL (Figure 2.7c). Beyond $Đ$ ~2, MIC did not further decrease. This behavior suggests that while chain transfer agents have historically been used to control antimicrobial activity through molecular weight and dispersity in linear polymers, they are only effective in crosslinked polymers to the extent they can control dispersity. The inclusion of high molecular weight polymers in crosslinked systems may dominate the antimicrobial behavior or work synergistically with lower MW polymers. AMPs are monodispersed, and previous design platforms for amphiphilic methacrylate copolymers have attempted to mimic this through narrow molecular weight dispersity. However, the collective effect of multiple monodispersed polymers binding to the membrane may result in behavior that mimics a higher dispersity system. For instance, two AMPs overlapping at a bacterial membrane may have the apparent effect of a single AMPs with 2x their molecular weight.

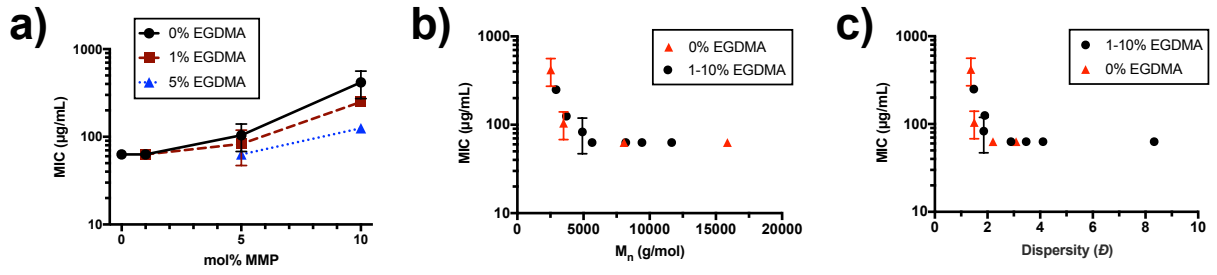

Figure 2.7. Effect of polymer size on antimicrobial activity of methacrylate random copolymers against *E. coli* as a factor of (a) MMP mol% content, (b) molecular weight, (c) and polymer dispersity. Data points and error bars represent the average and s.d. from data in three independent experiments (n=3).

Hemolytic Activity

To investigate mammalian cell toxicity, the lysis of human red blood cells (hemolysis) by methacrylate polymers was assessed and quantified as the polymer concentration to induce 50% hemoglobin release (HC_{50}). For polymers which concentrations ≤1000 μg/mL did not achieve 50% hemolysis, the %hemolysis at 1000 μg/mL was recorded (Table 2.7).

Effect of Polymer Composition

One challenge with amphiphilic antimicrobial polymers is the toxicity to human cells due to non-specific hydrophobic interactions, disrupting mammalian cell membranes. Selecting a polymer composition that appropriately balances cationic and hydrophobic composition is necessary to achieve potent antimicrobial activity and low toxicity to mammalian cells. As the mole percentage of EMA was increased, the HC_{50} activity of linear and crosslinked polymers decreased (Figure 2.8a). For example, P_a1 (0% EMA) had at HC50 >1000 μg/mL, which decreased to 60 (±40) μg/mL in P_b17 (32% EMA), and further decreased to 6 μg/mL in P_c33 (47% EMA). This indicates that increasing hydrophobic content results in increased hemolytic activity. Because increasing hydrophobic content increases both hemolytic and antimicrobial

activity, we sought to quantify the selectivity of polymers to bacterial cells over mammalian cells through a selectivity index (HC_{50}/MIC against *E.coli*) (Table 2.7, Appendix A). Selective activity exists at ratios >1, though increases to selectivity by increasing ratio value are also of interest. The copolymers with the most potent antimicrobial activity (smallest MIC values) and largest SI are from Series b (~30% EMA), including P_b26, P_b21, and P_b25 (Table 2.7). P_b21 had an MIC of 63 μg/mL and an HC_{50} of 540 (±210) μg/mL, resulting in a selectivity index of 8.6. P_b25 had an MIC of 104 (±36) μg/mL and an HC_{50} of >1000 μg/mL (30% hemolysis at 1000 μg/mL), resulting in a selectivity index of 9.6. P_b26 had an MIC of 83 (±36) μg/mL and an HC_{50} of 600 (±300) μg/mL, resulting in a selectivity index of 7.2. P_b21 and P_b25 are both linear polymers, while P_b26 contains 1% EGDMA. P_b25 and P_b26 have low M_n, 3,499 and 4,922 g/mol respectively, and low $Đ$, 1.5 and 1.86 respectively. P_b21 has a higher M_n of 8,064 g/mol, and a $Đ$ of 2.2. Together, these properties suggest that selective polymers have 1) amphiphilic balance of approximately 30% hydrophobic-70% cationic side chains, 2) low molecular weights in the range of 3,000-8,000 g/mol, and 3) polymer dispersity of ≤ 2.2. This would also suggest that hyperbranching does not increase the selectivity of polymers compared to comparable linear polymers, as can be seen in the case of P_b25 and P_b26.

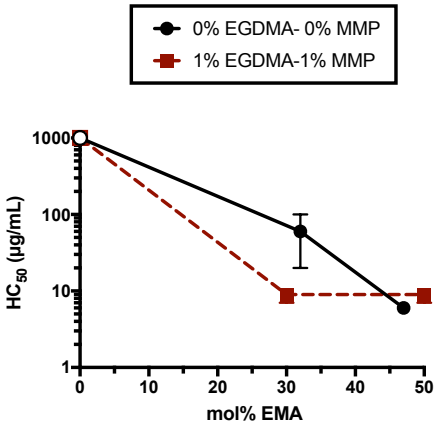

Figure 2.8. Hydrophobic content effect on RBC toxicity of methacrylate random copolymers. Data points and error bars represent the average and s.d. from data in three independent experiments (n=3).

Table 2.7. Antimicrobial activity (MIC) and hemotoxicity (HC_{50}) of Series b copolymers

		MIC (µg/mL)		HC_{50} (µg/mL)	*%Hemolysis at 1000 µg/mL*	Selectivity Index (HC_{50}/MIC *E. coli*)
		E. coli	***S. aureus***			
Series b	**P_b17**	63	125	60 (±40)	72 (±5)%	0.95
	P_b21	63	125	540 (±210)	59 (±5)%	8.57
	P_b22	63	125	9 (±2)	91 (±7)%	0.14
	P_b25	104 (±36)	125	N/A	30 (±5)%	9.62
	P_b26	83 (±36)	125	600 (±300)	66 (±8)%	7.23
	P_b27	63	125	9 (±2)	82 (±5)%	0.14
	P_b28	63	125	13 (±6)	95 (±18)%	0.21
	P_b29	417 (±144)	250	N/A	22 (±7)%	2.40
	P_b30	250	167 (±72)	N/A	19 (±9)%	4.00
	P_b31	125	167 (±72)	110 (±40)	64 (±10)%	0.88
	P_b32	63	208 (±72)	9 (±2)	90 (±5)%	0.14

Effect of EGDMA

The incorporation of EGDMA into methacrylate amphiphilic polymers has been shown capable of changing both antimicrobial and selectivity behavior, as earlier mentioned.

Increasing EGDMA content decreased HC_{50} values and the percentage hemolysis at 1000 μg/mL. For example, P_b30 (1% EGDMA) has a H_{C50} >1000 μg/mL and 22 (±7)% hemolysis at 1000 μg/mL, as compared to P_b32 which has a HC50 of 9 (±2) μg/mL and 90 (±5)% hemolysis at 1000 μg/mL. This suggests that increasing EGDMA increases hemolytic activity. Due to the calculation of a low number of crosslinks per polymer chain (<2) discussed previously, it is unlikely that EGDMA results in changes to polymer architecture. However, the resulting increase to hemolysis with EGMDA incorporation may be due to contributions to total hydrophobic content, which is supported by the previous polymer composition section. To further investigate the effect of EGDMA on cell selectivity, selectivity indices were compared (Table 2.7). Increasing EGDMA content decreased SI, such as in the case of P_b25 (9.6, 0 mol% EGDMA) P_b26 (7.3, 1 mol% EGDMA), and P_b28 (0.2, 4 mol% EGDMA) This result suggest that EGDMA decrease the selectivity of polymers towards bacterial cells over mammalian cells. While antimicrobial activity of these polymers slightly increased (MIC decrease from 104 μg/mL to 63 μg/mL), hemolytic activity increases significantly (HC_{50} >1000 μg/mL to 13 μg/mL). Therefore, it is likely that a consequence of EGDMA incorporation on polymer structures may be responsible for increased selectivity discussed above, while EGDMA incorporation generally results in increasing toxicity.

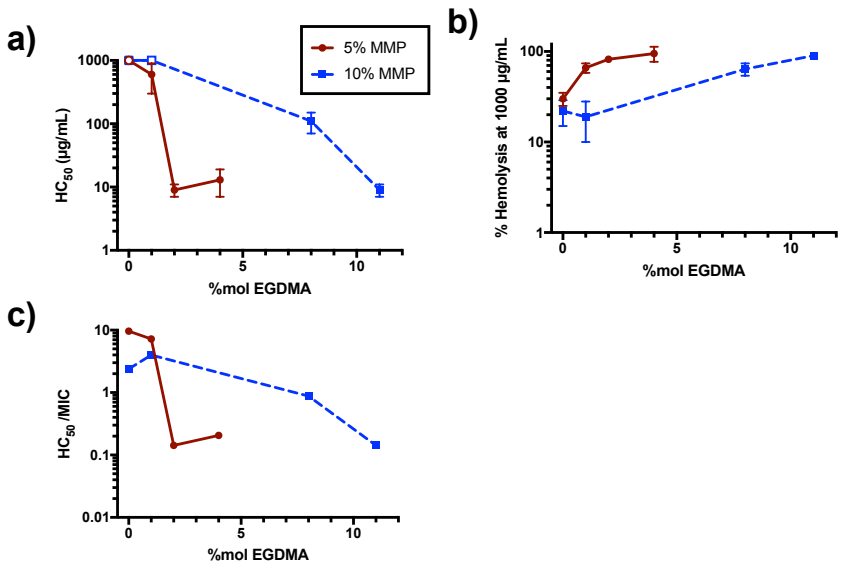

Figure 2.9. EGDMA content effect on RBC toxicity shown as (a) HC50 or (b) hemolysis at 1000 µg/mL polymer, and (c) polymer selectivity. Data points and error bars represent the average and s.d. from data in three independent experiments (n=3).

Effect of CTA, MW, Dispersity

Chain transfer agents control the degree of polymerization, and consequentially molecular weight, which are a factor in hemolytic activity. High molecular weight polymers have previously been shown to have high hemolytic activity.[69] The effect of CTA to control polymer chain length was utilized in this design. Increasing MMP content resulted in higher HC_{50} values, corresponding to decreased hemolytic activity. Additionally, increasing MMP increases the selectivity of polymers to bacterial cells over red blood cells, because of dramatic decreases in hemolytic activity rather compared to moderate decreases in antimicrobial activity. For example, the polymer P_b17 with 1% of MMP showed MIC of 63 µg/mL and HC_{50} of 60 (±40) µg/mL, but the polymer P_b29 with 10% MMP showed MIC of 417 (±144) µg/mL and HC50 of >1000 µg/mL. As MMP content controls molecular weight, we would expect to find that hemolysis increases as molecular weight increases. However, at approximately the same molecular weight, linear polymer without EGDMA P_b21 (Mn = 8,064 g/mol) had an MIC of 63

μg/mL and HC_{50} of 540 (±210) μg/mL and hyperbranched polymer with 1% EGDMA P_b27 (8,191 g/mol) showed MIC of 63 μg/mL and HC_{50} of 9 (±2) μg/mL. This behavior may be attributed to greater polydispersity of P_b27, ($Đ$ = 4.11) compared to linear P_b21 ($Đ$ = 2.21) due to the larger population of high molecular weight polymers that are very hemolytic.

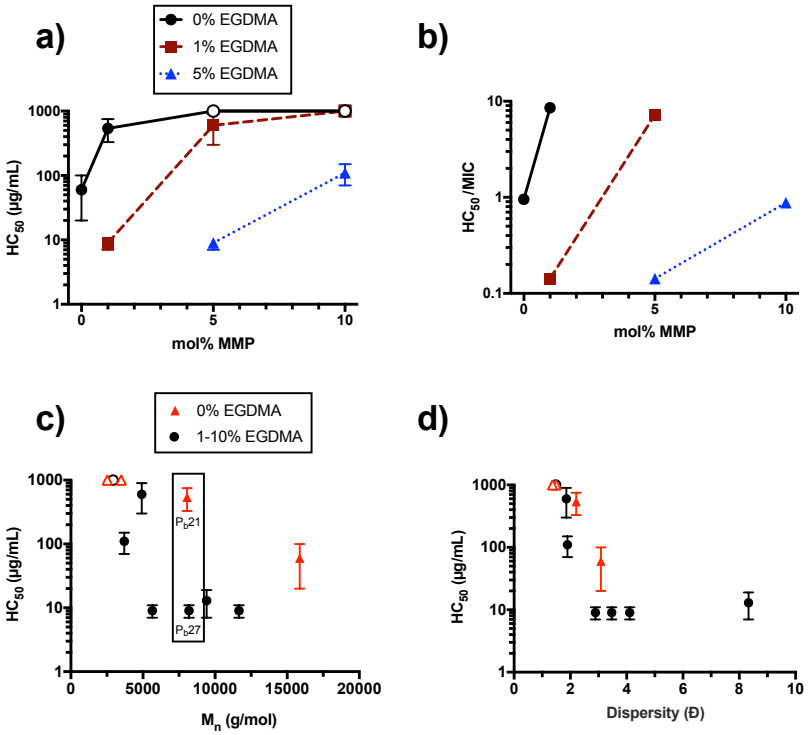

Figure 2.10. Effect of polymer size on RBC toxicity: (a) HC_{50} dependence on mol% MMP, (b) cell selectivity dependence on mol% MMP, (c) HC_{50} dependence on molecular weight, and (d) HC50 dependence on dispersity. Data points and error bars represent the average and s.d. from data in three independent experiments (n=3).

Discussion: Polymer Structure and Relationship with Antimicrobial and Hemolytic Activities

In this study, we aimed to explore the effect of hyperbranched polymers on antimicrobial and hemolytic activity as compared to traditional linear antimicrobial counterparts. Antimicrobial and hemolytic assays suggest that the activity of polymers with hyperbranched architecture are not an improvement from linear architecture. Antimicrobial

activity is dominated by the degree of hydrophobicity from EMA composition, and possible contributions from EGDMA, and molecular weight (i.e. the total number of hydrophobic groups). The hemolytic activity of hyperbranched polymers is increased from linear polymers of similar molecular weight. We propose that the increased hemolytic activity of hyperbranched polymers is due increased dispersity, specifically the contribution of high molecular weight polymers that are highly hemolytic.[69, 81]

The synthesis of hyperbranched polymers via free radical polymerization with crosslinking monomers was hypothesized to give rise to structures capable of mimicking the collective action of multiple AMP peptide chains at membrane surfaces. Based on the results of this study, we did not observe improved antimicrobial activity and selectivity in our hyperbranched polymers. We wonder if the resultant polymers are macromolecules which present multiple polymer chains as we initially designed. When we analyzed the data of polymer characterization, we found that, for the polymers which did not form gels during the polymerization, the number of crosslinkers in a polymer chain did not exceed 2. For example, P_b32 has DP of 14 determined by ^{1}H NMR. Because EGDMA is 11 mol% relative to the total number of monomers (as determined by ^{1}H NMR), one EGDMA molecule will be incorporated into every ~9 monomer units in a polymer chain. Therefore, P_b30 (DP = 14) has 1.5 EGDMA molecules in a polymer chain. If polymers contain only 1 crosslink, they are architecturally linear polymers that are extended through the crosslinking monomer to a second linear polymer. Therefore, they can be thought of as a longer linear chain, with short portions of the backbone extending away from the main/longest polymer chain. If polymers contain 2 crosslinks, they may suffer from restricted freedom of movement if both crosslinking

monomers associated in the same two chains, therefore having new architecture. However, in this study, the presence of 2 or more crosslinks resulted in polymer gelation, suggesting these conditions cannot be used to synthesize crosslinked polymers.

This model would suggest that only two polymer chains are linked together on average, suggesting that the majority is linear polymers, and a small fraction of polymers containing a crosslinking monomer. Based on this, we propose that these polymers do not have appropriately high crosslinker concertation per "chain" (i.e. CTA) to mimic the collective behavior of multiple polymers for membrane activity. Therefore, while this study is able to deduce the effects of inclusion of a crosslinking monomer on biological activity, we do not feel it is able to conclude the effects of hyperbranched architecture on antimicrobial and hemolytic activity based on the polymer collective design.

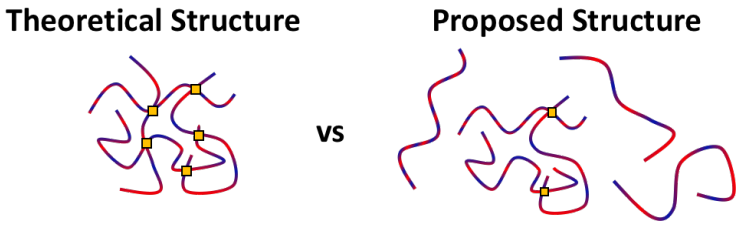

Figure 2.11. Theoretical structure of hyperbranched polymers by free radical polymerization with crosslinking monomers compared to the proposed structure of dilute crosslinked polymers that behavior as high molecular weight linear polymers.

Conclusions

In summary, amphiphilic primary ammonium copolymers composed of cationic 2-aminoethyl methacrylate (AEMA), ethyl methacrylate (EMA), and ethylene glycol dimethacrylate (EGDMA), were synthesized by free radical polymerization and evaluated for their antimicrobial and hemotoxic activity. Despite the presence of crosslinking monomers, we propose that polymers were primarily linear in structure based on calculated crosslinker/CTA

ratios, likely due to combined effects of low concentration of crosslinking agents and low molecular weight/DP target to mimic natural AMPs. While this approach is not an appropriate polymer model for the collective polymers responsible for membrane activity, these studies contributed and reinforced design factors for antimicrobial polymers. Antimicrobial and hemolytic activity both increased with percent hydrophobic composition and higher molecular weights. However, hemolytic activity is more sensitive to wider dispersity, suggesting mammalian cells may be more sensitive to high molecular weight polymers than bacterial cells. Additional research is necessary to determine polymer designs that appropriately mimic the behavior of multiples polymer on membranes in order to identify if multi-armed polymer architectures are a new tunable parameter for antimicrobial polymer designs.

Chapter 3 4-Armed Star-shaped polymer Architecture for Antimicrobial and Hemolytic Activities

Introduction

The increasing number of antibiotic-resistant bacterium has stimulated research into the development of therapeutic alternatives for conventional antibiotics.[174] While resistance has been increased at a growing rate[175], new conventional antibiotics do not address the issue of antibiotic-resistance development. Instead, this approach attempts to replace drugs that have become obsolete with new drugs, effectively racing antibiotic development and antibiotic-resistance. There is an emerging need for new antimicrobials that can overcome current resistance mechanisms and not contribute to the development of future resistances in bacteria. To that end, a recent approach has been the use of antimicrobial polymers which mimic host-defense antimicrobial peptides found in the innate immune system.[66-68] The barrier to clinical application of antimicrobial polymers has been the maintaining sufficient antimicrobial activity in the absence of mammalian cell toxicity.

As previously discussed, cationic random amphiphilic polymers have been one such design platform to explore structural factors that mimic AMPs, including polymer composition and molecular sizes.[155-165] Previous polymers have been primarily focused on tuning the balance of cationic and hydrophobic properties of the polymer in order to control selective membrane

activity. The cationic functionality of the polymer binds to the anionic bacterial cell membranes preferentially over more neutral mammalian membranes, followed by the insertion of hydrophobic groups into the lipid bi-layer to result in membrane disruption and ultimately cellular death. Achieving an optimal balance is often achieved by tuning polymer composition of cationic and hydrophobic monomers and has had good success in controlling polymer activities. However, we propose that further improvement of antimicrobial activity can be achieved by introducing multi-armed polymer architecture as a new tunable factor for polymer design. As we previously discussed in chapter 2, natural antimicrobial peptides are assembled to form pores on bacterial cell membranes or disrupt cell membrane structures. Therefore, we also hypothesize in this chapter that macromolecules presenting multiple antimicrobial polymer chains will show improved antimicrobial activity and selectivity. In the previous chapter, we attempted to synthesize hyperbranched polymers using crosslinking monomers by free radical polymerization but failed to achieve hyperbranched architecture. In this chapter, we will extend our approach to star-shaped polymers, which present a star-shaped structure with 4 polymer chains.

To test the hypothesis, we investigated a star-shaped polymer architecture with 4 polymer chains composed of cationic 2-aminoethyl methacrylate (AEMA) and ethyl methacrylate (EMA). The traditional antimicrobial polymer parameters of polymer composition and polymer size were explored within both architectures in order to examine each factors effect on antimicrobial and hemolytic activities. The ultimate goal of this study is to design 4-armed polymers with increased antimicrobial activity due to the collective polymer effect, and

increased selectivity towards bacterial cells due to the high density of cationic charge, as compared to linear copolymer counterparts.

Methods

Materials

Dichloromethane (DCM, Fisher Chemicals), hexane (Fisher Chemicals), trifluoracetic acid (TFA, Fisher Chemicals), methanol (MeOH, Fisher Chemicals), ethyl ether (Fisher Chemicals), copper (I) bromide (CuBr, Acros organics), 1,1,4,7,7-pentamethyldiethylenetriamine (PMDETA, Acros Organics), pentaerythritol tetrakis(2-bromoisobutyrate) (4f-BIB, Aldrich chemistry), and ethyl 2-bromo-2-methylpropionate (EBIB, Acros organics) were used as received. Tetrahydrofuran (THF, Fisher Chemicals) was dried over molecular sieves (3 Å). Ethyl methacrylate (EMA, Aldrich) was passed through a column of aluminum oxide (50-200 μm) to remove inhibitors prior to polymer synthesis. Boc-AEMA was synthesized as described in Chapter 2.

Escherichia coli (*E. coli* ATCC 25922) and *Staphylococcus aureus* (*S. aureus* ATCC 25923) were used as model bacteria evaluate antimicrobial activity. Human red blood cells (RBCs) (leukocytes reduced adenine saline added) were obtained from the American Red Cross Blood Services Southeastern Michigan Region and used prior to the out date indicated on each unit. Mueller Hinton Broth (MHB, BD and Company ©) and phosphate buffered saline (PBS, pH=7.4, Gibco®) were prepared according to manufacturer instructions and sterilized prior to use.

Synthesis of Linear Methacrylate Copolymers by ATRP

The synthesis of linear polymers via atom transfer radical polymerization (ATRP) was carried out following procedure modified from Dufresne.[176] Monomers (Boc-AEMA and EMA, 0.87 mmol, 20, 40 or 80 Eq) were dissolved in dry degassed THF (0.8 mL) with EBIB initiator (1 Eq) in a N_2 purged container. Concurrently, Cu(I)Br (1.1 Eq) and PMDETA (1.1 Eq) were dissolved in dry degassed THF (0.27 mL) in a second-round bottom flask, purged with N_2. The monomer/initiator solution was transferred to CuBr/PMDETA solution via syringe under N_2. Polymerization was carried out at 65 °C for 18 hours. The reaction was quenched by exposure to atmospheric oxygen, diluted with DCM (~2 mL) and passed through a neutral aluminum oxide column, followed by 8 mL of DCM to wash the column. Monomer conversion was confirmed by ^{1}H NMR. Solvent was evaporated under reduced pressure, the polymer residue dissolved in DCM and precipitated twice in hexanes. Fine white particulates were dried under vacuum overnight. ^{1}H NMR in CDCl3 was used to determine the degree of polymerization, composition and molecular weight of the boc-protected polymers. The degree of polymerization was determined by comparing integration of signal peaks from methylene in monomer side chains (~4 ppm) to that of the initiator methylene (~1.05 ppm) (^{1}H NMR found in Appendix B).

Removal of the boc protecting group to achieve a primary amine was performed by reacting polymers with trifluoracetic acid (TFA) for 20 minutes. A small amount of MMP was included to quench the formation of the carbo cations. TFA is harmful, and exposure to TFA should be limited. TFA was removed by blowing with nitrogen gas, which was subsequently passed through a NaOH solution. The polymer residue was dissolved in methanol (~0.5 mL) and

the solution precipitated twice in diethyl ether, resulting in white particulates. The precipitate was dried under high vacuum and subsequently dissolved in water and lyophilized. ^{1}H NMR in D2O was used to determine the monomer composition of final polymers. Overlapping peaks from both methyl and methylene signals of the initiator with monomer backbone and side chain peaks resulted in an inability to characterize degree of polymerization in the final polymer.

Synthesis of 4-armed Methacrylate Copolymers by ATRP

The synthesis of 4-armed methacrylate polymers via ATRP was carried out following procedure modified from Dufresne[176], as described above with the replacement of EBIB initiator with 4f-BIB (1 eq). The concentration of Cu(I)Br (4.4 Eq) and PMDETA (4.4 Eq) were increased to reflect the number of active end groups, and the reaction time was decreased to 5 hours. All other setup, reaction, and workup conditions remained the same as compared to linear polymer synthesis described above.

Characterization of methacrylate polymers

Gel permeation chromatography (GPC) analysis was performed using a Waters 1515 HPLC instrument equipped with Waters Styragel (7.8 × 300 mm) HR 0.5, HR 1, and HR 4 columns in sequence and detected by a differential refractometer (RI). Calibration curves were based on narrow dispersity polystyrene standards between 1,050-1,000,000 g/mol (Polymer Laboratories Ltd. And Polysciences, Inc.). Boc-protected polymers were characterized by gel permeation chromatography (GPC) to determine number average molecular weight (M_n) and weight-average molecular weight (M_w), and calculated dispersity ($Đ$).

Antimicrobial Activity

The minimum inhibitory concentration (MIC) of polymers against *E. coli* (ATCC 25922) and *S. aureus* (ATCC 25923) was determined in a standard microbroth dilution assay according to the Clinical and Laboratory Standards Institute guidelines with suggested modifications by R. E.W Hancock Laboratory (University of British Columbia, British Columbia, Canada)[169] and Giacometti et al.[170] Bacteria was grown overnight (~18 hours) in MHB at 37 °C with orbital shaking (180 rpm), and used as an inoculum by diluting overnight culture in MHB to a concentration of OD_{600}=0.1. The inoculated solution was then grown at 37 °C to the exponential phase (OD_{600}= 0.5-0.7, 2 hours). Final dilution to OD_{600}= 0.001, 2 x 10^5 CFU/mL, was made with MHB. Bacterial suspension (OD_{600}= 0.001, 90 µL/well) was transferred to a 96-well sterile round-bottom polypropylene plate. Polymers were dissolved in 0.01% acetic acid to achieve stock concentrations of 20 mg/mL. Serial 2-fold dilutions of polymers were prepared from stock solutions in PBS and transferred to the 96-well sterile round-bottom polypropylene plate for a final concentration of 7.8-1,000 µg/mL (10 µL/well). PBS was used as a solvent control in place of polymer. Plates were sealed with parafilm and incubated for 18 hours at 37 °C without shaking. MIC was defined as the lowest concentration of polymers to completely inhibit bacterial growth, as indicated by lack visual of turbidity. Assays were repeated a minimum of three times in triplicate on different days.

Hemolytic Activity

Hemolysis, the lysis of human red blood cells (RBCs), was used to assess the toxicity of polymers to human cells. A 10% solution of human RBCs in PBS was centrifuged at 2000 rpm for 5 minutes and washed with PBS x2 to remove initial hemoglobin. The number of RBCs in the

resulting solution was determined by counting chamber, and the solution diluted in PBS to give a final concentration go 3.33 x 10^8 cells/mL. After serial dilutions, polymers (10 µL) were transferred to a 96-well sterile round-bottom polypropylene plate, followed by the RBC suspension (90 µL). Plates were incubated 37 °C with orbital shaking (180 rpm) for 1 hour. Triton X-100 (0.1% v/v in water) was used as the positive lysis control and PBS used as a negative control. Following incubation, the plate was centrifuged at 2000 rpm for 5 minutes. The supernatant (5 µL) from each well diluted in PBS (100 µL) with thorough mixing in a 96-well flat-bottomed polystyrene plate. The absorbance of released hemoglobin (415 nm) was measured using a Varioskan Flash microplate reader (Thermo Fisher). The percentage hemolysis was determined relative to Triton X-100 (100%) and PBS negative control (0%). The polymer concentration causing 50% hemoglobin release (HC_{50}) was determined, and the hemolysis (%) at the highest concentration of polymer (1000 µg/mL) was reported if below 50%. Assays were repeated a minimum of three times in triplicate.

Results and Discussion

Polymer Design and Synthesis

In this study, we synthesized linear and 4-armed star-shaped polymers by atom transfer radical polymerization (ATRP). Polymer chain length was controlled by varying the feed mole ratio of monomers to initiator. For star-shaped polymers, boc-protected aminoethyl methacrylate (boc-AEMA) and ethyl methacrylate (EMA) are copolymerized using pentaerythritol tetrakis(2-bromoisobutyrate) as an initiator and CuBr/PMDTA catalyst/ligand, followed by deprotection of the boc-group using TFA to yield polymers with primary

ammonium groups (Figure 3.1). For linear polymers, ethyl 2-bromo-2-methylpropionate was used as an initiator.

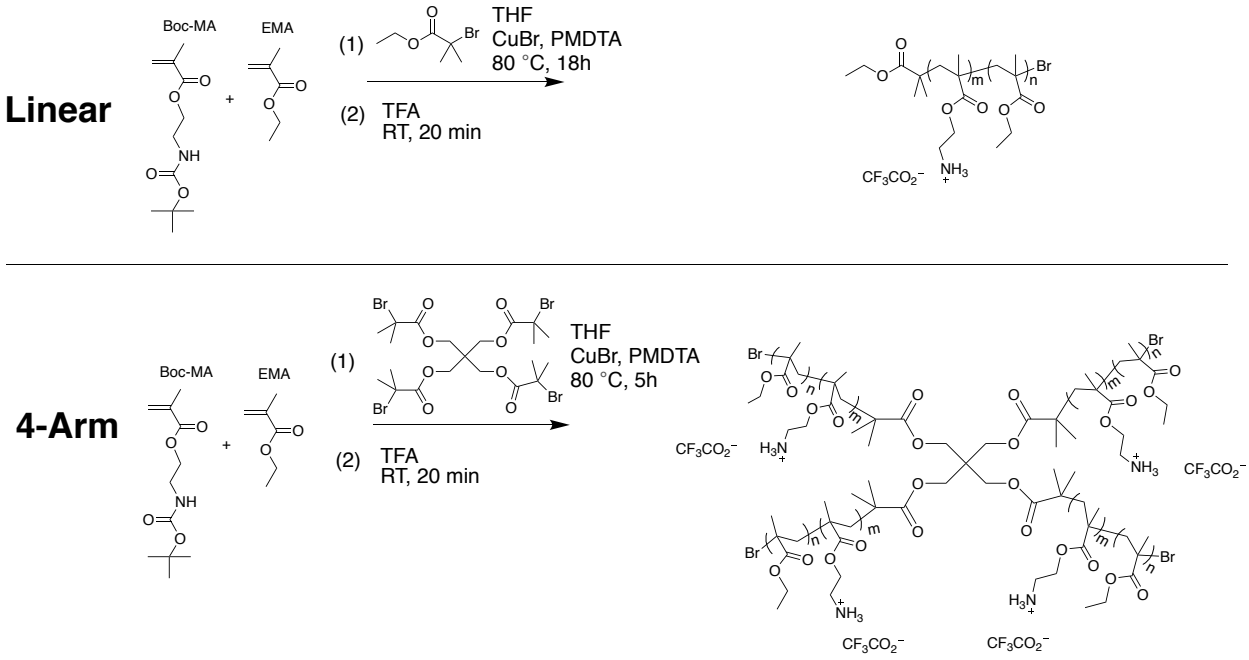

Figure 3.1. Synthesis scheme for linear and 4-armed methacrylate copolymers by ATRP.

Conversion/Yield

Following polymerization, the conversion of monomers to boc-protected polymers was determined by ^{1}H NMR, and yield determined by weight. Polymer conversion was determined by the integration or absence of signal peaks from methylene on the unsaturated monomer double bond. Linear polymers were fully converted in the 18-hour reaction time, while star-shaped polymers were fully converted in the 5-hour reaction time (Table 3.1). Boc-protected polymers were recovered by precipitation of DCM dissolved polymers in hexane with yields of 62-87%. Previously linear amphiphilic methacrylate copolymers were recovered by precipitation DCM dissolved polymers in hexane at higher yields (80-100%, Chapter 2). The lower yield in this case, despite 100% conversion, is hypothesized to be due to interaction of

polymers with the aluminum oxide column used to remove the copper complex. Alternative copper complex removal methods could be used in attempts to increase yield, such as washing with H_2O. Following deprotection, polymers were recovered with good yields of 85-94%.

Table 3.1 Polymerization conversion and yield of boc-protected and deprotected linear and 4-armed methacrylate copolymer, determined by ^1H NMR (conversion) and mass (yield).

	Monomer Feed Composition	**Target Total DP**	**Conversion**	**Boc-Protected Yield (%)**	**Deprotected Yield (%)**
P_L1	100% Boc-AEMA	20	100%	69	94
P_L2		40	100%	74	93
P_L3		80	100%	63	86
P_L4	70% Boc-AEMA-30% EMA	20	100%	71	89
P_L5		40	100%	66	91
P_L6		80	100%	67	86
P_L7	50% Boc-AEMA - 50% EMA	20	100%	70	92
P_L8		40	100%	62	89
P_L9		80	100%	71	90
P_S10	100% Boc-AEMA	20	100%	81	94
P_S11		40	100%	77	87
P_S12		80	100%	78	88
P_S13	70% Boc-AEMA-30% EMA	20	100%	73	86
P_S14		40	100%	72	90
P_S15		80	100%	75	90
P_S16	50% Boc-AEMA - 50% EMA	20	100%	77	90
P_S17		40	100%	87	89
P_S18		80	100%	74	88

Composition

Linear and 4-armed polymers were synthesized at three monomer compositions: 100 mol% boc-AEMA, 70 mol% boc-AEMA-30 mol% EMA, and 50 mol% boc-AEMA-50 mol% EMA. Amphiphilic ratio, or the balance of cationic to hydrophobic groups, has previously been used to control antimicrobial and hemolytic activities. Since the goal of this project is to improve upon the linear architecture of antimicrobial polymers through the use of 4-armed star-shaped

architecture, it is important to examine how the inherent activity of each polymer chain is reflected in the activity of whole macromolecules (star-shaped polymers) through comparison of activity between the star-shaped polymers and linear (arm) polymers. Polymer composition was controlled by varying the monomer feed composition of boc-AEMA and EMA. The boc-protected polymers were a good reflection of feed compositions (^{1}H NMR found in Appendix B). For example, polymers designed with a monomer composition of 70% boc-AEMA resulted in 74-78% boc-AEMA (linear) and 71-72% boc-AEMA (star-shaped) (Table 3.2). Following deprotection, the mole % of cationic monomer decreased slightly, suggesting preferential precipitation of hydrophobic polymers (^{1}H NMR found in Appendix B). Polymers designed with 70% boc-AEMA decreased to 69-71% boc-AEMA (linear) and 65-67% boc-AEMA (star-shaped) (Table 3.2). The ranges of monomer compositions were still considered is good reflection of molar monomer feed composition.

Table 3.2. Monomer feed composition, boc-protected monomer composition, and deprotected monomer composition of linear and 4-armed methacrylate copolymers.

	Monomer Feed Composition (mol%)			Boc-Protected Polymers (mol%)			Deprotected Polymers (mol%)	
	Boc-AEMA	**EMA**		**Boc-AEMA**	**EMA**		**AEMA**	**EMA**
P_L1	100	0		100	0		100	0
P_L2				100	0		100	0
P_L3				100	0		100	0
P_L4	70	30		74	26		69	31
P_L5				83	17		71	29
P_L6				78	22		70	30
P_L7	50	50		52	48		49	51
P_L8				59	41		51	49
P_L9				53	47		51	49
P_S10	100	0		100	0		100	0
P_S11				100	0		100	0
P_S12				100	0		100	0
P_S13	70	30		71	29		67	33
P_S14				70	30		65	35
P_S15				72	28		68	32
P_S16	50	50		51	49		43	57
P_S17				52	48		48	52
P_S18				54	46		49	51

Polymer Characterization

Degree of Polymerization, molecular weight and dispersity

Monomer/initiator ratio was varied to synthesize polymers with target molecular sizes. In general, the monomer/initiator ratio is expected to be the degree of polymerization because of the nature of living polymerization. In 4-armed star-shaped polymers, the degree of polymerization was determined by comparing the integrated areas of signals from the initiator core to that of polymer side chains in ^{1}H NMR spectra, providing the average degree of polymerization of total polymer arms.

In linear polymers, the DP of resultant polymers was not consistent with the target DP (Figure 3.2a); Polymers that targeted DP 20 resulted in DPs of 30-40, while polymers that targeted DP 80 resulted in DPs of 50-60 (Table 3.3). Target DP 40 polymers were closest to their goal with DPs of 37-53 (Table 3.3). On the other hand, the star-shaped polymers showed high DP than target DP (Table 3.3, Figure 3.2b). Molecular weights were calculated by DP and monomer composition (Table 3.2). Linear polymers were determined to be between 7,300-14,400 g/mol (Table 3.2, Figure 3.2c), while star-shaped polymers were between 5,700-24,100 g/mol (Table 3.2, Figure 3.2d), where the difference in MW was the factor of DP.

Gel permeation chromatography was used to determine M_n, M_w and D of linear and 4-armed copolymers. Linear polymers had M_n in the range of 5,000-10,300 g/mol and M_w in the range of 6,100-14,700 g/mol (Table 3.3). star-shaped polymers had M_n in the range of 5,000-9,800 g/mol and M_w in the range of 6,900-14,800 g/mol (Table 3.3). Despite the controlled nature of ATRP, polymer dispersity ($Đ$) of the linear systems was larger than expected between 1.23-1.43 (Table 3.3), with no apparent dependence on molecular weight of polymers (Figure 3.3a). Star-shaped systems were slightly higher where $Đ$ = 1.27-1.50 (Table 3.3, Figure 3.3b). The DP discrepancy and broad molecular distribution indicate that the polymerization was not controlled, and further optimization is necessary to obtain defined polymers.

Table 3.3. Size characterization of boc-protected linear and 4-armed methacrylate polymers by degree of polymerization, molecular weight, M_n, M_w, and $Đ$.

	DP (^{1}H NMR)	DP/Arm	Molecular Weight (g/mol) (^{1}H NMR)	M_n (g/mol) (GPC)	M_w (g/mol) (GPC)	$Đ$ (GPC)
P_L1	32	32	7,500	5,355	7,003	1.31
P_L2	37	37	8,642	7,342	9,749	1.33
P_L3	62	62	14,349	10,311	14,745	1.43
P_L4	30	30	6,153	5,248	6,577	1.25
P_L5	48	48	10,222	7,029	8,651	1.23
P_L6	60	60	12,386	10,269	13,889	1.35
P_L7	41	41	7,309	5,033	6,149	1.22
P_L8	53	53	9,814	6,138	7,967	1.30
P_L9	51	51	9,102	7,563	10,598	1.40
P_S10	29	7.3	7,353	5,000	6,922	1.38
P_S11	45	11.3	11,005	6,690	9,441	1.41
P_S12	91	22.8	21,506	9,335	13,588	1.46
P_S13	39	9.8	8,344	5,332	7,032	1.32
P_S14	62	15.5	12,763	7,394	10,564	1.43
P_S15	98	24.5	19,972	9,828	14,752	1.50
P_S16	29	7.2	5,713	6,421	9,308	1.45
P_S17	55	13.8	10,275	6,612	9,192	1.39
P_S18	133	33.3	24,111	9,490	12,084	1.27

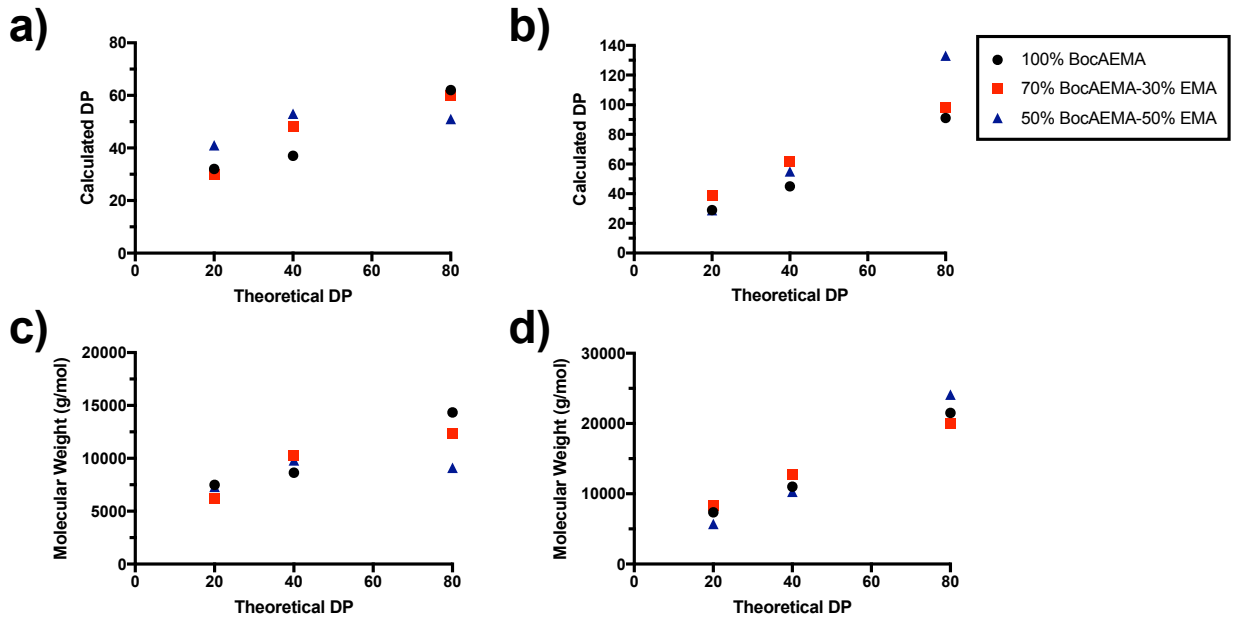

Figure 3.2. Degree of polymerization and molecular weight evaluation. Comparison of theoretical DP based on polymer design and calculated DP by H NMR in linear (a) and 4-armed (b) polymers. Molecular weights determined by calculated DPs by H NMR in linear (c) and 4-armed (b) polymers.

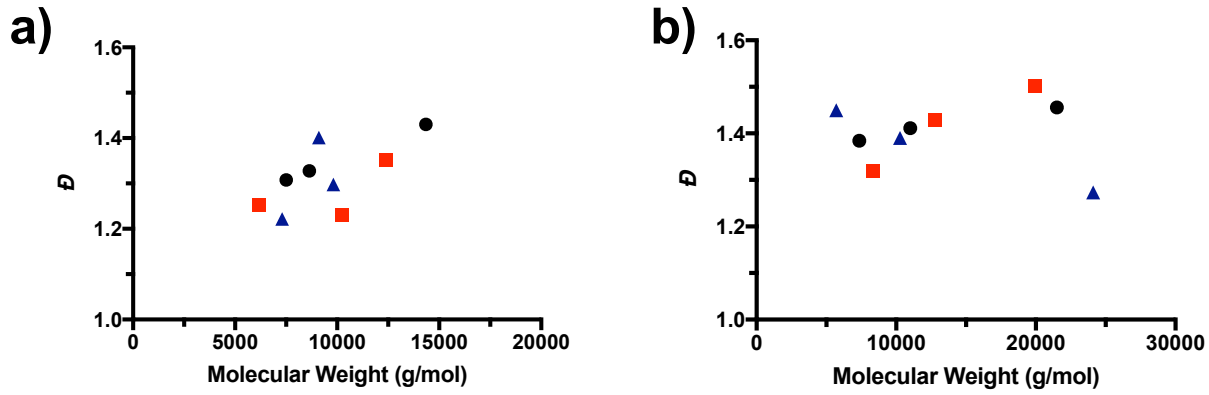

Figure 3.3. Polymer dispersity of (a) linear and (b) 4-armed star polymer systems.

Antimicrobial Activity

Next, we sought to investigate the relationship between polymer structure and antimicrobial efficacy. The antimicrobial activity of the polymers was quantified as the lowest

polymer concentration that completely inhibit bacterial growth, or the minimal inhibitory concentration (MIC), as the bacterial growth was determined by turbidity. The activity of polymers against Gram-negative *E. coli* and Gram-positive *S. aureus* were used as model bacterium. Gram-positive bacteria possess a thicker peptidoglycan cell wall as compared to Gram-negative bacteria, while Gram-negative bacteria possess two (cytoplasmic and outer) membranes. These differences in the membrane structure can give rise to different behavior of membrane-active membranes, because the polymers need to penetrate these cell wall and membranes to reach the cytoplasmic membranes to exert antimicrobial effects.

Effect of Polymer Composition

Cationic/hydrophobic ratio has been a way for previous designs of amphiphilic random copolymers to control antimicrobial efficacy. Increasing hydrophobic ratio increases antimicrobial activity[70, 172-173], as the hydrophobic segments inserts into the bacterial membrane to cause disruption and consequential cellular death. Against *E. coli*, increasing EMA content in linear and 4-armed polymers resulted in reduced MICs . For example, P_L1 (100% AEMA-0% EMA) had an MIC of >1000 μg/mL, which reduced to 63 μg/mL in P_L4 (70% AEMA-30% EMA), and further to 16 μg/mL in P_L7 (50% AEMA-50% EMA) (Figure 3.4a). The same behavior is evident in P_S10 (>1000 μg/mL), P_S 13 (63 μg/mL), and P_S 16 (16 μg/mL) (Figure 3.4a). Against *S. aureus*, increased EMA content slightly increased MICs in both linear and 4-armed polymers. P_L2 had a MIC of 63 μg/mL which increased to 125 μg/mL P_L5 and P_L7 (Figure 3.4b). P_S11 had an MIC of 63 μg/mL which increased to 250 μg/mL in P_S17 (Figure 3.4b). *S. aureus* has previously been reported to be sensitive to cationic charge density in copolymers, as opposed to hydrophobic content, which is supported in this study.

Table 3.4. Antimicrobial activity of linear and star-shaped polymers as measured by MIC against *E. coli* and *S. aureus*.

	MIC (μg/mL)	
	E. coli	***S. aureus***
P_L1	>1000	63
P_L2	250	63
P_L3	250	83 (±36)
P_L4	63	125
P_L5	63	125
P_L6	52 (±18)	83 (±36)
P_L7	16	125
P_L8	16	125
P_L9	16	208 (±72)
P_S10	>1000	63
P_S11	>1000	63
P_S12	>1000	63
P_S13	63	63
P_S14	31	104 (±36)
P_S15	31	104 (±36)
P_S16	16	250
P_S17	16	250
P_S18	16	250

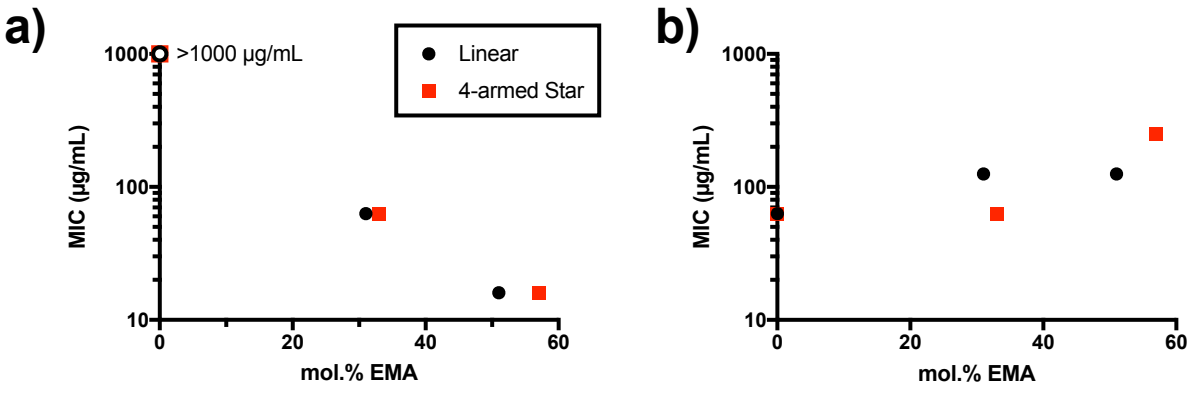

Figure 3.4. Hydrophobic content effect on antimicrobial activity of linear and 4-armed star methacrylate random copolymers (target DP 20) against (a) *E. coli* and b) *S. aureus*. Data points and error bars represent the average and s.d. from data in three independent experiments (n=3).

Effect of Polymer Size

Polymer size (i.e. degree of polymerization, molecular weight) has been previously shown to be an important factor in antimicrobial activity. Specifically, high molecular weight polymers have been shown to increase antimicrobial efficacy as compared to lower molecular weight polymers of similar composition, due to an increase in the total number of biologically active groups.[69] In linear methacrylate random copolymers in the range of 6,000-12,400 g/mol, molecular weight did not significantly alter MIC behavior. This can be seen in P_L4 (6,153 g/mol) had an MIC of 63 μg/mL as compared to P_L6 (12,386 g/mol) which had an MIC of 52 (±18) (Figure 3.5a). In cationic homopolymer, there was a decrease in MIC from >1000 μg/mL in P_L1 (7,500 g/mol) to 250 μg/mL in P_L2 (8,642 g/mol) and P_L3 (14,349 g/mol) (Table 3.4). Polymers with 4-armed structure exhibited a decrease in MIC with increasing molecular weight, such as in the case of P_S13 (8,344 g/mol) with an MIC of 63 μg/mL to P_S15 (19,972 g/mol) with an MIC of 31 μg/mL. These results indicate that increasing the number of active groups through increased molecular weight can help improve antimicrobial efficacy, though this approach appears minimally effective within the molecular weight ranges of 5,000-20,000 g/mol, which a maximum decrease of 1/2 MIC concentration.

Polymer dispersity may also be a factor for consideration in antimicrobial activity, as it is related to molecular weight. While AMPs are monodispersed, polymer systems are the cumulative effect of polymers of a range of molecular weights on bacterial membranes. In linear polymers, within the range of $Đ$ = 1.25-1.35, dispersity did not alter MIC values. This can be seen in P_L4 ($Đ$ = 1.25) had an MIC of 63 μg/mL as compared to P_L6 ($Đ$ = 1.35) which had an MIC of 52 (±18) (Figure 3.5b). In the case of 4-armed polymers, greater dispersity decreased

MICs. P_S13 ($Đ$ =1.32) had an MIC of 63 µg/mL which decreased in P_S15 ($Đ$ =1.5) to a MIC of 31 µg/mL (Figure 3.5b). It is interesting to note that polymers with greater dispersity (P_S15, P_S14) also had higher molecular weights. However, polymers with low molecular weight with high dispersity, such as P_S16 (5,713 g/mol, $Đ$ =1.45) have similar activity to high molecular weight polymers with low dispersity, such as P_S18 (24,111 g/mol, $Đ$ =1.27). Akin to the previous discussion, while in some cases dispersity did increase antimicrobial activity, it was only increased by a factor of 2 (MIC).

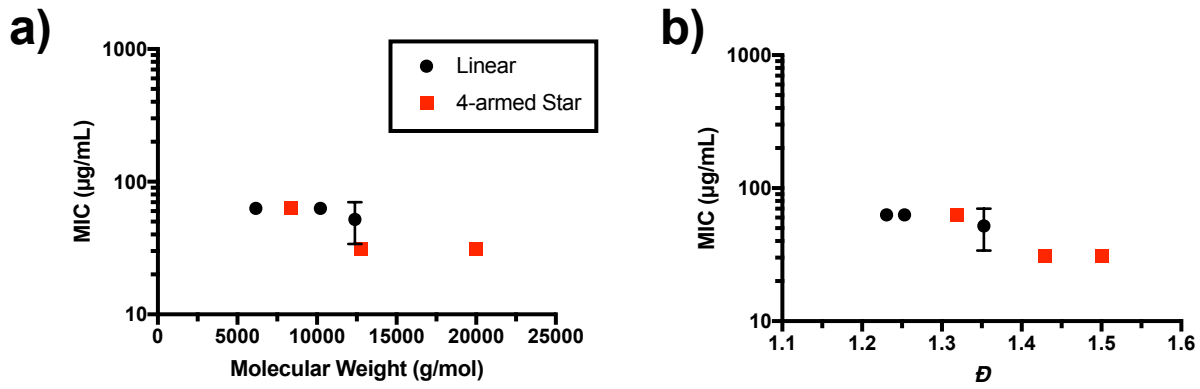

Figure 3.5. Effect of polymer size and dispersity on antimicrobial activity against *E. coli* of methacrylate random copolymers (70% AEMA-30% EMA) against *E. coli* as a factor of (a) molecular weight by ^{1}H NMR and (b) polymer dispersity. Data points and error bars represent the average and s.d. from data in three independent experiments (n=3).

Effect of 4-armed vs Linear Architecture

The purpose of this study was to examine the antimicrobial efficacy of 4-armed polymers compared to linear polymers, with the goal of improving antimicrobial efficacy due to a collective action of multiple polymer chains on the bacterial membrane. The theory of this study is that 4-armed architecture can mimic the collection of multiple polymer chains (i.e. 4) Therefore, it is necessary to compare 4-armed polymers with arm lengths equal to the total DP of linear polymers. The best comparison of antimicrobial activity can be seen in the case of

polymers designed at 70% AEMA-30% EMA, which demonstrates moderate antimicrobial activity.P_S15 has a total DP of 98, where each arm has a DP of 24.5, with a composition of 68% AEMA-32% EMA (Table 3.2, Table 3.3). There P_S15 is a representation of the collection of 4 polymers of DP 24.5. P_L4, with a DP of 30 and a composition of 69% AEMA-31% EMA, is therefore an appropriate linear analog to discuss the impact of 4-armed architecture (Table 3.2, Table 3.3). P_S15 has an MIC of 31 µg/mL, compared to P_L4 with an MIC of 63 µg/mL against *E. coli* (Table 3.4). This increase in the activity is not significant considering that the MIC values were determined by 2-fold dilution. This indicates that the collection of multiple polymer chains into a macromolecule has no have any significant enhancement in their antimicrobial efficacy against *E. coli* compared to the linear polymer. In polymers with 100% AEMA composition, 4-armed architecture does not affect MIC, such as in P_L1 (DP 32) and P_S12 (total DP 91, arm DP 22.8) which both have an MIC of >1000 µg/mL against *E. coli* (Table 3.4). Polymers with 50% AEMA-50% EMA composition have an increased MIC against *S. aureus* in 4-armed polymers, where P_S18 (DP 133, arm DP 33.3) has an MIC of 250 µg/mL compared to P_L7 (DP 41) with an MIC of 125 µg/mL. (Table 3.4). However, the efficacy against *E. coli* is unaffected, where P_S18 and P_L7 both have an MIC of 16 µg/mL (Table 3.4). For the activity of polymers against *S. aureus*, in similar to *E. coli*, these star-shaped polymers and linear analogues did not show any significant difference in the MIC values. These results suggest that the 4-arm star-shaped structure does not improve the activity of polymers.

To further examine the effect of 4-armed architecture on their antimicrobial activity, , we compared the antimicrobial activity of linear and 4-armed polymers of comparable total DPs and molecular weight. If the MIC of these polymers is same, the antimicrobial activity of

polymers is determined by the polymer size, but not the shape. Within the composition of 70% AEMA-30% EMA, P_L6 (12,385 g/mol) and P_S14 (12,763 g/mol) have the similar molecular weights (Table 3.3). P_S14 has a lower MIC of 31 μg/mL as compared to P_L6 which has an MIC of 63 μg/mL against *E. coli* (Table 3.4). The increase in the activity is not significant. P_L8 (9,814 g/mol) and P_S17 (10,275 g/mol) which have similar molecular weights and compositions of 50% AEMA-50% EMA (Table 3.2, Table 3.3), have MICs of 16 μg/mL against *E. coli* (Table 3.4). For the activity of polymers against *S. aureus*, the star-shaped and linear copolymers did not show any difference in their activity. These results indicate that 4-armed star and linear architectures do not significantly affect the antimicrobial activity of polymers.

Hemolytic Activity

To investigate mammalian cell toxicity, the lysis of human red blood cells (hemolysis) by methacrylate polymers was assessed and quantified as the polymer concentration to induce 50% hemoglobin release (HC_{50}). For polymers which concentrations ≤1000 μg/mL did not achieve 50% hemolysis, the %hemolysis at 1000 μg/mL was recorded (Table 3.5).

Effect of Polymer Composition

Non-specific hydrophobic interactions with mammalian cells has been a major challenge for amphiphilic antimicrobial polymers. Therefore, selecting polymer compositions that balance cationic and hydrophobic functionalities is critical to achieve both potent antimicrobial activity and low mammalian cell toxicity. In both linear and 4-armed polymers, as EMA content increases, HC_{50} values decrease (Table 3.5), indicating greater toxicity with increasing hydrophobic content. P_L2 had a HC_{50} value of >1000 μg/mL, which decreased to 414 (±16)

μg/mL in P_L5 (70% AEMA-30% EMA), and further decreased to 4.5 (±0.4) μg/mL in P_L8 (50% AEMA-50% EMA) (Figure 3.6). In 4-armed polymers, P_B11 had HC_{50} value of >1000 μg/mL, which decreased to 2.8 (±0.4) μg/mL in P_B14 (70% AEMA-30% EMA) and maintained comparable HC_{50} value of 3.1 (±0.2) μg/mL in P_B17 (Figure 3.6). This behavior may indicate a hydrophobic toxicity saturation in 4-armed polymers at 30% EMA. Linear polymers with compositions of 70% AEMA-30% EMA demonstrate the best selectivity towards bacterial cells, specifically P_L5 with a SI of 6.57 (Table 3.5). However, 4-armed polymers have comparably low selectivity ratios in both 30% EMA and 50% EMA compositions, due to the highly hemolytic nature of these polymers. P_B18 demonstrate the best selectivity with an SI of 0.26 (Table 3.5), which as the SI <1, does not indicate selective behavior.

Table 3.5. Hemolytic activity and selectivity of linear and 4-armed methacylrate copolymers.

	HC_{50} (μg/mL)	%Hemolysis at 1000 μg/mL	Selectivity Index (SI) (HC_{50}/MIC *E. coli*)
P_L1	>1000	46 (±5)	No HC_{50}/No MIC
P_L2	>1000	29 (±6)	No HC_{50}
P_L3	>1000	44 (±7)	No HC_{50}
P_L4	369 (±56)		5.86
P_L5	414 (±16)		6.57
P_L6	71 (±23)		1.37
P_L7	6.9 (±0.5)		0.43
P_L8	4.5 (±0.4)		0.28
P_L9	2.9 (±0.2)		0.18
P_S10	>1000	15 (±2)	No HC_{50}/No MIC
P_S11	>1000	43 (±6)	No HC_{50}/No MIC
P_S12	551 (±18)		No MIC
P_S13	10 (±2)		0.16
P_S14	2.8 (±0.4)		0.09
P_S15	3.6 (±0.9)		0.12
P_S16	2.7 (±0.1)		0.17
P_S17	3.1 (±0.2)		0.19
P_S18	4.2 (±0.6)		0.26

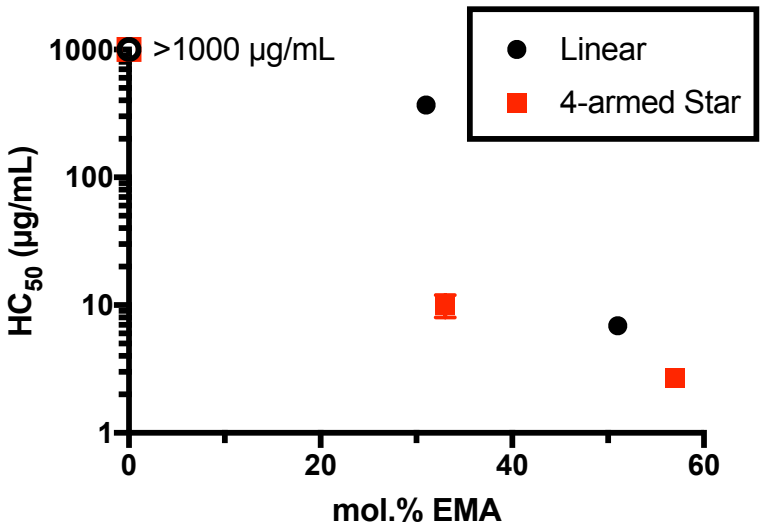

Figure 3.6. Hydrophobic content effect on RBC toxicity of methacrylate random copolymers. Data points and error bars represent the average and s.d. from data in three independent experiments (n=3).

Effect of Polymer Size

Molecular weight has been previously reported to affect hemolytic behavior, specifically where high molecular weight polymers have high hemolytic activity. [69] Linear polymers between 5,000-10,000 g/mol had similar hemolytic activity, as in the case of P_L4 (6,153 g/mol) with an HC_{50} of 369 (±51) μg/mL and P_L5 (10,222 g/mol) with an HC_{50} of 414 (±16) μg/mL (Figure 3.7a). Increasing molecular weight beyond 10,000 g/mol resulted in decreased HC_{50}, such as in P_L6 (12,386 g/mol) decreasing to 71 (±23) μg/mL (Figure 3.7a). 4-armed polymers also had a decrease in HC_{50} with increasing molecular weight, where P_S13 (8,344 g/mol) had an HC_{50} of 10 (±2) μg/mL which decreased to 2.8 (±0.4) μg/mL in P_S14 (12,763 g/mol) (Figure 3.7a). Alternatively, polymer dispersity may also contribute to hemolytic activity, because more disperse systems may contain only a small fraction of high molecular weight polymers that could significantly contribute to RBC membrane disruption. Indeed, as dispersity increases in linear polymers, HC_{50} decreases, such as in the case of P_L5 ($Đ$ = 1.23) at 414 (±16) μg/mL and P_L6 ($Đ$ = 1.35) at 71 (±23) μg/mL. Increasing dispersity also contributes to hemolytic activity in 4-armed polymers, where HC_{50} values decreased from 10 (±2) μg/mL in P_S13 to 2.8 (0.4) μg/mL in P_S14. Dispersity beyond 1.4 does not appear to significantly impact hemolytic activity, as seen in P_S15.

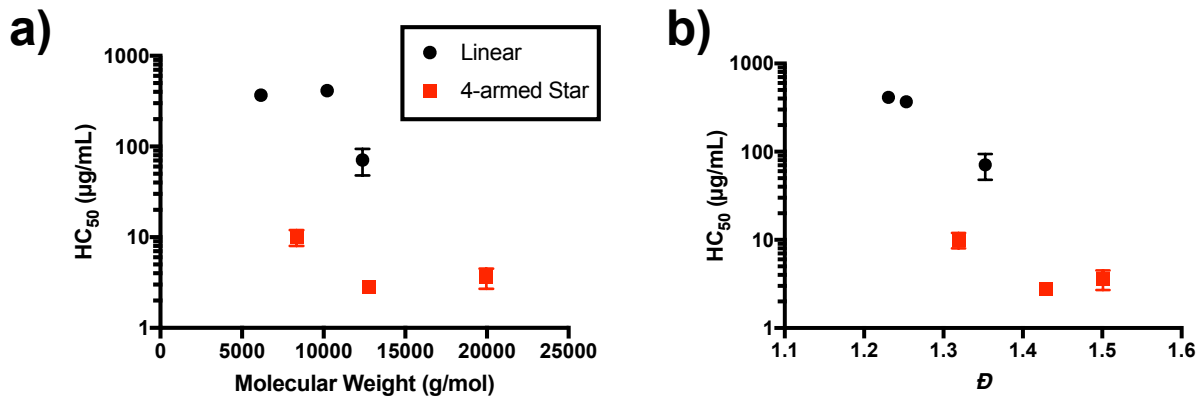

Figure 3.7. Effect of polymer size on RBC toxicity: (a) HC_{50} dependence on molecular weight determined by ^1H NMR and (b) HC_{50} dependence on dispersity. Data points and error bars represent the average and s.d. from data in three independent experiments (n=3).

Effect of 4-armed vs Linear Architecture

While the goal of this study was to utilize 4-armed polymers to enhance antimicrobial activity as compared to linear polymers, the same collective chain mechanism which we proposed to act against bacterial membranes may also act against mammalian cell membranes. Therefore, it is necessary to compare 4-armed star polymers with comparable arm DPs to linear DPs to assess the collective action of multiple chains working together in a macromolecule. P_L4 (DP=30) has an HC_{50} of 369 (±56) µg/mL (Table 3.5). However, P_S15 with arm DP = 24.5, which is close to P_L4, has an HC_{50} of 3.6 (±0.9) (Table 3.5), indicating significant enhancement in hemolytic activity. This enhancement of hemolytic activity by 4-armed architecture is apparent in all polymer compositions. P_L1 (DP = 32) has an HC_{50} of >1000 µg/mL, which his reduced to 551 (±18) µg/mL in P_S12 (arm DP = 22.8), and P_L7 (DP = 41) has an HC_{50} of 6.9 (±0.5) µg/mL which is reduced to 4.2 (±0.6) µg/mL in P_S18 (arm DP = 33.3 (Table 3.5)). This increased in hemolytic activity causes decreased selectivity ratios. For example, P_L4 has a selectivity of 5.86,

which is reduced to 0.12 in P_S15 (Table 3.5). This suggests that 4-armed architecture is responsible for decreasing selectivity of polymers towards bacteria over mammalian cells.

To verify that this effect was due to differences in polymer architecture and not differences in polymer size, polymers with comparable total DPs and molecular weights were compared. For example, P_L6 has a molecular weight of 12,385 g/mol (D= 1.35) compared to P_S14 with a molecular weight of 12,763 (D=1.43) (Table 3.5). However, P_L6 has a HC_{50} of 71 ($\pm$23) μg/mL, compared to P_S14 with a 2.8 ($\pm$0.4) μg/mL HC_{50} (Table 3.5). This trend is also apparent in P_L8 (9,814 g/mol) and P_S17 (10,275 g/mol), where P_L8 has a HC_{50} of 4.5 ($\pm$0.4) μg/mL and P_S17 has an HC_{50} of 3.1 ($\pm$0.2) μg/mL. These results indicate that the increase in hemolytic behavior is not the result of increased molecular weight, but rather suggests that a macromolecule containing multiple polymer chains disrupts mammalian cell membranes more effectively than individual linear polymers of comparable properties (i.e. composition, size).

Discussion: Membrane Sensitivity to 4-Armed Polymers

In this study, we sought to improve antimicrobial properties of amphiphilic copolymers through 4-armed architecture that may mimic the collective activity of multiple polymers attached to a bacterial membrane. Additionally, we hypothesized that higher density of cationic charge on 4-armed polymers would result in improved selectivity. In this study, we saw a slight increase in antimicrobial efficacy in 4-armed polymers as compared to linear polymers, suggesting that 4-armed structure can simulate the effect of multiple polymers accumulated on the membrane surface necessary for disruption. However, we also found that 4-armed polymers were significantly more hemolytic than linear polymers, and less selective than linear polymers. This hemolytic activity was observed in polymers of comparable composition,

molecular weight and dispersity, which suggests that the differences in hemolytic activity is the result of architecture. Therefore, the result suggests that 4-armed star-shaped polymer structure is not effective in improving the antimicrobial activity and selectivity. Previous research on antimicrobial peptides has proposed that pore formation in membranes needs 4-11 polymers to occur,[166-167] where peptide chains are supposed to aligned in the pore structure. From our results, 4 polymer chains may not be sufficient to form pores in bacterial membranes. Further studies that explore the use of polymers with more arms and different design of polymer structures would be useful in improving the activity of polymers.

Conclusions

In summary, amphiphilic primary ammonium copolymers composed of cationic 2-aminoethyl methacrylate (AEMA) and ethyl methacrylate (EMA) were synthesized by ATRP with linear or 4-armed initiators and evaluated for their antimicrobial and hemotoxic activity. Antimicrobial activity was a factor of polymer composition, size, and architecture (4-armed vs linear). Specifically, polymers with 4-armed architecture had decreased MICs by comparison to linear polymers against *E. coli*. However, 4-armed polymers were significantly more hemolytic than linear polymers of comparable designs, and therefore had reduced selectivity towards bacterial cells over mammalian cells. Further studies are necessary to evaluate this proposed mechanism but may provide useful experimental insight into the number of polymers necessary for bacterial membrane pore formation, and a new way to control amphiphilic polymer selectivity. While this study indicates that linear polymers are preferable design to 4-armed polymers due to their hemolytic activity, the increase of antimicrobial activity by 4-armed

architecture does prove multi-armed polymers could provide a new tunable parameter for polymer design if mammalian cell toxicity is overcome.

Chapter 4 Solution-Mediated Modulation of Bacterial Biofilm Formation by Synthetic Polymers

Introduction

Synthetic surfaces of medical devices and implants are susceptible to microbial colonization and biofilm formation[177-181], which contribute to at least 60% of healthcare-acquired infections.[182] Biofilms are difficult to treat by antibiotics, due to reduced metabolic activity and poor antibiotic penetration, which can also results in sub-lethal exposure and contribute to resistance development.[26, 183] Additionally, biofilms are physically robust, and difficult to remove mechanically. Specifically, *Pseudomonas aeruginosa* frequently develops into biofilms and consequently chronic infections of the respiratory system, especially in immunocompromised patients.[184-186] The prevention of biofilm formation is a primary challenge in modern biomaterials science in order to prevent chronic infections. It is therefore critically important to better understand the factors that govern biofilm formation and growth in order to create effective solutions to biofilm colonization.

The long-term goal of this study is to develop a new effective method to address the challenge of *P. aeruginosa* biofilm-associated infections. The main-stream approach in the general area of anti-biofilm materials is to modify device surfaces with antibacterial or anti-fouling polymers, which kill bacteria on contact or effectively repel them.[111-116, 119-121] However, while some recent approaches show promising results, it has been long-term scientific and

technical challenges to generate surface materials that can inherently overcome the sophisticated biological adhesion mechanisms of bacteria as well as meet requirements for use in products in terms of efficacy and manufacturing. In practice, once exposed to physiological conditions, modified surfaces suffer from a short lifetime due to protein and cell accumulations, while regenerative surfaces are of recent interest in the field.[122-123] In addition, most approaches require surface chemistries on existing products, which are generally chemically inert, and some products are not tolerant to chemical exposures. These problems lead us to explore a new bacterial target and an alternative approach to regulate biofilm formation. To that end, we hypothesize that the surface properties of planktonic bacteria in solution can be targeted to modulate bacterial aggregation/adhesion and thus prevent biofilm formation. Traditionally, polymers have been modified by multiple ligands that bind to bacterial cell surfaces, which block adhesion of bacteria to host cell ligands.[187-189] Instead, *what if bacterial surfaces were modified by adhesion of polymers to change their physicochemical and/or solution properties such that the bacteria cannot effectively attach on material surfaces?*

In academic research and industrial settings, many applications of polymers have been reported for their physical and biological efficacies through the direct interactions between polymers and bacteria. For example, the bacterial surface modification by cationic polymers and subsequent aggregate formation or flocculation have been utilized to separate bacteria from solution for water purification and bioreactors.[190-192] These polymers exploit the electrostatic interaction with negatively charged bacterial cell surfaces, which causes surface neutralization of bacterial surfaces, electrostatic patching and polymer bridging of bacterial cells, resulting in macroscopic aggregates or precipitates.[193-195] However, it remains unclear if

such polymer-induced aggregates favor the formation of mature biofilms or rather prevent it, while it may be intuitive that they may pre-set bacterial assembly for mature biofilm structures. Similarly, previous studies used cationic polymers as a bacteria sequestrant, which causes clustering of bacteria in solution, triggering quorum sensing cell-cell communications.[196-197] While these studies elegantly demonstrate translation of polymer-mediated cell clustering to biological response of bacteria, it is not clear if bacteria clusters in solution would contribute to biofilm formation or not.[155] There is a gap in our knowledge on how the polymer-bacteria interactions modulate biofilm formation. Such knowledge is critical to design and develop new anti-biofilm materials.

The mechanism of biofilm formation consists of several stages, including bacterial attachment to the surface, micro-colony formation, the production of extracellular matrix, and ultimately the formation of a mature biofilm.[198-199] The biofilm formation is orchestrated between bacteria on surfaces, involving changes in gene expression, spatial arrangement of bacteria and extracellular biopolymers, cell-cell communications, and timings of these events.[200] This natural mechanism of biofilm formation has been evolutionarily optimized to construct robust biofilms. This led us to hypothesize that disrupting the natural behavior of planktonic bacteria may cause sub-optimal changes in the biofilm development process, leading to decreased biofilm accumulation.

In this study, we take a step forward to understanding the polymer-bacteria interactions that govern biofilm formation toward the development of anti-biofilm polymers that exploit such interactions as our long-term goal. Specifically, because of its use in many applications already, this study is a first and important step to understand how cationic polymers induce

bacterial aggregates in solution and how the aggregates contribute to biofilm formation or prevention. Particularly, the purpose of this study is to provide foundational knowledge to guide future anti-biofilm approaches rather than elucidating the molecular mechanism of biofilm formation. P*seudomonas aeruginosa* PAO1 was chosen as a model bacterium for this study because of its nature as an opportunistic pathogen, which frequently develop into biofilms and consequently chronic infections.[184] We propose that cationic polymers used in this study result in concentration dependent suppression of biofilm development by planktonic bacteria sequestration.

Methods

Materials

Tryptic Soy broth (TSB, Thermo Scientific Oxoid™), Mueller Hinton broth (MHB, BD and Company ©), and phosphate buffered saline (PBS, pH=7.4, Gibco®) were prepared according to manufacturer instructions and autoclave sterilized prior to use. SYTO 9 and propidium iodide (PI) nucleic acid stains (Molecular Probes, OR) were used as prescribed by the product manual at 1.5 µL/mL. Crystal violet (Sigma-Aldrich) was diluted in Millipore water to a working concentration of 0.01% (wt/vol). MTT (3-(4,5-dimethylthiazol-2-yl)-2,5-diphenyltetrazolilum bromide, Thermo Scientific) was diluted in Millipore water to working concentration of 0.3% (wt/vol).

Polyethylene glycol (PEG, average M_n = 6,000 g/mol) and polyethylenimine (branched, M_n= ~60,000 g/mol by GPC) were used as received from Acros Organics™. Poly[(3-methacryloylamino)propyl] trimethylammonium chloride (P-1) and poly(2-acrylamido-2-

methylpropane sulfonic acid) (P-2) were synthesized by RAFT polymerization using a modified literature procedure2 and characterized by ^{1}H NMR and GPC (Appendix C). Stock solutions were prepared at 10 mg/mL in 0.01 % acetic acid). Further P-1 stock solutions were prepared by ten-fold dilutions in PBS (1000, 100, 10 µg/mL).

Pseudomonas aeruginosa (*P. aeruginosa*) PAO1 was received from Dr. Chuanwu Xi (Environmental Health Science, University of Michigan). *P. aeruginosa* cultures were prepared by suspension of a bacteria colony in TSB, collected from agar plate (<5 days old). Cultures were grown overnight (18 hours) at 37 °C at 180 rpm. Further preparations are as noted in subsequent methods.

Antimicrobial Activity: MIC Assay

The minimum inhibitory concentration (MIC) of polymers against *P. aeruginosa* (PAO1) was determined in a standard microbroth dilution assay according to the Clinical and Laboratory Standards Institute guidelines with suggested modifications by R. E.W Hancock Laboratory (University of British Columbia, British Columbia, Canada)[169] and Giacometti et al.[170] *P. aeruginosa* was grown overnight (~18 hours) in TSB at 37 °C with orbital shaking (180 rpm), and used as an inoculum by diluting overnight culture in TSB to a concentration of OD_{600}=0.1. The inoculated solution was then grown at 37 °C to the exponential phase (OD_{600}= 0.5-0.7, 2 hours). Final dilution to OD_{600}= 0.001, ~4 x 10^6 CFU/mL, was made with TSB. Bacterial suspension (OD_{600}= 0.001, 90 µL/well) was transferred to a 96-well sterile round-bottom polypropylene plate. Polymers were dissolved in 0.01% acetic acid to achieve stock concentrations of 20 mg/mL. Serial 2-fold dilutions of polymers were prepared from stock solutions in PBS and transferred to the 96-well sterile round-bottom polypropylene plate for a

final concentration of 7.8-1,000 μg/mL (10 μL/well). PBS was used as a solvent control in place of polymer. Plates were sealed with parafilm and incubated for 18 hours at 37 °C without shaking. MIC was defined as the lowest concentration of polymers to completely inhibit bacterial growth, as indicated by lack visual of turbidity. Assays were repeated a minimum of three times in triplicate on different days.

Growth Curve Assay

The effect of polymers on *P. aeruginosa* growth was assessed by optical density (OD_{600}). Disposable polystyrene cuvettes were sterilized by soaking in 70% EtOH solution for 1 hour and air dried. *P. aeruginosa* overnight cultures were diluted in TSB to desired concentration of OD_{600}= 0.001. A solution of bacterial suspension (OD_{600}= 0.001, 900 μL) and stock polymer (PEG, P-1 or P-2, 100 μL) was prepared in cuvettes, and cuvettes secured with parafilm to prevent contamination. Final polymer concentrations were 1,000 μg/mL or 100 μg/mL after dilution in the bacteria suspension. Solutions were incubated at 37 °C with shaking (180 rpm) except when removed for time of measurement. The optical density (OD_{600}) of dispersions were measured by optical density using a visible diode array spectrophotometer (WPA S800 Spectrawave, Biochrom). Measurements were taken at 2 and 4 hours, and then once an hour through 10 hours, and a final point taken at 18 hours. Triplicate measurements were carried out on separate days.

Flocculation Assay

The effect of polymers on bacteria aggregation and/or flocculation was assessed by optical density (OD_{600}). Disposable polystyrene cuvettes were sterilized by soaking in 70% EtOH

solution for 1 hour and air dried. *P. aeruginosa* overnight cultures were diluted in TSB to desired concentration of OD_{600}= 0.001. A solution of bacterial suspension (OD_{600}= 0.001, 900 µL) and stock polymer (PEG, P-1, P-2, or PEI 100 µL) was prepared in cuvettes, and cuvettes secured with parafilm to prevent contamination. Final polymer concentrations were 1,000 µg/mL or 100 µg/mL after dilution in the bacteria suspension. In contrast to growth curve assays, bacterial suspensions were kept at room temperature in the absence of stirring, to allow for bacteria to aggregate and precipitate in the absence of external forces. The optical density (OD_{600}) of dispersions were measured by optical density using a visible diode array spectrophotometer (WPA S800 Spectrawave, Biochrom). Measurements were taken at 0, 5 10 minutes, and subsequently every 10 minutes for the first hour, and every 20 minutes during the second hour. To prevent agitation of the bacterial suspension, cuvettes remained in the spectrophotometer for the entirety of the measurement time. Triplicate measurements were carried out on separate days.

Bacterial Aggregate Observation: Confocal Microscopy

P. aeruginosa overnight cultures were diluted in TSB to desired concentration of OD_{600}=1.0. Bacteria suspensions (OD_{600}= 1.0, 900 µL) were combined with stock polymer solutions or PBS (100 µL) to achieve final polymer concentrations (1,000-1 µg/mL) in an Eppendorf tube. SYTO 9 (1.5 µL) was added and incubated with suspensions for 15 minutes at room temperature in the absence of light without shaking, simultaneously allowing time for polymer-bacteria interaction. An aliquot (5 µL) was collected from the bottom of Eppendorf tube and deposited on glass microscope slides and covered with glass coverslips, with the

manual removal of air bubbles. Bacteria was examined by inverted confocal microscope using a 60x oil objective (Eclipse Ti-U, Nikon).

Bacterial Attachment: Confocal Microscopy

P. aeruginosa overnight cultures were diluted in TSB to desired concentration of OD_{600}= 0.001. Bacterial suspensions (OD_{600}= 0.001, 2.7 mL) were combined with stock polymer solutions or PBS (0.3 mL) to achieve final polymer concentrations (1,000-1 μg/mL). The prepared bacteria-polymer solutions were transferred to a clear cell culture dish (FD35-100, Fluorodish™) with glass window diameter of 23.5 mm, sealed with parafilm, and incubated for 15 minutes at 37 °C in the absence of shaking. Following incubation, the culture medium was carefully removed from the wells by micropipette to avoid disrupting attached cells. Wells were washed twice with an excess volume of PBS. Bacterial cells were stained by SYTO 9 (3.34 mM) in 0.85% NaCl solution for 15 minutes at room temperature in the absence of light without shaking. SYTO 9 solution was then removed by micropipette and cells washed once with 0.85% NaCl solution. Bacterial cells were examined by inverted confocal microscope (Eclipse Ti-U, Nikon) using a 60x oil objective.

Bacterial Formation Over Time: Confocal Microscopy

P. aeruginosa overnight cultures were diluted in TSB to desired concentration of OD_{600}= 0.001. Bacterial suspensions (OD_{600}= 0.001, 2.7 mL) were combined with stock polymer solutions (10,000-10 μg/mL, 0.3 mL) or PBS (0.3 mL) to achieve desired polymer concentrations (1,000-1 μg/mL). The prepared bacteria-polymer solutions were transferred to a clear cell culture dish (FD35-100, Fluorodish™) with glass window diameter of 23.5 mm, sealed with

parafilm, and incubated for 4 hours at 37 °C in the absence of stirring. Following incubation, the culture medium was carefully removed from the wells by micropipette to avoid disrupting biofilms. Wells were washed twice with an excess of PBS. Biofilms were stained by SYTO 9 (3.34 mM) and/or propidium iodide (20 mM) in 0.85% NaCl solution for 20 minutes at room temperature in the absence of light without shaking. SYTO 9-PI solution was then removed by micropipette and biofilms washed once with 0.85% NaCl solution. Biofilms were examined by inverted confocal microscope (Eclipse Ti-U, Nikon) using a 60x oil objective at of 2, 4, 8 and 24 hours.

Biofilm Formation and Polymer Exposure for Total Biomass, Direct Enumeration and Metabolic Activity

Biofilm growth was performed with modifications to previous literature methods.[201-202] 12 mm diameter borosilicate glass coverslips (Fisherbrand™) were sterilized in 70 vol% ethanol for a minimum of 1 hour and allowed to air dry. A thin strip of label tape was placed on the bottom wells of a sterile 12-well polystyrene plates (Corning® Costar®) to facilitate coverslip retrieval, and the plate sprayed with 70 vol% ethanol and allowed to dry completely. Coverslips were placed 1 per well, with the entire coverslip being flush with the well bottom. *P. aeruginosa* overnight cultures were diluted in TSB to desired concentration of OD_{600}= 0.001 Bacteria solution (900 µL) was added to each well to fully immerse the coverslip. Polymer stock solutions or PBS (100 µL) were then added to wells to achieve desired polymer concentrations (1,000-1 µg/mL). TSB with PBS (100 µL) was also assayed along with the test samples to confirm no bacterial contamination. Plates were wrapped in parafilm and incubated for 24 hours at 37 °C in the absence of shaking.

Evaluation of Total Biomass by Crystal Violet

Biofilms were generated as described in the previous section. Following incubation, the supernatant was removed from the wells by micropipette. Wells were washed twice with excess PBS. Crystal violet (CV, 0.01%, 1000 µL) solution was introduced to wells by micropipette and used to stain the biofilm for 15 minutes at room temperature without shaking. CV was removed from the wells by micropipette, and wells were rinsed twice with PBS, and the solution discarded. In order to maintain a consistent biofilm area, coverslips (with adhered biofilms) were removed and transferred to a new sterile 12-well plate using forceps, by holding a coverslip edge carefully as to not disrupt the biofilm. Ethanol (100%, 1000 µL) was used to extract CV from the biofilms for 10 minutes at room temperature and the biofilm manually disrupted by micropipette agitation of the solution and scraping. An aliquot of the solution (200 µL) was transferred to 96-well round-bottom plate, which was centrifuged at 1000 rmp for 5 minutes in order to reduce the impact of cellular debris in solution. Aliquots (25 µL) of solution were then transferred to untreated, sterile polystyrene 96-well flat-bottom plate containing ethanol (75 µL) to create 1:4 solutions and the OD_{595} was obtained on a Varioskan Flash microplate reader (Thermo Fisher). Experiments were carried out in duplicate on three separate days. Daily averages were calculated from duplicates and used to determine a grand average and standard error of the mean (n=3).

Evaluation of Viable Bacteria by Direct Enumeration

Biofilms were generated as described in the previous section. Following incubation, the supernatant was removed from the wells by micropipette. Wells were washed twice with PBS (1000 µL), and the solution discarded. Washed coverslips (with adhered biofilms) were

removed and transferred to 15 mL conical tubes containing PBS (3 mL) using forceps, by holding a coverslip edge carefully as to not disrupt the biofilm. Coverslips in PBS were sonicated for 10 minutes to fully disrupt biofilms and dispersed bacteria in solution. 10-fold serial dilutions were performed in PBS, and an aliquot of samples (100 µL) was plated on TSB agar plates. The agar plates were incubated overnight (~18 hours) at 37 °C, and the number of viable colonies was counted. An appropriate dilution was selected from agar plate contained 30-300 colonies, the accepted range of countable colonies.[203] Experiments were carried out in duplicate on three separate days. Daily averages were calculated from duplicates and used to determine a grand average and standard error of the mean (n=3).

Evaluation of Metabolic Activity by MTT

Biofilms were generated as described in the previous section. Following incubation, the supernatant was removed from the wells by micropipette. Wells were washed twice with PBS (1000 µL), and the solution discarded. To each well, a premixed solution of PBS (750 µL) and 0.3% MMT (250 µL) were added and allowed to incubate for 2 hours at 37 °C in the absence of stirring. The solution was removed by micropipette and the wells washed with PBS, and the solution discarded. Washed coverslips were removed and transferred to a new 12-well plate using forceps, by holding a coverslip edge carefully as to not disrupt the biofilm. A solution of DMSO (750 µL) and glycine buffer solution (pH 10.5, 126 µL) was added to each well with coverslip and the biofilms manually disrupted by solution agitation and scraping and allowed to incubate at room temperature for 15 minutes. Aliquots (100 µL) of solution were then transferred to untreated, sterile polystyrene 96-well-plate containing ethanol (75 µL) to create 1:4 solutions and the OD_{570} was obtained on a Varioskan Flash microplate reader (Thermo

Fisher). Experiments were carried out in duplicate on three separate days. Daily averages were calculated from duplicates and used to determine a grand average and standard error of the mean (n=3).

Results

Polymer Design, Synthesis and Characterization

Cationic functionality on polymers have previously been utilized to facilitate electrostatic binding to anionic bacterial membrane. To test the hypothesis that cationic polymers are capable of modulating biofilm behavior through assembly disruption, model cationic polymer poly[(3-methacryloylamino)propyl] trimethylammonium chloride (P-1) was synthesized (Figure 4.1). P-1 design was chosen for this study because the quaternary ammonium groups provide permanent cationic charges, while some conventional cationic polymers such as poly(ethylene imine)s contain primary ammonium groups. In contrast to primary ammoniums, quaternary ammonium groups are pH-independent, which would minimize the effect of microenvironment pH in bacteria on the binding behavior of polymer chains onto the bacterial surface. As a control to assess the effects of a non-neutral polymer charge, poly(2-acrylamido-2-methylpropane sulfonic acid) (P-2) was synthesized, which contains sulfonate groups, which are negatively charged in a broad range of pH (Figure 4.1). Similar degrees of polymerization (~100) between P-1 and P-2 was selected to ensure comparable number of charges.

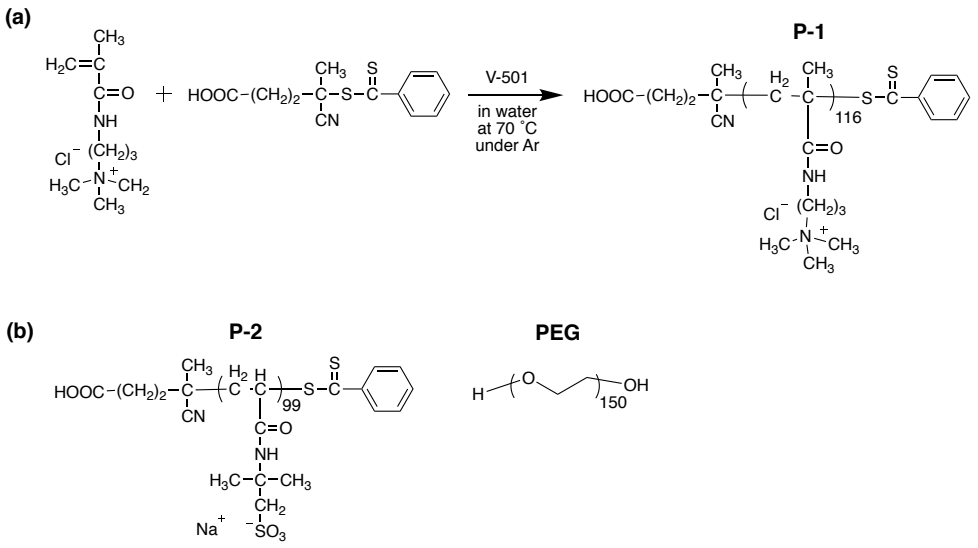

Figure 4.1. Synthesis scheme of (a) P-1 and (b) structures of P-2 and PEG.

P-1 and P-2 were synthesized by RAFT polymerization in order to achieve controlled molecular weight with narrow dispersity (Đ) (Figure 4.1). ^{1}H NMR analysis confirmed the polymerization and removal of residual monomers (Appendix C). The degree of polymerization (DP) was determined by comparing of integral intensity ratio of peaks from the chain transfer agents (P-1: *f*; P-2: *e*) to methylene and methyl in the polymer side-chains (P-1: *c+e*; P-2: *d*) (Table 4.1). The number-average molecular weight (M_n) was calculated using DP and molecular weights of monomer and RAFT agent. GPC was used to determine M_n, molecular weight (M_w), and *Đ*, which were compared to M_n determined by ^{1}H NMR. The molecular weights of these polymers are ~20,000 g/mol, which is relatively smaller than conventional polymers used as flocculants. Lower molecular weight polymers (~20,000 g/mol) were utilized as an initial model for this study to focus on the charge effects on bacterial aggregation and biofilm formation rather than the effect of polymer sizes and a combined effect with polymer bridging[204-205] in order to elucidate a simple rule in polymer-bacteria interactions for biofilm modulation.

Table 4.1. Polymer characterization of P-1 and P-2.

	DP	M_n (^{1}H NMR)	M_n (GPC)	M_w (GPC)	$Đ$
P-1	116	25,900	19,600	20,580	1.05
P-2	99	20,589	15,333	20,392	1.33

Planktonic Bacteria-Polymer Interactions and Consequences

Planktonic bacteria offer a favorable target for biofilm prevention. Once formed, biofilms are difficult to treat or remove, and thus prevention of biofilm formation from individual cells is highly desirable. Approaches that attempt to mitigate planktonic bacteria attachment through materials modification suffer both from short lifetimes, as well as limited applications to surfaces. Targeting planktonic bacteria offers the advantage that this approach is not reliant on a surface platform, and therefore could be applicable also to biotic surfaces such as biofilm related tissue infections. Additionally, the anionic surface of bacterial membranes is a universal target for a broad spectrum of bacteria. The interaction of planktonic bacteria with polymers, and their resulting consequences in solution, are hypothesized to affect the development of biofilms, as bacteria attachment is the first step to biofilm formation. Modulation of planktonic bacteria behavior could therefore effect biofilm development due to sub-optimal assembly.

Biostatic, Biocidal and/or Antimicrobial Effect of Polymers

Some cationic polymers have been reported to exert biocidal or biostatic behavior.[206-208] Biocidal behavior occur when bacteria are completely killed following exposure to material, while biostatic behavior occurs when bacterial growth is inhibited. Materials that eradicate only a portion of bacteria are considered biostatic. For the purposes of this chapter, antimicrobial activity will include both of these terms, where agents are biostatic at MIC concentration and

biocidal at higher concentrations. Typically, antimicrobial cationic polymers function act as biocidal agents through membrane disruption, where cationic segments adsorb onto the anionic bacteria surface and hydrophobic sections the polymer create catastrophic defects in the membrane which release essential cellular components and ions.

Bacterial Growth Curve

To determine if P-1 exhibited either biostatic or biocidal effects, the growth behavior of *P. aeruginosa* was observed during log phase growth by optical density (OD) at dilute (OD_{600}=0.001) concentrations in TSB nutrient broth at 37 °C with stirring. In dilute bacteria concentrations, high P-1 concentrations (1000 μg/mL) resulted in an increase in optical density during the first 4 hours but did not subsequently change growth behavior (Figure 4.2). The high OD value is likely due to flocculation ability of highly cationic polymers, which is a physical aggregation of bacteria in solution resulting in greater light scattering from large aggregates and was further explored subsequently. Lower concentrations of P-1 did not induce noticeable changes in OD and likewise did not affect bacterial proliferation (Figure 4.2). Neither P-2 or PEG exhibited any changes to the bacterial growth behavior (Figure 4.2), suggesting no biostatic or biocidal activity. After 18 hours of growth, the optical density of bacteria was ~2.5 for all polymers, indicating polymers had no effect on the maximum load of stationary phase bacteria.

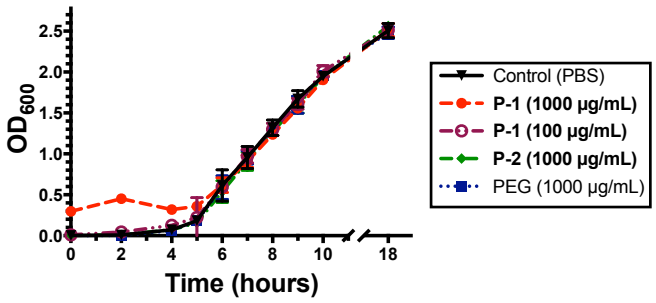

Figure 4.2. Effect of polymers on planktonic *P. aeruginosa* growth behavior in Tryptic Soy broth (TSB) with stirring in the presence of P-1, P-2 or PEG at 1000 µg/mL. The data points and error bars represent the average and standard deviation from three independent experiments (n = 3).

Minimum Inhibitory Concentration (MIC)

The antimicrobial activity of P-1 was determined using the standard protocol as the minimum inhibitory concentration (MIC)[169-170], which is the concentration of polymer necessary to inhibit growth of bacteria during long term incubation (~18 hours). The antimicrobial activity of polymers was evaluated against exponential phase *P. aeruginosa* (in TSB and MHB), as well as *E. coli* (in MHB) and *S. aureus* (in MHB), which are protocol standards. P-1, P-2 and PEG did not show any growth inhibition effect against *P. aeruginosa* in both TSB and MHB up to 1000 µg/mL, the highest concentration tested. The MICs against *E. coli* and *S. aureus* were likewise >1000 µg/mL for all polymers. This suggests that no polymers may not bind to bacterial membranes, such as in the case of P-2 due to charge repulsion, or binding does not result in membrane disruption, such as in the case of PEG or P-1. Antimicrobial activity is derived from hydrophobic groups disrupting the bacterial membrane. It is important to note that MIC reflects inhibition of bacterial growth, or bacteriostatic activity, as opposed to a measure of killing capacity, or bactericidal activity. However, presence of bacterial growth indicates lack of bacteriostatic or bactericidal effect.

Bacterial Aggregation and Flocculation

Charged polymers have been used to aggregate or flocculate charged molecules for applications such as waste water treatment or bioreactors.[190-192] Cationic polymers have been previously used to induce bacterial aggregation and flocculation by interacting with bacterial surfaces which have high net negative charge.[209] Electrostatic interactions between bacteria surfaces and polymers can result in surface neutralization, electrostatic patching and polymer bridging of bacterial cells, resulting in macroscopic aggregates or precipitates due to changes in repulsive and attractive forces.[193-195] Bacteria aggregation is a simple way to observe a change exerted on bacteria behavior by a material through changing only physical properties. Interestingly, bacteria aggregation has been linked to consequential biological signaling, in which cationic polymers have been used to trigger cell-cell communications through bacteria clustering.[196-197]

Bacterial Flocculation

Optical density was used to evaluate the aggregation of diluted stationary phase bacteria when exposed polymers with various charges, specifically P-1 (linear cationic) in comparison to PEI (branched cationic), which is a known flocculant, in addition to P-2 (anionic) and PEG (neutral). As compared to the bacterial growth curves presented in Figure 4.2, bacteria (OD_{600}=0.001) in TSB broth and polymers were combined and kept stationary at room temperature to allow bacteria to settle naturally. As aggregation is due to interactions between polymer chains and bacteria, changes in optical density were assessed at both dilute and concentrated bacteria suspensions, as behavior is likely dependent on the ratio of polymer chains to bacteria surfaces. At both dilute and high bacteria concentrations, PEI quickly and

effectively aggregates bacteria, evident by a sharp increase in OD, followed by a gradual reduction in OD as aggregates precipitate to the bottom of the solution (Figure 4.3). Likewise, P-1 (1000 µg/mL) also induced aggregation and a slow reduction in OD suggesting some aggregate settling (Figure 4.3). Lower concentration of P-1 (100 µg/mL) did not induce noticeable change in OD (Figure 4.3). As bacteria aggregation is due to the disruption of stable suspension dynamics, primarily electrostatic repulsive forces between negatively charged bacteria, the amount of cationic charge, such as polymer concentration or number of charged groups in the case of branched PEI, is responsible for the varying degrees of aggregation. P-2 and PEG failed to induce changes in optical density even in dilute bacteria solutions (Figure 4.3), results which are consistent with electrostatically driven aggregation. Control bacteria suspension, which replace polymer with PBS, show no spontaneous aggregation. However, *P. aeruginosa* has been reported to autoaggregate in liquid cultures, specifically at high bacteria concentrations, in which bacteria aggregates are incorporated into the bacteria suspension along with individual planktonic bacteria, which could not be detected through changes to optical density.[210]

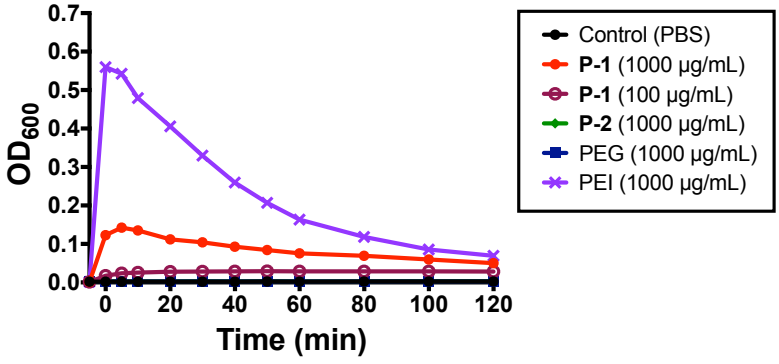

Figure 4.3. Effect of polymers on planktonic *P. aeruginosa* solution behavior. Representative data of optical density of *P. aeruginosa* in TSB incubated with P-1, P-2, PEG, or PEI at 1000 µg/mL, and PBS at room temperature without stirring. The polymers were added into the bacterial suspension at time 0.

Observation of Bacteria Aggregates

The presence of aggregates in liquid cultures was confirmed by fluorescence microscopy. Higher bacteria density (OD_{600}=1.0) was used to better visualize bacteria. In cultures of *P. aeruginosa* without any polymers, bacterial cells were observed in a diversity of aggregate sizes up to 50 µm diameter in addition to individual planktonic cells (Figure 4.4). This is consistent with previous reports of autoaggregation in nutrient deficient medium, such is the case of stationary phase bacteria.[210] With the addition of PEG or P-2, the aggregates did not dissociate nor increase in size, indicating neutral or anionic charged polymers do not perturb bacteria surface charge (Figure 4.4). At higher concentrations of P-1 (1000 and 100 µg/mL), large aggregates up to 200 µm diameter became evident in addition to smaller aggregates (20-50 µm) (Figure 4.4), suggesting cationic charged polymers are sufficient concentration can modulate the behavior of planktonic bacteria through charge. These results are consistent with optical density aggregation behavior, in which high concentrations of cationic polymer disrupt the normal state of planktonic bacteria through increased aggregation, such as by increasing the size of aggregates. While analysis of aggregate distribution in liquid cultures was considered, the size of both naturally occurring autoaggregates and cationic polymer induced aggregates are beyond the capabilities of dynamic light scattering (<10 µm) and should be an area of further study in the future. At this time, it is not hypothesized that controlling the size or distribution of aggregates would affect resulting biofilm behavior.

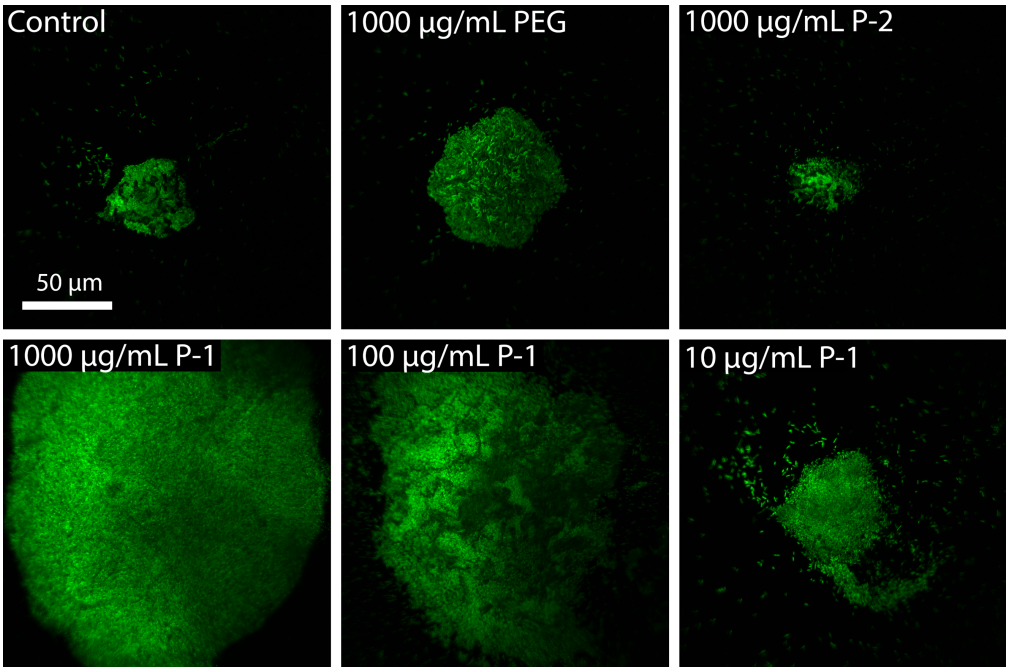

Figure 4.4. Representative images depicting aggregates of 1.0 OD_{600} solutions following 15 min incubation with polymers solutions in PBS.

Depending on size, aggregates may settle over time due to gravitational effects and alter the behavior of bacteria with surfaces. Computational models have suggested that the introduction of bacteria aggregates on a surface can result in changes to biofilm formation and behavior, due to increased access to nutrients compared to individual cells by height advantage.[210-211] Biofilm formation begins with planktonic cells attaching to a surface, such as in a low bacteria concentration environment. Therefore, to assess if P-1 induced aggregates significantly affected bacterial attachment behavior, fluorescence microscopy was used to visualize glass surfaces after 4 hours of exposure to static dilute *P. aeruginosa* cultures. At dilute concentrations, large aggregates were not evident in the bacterial attachment layer, which was instead composed of a similar distribution of individual cells (Figure 4.5). While aggregates may have settled on the surface, washing may have removed them by sheer due to increased height, suggesting they only loosely attach to surfaces. This weak attachment of aggregates is

consistent with bacteria attachment behavior, during which bacteria first attach reversibly by non-specific forces, followed by ligand based irreversible attachment. In aggregates, only bacteria in contact with the surface would undergo irreversible attachment, in which case the bulk of aggregates may be easily removed.

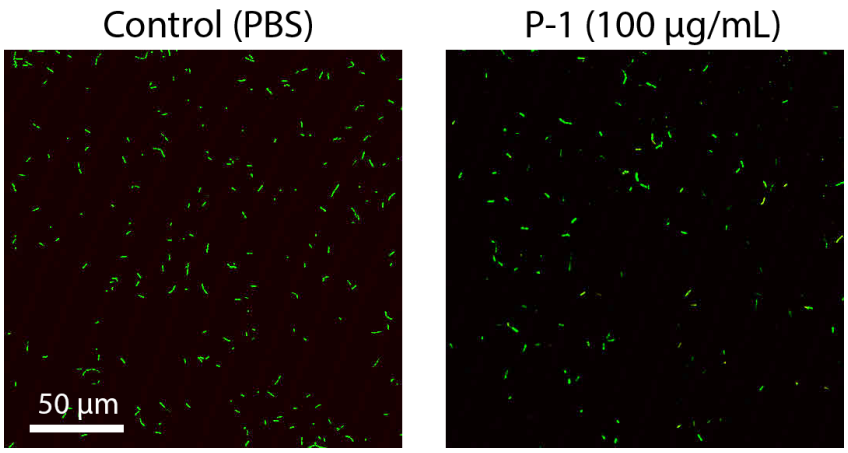

Figure 4.5. Representative images depicting bacterial attachment on surface of glass petri dish (1 hour) of 0.001 OD_{600} bacteria solution co-incubated with P-1.

Polymer Co-incubation Effect on Mature Biofilms

This work hypothesized that cationic polymers would bind to planktonic bacteria prior to their attachment and propagation into biofilms, and consequentially change their attachment behavior and subsequent biofilms formed. In order to evaluate the downstream effects of polymer interactions with planktonic bacteria, it was necessary to evaluate the properties of biofilms developed under co-incubation conditions.

Total Biomass

We evaluated the total biomass of *P. aeruginosa* biofilm as a measure of biofilm formation to determine if the polymers enhance or inhibit biofilm formation. Crystal violet (CV) staining has been an established method in biofilm microbiology to quantify the total biomass

of biofilms owing to electrostatic binding of cationic CV to the anionic biopolymers of extracellular matrix and bacterial membranes in the biofilm.[212-213] The amount of CV adsorbed onto biofilms, extracted and characterized by absorbance reflects the total biomass of biofilms.

P. aeruginosa was incubated with the polymers in a range of polymer concentrations for 24 hours, sufficient time for polymers to interact with planktonic bacteria and a biofilm to develop during polymer-bacteria interactions. The total biomass in the presence of neutral PEG and anionic P-2 did not differ significantly from control biofilms (Figure 4.6). In the presence of P-1, total biomass by CV was decreased (Figure 4.6). This effect is concentration dependent, where biomass reduction is only evident at P-1 concentrations ≥ 100 μg/mL (Figure 4.6). The lack of change in biomass by PEG and P-2 suggest that the reduced biomass is the result of specifically cationic polymers. Furthermore, the concentration dependence suggests a total charge dependent effect. The change in total biomass may reflect several events: a lower quantity of biofilm development, polymers eradicated biofilms once developed a more fragile structure in biofilms causing removal during washing, and/or a change in biofilm properties reducing the binding efficiency of CV stain.

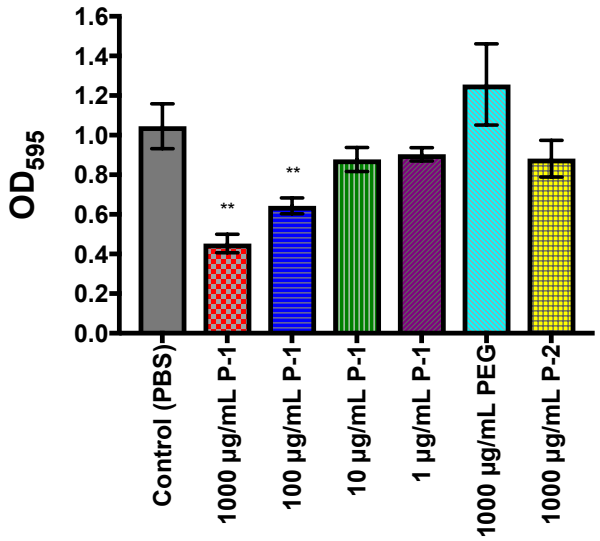

Figure 4.6. Crystal violet evaluation of polymer-modulated biofilm formation. Total biomass dependence on polymer concentration after 24 hours of incubation in the presence of P-1, PEG, or P-2. PBS was used as a positive control. The experiment was performed in duplicate, and the absorbance was determined as the average of data for each experiment. The data points and error bars represent the average and s.d from data in three independent experiments (n = 3), with significance (**p< 0.01) indicated against control (PBS).

Viable Bacteria

Biofilms are heterogenous structures of extracellular matrix and microbial cells, both live and dead. When considering infection persistence, only live or viable cells are responsible. Therefore, to determine if polymers reduced the number of viable bacteria within biofilms, direct enumeration of colony forming units was conducted. *P. aeruginosa* was incubated with the polymers in a range of polymer concentrations for 24 hours, under which conditions biofilms were formed.

In the absence of polymers, biofilms contained 5.4 (±2.5) x 10^8 CFU/cm^2 viable bacteria. Incubation with PEG and P-2 did not significantly alter the viable bacteria load as compared to the control, with counts of 4.9 (±2.3) and 5.7 (±4.3) x 10^8 CFU/cm^2 respectively (Figure 4.7). When biofilms were formed in the presence of 1000 µg/mL P-1, the number of viable bacteria was reduced to 7.7 (±5.5) 10^7 CFU/cm^2 (Figure 4.7), which corresponds to an 86% reduction. As

P-1 concentration decreases however, the bacterial load approaches levels similar to the control. Therefore, reduction in viable bacteria is both a result of polymer charge and polymer concentration. These results support findings by CV that P-1 inhibits biofilm development, decreasing both biofilm matrix and viable cells. As P-1 has no antimicrobial activity, the reduction in viable cells is the result of inhibited biofilm growth.

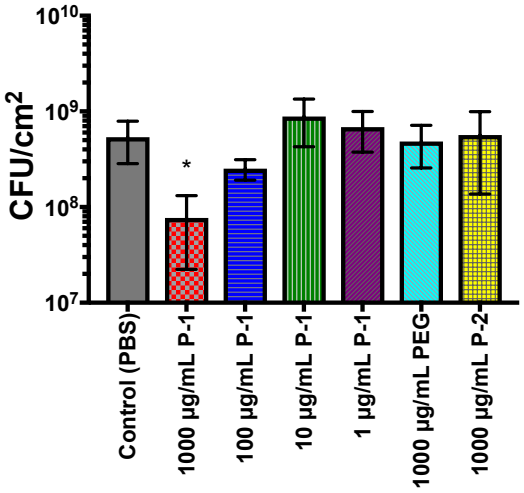

Figure 4.7. Viable bacteria evaluation of polymer-modulated biofilm formation. Viable bacteria dependence on polymer concentration after 24 hours of incubation in the presence of **P-1**, PEG, or **P-2**. PBS was used as a positive control. The experiment was performed in duplicate, and the absorbance was determined as the average of data for each experiment. The data points and error bars represent the average and s.d from data in three independent experiments (n = 3), with significance (**p< 0.01) indicated against control (PBS).

Metabolic Activity

Cellular activity for biofilm bacteria is reported lower as compared to planktonic bacteria and is a potential cause of poor antibiotic efficacy. Bacteria found in the interior of the biofilm have lower metabolic activity likely due to oxygen limitation[28], and are considered to be in a dormant state. Structural changes to the biofilm may result in increased availability of oxygen and nutrients to interior bacteria, resulting in changes to metabolic activity caused by incorporation of charged or uncharged polymers into the biofilm matrix. Therefore, the

metabolic activity of biofilm bacteria was evaluated by MTT assay, a colorimetric assay in which MTT is converted to formazan by mitochondrial reductase, and the absorbance of formazan at 570 nm is correlated to the amount of metabolic activity. MTT assays are also often used as indication of viable bacteria, assuming all bacteria in the study are at the same level of metabolic activity, where the amount of formazan converted correlates to the number of viable bacteria present. In this case, previous data indicates comparable number of viable bacteria, and therefore MTT assay will provide information regarding the metabolic activity of bacteria in the biofilm, and/or to corroborate the direct enumeration results.

P. aeruginosa was incubated with the polymers in a range of polymer concentrations for 24 hours and allowed to form biofilms, and biofilms were subsequently assessed by MTT assay. Biofilms grown in the presence of PEG and P-2 demonstrated similar metabolic activity to control biofilms (Figure 4.8), which supports direct enumeration, and indicates bacteria are at similar metabolic states. The reduction of metabolic activity at 1000 μg/mL P-1 (Figure 4.8) is consistent with the lower number in viable bacteria found by direct enumeration. As P-1 concentration decrease, metabolic activity is recovered (Figure 4.8), supporting the finding of similar amounts of viable bacteria, and indicating similar metabolic activity. These findings corroborate direct enumeration studies indicating bacterial reduction only in the presence of high concentrations of P-1, indicating cationic charge and sufficient charge is necessary to reduce biofilm accumulation.

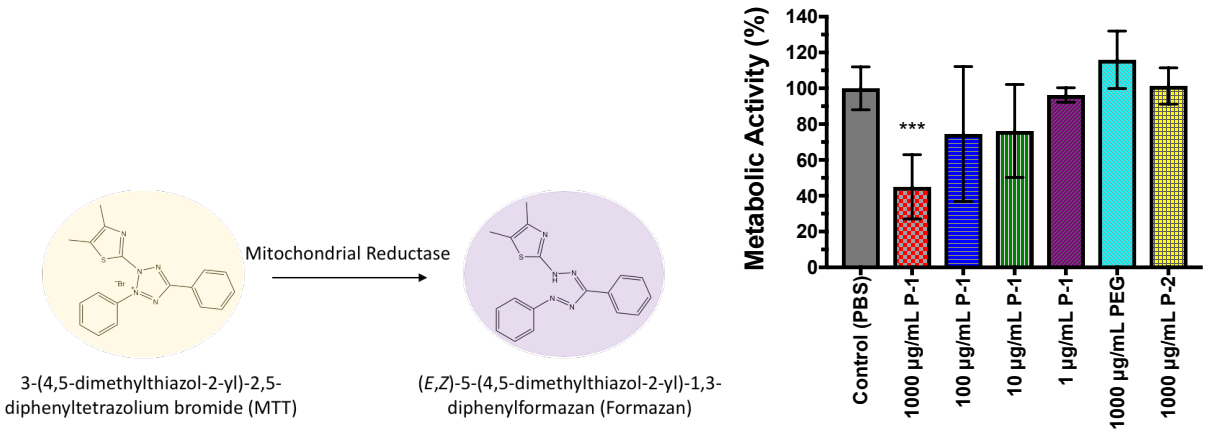

Figure 4.8. Metabolic activity of *P. aeruginosa* bacteria in biofilms measured by MTT colorimetric assay, through the reduction of MTT to formazan. Metabolic activity dependence on polymer concentration after 24 hours of incubation in the presence of **P-1**, PEG, or **P-2**. PBS was used as a positive control. The experiment was performed in duplicate, and the absorbance was determined as the average of data for each experiment. The data points and error bars represent the average and s.d from data in three independent experiments (n = 3), with significance (**p< 0.01) indicated against control (PBS).

Biofilm Formation Over Time

Biofilm development begins from the attachment of planktonic bacteria to a surface, though previous research has reported bacteria aggregates may seed surfaces and change biofilm behaviors, such as early switching of bacteria biofilm phenotype that consequentially changes biofilm formation behavior.[211, 214] Therefore, the accumulation and development of *P. aeruginosa* bacteria into biofilms was observed through confocal microscopy in the absence and presence of P-1 (1000 µg/mL). The formation of 3-dimensional structures can be seen observed in as little as 2 hours, originating from a layer of single cell attachments to the surface (Figure 4.9). After 4 hours, the biofilm has thickened with a dispersion of live bacteria throughout, which divide and more densely populate the biofilm after 8 hours (Figure 4.9). In the presence of P-1, biofilms appear to be initiated by single bacterium, or small clusters of bacteria (diameter<10 µm), but do not appear to include large aggregates that dominate the biofilm (Figure 4.9). After 4 hours, the biofilm thickens and becomes densely populated with

live bacteria after 8 hours, such as was seen in the case of control bacteria (Figure 4.9). Further studies that probe the comparative properties of biofilms as they develop, such as cellular density or surface roughness, should be aspects of future research to determine if incubation with P-1 results in changes to the biofilm structure during development, and if such changes are maintained at longer lifetimes.

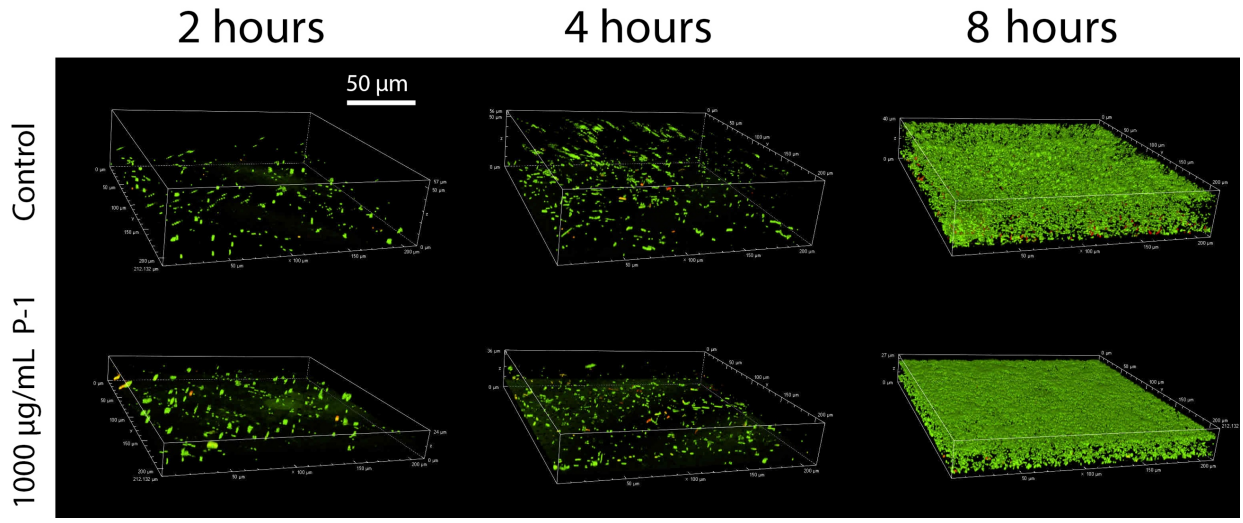

Figure 4.9. Representative three-dimensional renderings of *P. aeruginosa* biofilm development over 2, 4, and 8 hours in the absence (control) and presence of P-1 (1000 µg/mL).

Proposed Polymer-Modulated Biofilm Formation Mechanism

This study indicated that the co-incubation of cationic polymers results in the reduction of biofilm accumulation. As this reduction is not due to the biocidal or biostatic effects, we propose a new mechanism through the cationic polymer-bacteria interactions (Figure 4.10). The observed cellular aggregation of bacteria in the presence of cationic polymers results in bacteria sequestration in solution. The cationic polymers bind to the anionic surface of bacteria, which either results in surface charge neutralization which reduces repulsive activity between bacteria, or electrostatic bridging between cationic and anionic portions of adjacent bacteria.

This aggregation sequesters bacteria, reducing the number of planktonic bacteria that can attach to a surface to begin biofilm formation. Increasing the concentration of polymer more effectively result in sequestering the bacteria away from attaching surfaces. However, the polymer-bacteria interaction appears not to change the inherent ability of bacteria to attach to surface and form biofilms. The bacteria eventually do attach divide and propagate as normal. The polymers can delay the biofilm formation. Studies that would further help elucidate the mechanism of action include identifying the relationship between polymer concentration, aggregate size and degree of biofilm suppression. Additionally, further studies that monitor the accumulation of biomass and viable bacteria over time both during early development (2-12 hours), and beyond 24 hours would be useful to identify a point at which this approach no longer effectively combats biofilms, such as would be necessary for application in combination therapy studies. To the authors knowledge, no other studies have proposed a mechanism by which charged polymers are used to target bacteria surfaces for non-toxic prevention of biofilm formation.

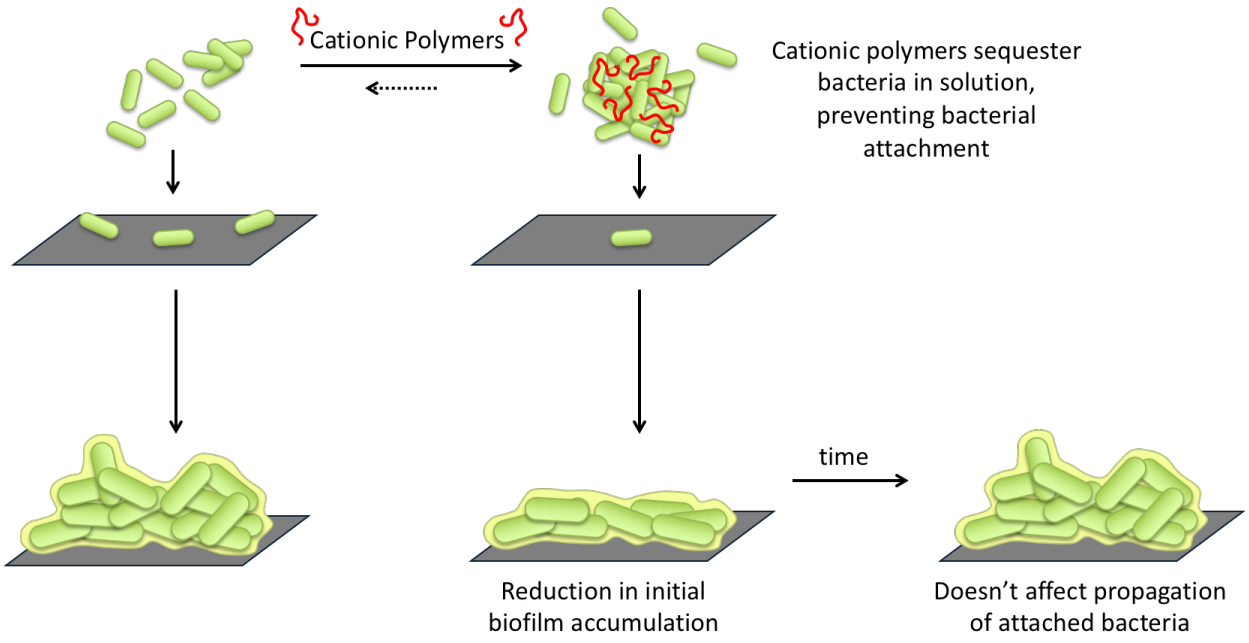

Figure 4.10. Proposed mechanism for cationic polymer modulation of biofilm behavior through planktonic bacteria interactions. Cationic polymers are proposed to sequester bacteria in solution, preventing bacterial attachment to surfaces, and consequentially suppression biofilm accumulation.

Conclusions

In summary, cationic poly[(3-methacryloylamino)propyl] trimethylammonium chloride (P-1) is capable of modulating planktonic and biofilm bacteria behavior through electrostatic interactions. Specifically, P-1 has been shown to induce concentration dependent bacteria aggregation in solution, indicating changes to the physiochemical surface of bacterial membranes. Despite no direct antimicrobial action, P-1 suppressed biofilm accumulation of both matrix and viable bacteria when concentrations ≥100 µg/mL were incubated with planktonic bacteria during biofilm development, while neutral and anionic polymers did not. We propose that cationic polymers can sequester planktonic bacteria in solution through electrostatic interactions, preventing bacteria attachment and consequentially reducing biofilm formation. This method of biofilm prevention could be useful in clinical applications in

combination with existing antibiotics to reduce the necessary antibiotic load by suppressing biofilm development at early stages. Our findings provide a mechanistic link between the physical-interactions of planktonic bacteria and biofilm biological consequences, useful to develop versatile anti-biofilm polymers to modulate not only bacteria-material interactions, but also interfere bacteria-host interactions for infection prevention.

Chapter 5 Membrane Targeting Cationic Polymers for Increased Tobramycin Susceptibility of Dormant Biofilm Bacteria

Introduction

Bacterial biofilms are a continuing problem in the healthcare community, and long-term effectiveness of current anti-biofilm methods has proven challenging. Bacterial biofilms can form on abiotic surface, such as implanted medical devices, as well as biotic surfaces, such as tissue.[215] They are responsible for 65-80% of infections [23-24], and once established, are difficult to treat due to increased antibiotic tolerance.[39] Specifically, *Pseudomonas aeruginosa* frequently develops into biofilms and consequently chronic infections of the respiratory system, especially in immunocompromised patients such as those with cystic fibrosis.[184-186, 216]

P. aeruginosa biofilms in the respiratory system are typically treated by inhaled antibiotics, such as tobramycin. Combination therapies with multiple antibiotics have been explored, and while they may prove more effective to single-drug therapy, they also increase risk of multi-drug antibiotic resistance development due to biofilm hypermutability, which would hinder future treatment options.[217-219] Enzymes that degrade the biofilm matrix have been shown to enhance antibiotic efficacy by improving antibiotic penetration.[92-95] However, the degradation of the biofilm matrix promotes biofilm detachment, which allows portions of the biofilm to be disperses and potentially seed new biofilms throughout the body. Inhibition of quorum sensing has also been a target for enhanced antibiotic efficacy, due to its involvement

in multiple virulence factors such as the production of extracellular enzymes for antibiotic deactivation.[220-222] Unfortunately, the quorum sensing pathways are highly complex and their effects and role in biofilms are not well defined.

Metabolically inactive bacteria or dormant bacteria are another challenge to antibiotic treatment, especially in biofilms. Bacteria in biofilm have reduced rate of metabolism and cell division, but can revert to an metabolically active state even after extended period of times.[223-224] Dormancy occurs when the environment is not favorable, such as low nutrient or oxygen accessibility, as is the case for embedded biofilm bacteria.[28, 142, 224-226] Because many antibiotics target pathways for cellular repair and/or division (i.e. cell wall synthesis inhibitors, protein synthesis inhibitors), dormancy related repressed cellular activity have been theorized to be a cause of reduced antibiotic efficacy.[28, 149, 225] Additionally, has been proposed that dormant bacterial may also have reduced antibiotic uptake, because it is an energy-dependent process.[227-228] Previous studies has investigated overcoming dormancy related antibiotic tolerance in *P. aeruginosa* biofilms[229], such as through using molecules to generate a proton-motive force to increase tobramycin uptake[151, 230], stimulating bacterial to a higher metabolic state through motility[150] or signaling molecules[231], or conjugation of antibiotics with antimicrobial peptides that disrupt the bacterial membrane for enhanced antibiotic penetration.[232]

In our previous research (chapter 4), cationic poly[(3-methacryloylamino)propyl] trimethylammonium chloride bound to bacterial membranes to modulate physiochemical behavior during biofilm assembly. In this study, we will explore the application of this cationic polymer for treatment of developed biofilms. Specifically, the aim of this study is to determine

if cationic polymers can be used to increase antimicrobial susceptibility of dormant bacterial cells through non-disruptive membrane binding. This study will extend the application of cationic polymers from use in preventative biofilm approaches to active treatment approaches, providing a multi-pronged strategy to combat biofilm infections.

Methods

Materials

Tryptic Soy broth (TSB, Thermo Scientific Oxoid™), Mueller Hinton broth (MHB, BD and Company ©), and phosphate buffered saline (PBS, pH=7.4, Gibco®) were prepared according to manufacturer instructions and autoclave sterilized prior to use. SYTO 9 and propidium iodide (PI) nucleic acid stains (Molecular Probes, OR) were used as prescribed by the product manual at 1.5 µL/mL. Crystal violet (Sigma-Aldrich) was diluted in Millipore water to a working concentration of 0.01% (wt/vol). MTT (3-(4,5-dimethylthiazol-2-yl)-2,5-diphenyltetrazolilum bromide, Thermo Scientific) was diluted in Millipore water to working concentration of 0.3% (wt/vol). Cyanin-5 NHS ester was purchased from Lumiprobe. Diisopropylethylamine, tobramycin and solvents were purchased from Fisher Scientific. 3-(Methacrylamido)propyltrimethylammonium chloride (MAPTAC, 95%) from Wako Pure Chemical and Fluorescein *o*-acrylate (AAcF, 97%) from Sigma-Aldrich were used as received without further purification. 4-Cyanopentanoic acid dithiobenzoate (CPD), used as a chain transfer agent (CTA), was synthesized according to the method reported by Mitsukami and co-workers.[233] 2,2'-Azobis(isobutyronitrile) (AIBN, 98%) was used as received. Water was purified with an ion-exchange system.

Poly[(3-methacryloylamino)propyl] trimethylammonium chloride (**P-1**) were synthesized by RAFT polymerization as described in Chapter 4 and characterized by ^{1}H NMR and GPC (Appendix C). Stock solutions were prepared at 10 mg/mL in 0.01 % acetic acid). Further P-1 stock solutions were prepared by ten-fold dilutions in PBS (1000, 100, 10 µg/mL).

Pseudomonas aeruginosa (*P. aeruginosa*) PAO1 was received from Dr. Chuanwu Xi (Environmental Health Science, University of Michigan). *P. aeruginosa* cultures were prepared by suspension of a bacteria colony in TSB, collected from agar plate (<5 days old). Cultures were grown overnight (18 hours) at 37 °C at 180 rpm. Further preparations are as noted in subsequent methods.

Cy5-tobramycin was synthesized by Dr. Rajani Bhat (University of Michigan) using the reaction of Cy5-NHS ester (10 mg, 1.62 x 10^{-2} mmol, 1 eq), Tobramycin (8 mg, 1.79 x10^{-2} mmol, 1.1 eq) and N,N-diisopropylethylamine (10mg, 7.7 x10^{-2} mmol, 5 eq). Compounds were dissolved in DMSO (0.7 mL) and reacted in the absence of light for 20 hours. DMSO was evaporated by N_2 gas. The resultant solid was dissolved in minimum quantity of methanol and purified by flash column using DCM:Methanol:NH_4OH (5:4:1) as the eluent. Refractive index (R_f) of dye-antibiotic conjugate was seen to be 0.4.

Fluorescein labeled PMAPTAC was prepared by Yusa and colleagues (University of Hyogo). MAPTAC (1.81 g, 8.18 mmol), AAcF (32.6 mg, 0.0844 mmol), CPD (23.7 mg, 0.0846 mmol), and AIBN (6.80 mg, 0.0414 mmol) were dissolved in methanol (5.20 g). The solution was heated at 60 °C for 8h under argon atmosphere. After the polymerization, ^{1}H NMR was measured to determine the monomer conversion (= 41.1%). The polymerization mixture was dialyzed against pure water for one day. The polymer (P(MAPTAC/$AAcF_3$)$_{63}$) was recovered with

a freeze-drying technique (0.420 g, 22.5%). Degree of polymerization (DP) was 63 estimated by ^{1}H NMR (Appendix D). Number-average molecular weight (M_n) and molecular weight distribution (M_w/M_n) were estimated by gel-permeation chromatography (GPC) to be 1.40×10^4 and 1.04, respectively (Appendix D). The AAcF content in the copolymer was 3 mol% estimated from UV-vis absorption spectra (Appendix D).

Antimicrobial Activity: MIC Assay

The minimum inhibitory concentration (MIC) of antibiotics against *P. aeruginosa* (PAO1) was determined in a modified microbroth dilution assay according to the Clinical and Laboratory Standards Institute guidelines with suggested modifications by R. E.W Hancock Laboratory (University of British Columbia, British Columbia, Canada)[169] and Giacometti et al.[170] Bacteria was grown overnight (~18 hours) in TSB at 37 °C with orbital shaking (180 rpm), and regrown to the exponential phase (OD_{600}= 0.5-0.7, 2 hours). Dilution with TSB resulted in a bacteria suspension with an OD_{600}= 0.001, ~4 x 10^6 CFU/mL. Stock solutions of tobramycin (1 mg/mL), ciprofloxacin (0.1 mg/mL), ceftazidime (1 mg/mL), and H_2O_2 (500 mM) were serially diluted to working concentrations in PBS and added to 96-well sterile round-bottom polypropylene plate wells (10 µL). PBS was used as a solvent control. A stock of dilute bacterial suspensions (OD_{600}= 0.001) was divided (4.5 mL), to which half an aliquot (0.5 mL) of P-1 was added to achieve a concentration of 1000 µg/mL, and the remaining half an aliquot of PBS. Dilute suspensions were then added to the wells of plates (90 µL). Plates were incubated for 18 hours at 37 °C. MIC was defined as the lowest concentration of antibiotics to completely inhibit bacterial growth. Assays were repeated a minimum of three times in triplicate on different days.

Biofilm Formation and Polymer Exposure for Total Biomass, Direct Enumeration and Metabolic Activity

Biofilm growth was performed with modifications to previous literature methods.[201-202] 12 mm diameter borosilicate glass coverslips (Fisherbrand™) were sterilized in 70 vol% ethanol for a minimum of 1 hour and allowed to air dry. A thin strip of label tape was placed on the bottom wells of a sterile 12-well polystyrene plates (Corning® Costar®) to facilitate coverslip retrieval, and the plate sprayed with 70 vol% ethanol and allowed to dry completely. Coverslips were placed 1 per well, with the entire coverslip being flush with the well bottom. *P. aeruginosa* overnight cultures were diluted in TSB to desired concentration of OD_{600}= 0.001. Bacteria solution (900 µL) was added to each well to fully immerse the coverslip. PBS (100 µL) was then added to each well. TSB with PBS (100 µL) was also assayed along with the test samples to confirm no bacterial contamination. Plates were wrapped in parafilm and incubated for 24 hours at 37 °C in the absence of shaking.

To assess the effects of polymer exposure on biofilms, the culture medium was removed from the wells by micropipette following incubation. Wells were washed with excess PBS. Polymer stock solutions were added to biofilms to achieve final polymer concentrations between 1-1000 µg/mL and incubated at room temperature for 2 hours in the absence of shaking. Solution was then removed, and the biofilms washed with excess PBS.

Evaluation of Total Biomass by Crystal Violet

Biofilms were generated as described in the previous section. Crystal violet (CV, 0.01%, 1000 µL) solution was introduced to wells by micropipette and used to stain the biofilm for 15 minutes at room temperature without shaking. CV was removed from the wells by

micropipette, and wells were rinsed twice with PBS, and the solution discarded. In order to maintain a consistent biofilm area, coverslips (with adhered biofilms) were removed and transferred to a new sterile 12-well plate using forceps, by holding a coverslip edge carefully as to not disrupt the biofilm. Ethanol (100%, 1000 µL) was used to extract CV from the biofilms for 10 minutes at room temperature and the biofilm manually disrupted by micropipette agitation of the solution and scraping. An aliquot of the solution (200 µL) was transferred to 96-well round-bottom plate, which was centrifuged at 1000 rmp for 5 minutes in order to reduce the impact of cellular debris in solution. Aliquots (25 µL) of solution were then transferred to untreated, sterile polystyrene 96-well flat-bottom plate containing ethanol (75 µL) to create 1:4 solutions and the OD_{595} was obtained on a Varioskan Flash microplate reader (Thermo Fisher). Experiments were carried out in duplicate on three separate days. Daily averages were calculated from duplicates and used to determine a grand average and standard error of the mean (n=3).

Evaluation of Viable Bacteria by Direct Enumeration

Biofilms were generated as described in the previous section. Washed coverslips (with adhered biofilms) were removed and transferred to 15 mL conical tubes containing PBS (3 mL) using forceps, by holding a coverslip edge carefully as to not disrupt the biofilm. Coverslips in PBS were sonicated for 10 minutes to fully disrupt biofilms and dispersed bacteria in solution. 10-fold serial dilutions were performed in PBS, and an aliquot of samples (100 µL) was plated on TSB agar plates. The agar plates were incubated overnight (~18 hours) at 37 °C, and the number of viable colonies was counted. An appropriate dilution was selected from agar plate contained 30-300 colonies, the accepted range of countable colonies.[203] Experiments were

carried out in duplicate on three separate days. Daily averages were calculated from duplicates and used to determine a grand average and standard error of the mean (n=3).

Evaluation of Metabolic Activity by MTT

Biofilms were generated as described in section Chapter 0. To each well, a premixed solution of PBS (750 µL) and 0.3% MMT (250 µL) were added and allowed to incubate for 2 hours at 37 °C in the absence of stirring. The solution as removed by micropipette and the wells washed with PBS. Washed coverslips were removed and transferred to a new 12-well plate. A solution of DMSO (750 µL) and glycine buffer solution (pH 10.5, 126 µL) was added to each well, the biofilms manually disrupted, and allowed to incubate at room temperature for 15 minutes. Aliquots (100 µL) of solution were then transferred to untreated, sterile polystyrene 96-well-plate containing ethanol (75 µL) to create 1:4 solutions and the OD_{570} was obtained on a Varioskan Flash microplate reader (Thermo Fisher). Experiments were carried out in duplicate on three separate days. Daily averages were calculated from duplicates and used to determine a grand average and standard error of the mean (n=3).

Biofilm Formation, Polymer Exposure and Cy5-Tobramycin Exposure for Confocal Microscopy

An overnight culture of *P. aeruginosa* was diluted to 0.001 OD_{600} in TSB. Bacteria solution (OD_{600}= 0.001, 2.7 mL) and PBS (0.3 mL) was added to a clear cell culture dish (FD35-100, Fluorodish™) with glass window diameter of 23.5 mm. Dishes were wrapped in parafilm and incubated 24 hours at 37 °C in the absence of shaking. Following incubation, the culture medium was removed from the dish by micropipette. Biofilms were washed twice with excess PBS. Polymer solutions (2 mL, 100 µg/mL) were added to biofilm dishes (or PBS for control

biofilms) and incubated for 2 hours at room temperature without shaking. Polymer solution was then removed, and the biofilms washed twice with excess PBS. Biofilms were stained by SYTO 9 (3.34 mM) and/or propidium iodide (20 mM) in 0.85% NaCl for 20 minutes at room temperature in the absence of light without shaking. SYTO 9-PI solution was then removed by micropipette and biofilms washed once with 0.85% NaCl solution. Biofilms were examined by inverted confocal microscope (Eclipse Ti-U, Nikon) using a 60x oil objective.

Fluorescein labeled P-1 (F-P-1) was utilized to assess polymer penetration and location of P-1 within biofilms. F-P-1 was incubated with 24h biofilms for 2 hours at room temperature prior to biofilm washing and staining with PI as described above.

Cy-5 labeled tobramycin (1 mg/mL, 2 mL) utilized to assess antibiotic penetration of natural biofilms and P-1 exposed biofilms. Cy-5 tobramycin was incubated for 2 hours at room temperature prior to biofilm staining. Tobramycin solution was then removed, the biofilms washed with excess PBS, and the biofilm stained with SYTO 9 and imaged as described above.

Membrane Potential Measurement by $DisC_3$-(5)

The effect of polymer binding on membrane potential was evaluated for stationary and exponential phase *P. aeruginosa* cultures by $DiSC_3$-(5).[78] An overnight culture of *P. aeruginosa* (~18 hours) grown in TSB. Overnight cultures were used as stationary phase bacteria as analogs for biofilm dormant cells. Exponential phase bacteria were used for comparison, which were achieved by using overnight culture inoculated diluted in TSB at 37 °C with orbital shaking (180 rpm) for 2 hours (OD_{600} of 0.5-0.8). Bacterial solutions were centrifuged at 1,700 x g for 10 minutes to yield bacterial pellets and the supernatant broth removed by pipette. Bacteria was washed by resuspended in HEPES buffer (5 mM, pH 7.2), centrifuging, removal of wash buffer,

and resuspension in HEPES buffer to an OD_{600} of 0.05. Bacteria suspensions (95.5 µL) were added to a sterile flat-bottom polystyrene-wells. A stock solution of $DiSC_3$-(5) in DMSO (0.1 mM, 0.5 µL) was transferred to the bacteria suspension and stirred for 180 seconds to reach stable fluorescence intensity due to accumulation of dye on the bacterial membranes, with a final $DiSC_3$-(5) concentration of 0.5 µM. After 180 seconds, stock polymer solutions in PBS (or PBS for control) were added to the bacterial solutions (10 µL), to achieve final polymer concentrations of 1-1,000 µg/mL. The fluorescence intensity was monitored using a Varioskan Flash microplate reader (Thermo Fisher) with an excitation and emission wavelengths of 622 nm and 670 nm, respectively. Experiment were carried out in quadruplicate on three separate days (n=3).

Combination Treatment by P1 and Tobramycin

Biofilms were generated as described in the previous section, with stock polymer stock incubation for 2 hours at room temperature to achieve polymer concentrations of 1-1,000 µg/mL. Following polymer incubation, supernatant was removed by pipette and the wells washed with excess PBS. Stock solution of tobramycin (100 µg/mL, 1 mL) were added to each well and incubated at room temperature for 2 hours in the absence of shaking. Following tobramycin treatment, the solution was removed, and wells washed with excess PBS. Washed coverslips were removed and transferred to 15 mL conical tubes containing PBS (3 mL). Coverslips in PBS were sonicated for 10 minutes to fully disrupt biofilms and dispersed bacteria in solution. 10-fold serial dilutions were performed in PBS, and an aliquot of samples (100 µL) was plated on TSB agar plates. The agar plates were incubated overnight (~18 hours) at 37 °C, and the number of viable colonies was counted. An appropriate dilution was selected from agar plate contained 30-300 colonies, the accepted range of countable colonies.[203] Experiments

were carried out in duplicate on three separate days. Daily averages were calculated from duplicates and used to determine a grand average and standard error of the mean (n=3).

Results

Polymer Post-Treatment Effect on Mature Biofilms

In this study, naturally formed biofilms were challenged with cationic polymer P-1 (Figure 5.1) to determine the penetration of the cationic polymer through the biofilm matrix and binding to bacteria, as well as the effect on bacterial cell viability and biofilm structure.

P-1
M_n (^{1}H NMR): 25,900
M_n (GPC): 19,600
M_w (GPC): 20,580
$Đ$: 1.05

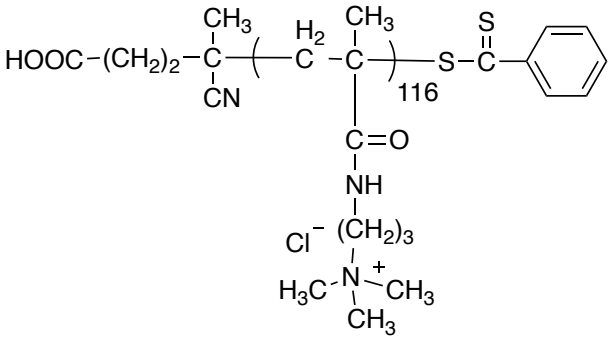

Figure 5.1. Chemical structure and characterization of cationic poly[(3-methacryloylamino)propyl] trimethylammonium chloride (P-1).

Polymer Penetration through Biofilm and binding to bacteria

Biofilms are composed of bacteria embedded in an extracellular polymeric substance (EPS). Previous studies have demonstrated that cationic antibiotic molecules have difficulty penetrating through the biofilm to embedded bacteria due to the anionic nature of the EPS. Similarly, P-1 may also be trapped in the biofilm matrix due to the cationic property of polymer and large molecular size. In order to access if P-1 is able to penetration through the biofilm matrix, biofilms are treated with fluorescently labeled P-1, and the distribution of P-1 was

examined by confocal microscopy. The images indicated that the florescence from P-1 was observed through the entire biofilm (Figure 5.2), suggesting that P-1 could fully penetrates through the biofilm matrix to the bacteria attached at the glass surface. Furthermore, the fluorescence from P-1 also matched with those from bacteria embedded in the biofilm, suggesting that P-1 had access to bacteria.

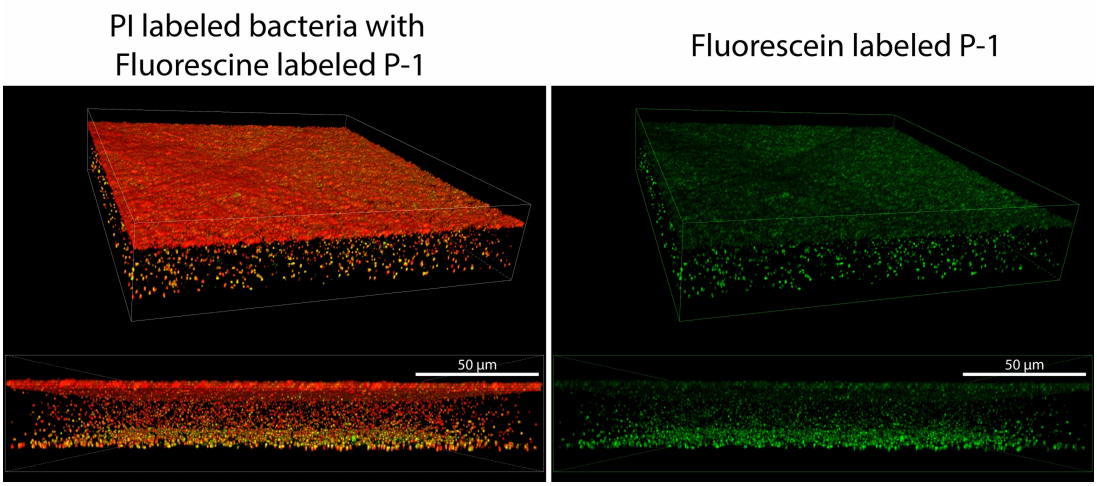

Figure 5.2. Representative three-dimensional renderings of P-1 (100 µg/mL) penetration into *P. aeruginosa* biofilms grown for 24 hours.

Biofilm removal and killing of bacteria

Cationic polymers have been reported to remove biofilms to some extent. The interaction of cationic polymers with biofilms may change the biofilm matrix structures or solubilize the matrix biopolymers, resulting in removal of biofilms. In addition, cationic polymers have been reported to kill bacteria while P-1 did not show any growth inhibition (Chapter 4). To examine these effects of P-1 on biofilms, the quantity of viable bacteria after polymer treatment was assessed. *P. aeruginosa* biofilms grown for 24 hours contained 2.15 ($\pm$1.0) x 10^8 CFU/cm^2 viable bacteria (Figure 5.3). After treatment by P-1, the biofilm contained 1.99 ($\pm$0 .4) x 10^8 CFU/cm^2 at 1 µg/mL, and higher concentrations of P-1 did not decrease viable

bacteria, for example 2.3 ($\pm$0.8) x 10^8 CFU/cm^2 at 1000 µg/mL (Figure 5.3). There is no difference in viable bacteria in biofilms treated with P-1 and control biofilms. This indicates that P-1 did not affect the biofilm and bacteria.

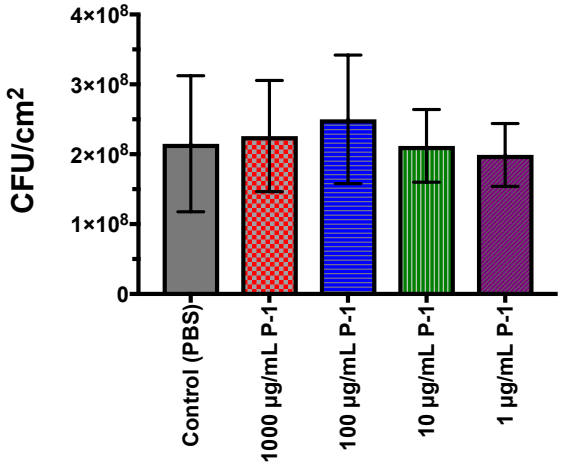

Figure 5.3. Viable bacteria evaluation of polymer challenged *P. aeruginosa* biofilms. Viable bacteria dependence on polymer concentration after challenging 24-hour biofilms with of incubation in the presence of P-1 (2 hours). The experiment was performed in duplicate, and the absorbance was determined as the average of data for each experiment. The data points and error bars represent the average and s.d from data in three independent experiments (n = 3), with significance (**p< 0.01) indicated against control (PBS).

Biofilm Structure

The previous result suggests that there is no change in cell viability and biofilm when treated with P-1. We further probed into the biofilm structures after polymer treatment using confocal microscopy. The biofilms were scanned for a z-axis sections of biofilms, and stacks reassembled to form 3-dimensional renderings. The control biofilms had a dense homogeneous layer of bacteria attached to the glass surface, and bacteria were distributed throughout the biofilm matrix, giving approximately 75 µm thickness (Figure 5.4). The biofilm surface has a higher density of bacteria. We speculate this was artifact by compressing the top layer of biofilm during washing or planktonic bacteria loosely bound to the biofilm surface. While live bacteria were found throughout the biofilm, membrane compromised (dead) bacteria were

found primarily at the glass surface, which might reflect depletion of nutrient and oxygen at the bottom of biofilm. When the biofilm was challenged with cationic polymer P-1, no significant structural changes such as voids or significant reduction in biofilm thickness was observed (Figure 5.4).

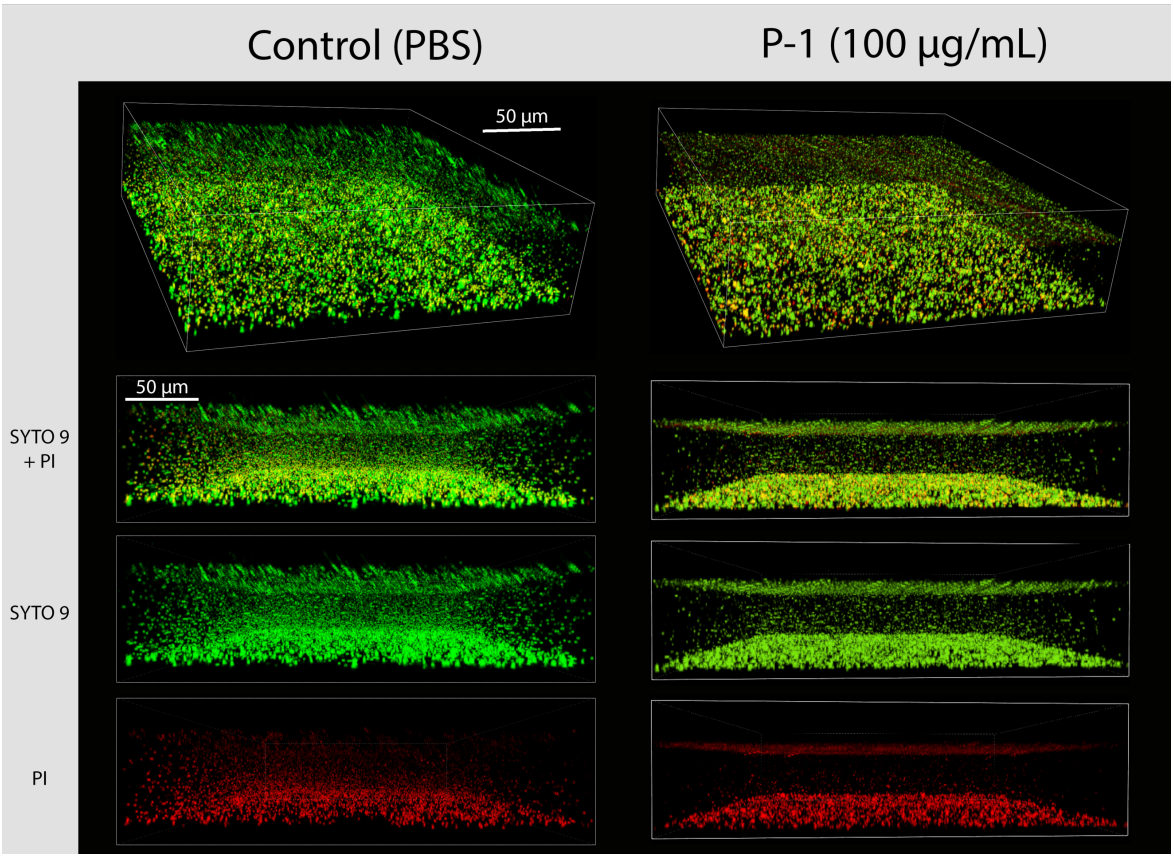

Figure 5.4. Representative three-dimensional renderings of naturally forming biofilms (control) and biofilms challenged with 100 µg/mL P-1 for 2 hours.

Metabolic Activity

Bacteria in biofilms reduce their metabolic activity because of low nutrient and oxygen availability. Consequentially, they are tolerant to antibiotics because antibiotics target metabolically active bacteria. Here we examined the effect of P-1 on the metabolic activity of bacteria in biofilms. The metabolic activity of bacteria within *P. aeruginosa* biofilms were

assessed by MTT assay after challenged with P-1 at various concentrations. At low P-1 concentrations, metabolic activity was similar to unchallenged control biofilms (Figure 5.5a). At the concentrations of 100 and 1000 µg/mL, metabolic activity of bacteria in the biofilm was enhanced by 40-50 % as compared to the control (Figure 5.5a). The direct enumeration data from this study indicated the same number of viable bacteria in biofilms with and without polymer treatment (Figure 5.3). Therefore, the result suggest that bacteria had increased metabolic activity, approximately 50% higher than the control (Figure 5.5b). To further examine this effect, increases to metabolic activity per bacteria was calculated by divining the OD reading with the number of viable bacteria (Figure 5.5c). There was a statically significant difference in the metabolic activity between biofilms treated by 1000 µg/mL of P-1 and control. This result suggests that P-1 might "awaken" the dormant bacteria in biofilms into metabolically active state.

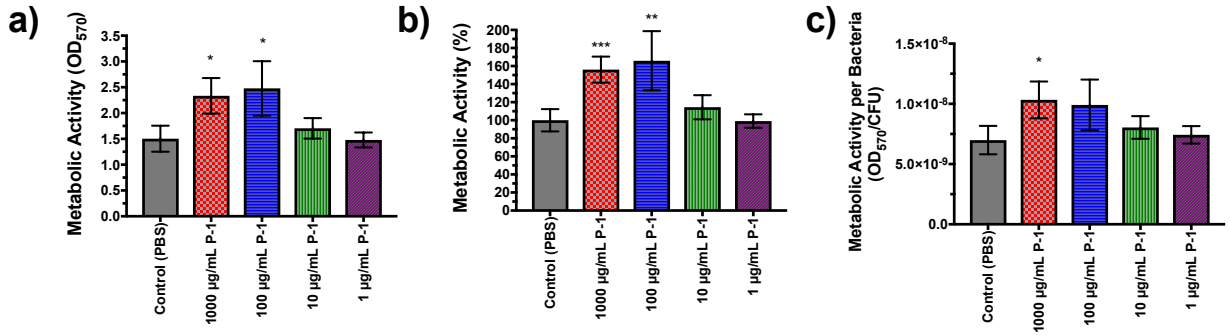

Figure 5.5. Metabolic activity of polymer challenged *P. aeruginosa* biofilms by MTT assays. A) Metabolic activity as indicated by the absorbance of solubilized formazan crystals formed by metabolic conversion of MTT. B) Metabolic activity normalized to control biofilms. C) Metabolic activity normalized to the average number of viable bacteria. The experiment was performed in duplicate, and the absorbance was determined as the average of data for each experiment. The data points and error bars represent the average and s.d from data in three independent experiments (n = 3), with significance (**p< 0.01) indicated against control (PBS).

Bacterial Membrane Potential

Because the P-1 cationic polymer chains of are likely to bind to anionic bacterial cell membranes, we hypothesize that the cationic polymer acts on bacterial cell membranes to enhance the metabolic activity. To test the hypothesis, we examined the effect of polymer on the membrane potential of bacteria. We used planktonic bacteria in the stationary phase as a model for dormant bacteria in biofilms. $DiSC_3$-(5) is a fluoresce dye that are sensitive to membrane potential; this dye molecule binds to and accumulates on the bacterial membrane when the membrane is hyperpolarized, and as the membrane potential is increased, more dye molecules bind to membranes. While the dye free in water is fluorescent, the high concentrations of dye molecules on membranes results in fluoresce quenching. Therefore, fluorescence from the dye reflect the membrane potential; where greater the membrane potential, lower fluorescence intensity from the dye. Alternatively, if membranes become compromised, membrane potential is reduced to zero, and the dye doesn't bind to the membranes, resulting in no change in fluorescence. The fluorescence of $DiSC_3$-(5) in bacterial suspension was decreased immediately after addition of P-1 (Figure 5.6a), indicating an increase in membrane potential. The fluorescent intensity continued to decrease over time (Figure 5.6a), which may reflect the time necessarily for the polymer to bind to the membrane surface or for the bacteria to respond to the polymer binding. The $DiSC_3$-(5) fluorescence was significantly decreased at 1 μg/mL (Figure 5.6b), indicating even low concentrations of P-1 are capable of increasing the membrane potential. Additionally, concentrations beyond 1 μg/mL do not decrease the fluorescence intensity (Figure 5.6b). In addition, P-1 also increased the membrane potential of bacteria in the exponential phase, indicating that the effect of polymer

is not specific to the bacteria in the stationary phase (Figure 5.6b). These results suggest that the binding of polymer chains to bacterial cell membranes may directly cause enhancement of membrane potential. It has been reported that the uptake of tobramycin is dependent on the membrane potential; as the membrane potential is increased, the uptake is increased.[227, 230, 234] In combined with the result of enhanced metabolic activity (Figure 5.5), it may be possible that P-1 increase the susceptibility of bacteria in biofilms against tobramycin. We will first examine the penetration of tobramycin into biofilm and determine the efficacy of tobramycin in combination with P-1 to test this hypothesis.

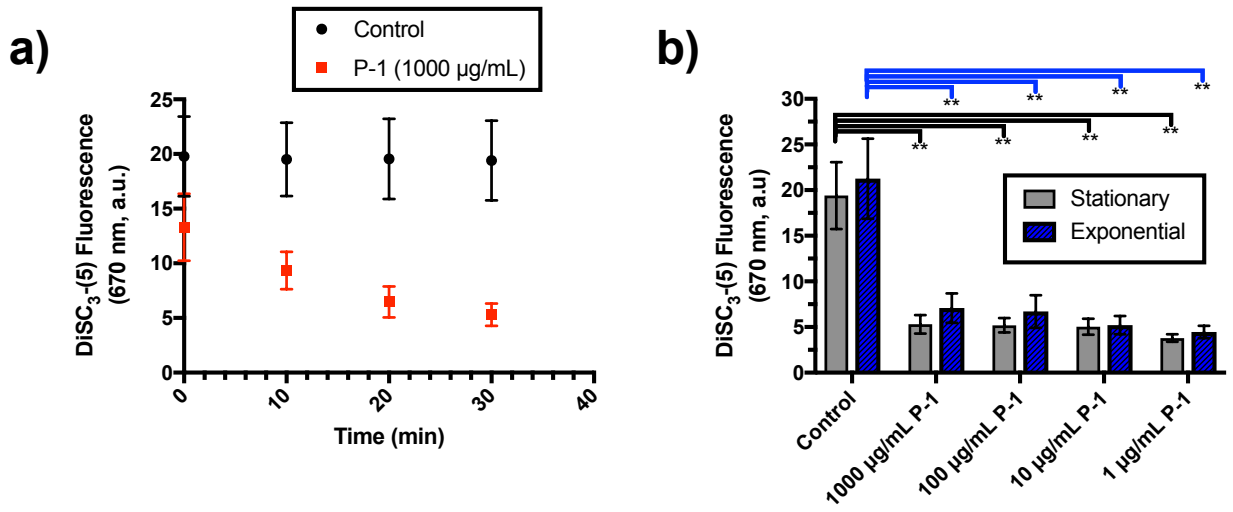

Figure 5.6. Membrane potential of planktonic *P. aeruginosa* measured by DiSC3-(5). (a) Fluorescence intensity after the introduction of P-1 to stationary phase bacteria. (b) Fluorescence intensity of stationary phase bacteria after 30 minutes of binding to P-1 at varying concentrations. The experiment was performed in quadruplicate, and the fluorescence was determined as the average of data for each experiment. The data points and error bars represent the average and s.d from data in three independent experiments (n = 3), with significance (**p< 0.01) indicated against control (PBS).

Tobramycin Penetration through Mature Biofilms

A commonly cited challenge of anti-biofilm treatment is the penetration of antibiotics through the matrix in order to access interior bacteria.[28, 32, 235] This may be true in the case of cationic antibiotics such as tobramycin, which may be sequestered in the anionic matrix away

from bacteria. First, we investigated the penetration of tobramycin though the biofilm matrix using Cy5-labeled tobramycin. The fluorescence image showed that the fluoresce from Cy5 were observed though the entire biofilm structure, tobramycin molecules were able to fully penetrate to the biofilm to the bacteria attached at the substrate (Figure 5.7). This result is inconstant with the previous reports in literature, showing incomplete dye penetration. We speculate that this inconstancy is due to the use of static biofilms as opposed to flow-cell biofilms which are more physically robust and have different matrix structures, or a factor of long exposure times that overcome retarded penetration. P-1 challenged biofilms treated with tobramycin also indicated the penetration of antibiotic was not hindered (Figure 5.7), suggesting that P-1 will not affect the penetration of tobramycin in biofilm bacteria.

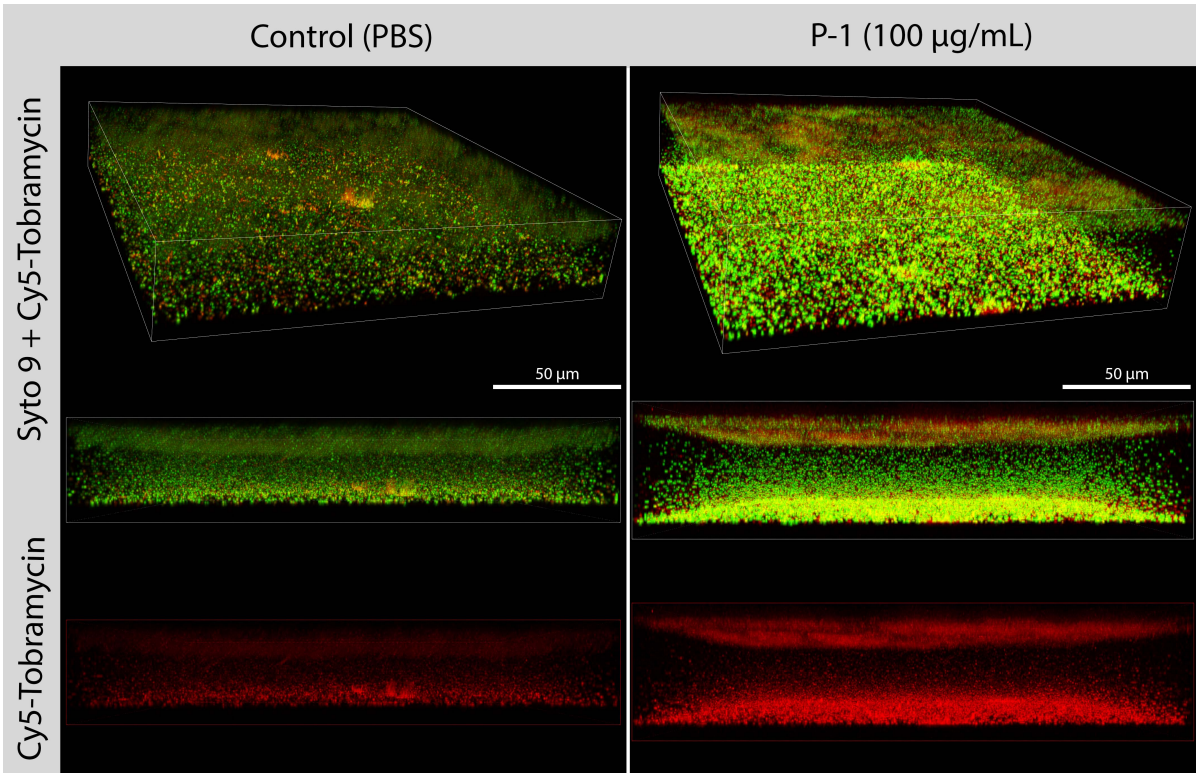

Figure 5.7. Representative three-dimensional renderings of Cy5-labeled tobramycin penetration through *P.* aeruginosa biofilms. Tobramycin is able to fully penetrate through the anionic matrix to access the inner-most cells bound to the substrate.

Cationic Polymer-Tobramycin Combined Treatment Efficacy

P. aeruginosa biofilms are highly resistant against antimicrobial agents, which is one of the primary challenges to the treatment of biofilm associated infections. Due to the increase in metabolic activity and membrane potential of bacteria when challenged with P-1, we hypothesized that a combination treatment of P-1 followed by tobramycin may increase the efficacy of tobramycin treatment. Despite tobramycin having an MIC of 0.3 μg/mL, treatment of control biofilms with 100 μg/mL tobramycin (>100x MIC) resulted in an 82% reduction of bacteria (Figure 5.8) compared to pre-treatment viability studies (Figure 5.3), less than a 1 log reduction in viable bacteria. This indicates that the static biofilms are a good representation of the antibiotic tolerant systems seen in clinical applications. When pre-treated with P-1, bacterial load was reduced by 71-82% (Figure 5.8). This reduction is comparable to the control, and therefore suggests no change in the efficacy of tobramycin on biofilms pre-treated with P-1. The lack of efficacy change suggests that despite change in membrane potential and metabolic activity as suggested by MTT (Figure 5.5), dormant bacteria in biofilms maintain additional tolerance mechanisms that cannot be overcome with cationic polymers alone. Alternatively, the efficacy of tobramycin was already saturated under this condition, and the effect of P-1 did not enhance the efficacy anymore.

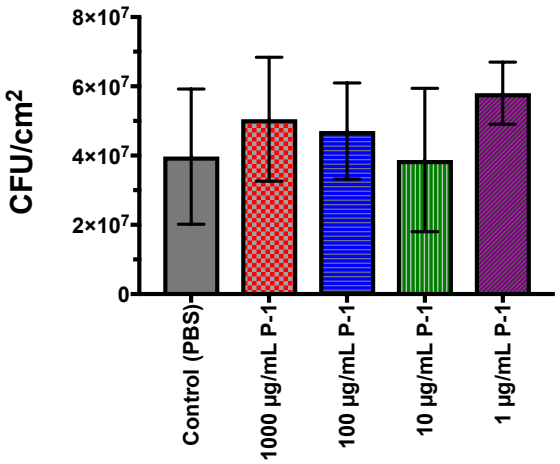

Figure 5.8. Combination therapy of P-1 challenged *P. aeruginosa* biofilms followed by treatment by tobramycin (100 µg/mL). The experiment was performed in duplicate, and the absorbance was determined as the average of data for each experiment. The data points and error bars represent the average and s.d from data in three independent experiments (n = 3), with no significance indicated against control (PBS).

Proposed Mechanism: Awakened Bacteria

The results suggest that P-1 increase the membrane potential and metabolic activity in *P. aeruginosa.* When cationic polymers have bind to the bacterial membranes, there is an increase in metabolic activity as indicated by MTT assay. This enhanced metabolic activity occurs at P-1 concentrations $\geq$1000 µg/mL, whereas increased membrane potential occurs at $\geq$1 µg/mL P-1, suggesting that the enhancement of metabolic activity is not reliant on membrane potential. While it is possible that enhanced metabolic activity measured by MTT assay could be the result of increased uptake of MTT, and that uptake is the rate limiting step of the MTT to formazan conversion. If this was the case, we hypothesize that all concentrations of P-1 would show enhanced metabolic activity, as they have similar membrane potentials. The exact mechanism of enhanced cellular activity by cationic polymer binding is an area for further examination but may be related to an increase in nutrient uptake due to increased PMF, as conversely PMF decreases in nutrient limited conditions.

The challenge of antibiotic treatment of dormant bacteria is due to multiple factors. For the purposes of this study, we will limit the discussion to the challenges of tobramycin, a clinically relevant antibiotic for the treatment of *P. aeruginosa* biofilms, particularly in cystic fibrosis patients. Antibiotics must have access to the target area of the cell, through cellular uptake. For tobramycin, this involves crossing the membrane barrier and binding to the ribosome. Once the antibiotic has entered the cell, cellular activity determines the internal effectiveness of the antibiotic. Once tobramycin has bound to the ribosome, its role is to inhibit the initiation of protein synthesis, thus it is only effective when cells are attempting to initiate protein synthesis. A final barrier to antibiotic efficacy, especially in the case of *P. aeruginosa*, are bacterial efflux systems that actively expel the antibiotic from the cell.[236-238] Therefore, in totality, the effectiveness of antibiotics is dependent on 1) the uptake of the antibiotic, 2) cellular activity of the bacteria, and 3) retention of the antibiotic at the target site.

In order to explain the results of this study, we propose the following reasons why the copolymers did not enhance the susceptibility of *P. aeruginosa* in biofilm to tobramycin.
(1) No increase in tobramycin uptake. The uptake of tobramycin by *P. aeruginosa* has been reportedly liked to membrane potential.[227, 230, 234] In dormant biofilm bacteria, the membrane potential of *P. aeruginosa* is reduced due to environmental conditions of pH an oxygen accessibility [239-240], which consequentially reduces the uptake of tobramycin into cells. Our result indicated that the binding of cationic polymers to the bacterial membrane increases membrane potential (Figure 5.6) Because the membrane potential has been previously linked to tobramycin uptake, we postulated cationic polymers could consequentially increase tobramycin uptake into the cells, resulting in increased susceptibility to tobramycin. However,

the lack of the enhanced activity may result from no enhancement in tobramycin update. It is necessary to determine absolute tobramycin uptake by control and P-1 bound bacteria to determine if tobramycin uptake is affected by P-1 increased membrane potential.

(2) Efflux pumps. We propose the lack of enhancement is related to the role of effective efflux pumps in *P. aeruginosa* bacteria, which can quickly remove harmful antibiotics from cells.[26, 40, 241-242] Efflux pumps are energy dependent, thus if metabolic activity is increased as this study suggests, efflux pumps may also work more effectively to remove antibiotics.[236, 242-243] Thus, as there is no increase in antibiotic susceptibility, this suggests that the rate of efflux is greater than either the rates of tobramycin uptake or cellular activity necessary for antibiotic activity.

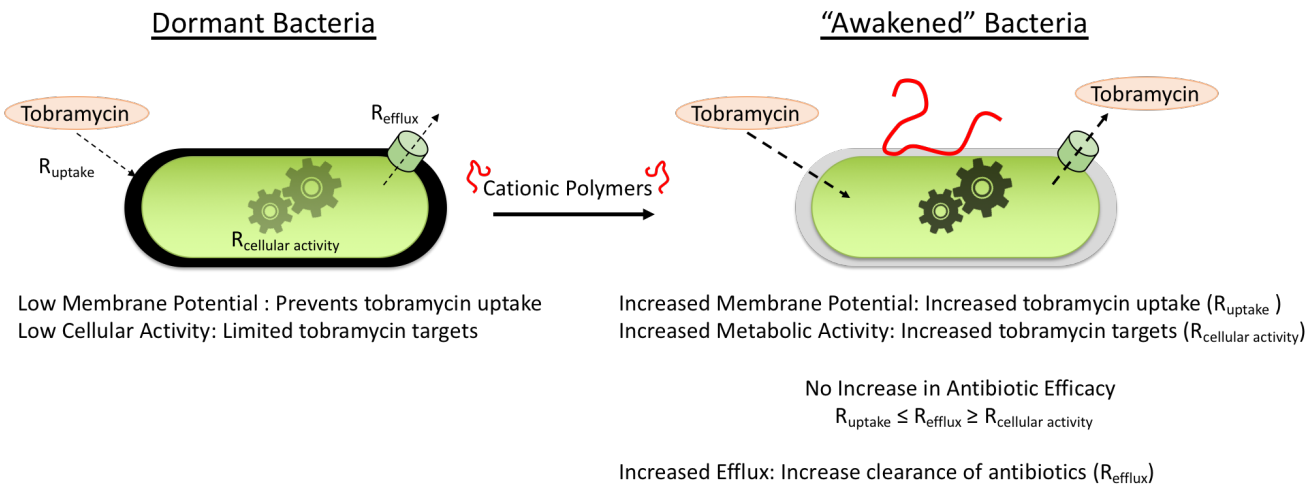

Figure 5.9. Proposed mechanism of cationic polymer "awakening" of dormant bacteria, where tobramycin uptake and cellular activity are enhanced, but bacterial susceptibility is not enhanced, proposed to due to enhanced efflux systems.

Conclusions

In summary, cationic poly[(3-methacryloylamino)propyl] trimethylammonium chloride (P-1) is capable of modulating the behavior of dormant bacteria behavior through electrostatic

binding. Specifically, P-1 has been shown to increase the membrane potential of stationary phase bacteria, where reduction in membrane potential has previously been linked to decreased antibiotic uptake. Additionally, P-1 interaction with dormant biofilm bacteria increases their metabolic activity ~50% at concentrations $\geq$1000 μg/mL. However, despite indications that antibiotics would have increased susceptibility due to increased uptake and increased cellular activity, there was no synergistic effect of P-1 and tobramycin in combination treatments. We propose that this is due to simultaneous stimulation of efflux systems in *P. aeruginosa* bacteria, which remove tobramycin at a greater rate than can be overcome by increased uptake or increased cellular activity. This approach to "awaken" dormant bacteria provides new insight into mechanism of biofilm tolerance. Future studies that combine this "awakening" approach with approaches that enhance metabolic activity may be effective at overcoming efflux dominance. The findings here provide a potential new route to enhance the treatment of biofilm infections through bacteria behavior modulation that is applicable for difficult to access biofilms, including those on tissue surfaces such as those in cystic fibrosis patients.

Chapter 6 Conclusions and Future Directions

In this dissertation, two different approaches have been explored to combat bacterial infections. New therapeutic agents were synthesized using random amphiphilic methacrylate copolymer design, with multi-armed architectures designed to mimic the multi-polymer mechanism of membrane disruption for antimicrobial activity. Additionally, cationic polymers were utilized to modulate the formation and behavior of *P. aeruginosa* biofilms.

Hyperbranched and 4-arm Star-Shaped Polymers as Antimicrobial Agents

One goal of work in this dissertation was to design cationic amphiphilic copolymers with potent antimicrobial activity and selective activity towards bacterial cells over mammalian cells, for applications as alternative antibiotics. In order to accomplish that, this work specifically focused on the use of architecture as a new tunable factor for polymer design. The hypothesis of this work was the macromolecules presenting multiple antimicrobial polymer chains would show improved antimicrobial activity and membrane selectivity. This hypothesis was based on the need for collective action of multiple polymers for membrane disruption (antimicrobial activity), and the localization of cationic charge for improved electrostatic interactions. In chapter 2, randomly branched copolymers synthesis was attempted through incorporation of a crosslinking monomer by free radical polymerization in the presence of chain transfer agent. However, the polymers were synthesized by this approach were not hyperbranched, but lightly

crosslinked high MW polymers. The finding of this study indicates that the resulting polymer structures were not branched, and high molecular weight polymers were responsible for their apparent increase in antimicrobial and hemolytic activities compared to linear polymers with comparable molecular weights. In chapter 3, 4-armed star-shaped polymers were synthesized by ATRP using a core molecule functionalized with 4 initiators. Compared to linear polymers with the molecular weight comparable to the whole star-shaped molecule or arm polymer chain, the antimicrobial activity of 4-armed star-shaped polymers was not affected by the polymer shape. However, the hemolytic activity of 4-armed star-shaped polymers was increased compared to linear polymer counterparts. Therefore, we conclude that the enhancement of hemolytic activity is due to the polymer architecture.

In conclusion, we successfully synthesized polymers presenting macromolecules with 4-arms of amphiphilic polymer chains. While we hypothesized this architecture would improve antimicrobial activity and selectivity, the results appeared not to support this hypothesis, instead not affecting antimicrobial activity and reducing selectivity. A potential problem with this approach may be that the number of arms is too low to successfully mimic the collection of multiple polymer chains at bacterial membranes. Experimentally, the formation of pores in lipid bilayers has been observed as a result of AMPs and is related to AMP concentration. Based on the size of the observed pores, calculation of the number of AMPs necessary for pore formation have been calculated to be between 4-11[166-167], depending on the pore formation model and AMP. Because it is not possible for a single AMP to form a pore, it has been experimentally determined that multiple AMPs are necessary for membrane disruption. Therefore, future studies should pursue examining multi-armed polymers with greater than 4 arms (i.e. 6, 8, 10)

with the hypothesis that at a critical number of arms, antimicrobial activity will improve beyond the linear polymer design. However, we suspect that multi-armed architecture will still induce increased hemolysis compared to linear polymers, as seen in this study because they will maintain the multi-armed architecture observed to be harmful to RBCs. Another possibility is exploration of a different shape of polymers, such as cyclic polymer structures. While no studies have explored cyclic antimicrobial polymers, research performed on cyclic antimicrobial peptide analogs of α-helix indicate cyclization reduces hemolytic activity.[244-247] This may indicate that the constrained cyclic structure restricted the peptide to adapt an amphiphilic conformation in cell membranes. This in turn disfavors the insertion of peptide chain into human cell membranes in which the lipids are generally packed while bacterial cell membranes can accommodate the distorted peptide conformation. This effect results in reduced hemolytic activity. Our laboratory has demonstrated that random copolymers also adopt an amphiphilic conformation in which the cationic and hydrophobic side chains are segregated into the opposite side of polymer backbone.[80] Therefore, cyclic polymer structures may also provide distorted amphiphilic conformations of polymer chains capable of selectively disrupt bacterial cell membranes over human cell membranes.

Cationic Polymers for Biofilm Mitigation

The second goal of this dissertation was to utilize cationic polymers to modulate biofilm behavior, through formation and increased sensitivity against antibiotics. Specifically, we hypothesized that disrupting the natural behavior of planktonic bacteria may cause sub-optimal changes in the biofilm development process, leading to decreased biofilm accumulation.

Furthermore, we hypothesized that treatment of cationic polymers to existing biofilms may sensitize them to traditional antibiotics.

In chapter 4, we found that the incubation of planktonic bacteria with a cationic polymer reduced biofilm formation through both biomass and viable bacteria. We proposed a new mechanism of biofilm prevention, specifically that cationic polymers sequester bacteria in solution and prevent attachment to the surface. Therefore, this study supported our hypothesis that targeting planktonic bacteria behavior could result in sub-optimal biofilm development. The next step to further this approach for clinical application would be an evaluation of toxicity against mammalian cells. Previous studies have reported cationic polymer toxicity to mammalian cells.[248] Future studies should be conducted to reduce the cationic functionalities by for example, reducing polymer size and designing cationic copolymers with neutral side chains.

In chapter 5, the hypothesis was that cationic polymers could be used to increase antimicrobial susceptibility of dormant bacterial cells through non-disruptive membrane binding. The finding of this study was that the treatment of developed biofilms with a cationic polymer increased the metabolic activity of embedded bacteria but did not sensitize the bacteria to tobramycin. While this finding did not agree with our hypothesis of increased sensitization by the interactions between the cationic polymers and bacteria, the finding that a change in bacteria metabolic activity offers a promising avenue for future research. A problem with this approach is the potential pitfalls for antibiotic failures; antibiotic efficacy is dependent on uptake, cellular activity and retention of the antibiotic in the cell, and cationic polymer binding may only promote uptake based on changes in proton motive force. If any of these

steps is hampered, the antibiotic would fail. Based on the finding that cationic polymers can increased bacterial proton motive force, our new hypothesis is that cationic polymers can increase antibiotic uptake, based on the observation of increased membrane potential. Additional approaches must be used in combination with cationic polymers to improve antibiotic sensitivity, such as efflux pump inhibiting molecules or metabolites that increased cellular activity to a rate beyond efflux activity. In this way, systematic studies may be conducted that control barriers to antibiotic efficacy in order to identify the effect of cationic polymers on dormant bacteria behavior. Characterizing antibiotic concentration in bacteria, and the use of antibiotics with external or internal cellular targets, would be essential studies to confirm the role of cationic polymers in antibiotic uptake.

Future Prospective of Cationic Polymers for Infection Prevention

Synthetic cationic polymers offer a potential platform for bacterial infection prevention. If the challenges of adequate antimicrobial efficacy with selectivity towards bacterial cells can be overcome, random amphiphilic methacrylate polymers have promising applications as topical therapeutic agents at infection sites, such as in creams or integrated into wound dressings. These would be a significant new contribution to the field of medicine, providing not only a new kind of therapeutic, but agents that have low chance of resistance development and can overcome current resistances against a broad spectrum of bacteria. Once the mechanism of cationic polymer related biofilm prevention and sensitization are addressed, there are many potential applications both alone and with traditional antibiotics. Alone they could be incorporated as anti-biofilm agents in products such as mouth wash to prevent oral biofilms associated with dental carries, where the agent could be delivered in high concentrations at

regular dosages and limited exposure to mammalian cells for long term biofilm prevention. In combination with traditional antibiotics, they could be used in the treatment of *P. aeruginosa* biofilms in cystic fibrosis lungs, simultaneously sensitizing existing biofilms to co-administered therapeutics and preventing new biofilm growth from developing. The future of these synthetic cationic polymers relies on 1) identifying new polymer designs for targeted application and 2) delineating the mechanisms of polymer activity for effective biofilm infection mitigation and treatment.

Appendices

Appendix A. Characterization of Chapter 2 Crosslinked Copolymers

^{1}H NMR spectra of Series a polymer

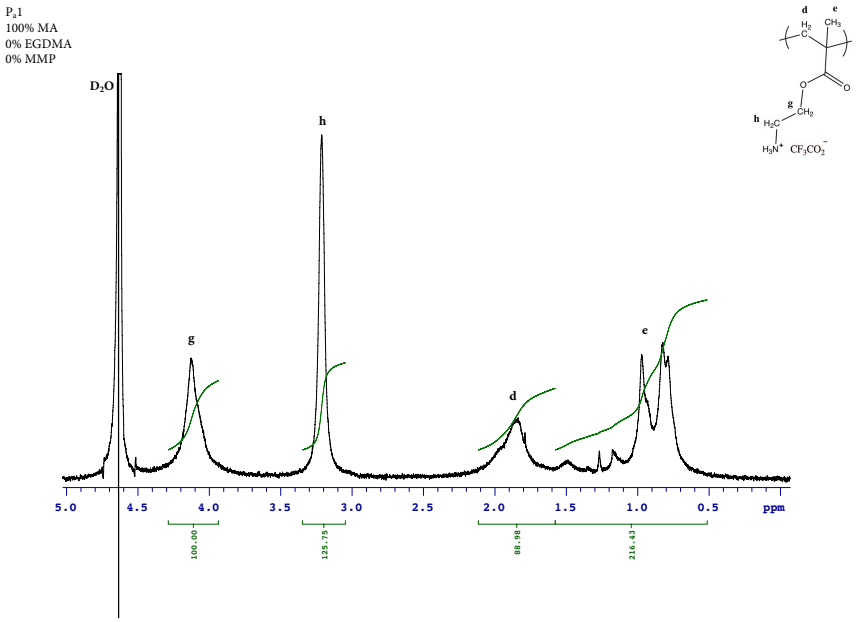

Figure A.1. ^{1}H NMR spectra of P_a1

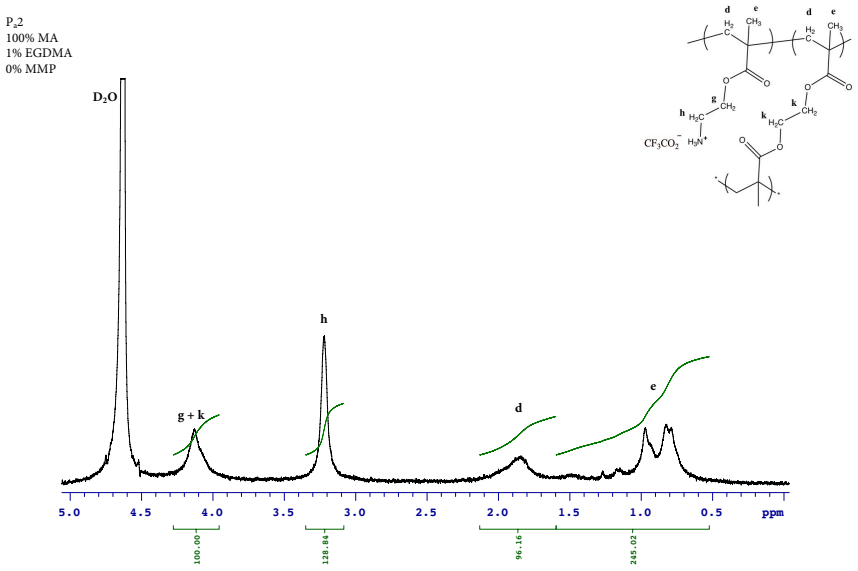

Figure A.2. ^{1}H NMR spectra of P_a2

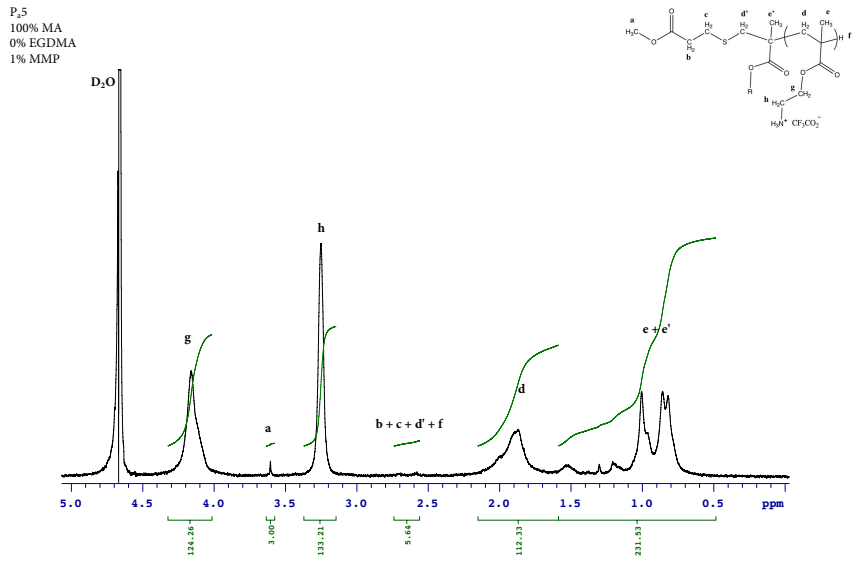

Figure A.3. ^{1}H NMR spectra of P_a5

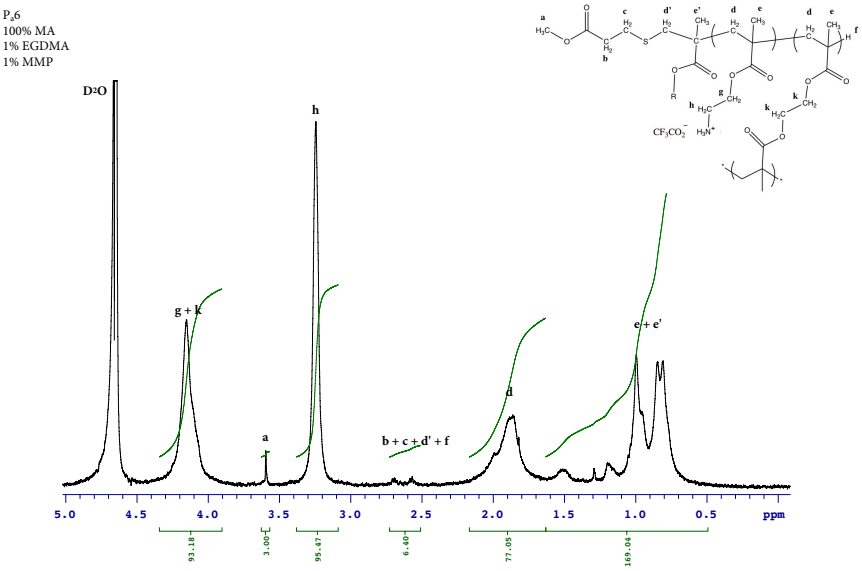

Figure A.4. ^{1}H NMR spectra of P_a6

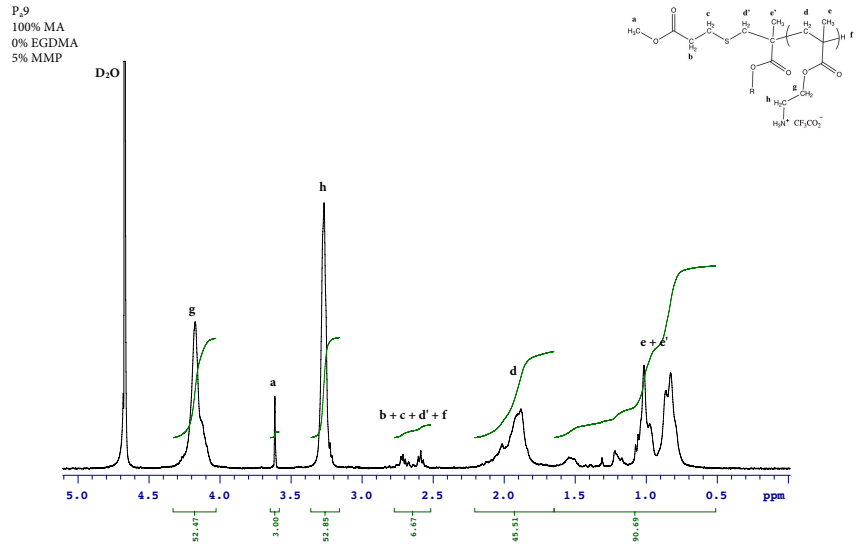

Figure A.5. ^{1}H NMR spectra of P_a9

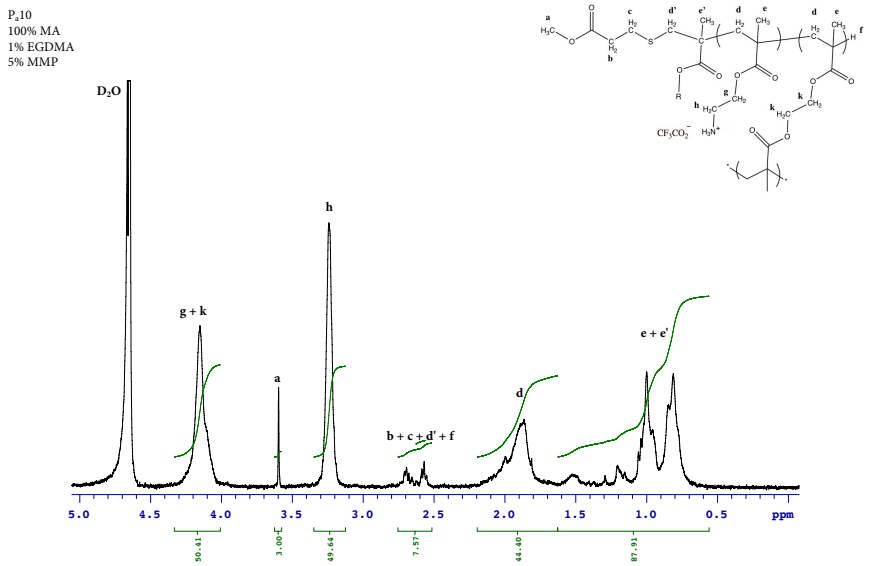

Figure A.6. ^{1}H NMR spectra of P$_a$10

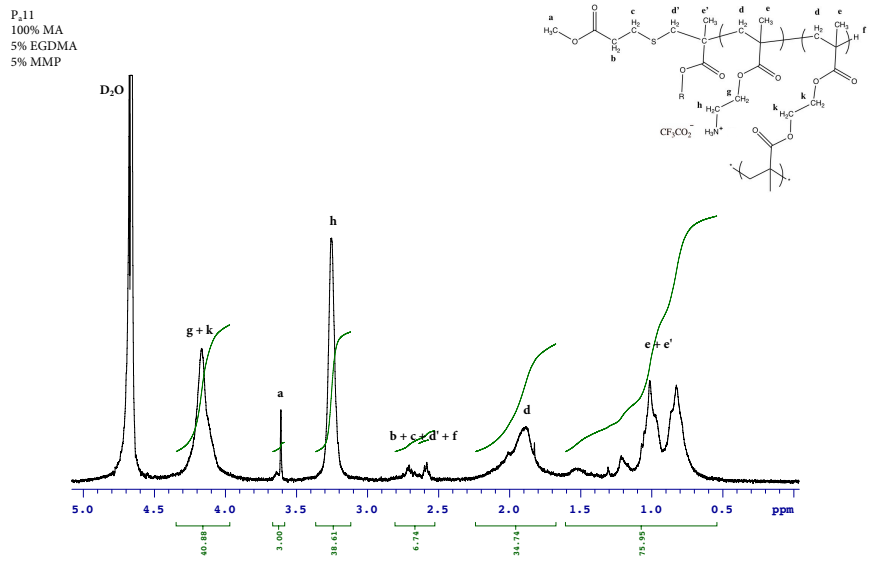

Figure A.7. ^{1}H NMR spectra of P$_a$11

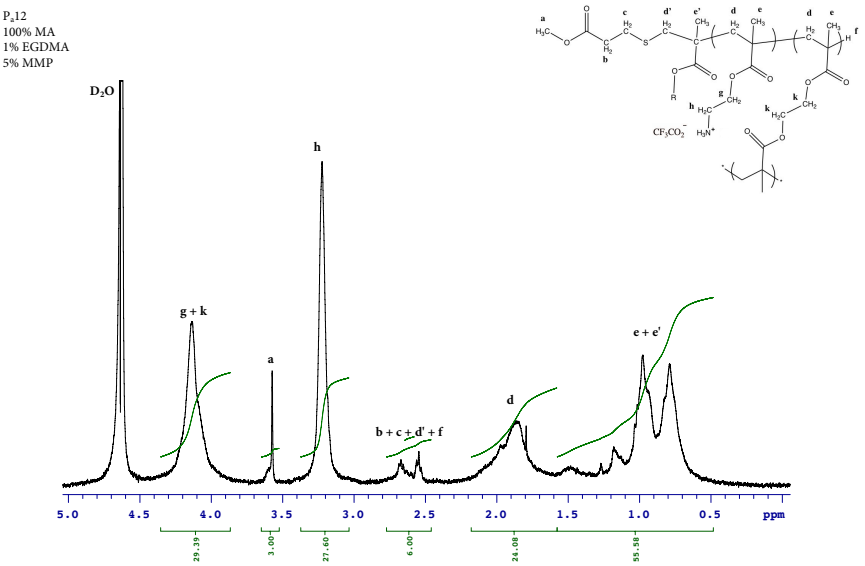

Figure A.8. ^{1}H NMR spectra of P$_a$12

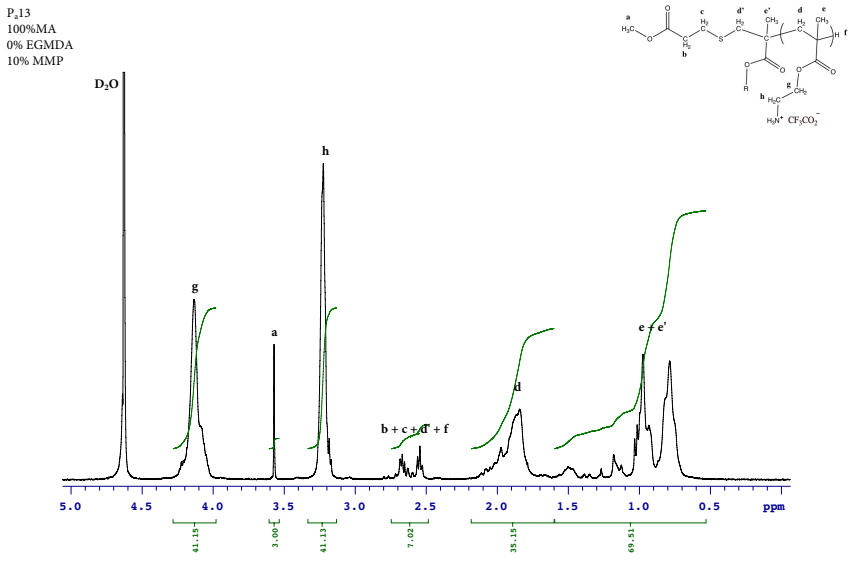

Figure A.9. ^{1}H NMR spectra of P$_a$13

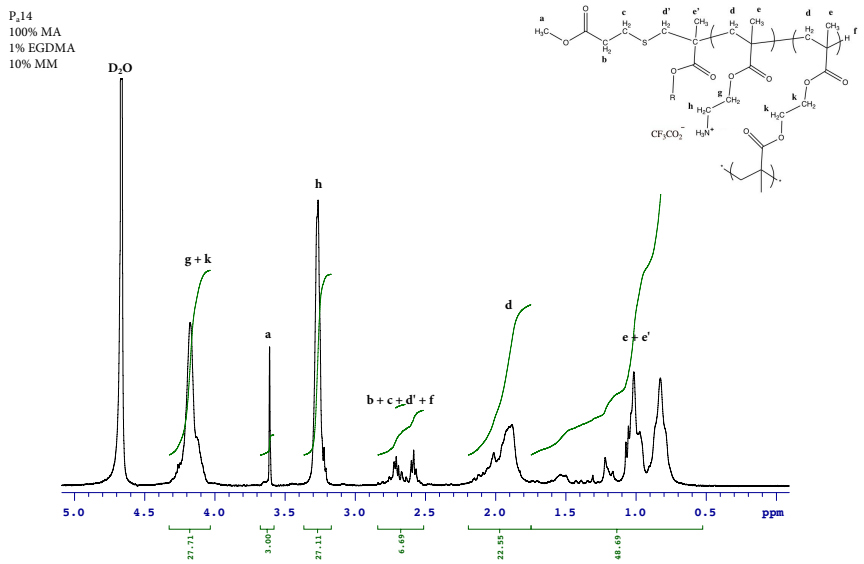

Figure A.10. ^{1}H NMR spectra of P$_a$14

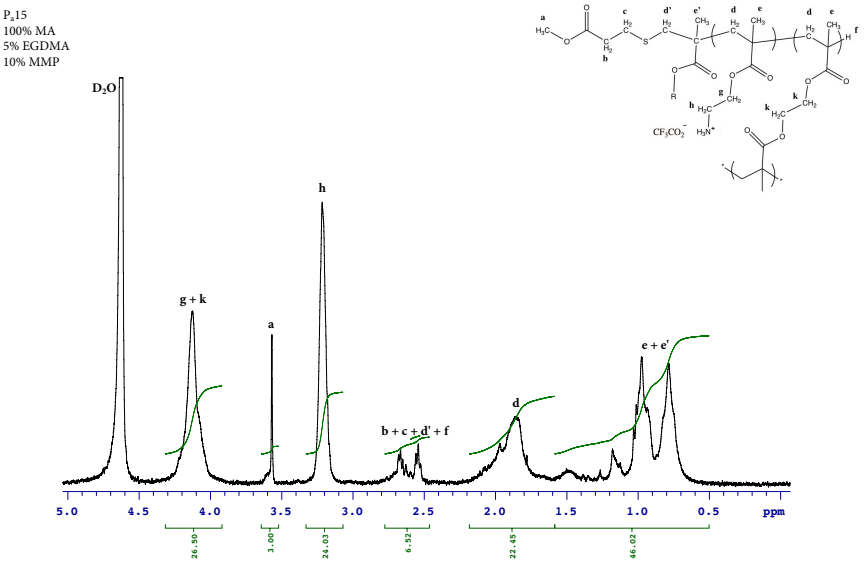

Figure A.11. ^{1}H NMR spectra of P$_a$15

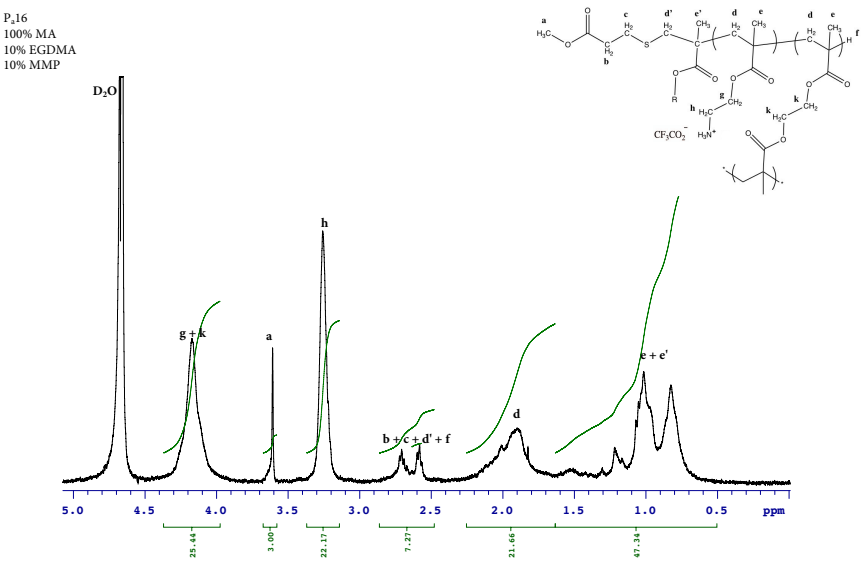

Figure A.12. ^{1}H NMR spectra of P$_a$16

A.A.2. ^{1}H NMR spectra of Series b copolymers

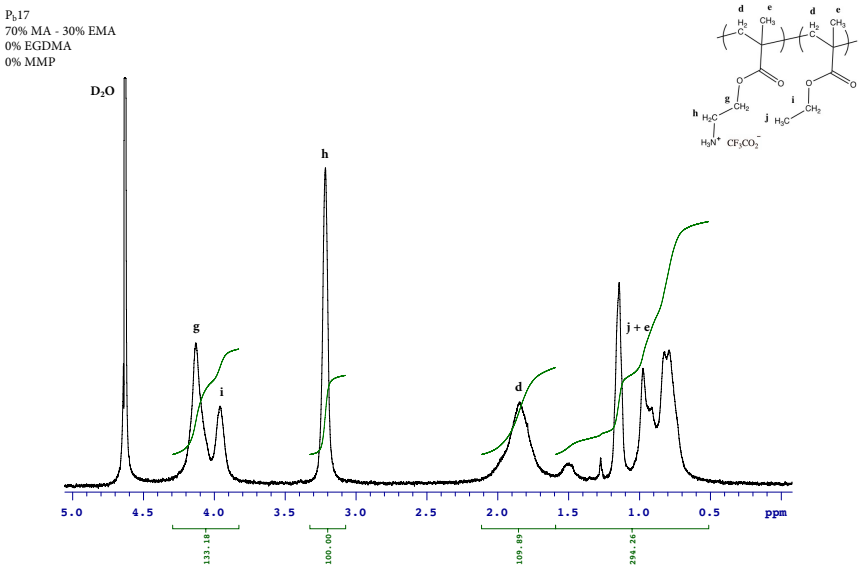

Figure A.13. ^{1}H NMR spectra of P_b17

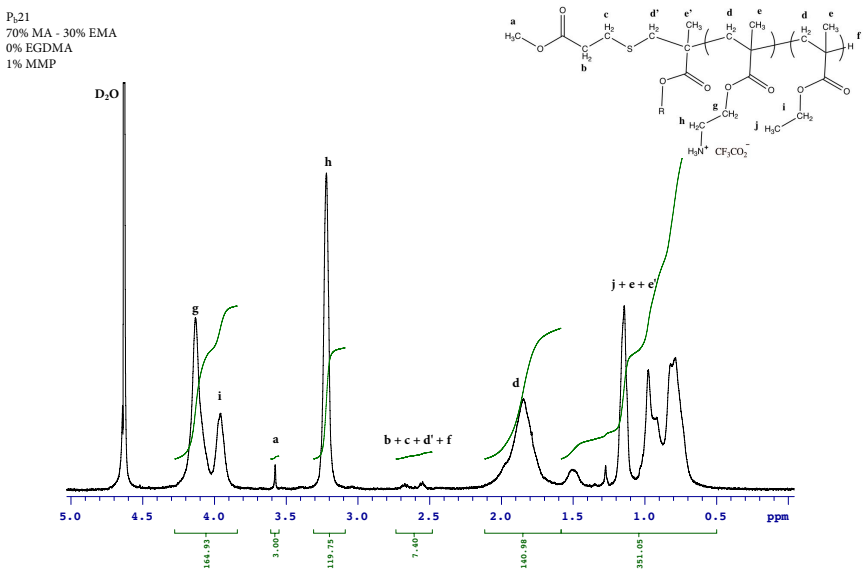

Figure A.14. ^{1}H NMR spectra of P_b21

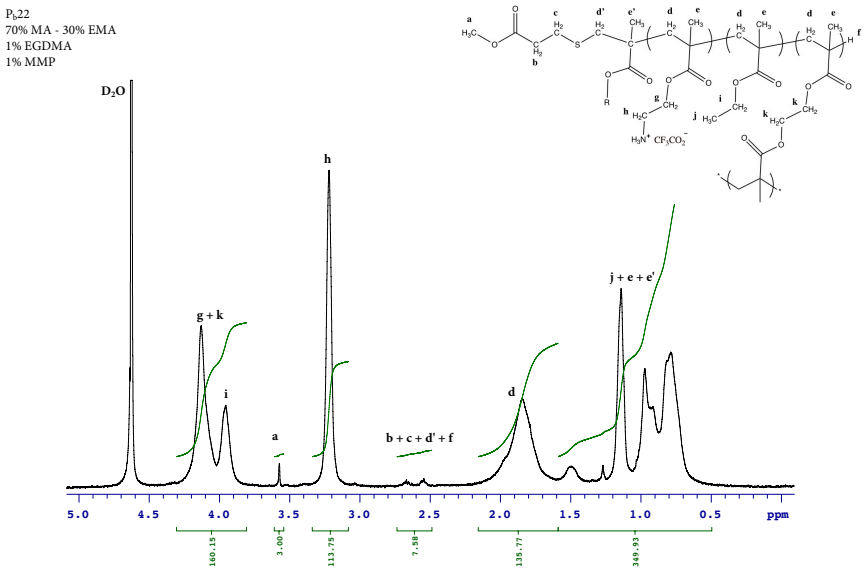

Figure A.15. ^{1}H NMR spectra of P_b22

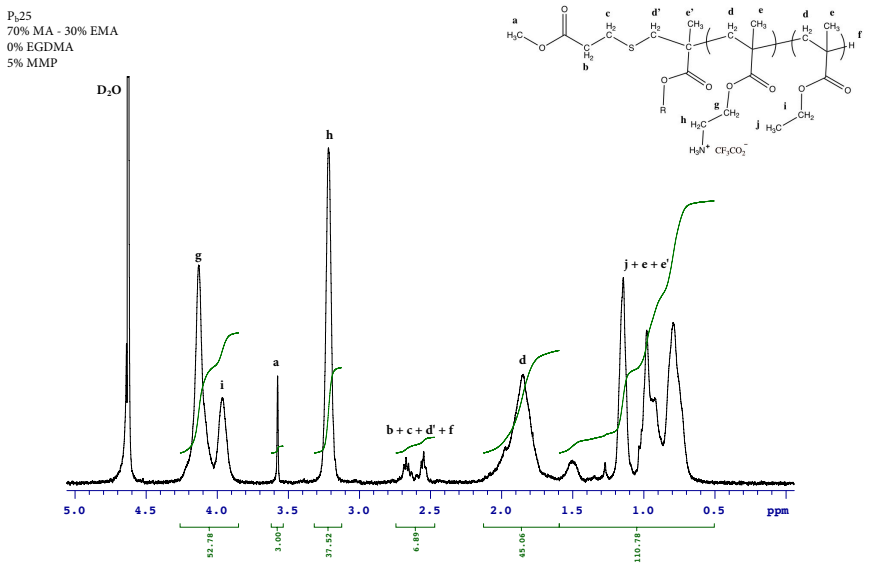

Figure A.16. ^{1}H NMR spectra of P_b25

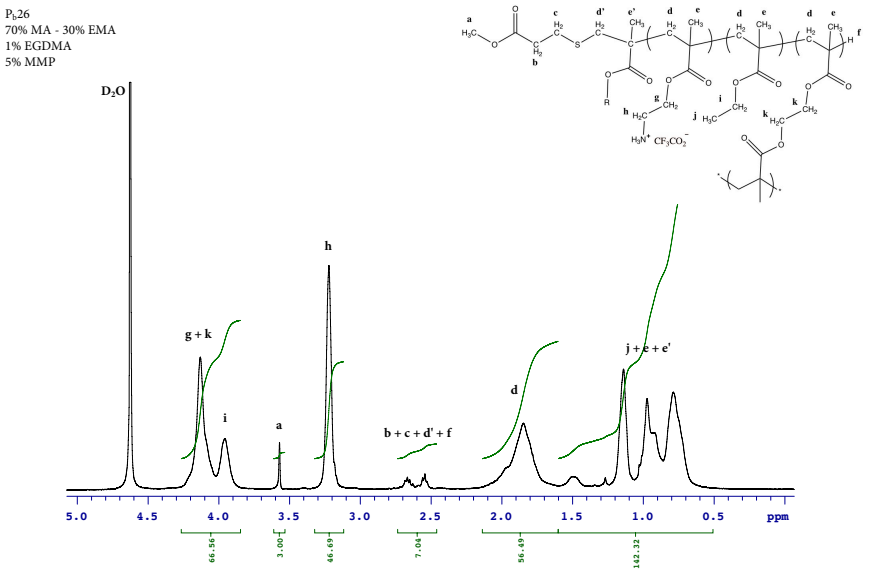

Figure A.17. ^{1}H NMR spectra of P_b26

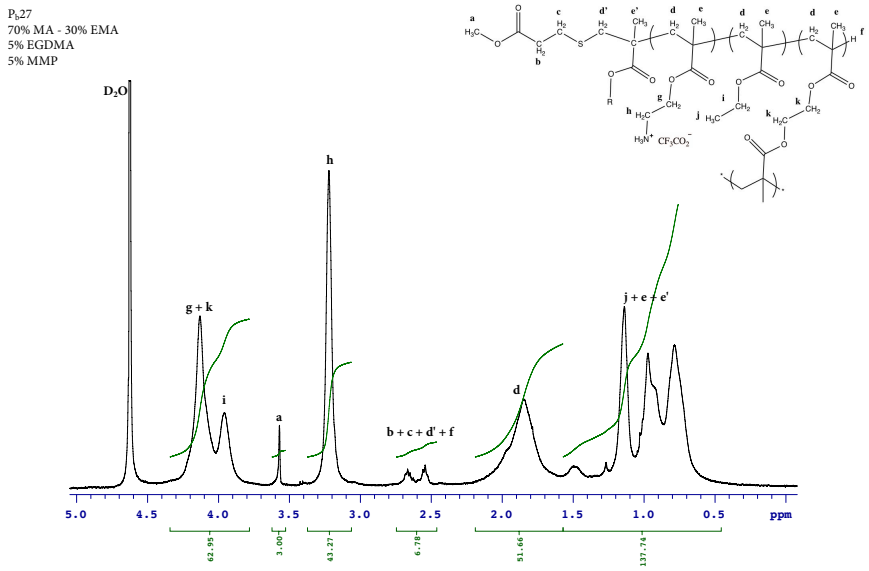

Figure A.18. ^{1}H NMR spectra of P_b27

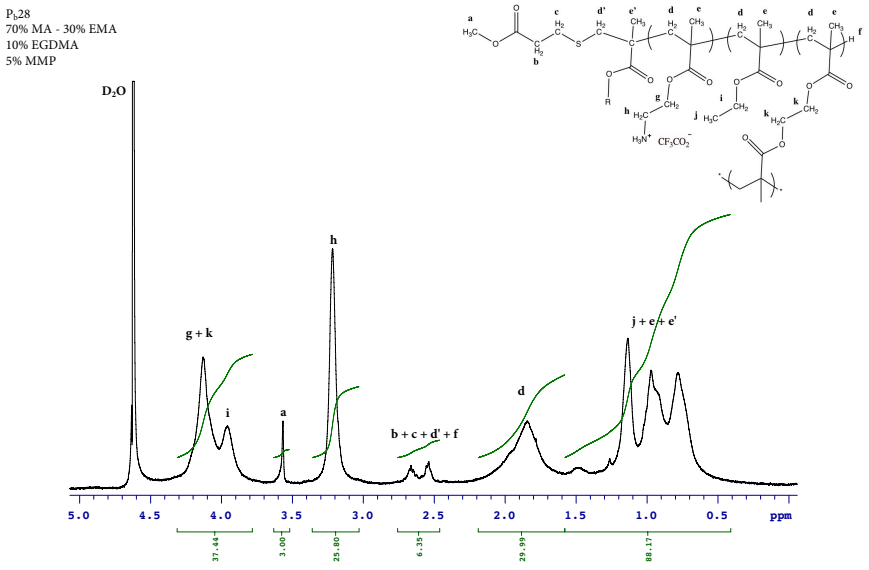

Figure A.19. ^{1}H NMR spectra of P_b28

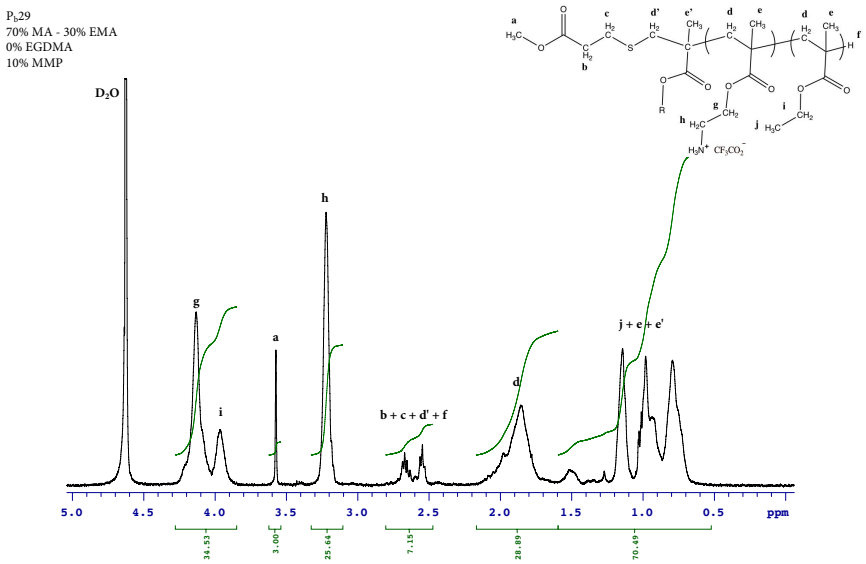

Figure A.20. ^{1}H NMR spectra of P_b29

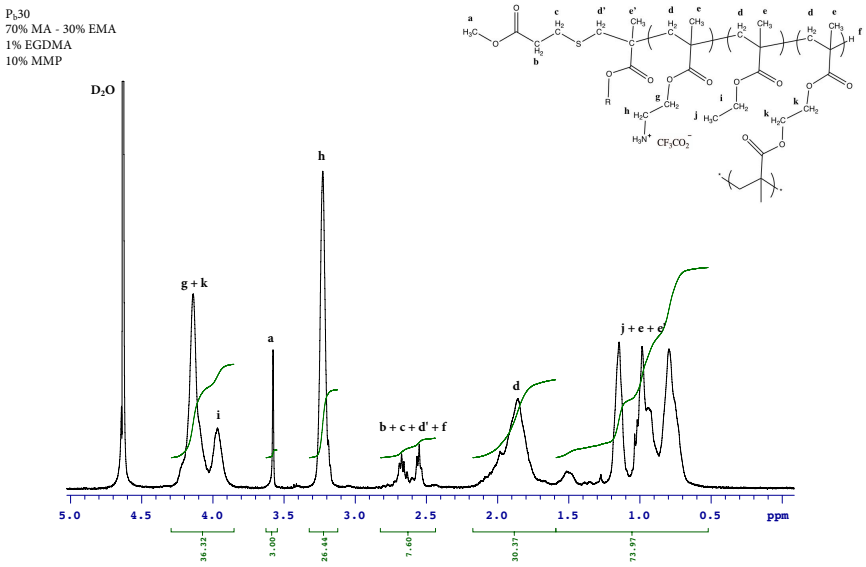

Figure A.21. ^{1}H NMR spectra of P_b30

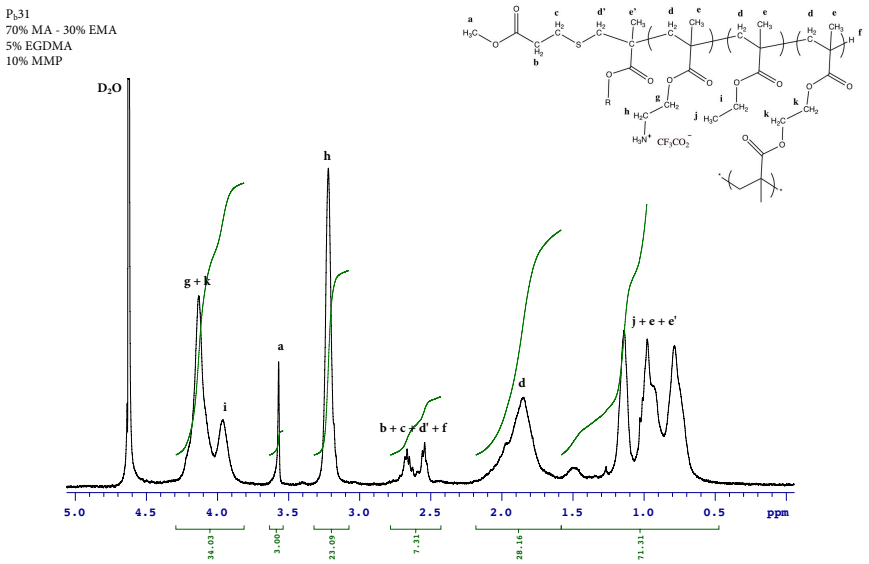

Figure A.22. ^{1}H NMR spectra of P_b31

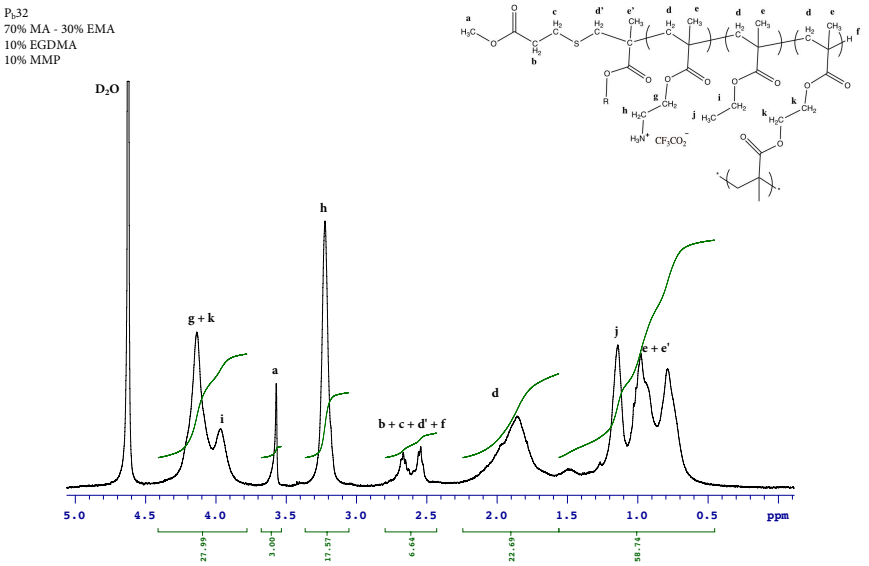

Figure A.23. ^{1}H NMR spectra of P_b32

A.A.3. 1H NMR spectra of Series c copolymers

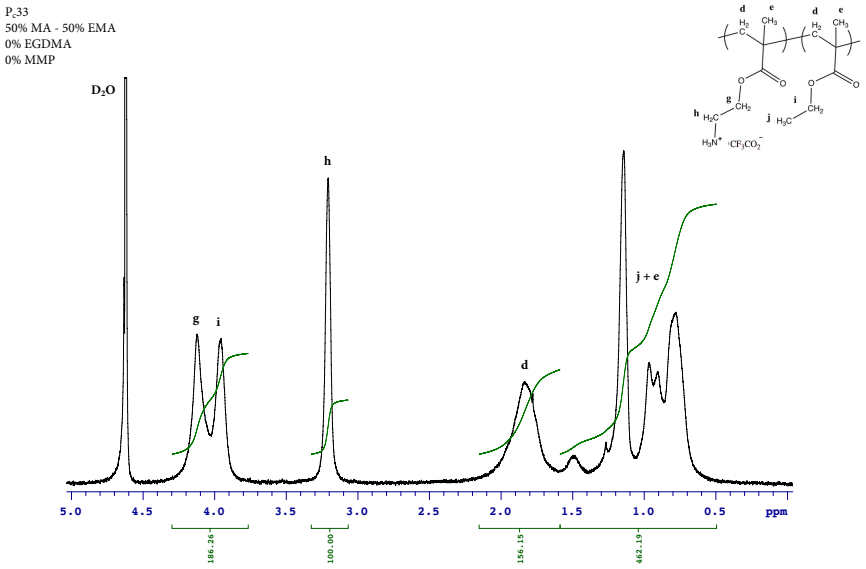

Figure A.24. ^{1}H NMR spectra of P_c33

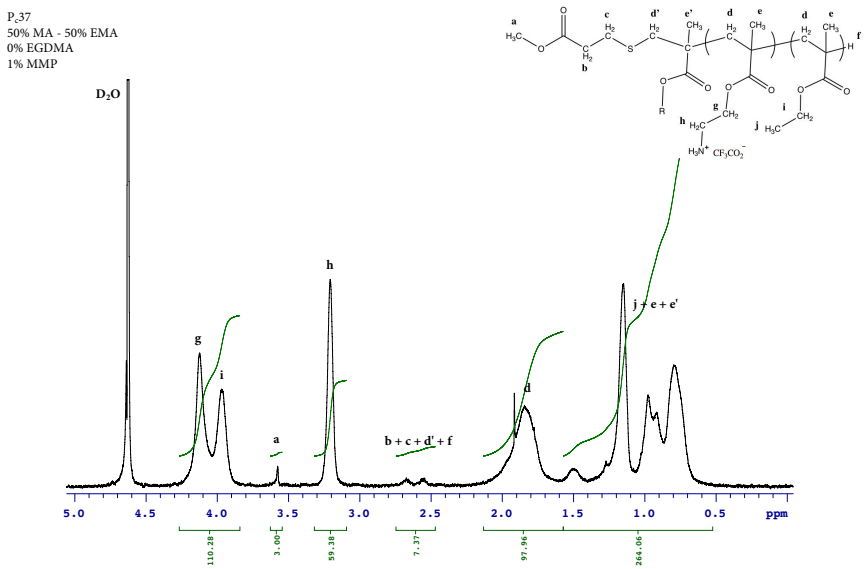

Figure A.25. ^{1}H NMR spectra of P_c37

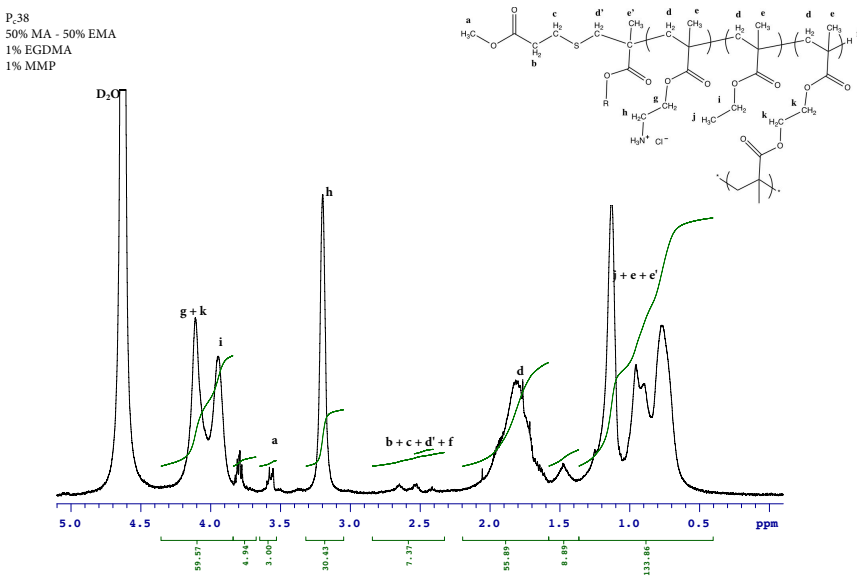

Figure A.26. ^{1}H NMR spectra of P_c38

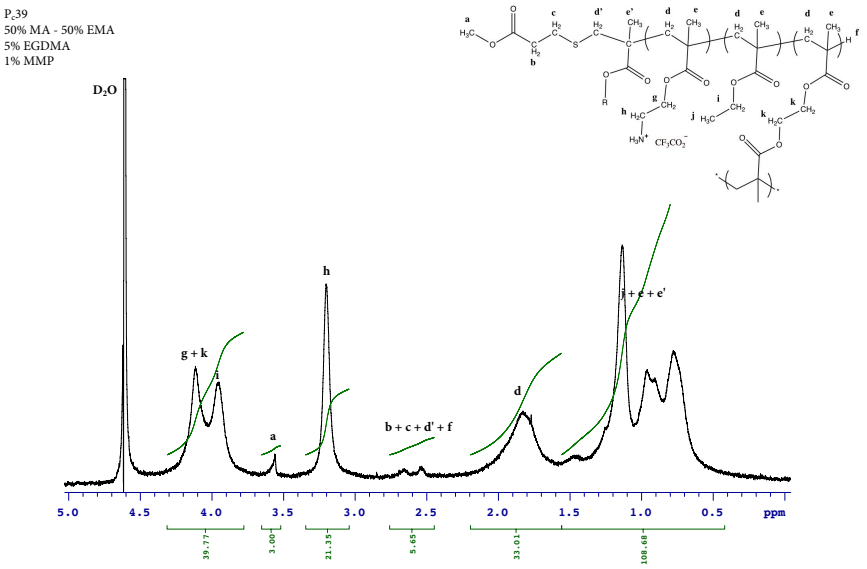

Figure A.27. ^{1}H NMR spectra of P_c39

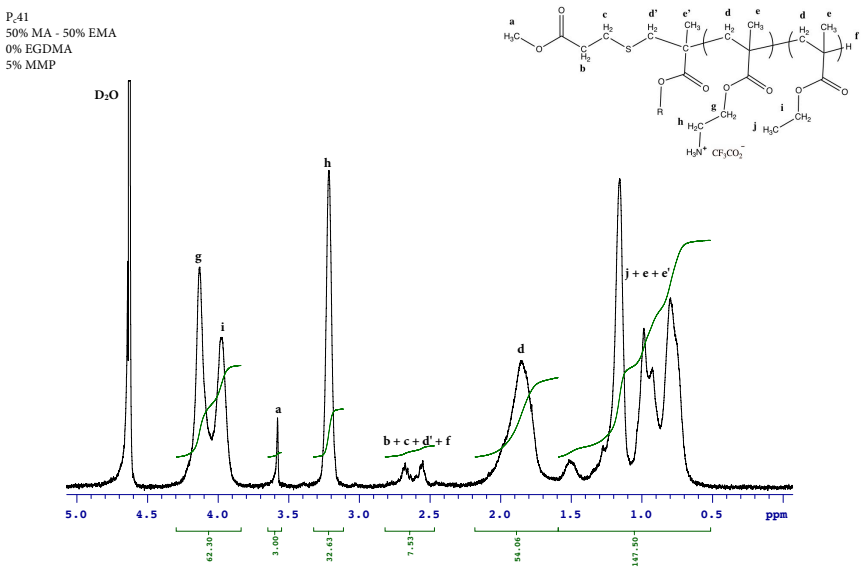

Figure A.28. ^{1}H NMR spectra of P_c41

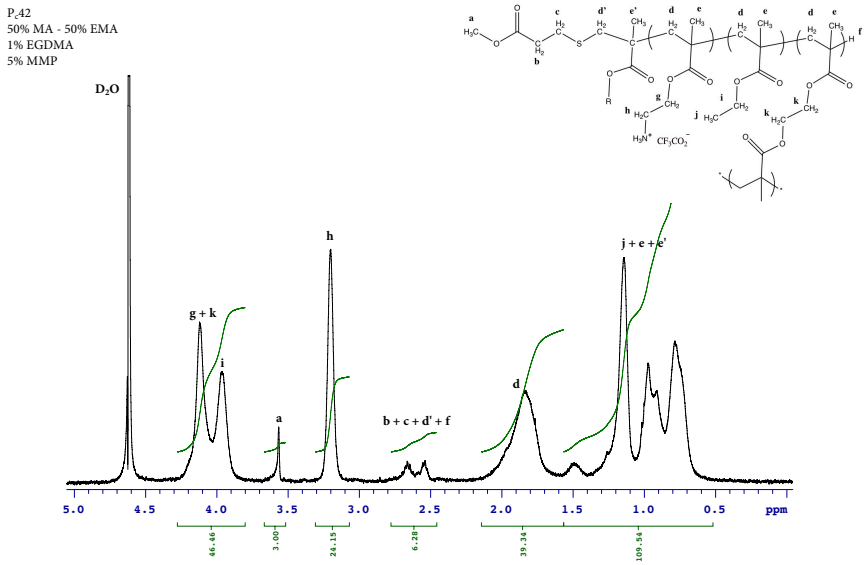

Figure A.29. ^{1}H NMR spectra of P_c42

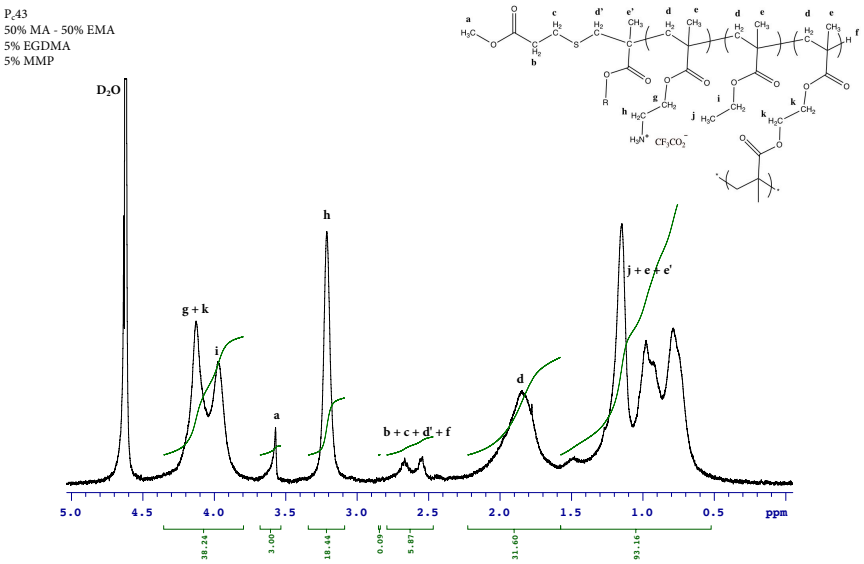

Figure A.30. ^{1}H NMR spectra of P_c43

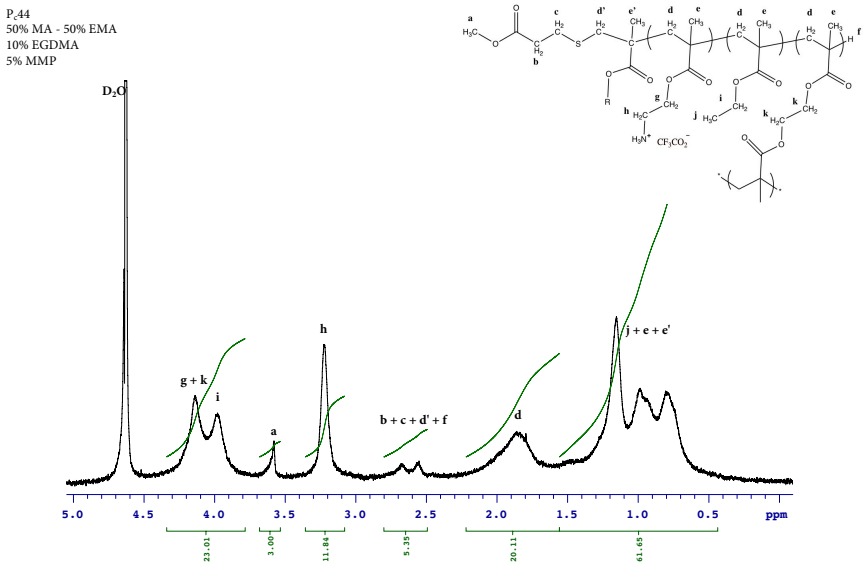

Figure A.31. ^{1}H NMR spectra of P_c44

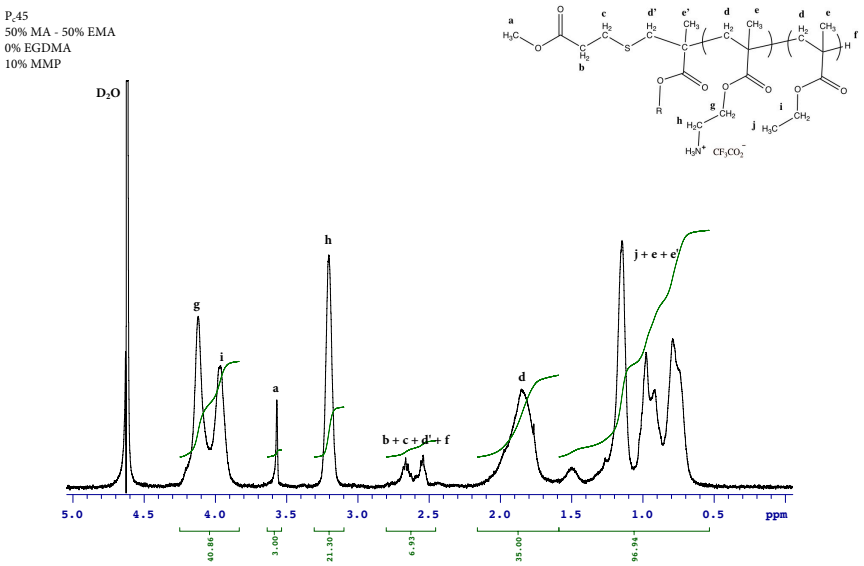

Figure A.32. ^{1}H NMR spectra of P_c45

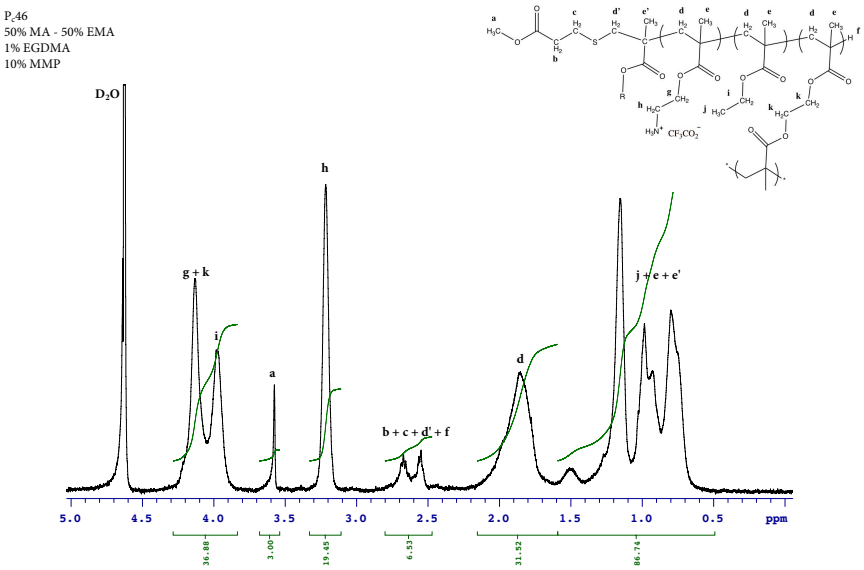

Figure A.33. ^{1}H NMR spectra of P_c46

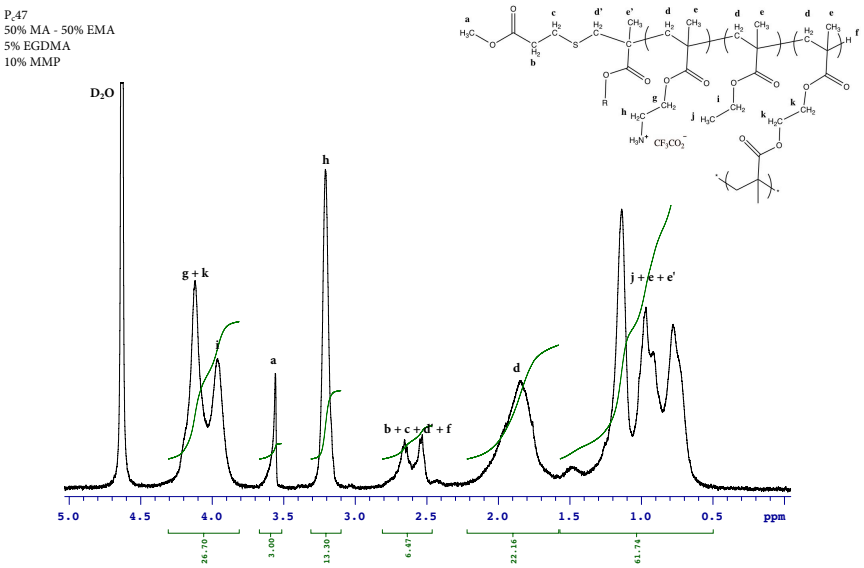

Figure A.34. ^{1}H NMR spectra of P_c47

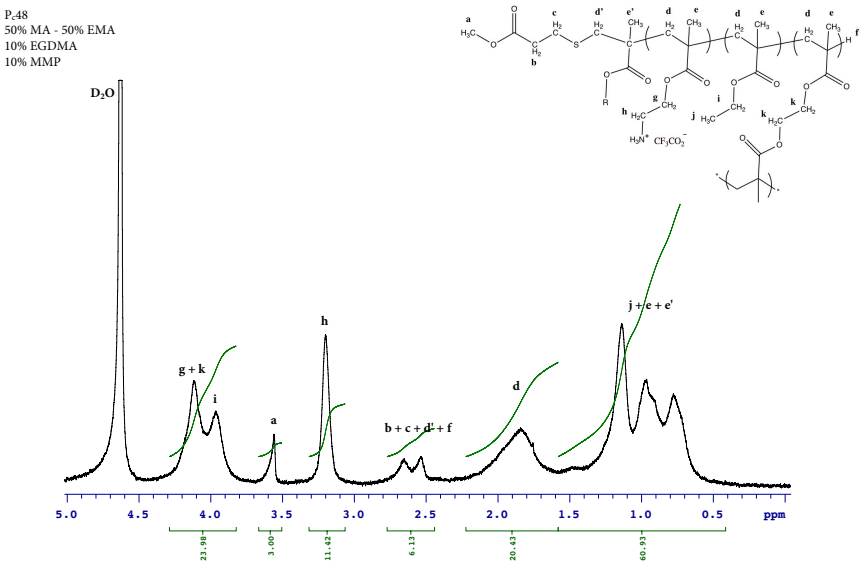

Figure A.35. ^{1}H NMR spectra of P_c48

A.A.4 ^{1}H NMR spectra of Series d copolymers

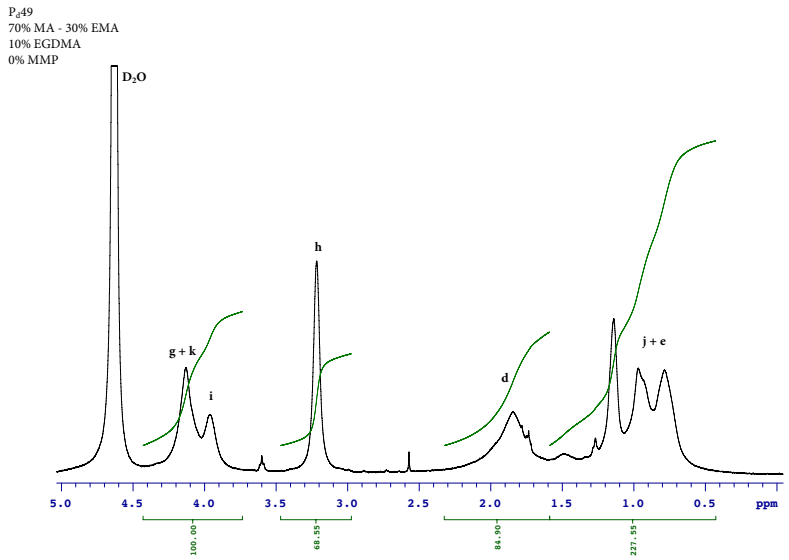

Figure A.36. ^{1}H NMR spectra of P$_d$49

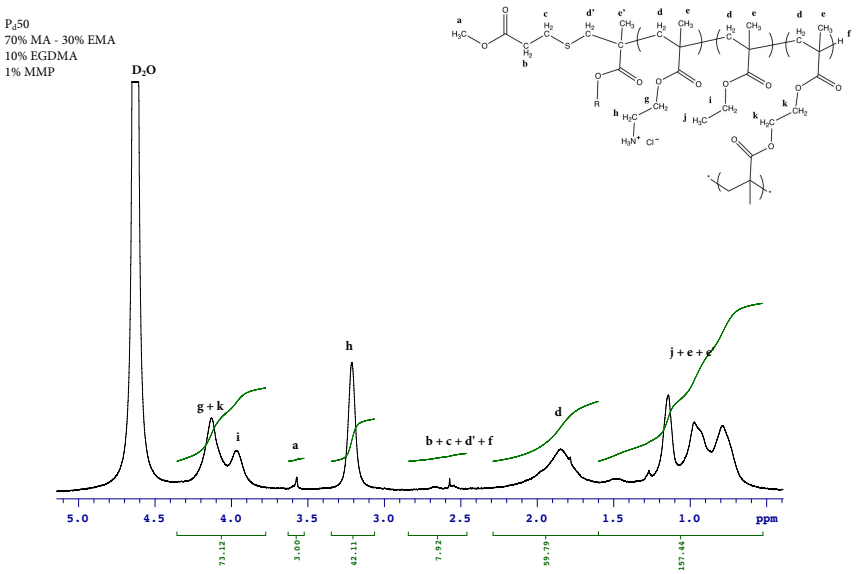

Figure A.37. ^{1}H NMR spectra of P$_d$50

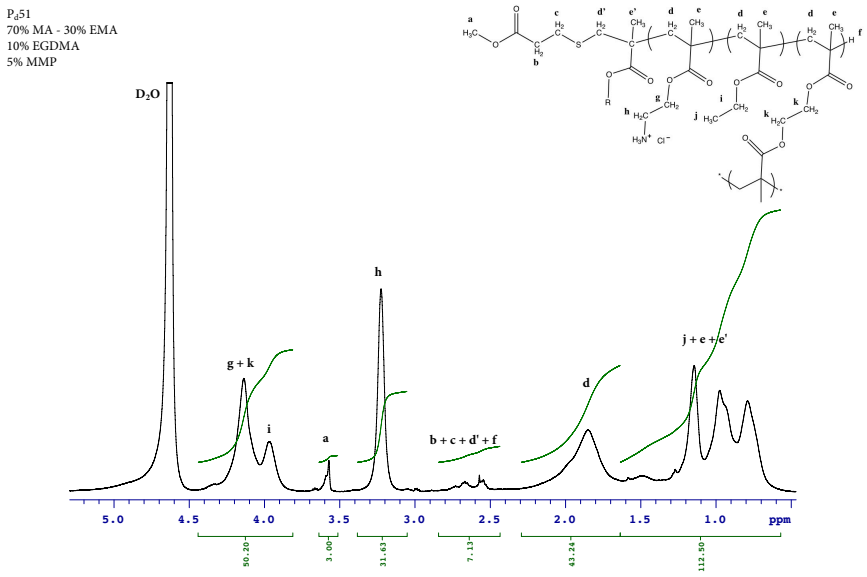

Figure A.38. ^{1}H NMR spectra of P_d51

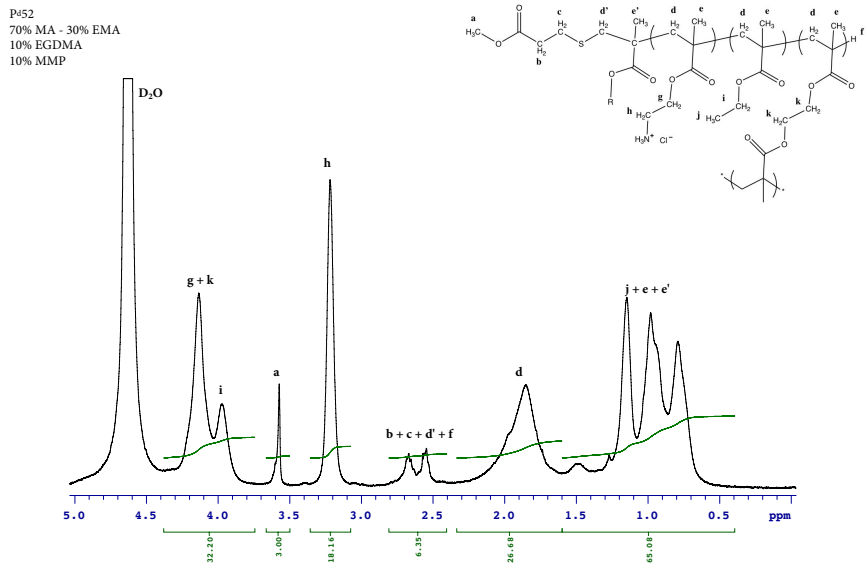

Figure A.39. ^{1}H NMR spectra of P_d52

A.A.5. Sample calculations of monomer conversion and monomer composition

Calculation of Conversion Rate

Calculated from crude polymer ^{1}H NMR

$$\%Conversion = 1 - \frac{1}{\left[\frac{\int d}{2}\right]}$$

Calculation of molar composition of final polymer products

$$F_{EMA} = \left(\frac{H_i}{H_i + H_{gk}}\right) \int g + k + i$$

$$F_{EGDMA} = \frac{\left(\left(\frac{H_{gk}}{H_i + H_{gk}}\right) \int g + k + i\right) - \int h}{\int g + k + i}$$

$$F_{MA} = 1 - F_{EMA} - F_{EGDMA}$$

H_i= height of peak i integration

H_{gk}= height of peak g + k integration

F_{MA}= mol fraction of MA

F_{EMA}= mol fraction of EMA

F_{EGDMA}= mol fraction of EGDMA

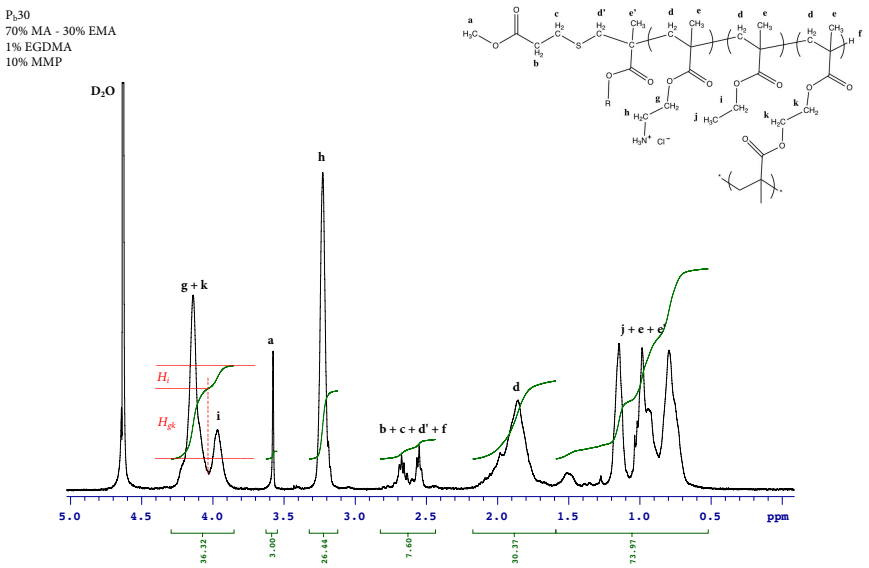

Figure A.40. Sample H NMR of calculation of molar composition of polymer P_b30

<u>Calculation of Apparent Degree of Polymerization (DP)</u>

$$DP = \frac{\int (g + k + i)}{(2f_{MA} + 2f_{EMA} + 4f_{EGDMA})}$$

f_{MA}= mol fraction of MA

f_{EMA} = mol fraction of EMA

f_{EGDMA} = mol fraction of EGDMA

Where the multiplier is the number of protons (2 or 4) on the associated carbon in MA, EMA or EDMA

A.A.6. Characterization Series a, Series c, and Series d polymers

Table A.1. Comparison of monomer feed composition to polymer composition calculated by H-NMR for Series a.

		Monomer Feed Composition (%)			Polymer Composition, H-NMR (%)		
		AEMA	**EMA**	**EGDMA**	**MA**	**EMA**	**EGDMA**
Series a	**P_a1**	100.0	0.0	0.0	100	0	0
	P_a2	99.0	0.0	1.0	99	0	1
	P_a3	95.2	0.0	4.8	Gel	Gel	Gel
	P_a4	90.9	0.0	9.1	Gel	Gel	Gel
	P_a5	100.0	0.0	0.0	100	0	0
	P_a6	99.0	0.0	1.0	99	0	1
	P_a7	95.2	0.0	4.8	Gel	Gel	Gel
	P_a8	90.9	0.0	9.1	Gel	Gel	Gel
	P_a9	100.0	0.0	0.0	100	0	0
	P_a10	99.0	0.0	1.0	98	0	2
	P_a11	95.2	0.0	4.8	94	0	6
	P_a12	90.9	0.0	9.1	96	0	4
	P_a13	100.0	0.0	0.0	100	0	0
	P_a14	99.0	0.0	1.0	98	0	2
	P_a15	95.2	0.0	4.8	90	0	10
	P_a16	90.9	0.0	9.1	87	0	13

Table A.2. Comparison of monomer feed composition to polymer composition calculated by H-NMR for Series c.

		Monomer Feed Composition (%)			Polymer Composition, H-NMR (%)		
		MA	EMA	EGDMA	MA	EMA	EGDMA
Series c	P_c33	50.0	50.0	0.0	53	47	0
	P_c34	49.5	49.5	1.0	Gel	Gel	Gel
	P_c35	47.6	47.6	4.8	Gel	Gel	Gel
	P_c36	45.5	45.5	9.1	Gel	Gel	Gel
	P_c37	50.0	50.0	0.0	59	41	0
	P_c38	49.5	49.5	1.0	51	50	1
	P_c39	47.6	47.6	4.8	54	45	1
	P_c40	45.5	45.5	9.1	Gel	Gel	Gel
	P_c41	50.0	50.0	0.0	60	40	0
	P_c42	49.5	49.5	1.0	52	44	4
	P_c43	47.6	47.6	4.8	48	43	9
	P_c44	45.5	45.5	9.1	52	42	6
	P_c45	50.0	50.0	0.0	53	47	0
	P_c46	49.5	49.5	1.0	53	41	6
	P_c47	47.6	47.6	4.8	50	40	10
	P_c48	45.5	45.5	9.1	47	42	11

Table A.3. Comparison of monomer feed composition to polymer composition calculated by H-NMR for Series d.

		Monomer Feed Composition (%)			**Polymer Composition, H-NMR (%)**		
		MA	EMA	EGDMA	MA	EMA	EGDMA
Series d	P_d49	63.6	27.3	9.1	69	26	5
	P_d50				58	32	10
	P_d51				63	34	3
	P_d52				57	29	14

Table A.4. Polymerization conversion and yield of Series a homopolymer.

						Boc-Protected	Deprotected
				State	% Conversion	% Yield	% Yield
Series a	P_a1	0% MMP	0% EGDMA	Liquid	96	89	86
	P_a2		1% EGDMA	Liquid	95	93	71
	P_a3		5% EGDMA	Gel	Gel	Gel	Gel
	P_a4		10% EGDMA	Gel	Gel	Gel	Gel
	P_a5	1% MMP	0% EGDMA	Liquid	96	100	100
	P_a6		1% EGDMA	Liquid	95	99	80
	P_a7		5% EGDMA	Gel	Gel	Gel	Gel
	P_a8		10% EGDMA	Gel	Gel	Gel	Gel
	P_a9	5% MMP	0% EGDMA	Liquid	94	100	100
	P_a10		1% EGDMA	Liquid	92	100	80
	P_a11		5% EGDMA	Liquid	89	100	96
	P_a12		10% EGDMA	Liquid	94	93	86
	P_a13	10 %MMP	0% EGDMA	Liquid	92	97	100
	P_a14		1% EGDMA	Liquid	85	86	98
	P_a15		5% EGDMA	Liquid	88	95	88
	P_a16		10% EGDMA	Liquid	98	99	84

Table A.5. Polymerization conversion and yield of Series c copolymer.

						Boc-Protected	Deprotected
				State	% Conversion	% Yield	% Yield
Series c	P_c33	0% MMP	0% EGDMA	Liquid	98	100	100
	P_c34		1% EGDMA	Gel	Gel	Gel	Gel
	P_c35		5% EGDMA	Gel	Gel	Gel	Gel
	P_c36		10% EGDMA	Gel	Gel	Gel	Gel
	P_c37	1% MMP	0% EGDMA	Liquid	99	100	100
	P_c38		1% EGDMA	Liquid	97	100	84
	P_c39		5% EGDMA	Liquid	96	100	92
	P_c40		10% EGDMA	Gel	Gel	Gel	Gel
	P_c41	5% MMP	0% EGDMA	Liquid	98	100	100
	P_c42		1% EGDMA	Liquid	96	91	99
	P_c43		5% EGDMA	Liquid	96	87	100
	P_c44		10% EGDMA	Liquid	97	86	100
	P_c45	10 %MMP	0% EGDMA	Liquid	98	86	100
	P_c46		1% EGDMA	Liquid	99	76	100
	P_c47		5% EGDMA	Liquid	99	95	90
	P_c48		10% EGDMA	Liquid	99	82	90

Table A.6. Polymerization conversion and yield of Series d copolymer.

						Boc-Protected	Deprotected
				State	% Conversion	% Yield	% Yield
Series d	P_d49	0% MMP	10% EGDMA	Liquid	90	82	97
	P_d50	1% MMP		Liquid	87	72	100
	P_d51	5% MMP		Liquid	90	76	100
	P_d52	10% MMP		Liquid	87	76	97

Table A.7. Characterization by GPC of Series a homopolymers

		MW (g/mol) (^{1}H NMR)	M_n (g/mol) (GPC)	M_w (g/mol) (GPC)	$Đ$ (GPC)
Series a	P_a1	No CTA	32595	129391	3.97
	P_a2	No CTA	65237	371016	5.69
	P_a5	14369.1779	13399	29018	2.17
	P_a6	10759.748	14299	41408	2.90
	P_a9	6067.52586	4500	7410	1.65
	P_a10	5812.64805	4249	7586	1.79
	P_a11	4686.74156	7357	22638	3.08
	P_a12	3379.1705	9376	61641	6.57
	P_a13	4758.5037	3419	5042	1.47
	P_a14	3195.16916	2837	4087	1.44
	P_a15	3020.6078	3588	6304	1.76
	P_a16	2887.16932	4594	12715	2.77

Table A.8. Characterization by GPC of Series c copolymers

		MW (g/mol) (^{1}H NMR)	M_n (g/mol) (GPC)	M_w (g/mol) (GPC)	$Đ$ (GPC)
Series c	P_c33	No CTA	15772	51085	3.23896779
	P_c37	10104.5087	6125	20924	3.41616327
	P_c38	5272.09273	6680	17002	2.54520958
	P_c39	3544.22366	6270	78854	12.5763955
	P_c41	5744.78268	3373	5137	1.52297658
	P_c42	4144.59625	2877	4550	1.58150852
	P_c43	3402.1019	6108	21784	3.5664702
	P_c44	2072.01829	10252	256014	24.972103
	P_c45	3600.2555	2537	3443	1.3571147
	P_c46	3342.59151	2961	5082	1.71631206
	P_c47	2417.91996	5332	15679	2.94054764
	P_c48	2139.54836	15772	51085	3.23896779

Table A.9. Characterization by GPC of Series d copolymers

		MW (g/mol) (^{1}H NMR)	M_n (g/mol)	M_w (g/mol)	Đ
Series d	P_d49	No CTA	7299	63064	8.64
	P_d50	6869.00305	12926	44294	3.43
	P_d51	4780.53194	7214	18491	2.56
	P_d52	2441.55405	4826	8697	1.80

Table A.10. Degree of polymerization and average crosslink density as determined by ^{1}H-NMR for Series a homopolymer. Average crosslink/CTA ratio denoted by * are theoretical calculations of gelled polymers based on linear comparable compositions.

		Apparent DP	**Average #Crosslink/CTA Ratio**
Series a	**P_a1**	No CTA	No CTA
	P_a2	No CTA	No CTA
	P_a3	Gel	No CTA
	P_a4	Gel	No CTA
	P_a5	62	No EGDMA
	P_a6	46	0.5
	P_a7	Gel	3.1*
	P_a8	Gel	6.2*
	P_a9	26	No EGDMA
	P_a10	25	0.5
	P_a11	19	1.1
	P_a12	14	0.6
	P_a13	21	No EGDMA
	P_a14	14	0.3
	P_a15	12	1.3
	P_a16	11	1.7

Table A.11. Degree of polymerization and average crosslink density as determined by ^{1}H-NMR for Series c copolymers. Average crosslink/CTA ratio denoted by * are theoretical calculations of gelled polymers based on linear comparable compositions.

		Apparent DP	**Average #Crosslink/CTA Ratio**
Series c	**P_c33**	No CTA	No CTA
	P_c34	Gel	No CTA
	P_c35	Gel	No CTA
	P_c36	Gel	No CTA
	P_c37	55	No EGDMA
	P_c38	29	0.3
	P_c39	20	0.2
	P_c40	Gel	11.0*
	P_c41	31	No EGDMA
	P_c42	22	0.9
	P_c43	18	1.7
	P_c44	11	0.7
	P_c45	20	No EGDMA
	P_c46	17	1.1
	P_c47	12	1.4
	P_c48	11	1.3

Table A.12. Degree of polymerization and average crosslink density as determined by ^{1}H-NMR for Series d copolymers. Average crosslink/CTA ratio denoted by * are theoretical calculations of gelled polymers based on linear comparable compositions.

		Apparent DP	Average #Crosslinks/CTA Ratio
Series d	P_d49	No CTA	No CTA
	P_d50	33	3.6
	P_d51	24	0.8
	P_d52	14	1.6

A.A.7. Antimicrobial activity of Series a, Series c, and Series d polymers

Table A.13. Antimicrobial activity (MIC) and hemotoxicity (HC_{50}) of Series a polymer

		MIC (μg/mL)		HC_{50} (μg/mL)	*%Hemolysis at 1000 μg/mL*	Selectivity Index (HC_{50}/MIC *E. coli*)
		E. coli	*S. aureus*			
Series a	P_a1	208 (±72)	83 (±36)	N/A	8 (±2)%*	No HC_{50}
	P_a2	208 (±72)	62.5	N/A	3 (±2)%*	No HC_{50}
	P_a5	167 (±72)	42 (±18)	N/A	12 (±2)%	No HC_{50}
	P_a6	417 (±144)	62.5	N/A	11 (±3)%*	No HC_{50}
	P_a9	208 (±72)	83 (±36)	N/A	1 (±1)%	No HC_{50}
	P_a10	>1000	83 (±36)	N/A	0%	No HC_{50}
	P_a11	>1000	83 (±36)	N/A	4 (±1)%*	No HC_{50}
	P_a12	>1000	104 (±36)	N/A	2 (±1)%*	No HC_{50}
	P_a13	208 (±72)	104 (±36)	N/A	0%	No HC_{50}
	P_a14	>1000	167 (±72)	N/A	0%	No HC_{50}
	P_a15	>1000	167 (±72)	N/A	0%	No HC_{50}
	P_a16	>1000	104 (±36)	N/A	2 (±1)%	No HC_{50}

Table A.14. Antimicrobial activity (MIC) and hemotoxicity (HC_{50}) of Series c copolymer

		MIC (μg/mL)		HC_{50} (μg/mL)	Selectivity Index (HC_{50}/MIC *E. coli*)
		E. coli	*S. aureus*		
Series c	P_c33	31	167 (±72)	6	0.19
	P_c37	16	104 (±36)	8 (±1)	0.50
	P_c38	16	125	9 (±2)	0.56
	P_c39	42 (±18)	167 (±72)	9 (±2)	0.21
	P_c41	16	42 (±18)	13 (±2)	0.81
	P_c42	13 (±5)	52 (±18)	9 (±2)	0.69
	P_c43	8	83 (±36)	9 (±2)	1.13
	P_c44	26 (±9)	167 (±72)	9 (±2)	0.35
	P_c45	10 (±5)	26 (±9)	27 (±4)	2.70
	P_c46	13 (5)	52 (18)	17 (1)	1.31
	P_c47	8	63	16 (1)	2.00
	P_c48	16	125	12 (1)	0.75

Table A.15. Antimicrobial activity (MIC) and hemotoxicity (HC_{50}) of Series d copolymer

		MIC (μg/mL)		HC_{50} (μg/mL)	Selectivity Index (HC_{50}/MIC *E. coli*)
		E. coli	*S. aureus*		
Series d	P_d49	62.5	125	5 (±1)	0.08
	P_d50	62.5	125	7 (±1)	0.11
	P_d51	62.5	125	11(±3)	0.18
	P_d52	62.5	125	25 (±3)	0.40

Appendix B. Characterization of Chapter 3 Copolymers

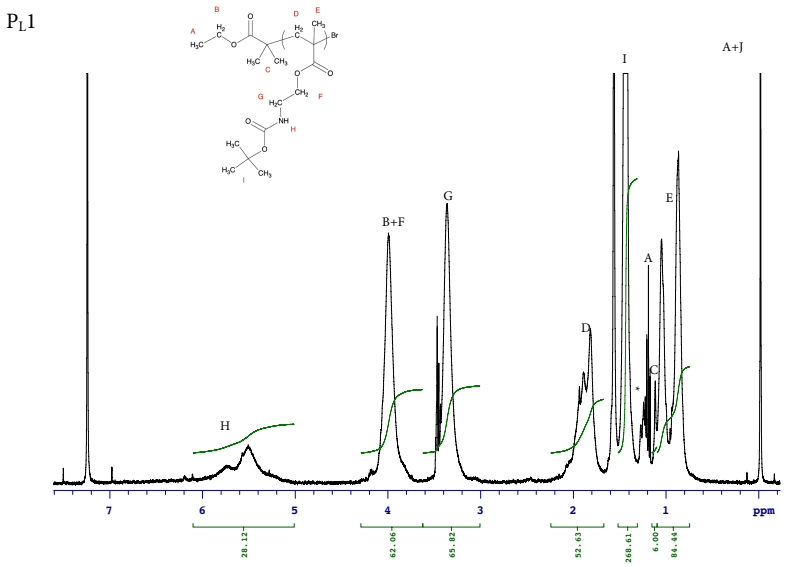

*H substitution of Br terminated polymer chains

Figure B.41. ^{1}H NMR spectra of boc-protected P_L1

P_L2

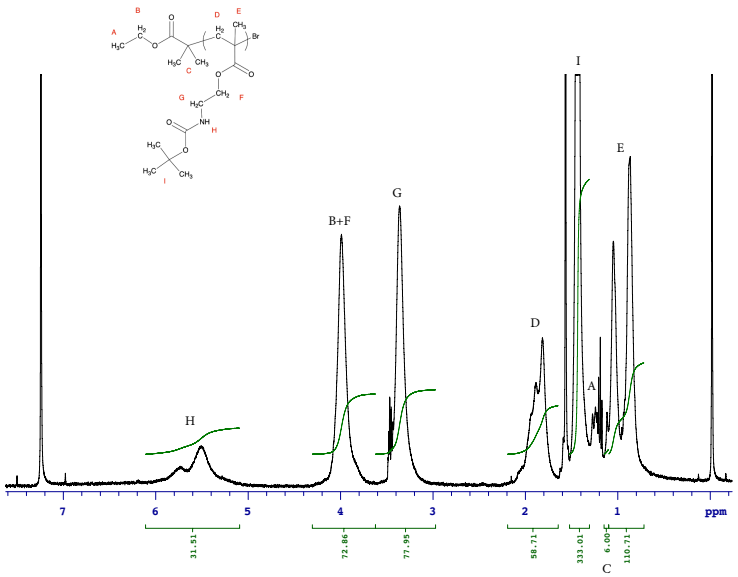

Figure B.42. ^{1}H NMR spectra of boc-protected P_L2

P_L3

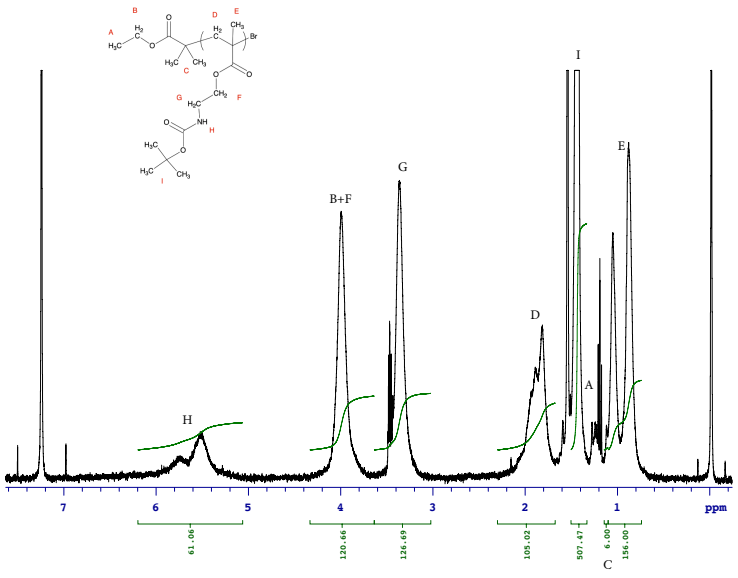

Figure B.43. ^{1}H NMR spectra of boc-protected P_L3

P_L4

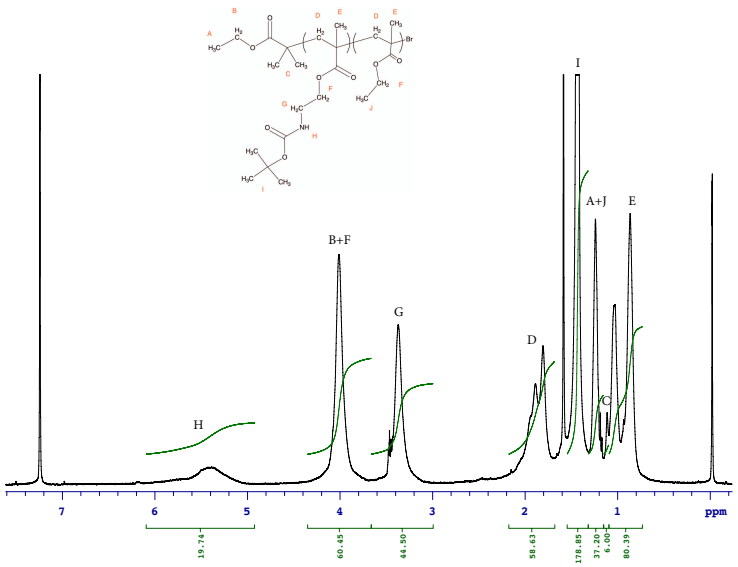

Figure B.44. ^{1}H NMR spectra of boc-protected P_L4

P_L5

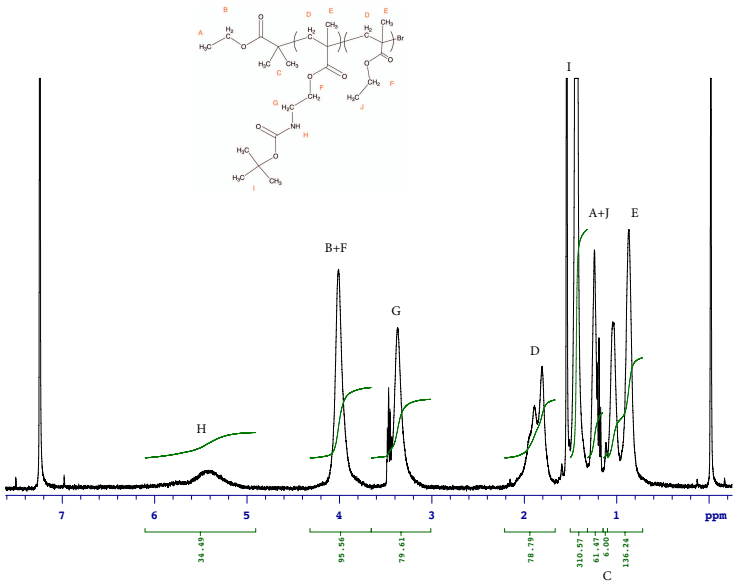

Figure B.45. ^{1}H NMR spectra of boc-protected P_L5

P_L6

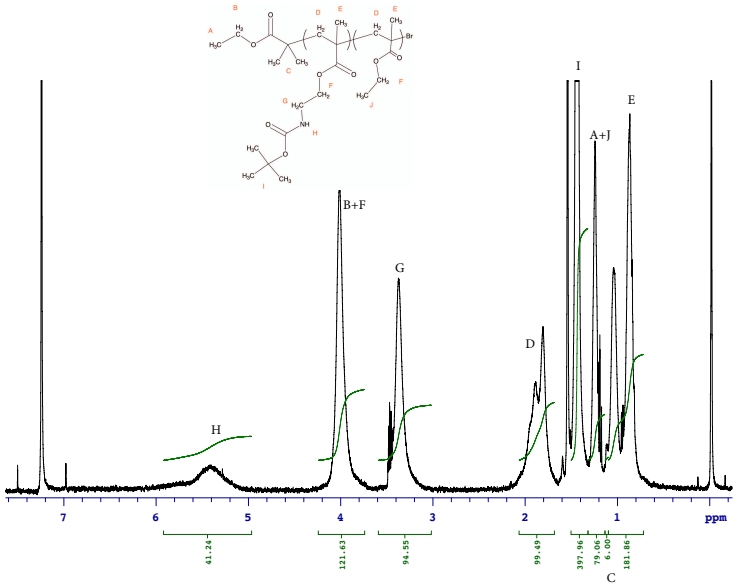

Figure B.46. ^{1}H NMR spectra of boc-protected P_L6

P_L7

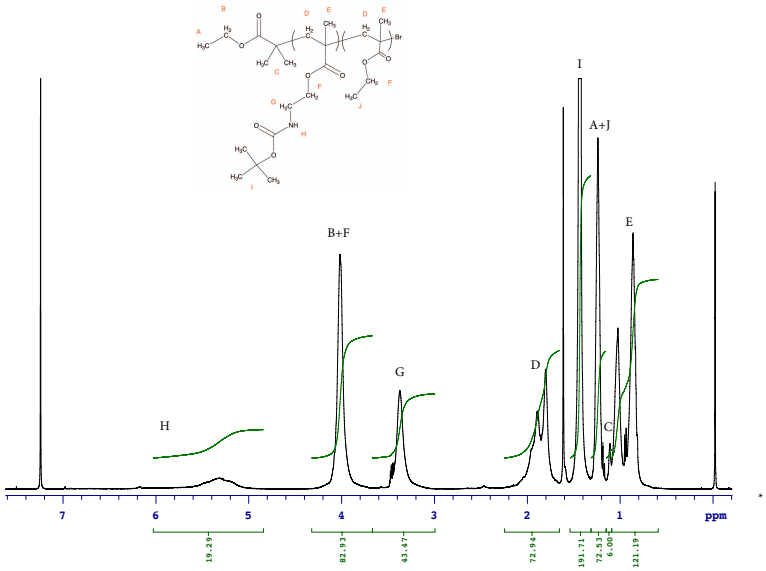

Figure B.47. ^{1}H NMR spectra of boc-protected P_L7

P_L8

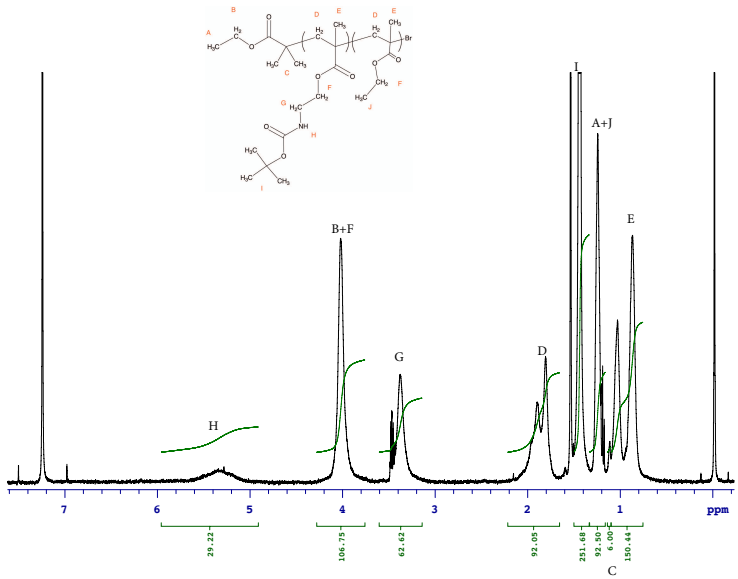

Figure B.48. ^{1}H NMR spectra of boc-protected P_L8

P_L9

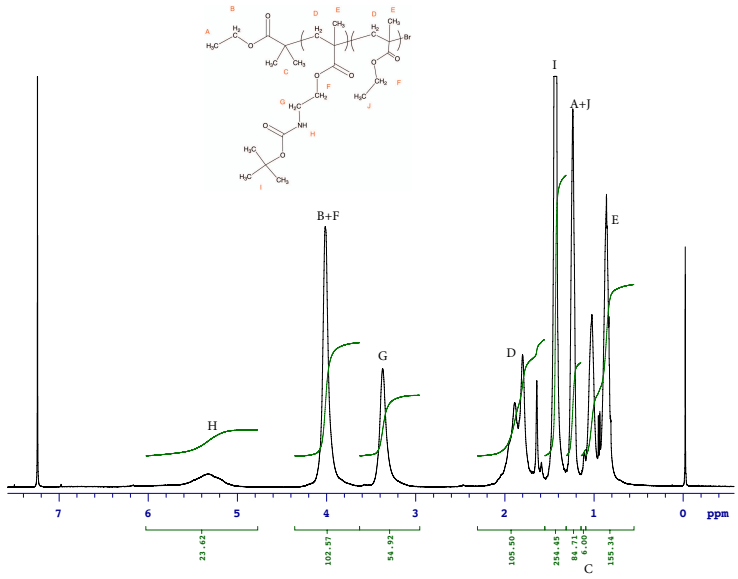

Figure B.49. ^{1}H NMR spectra of boc-protected P_L9

P_S10

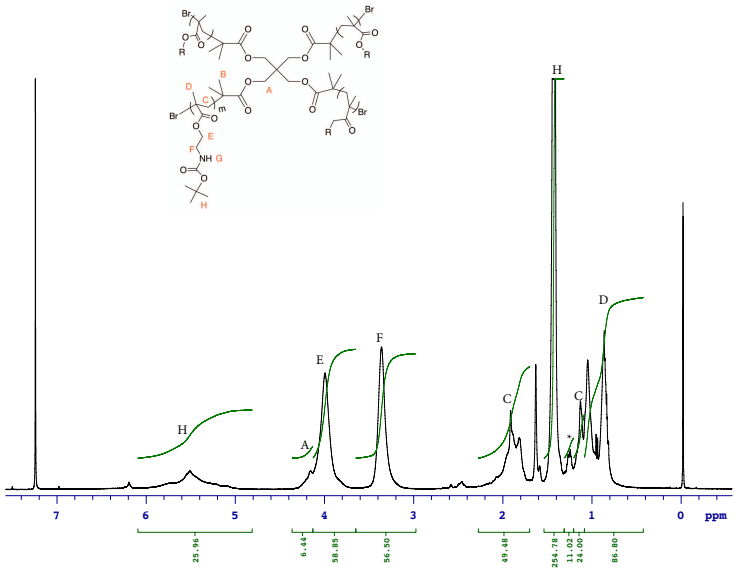

*H terminated branches due to Br removal

Figure B.50. ^{1}H NMR spectra of boc-protected P_S10

P_S11

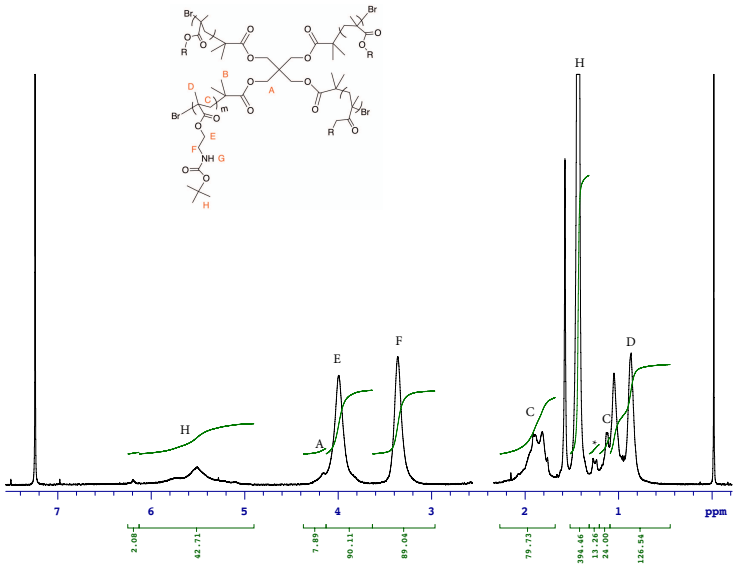

*H terminated branches due to Br remocal

Figure B.51. ^{1}H NMR spectra of boc-protected P_S11

P_S12

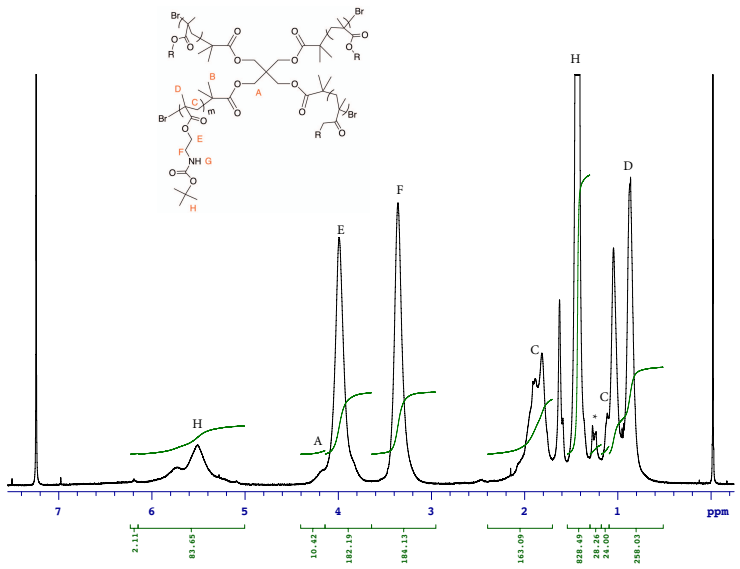

H terminated branches due to Br remocal

Figure B.52. ^{1}H NMR spectra of boc-protected P_S12

P_S13

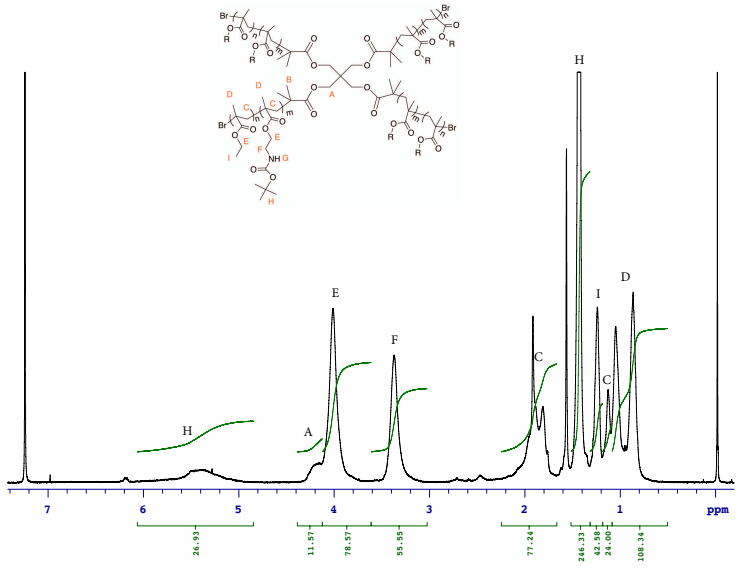

Figure B.53. ^{1}H NMR spectra of boc-protected P_S13

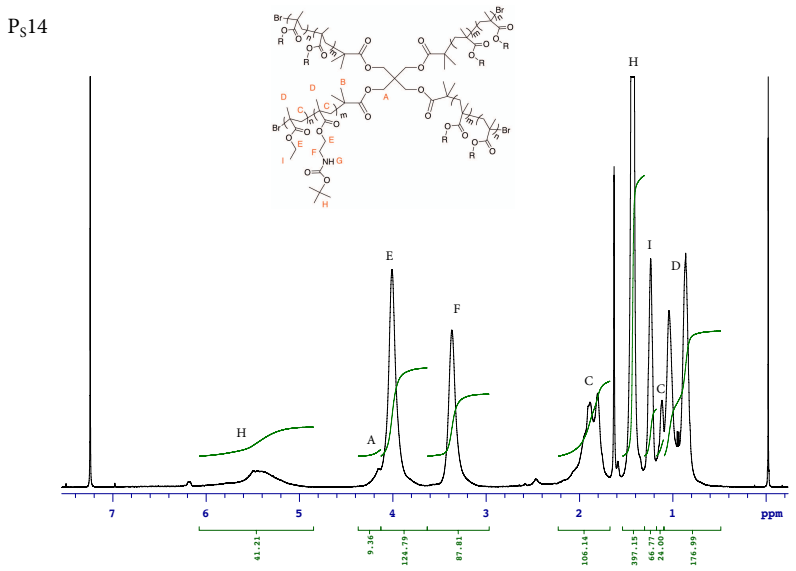

Figure B.54. ^{1}H NMR spectra of boc-protected P_S14

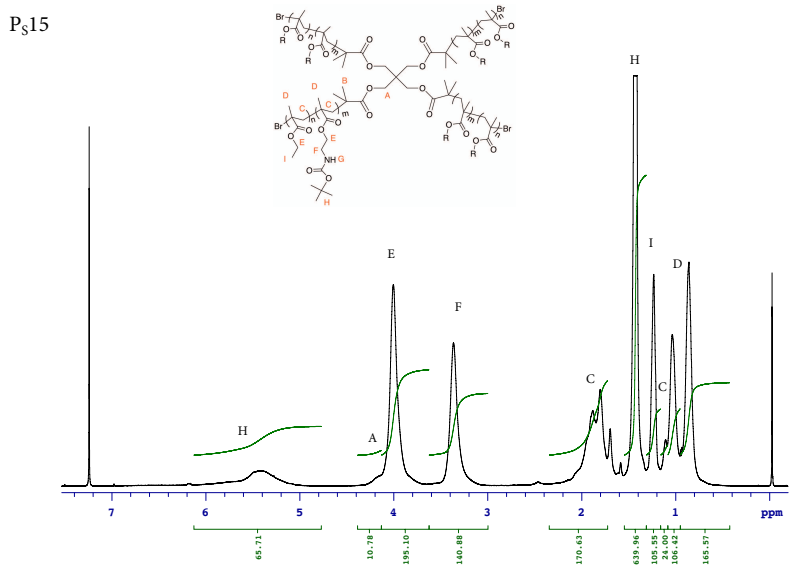

Figure B.55. ^{1}H NMR spectra of boc-protected P_S15

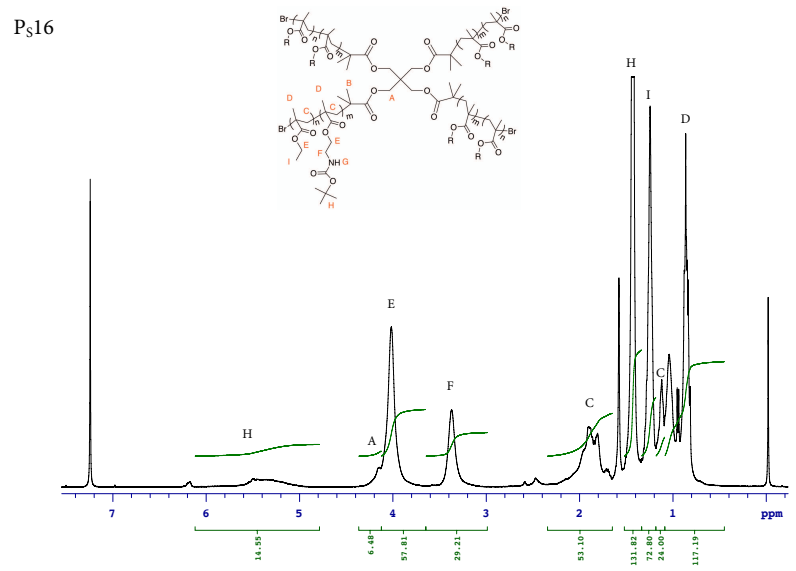

Figure B.56. ^{1}H NMR spectra of boc-protected P_S16

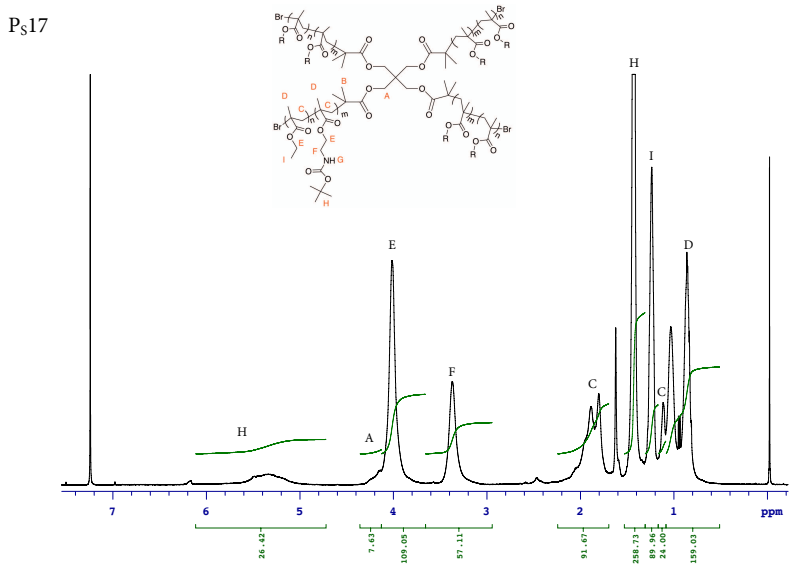

Figure B.57. ^{1}H NMR spectra of boc-protected P_S17

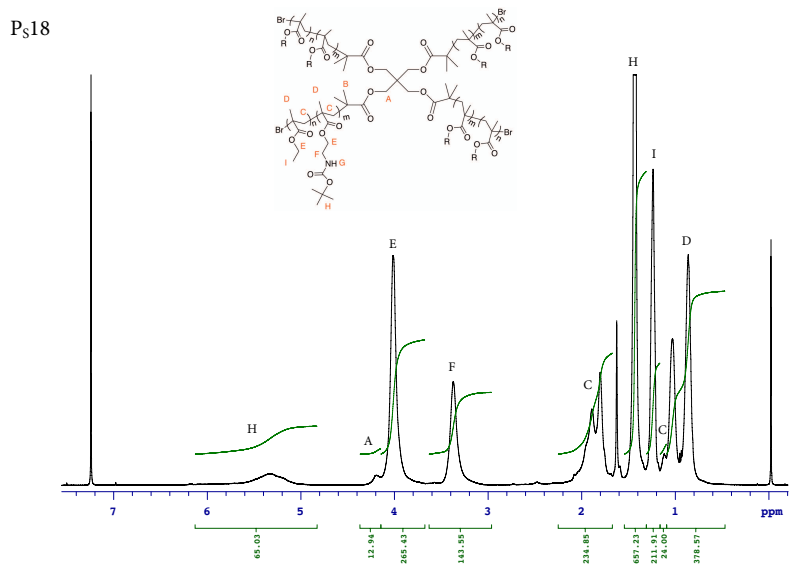

Figure B.58. ^{1}H NMR spectra of boc-protected P_S18

A.B.2. ^{1}H NMR spectra of deprotected AEMA-EMA copolymers

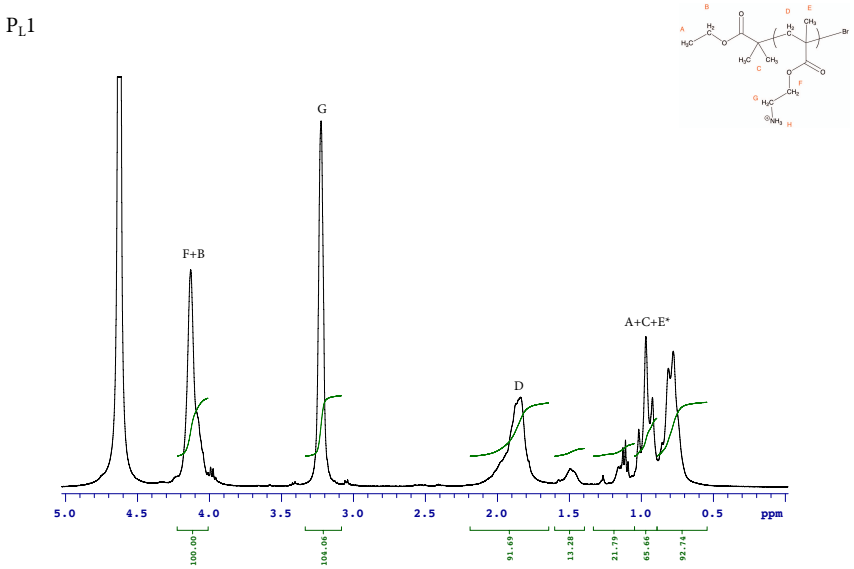

*H substition of Br terminated polymer chains

Figure B.59. ^{1}H NMR spectra of P_L1

P_L2

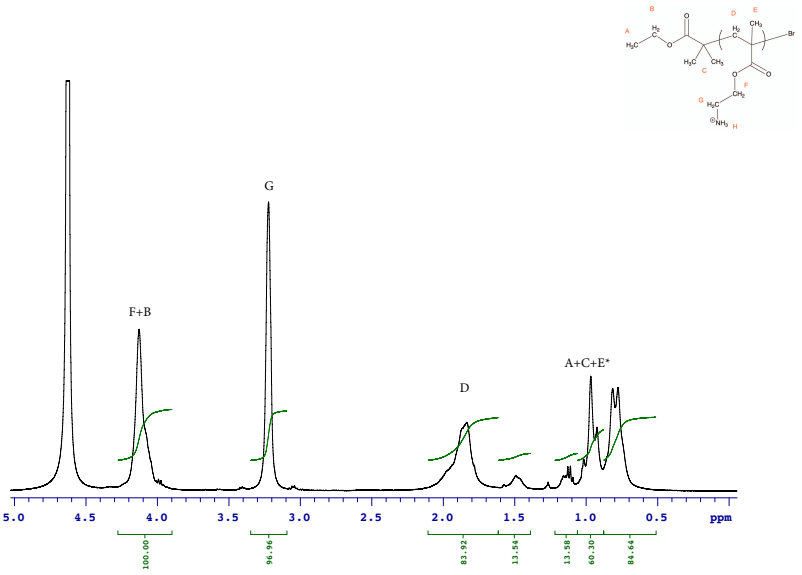

*H substition of Br terminated polymer chains

Figure B.60. ^{1}H NMR spectra of P_L2

P_L3

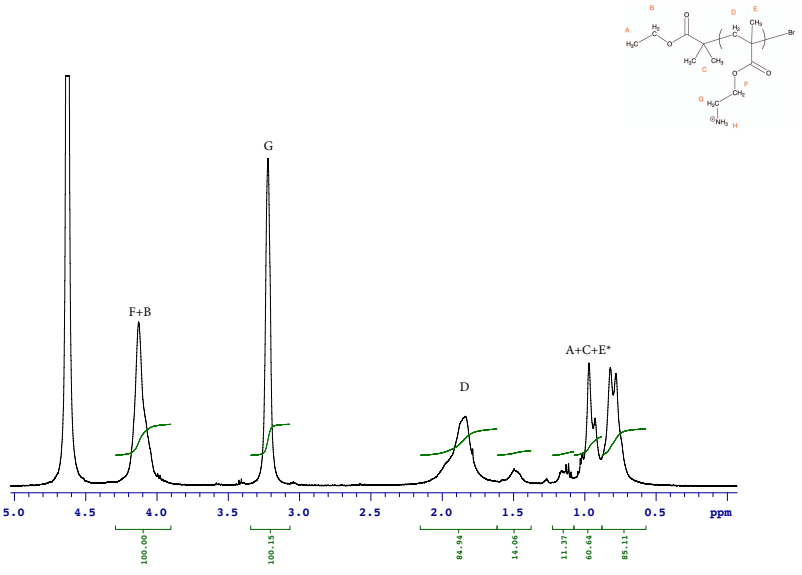

H substition of Br terminated polymer chains

Figure B.61. ^{1}H NMR spectra of P_L3

P_L4

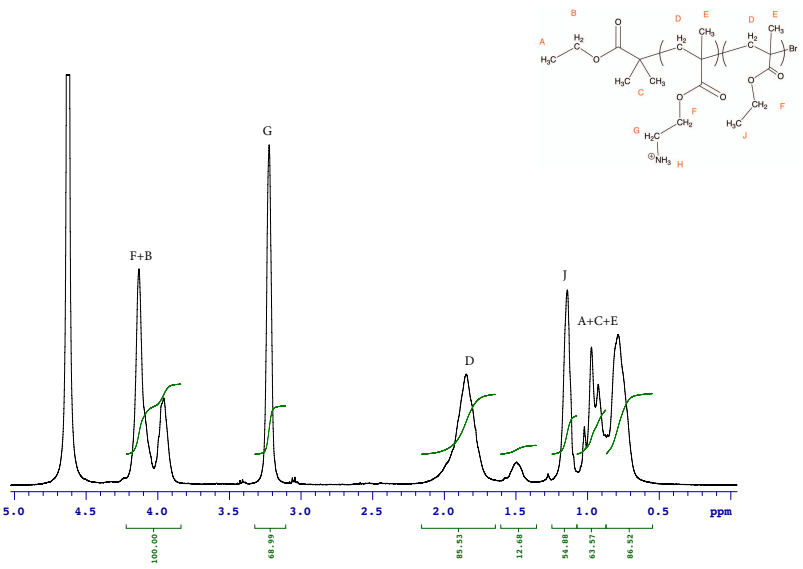

Figure B.62. ^{1}H NMR spectra of P_L4

P_L5

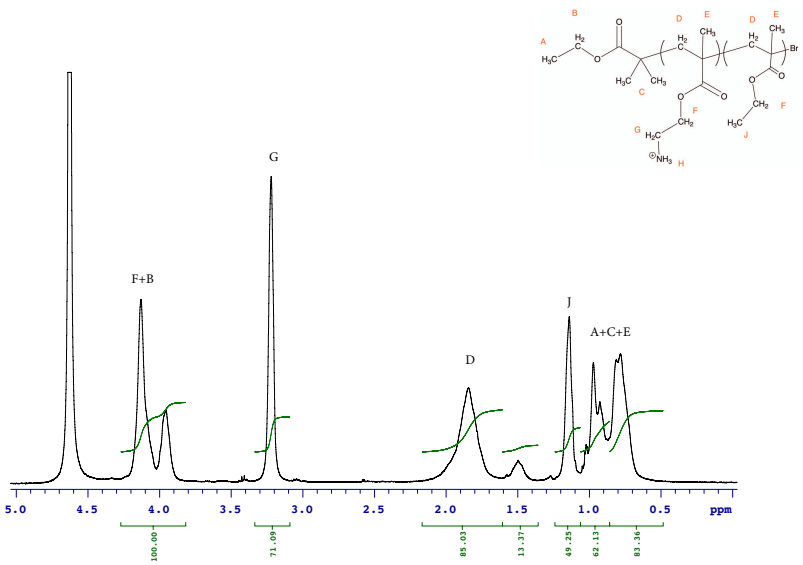

Figure B.63. ^{1}H NMR spectra of P_L5

P_L6

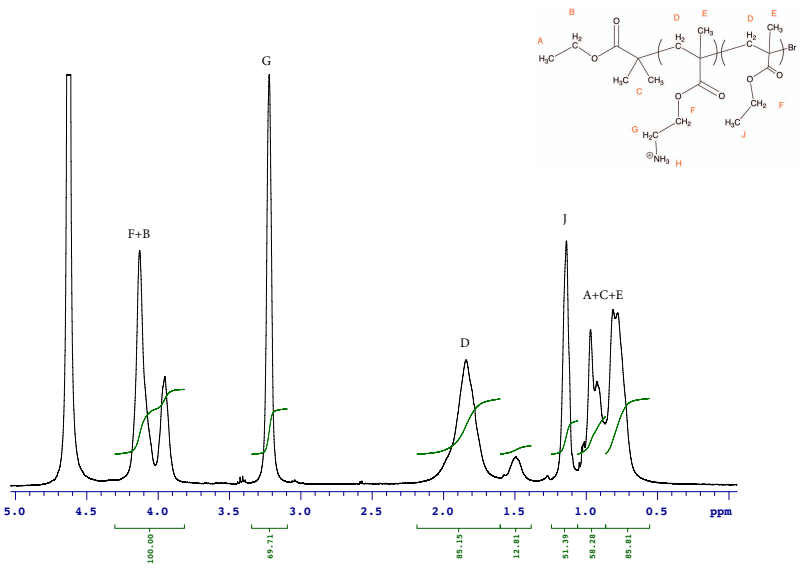

Figure B.64. ^{1}H NMR spectra of P_L6

P_L7

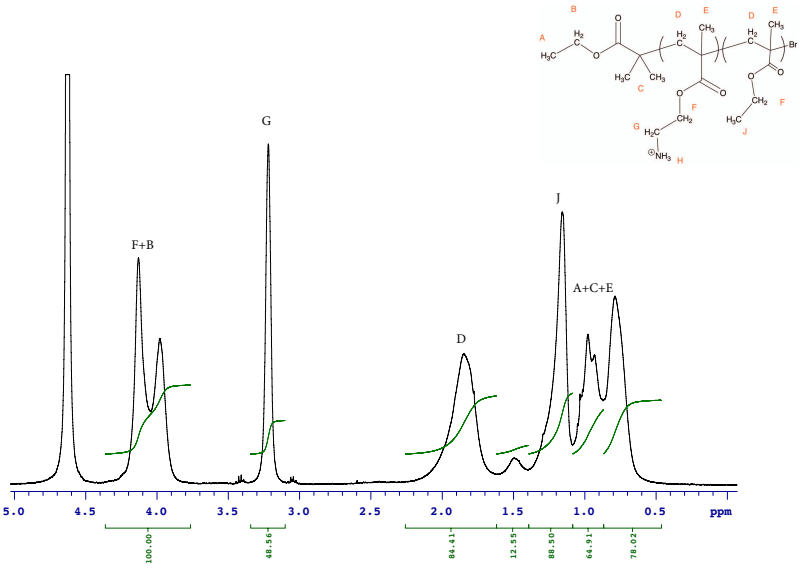

Figure B.65. ^{1}H NMR spectra of P_L7

P_L8

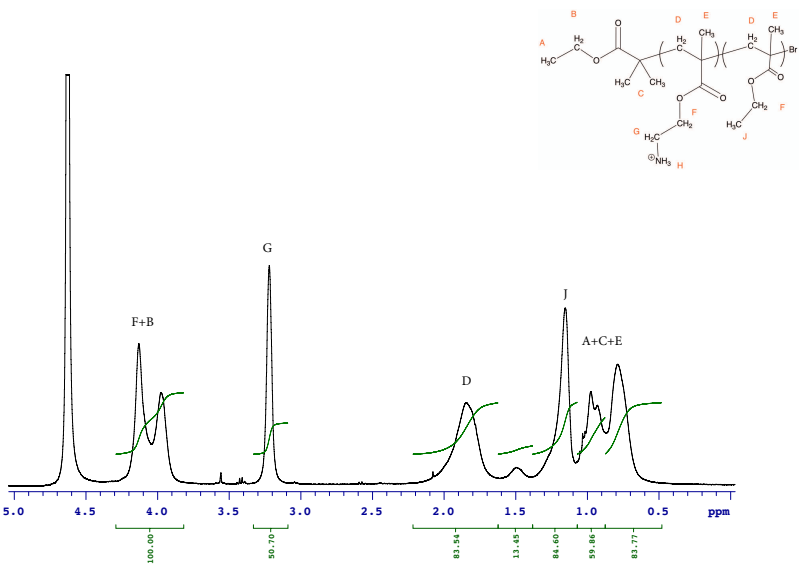

Figure B.66. ^{1}H NMR spectra of P_L8

P_L9

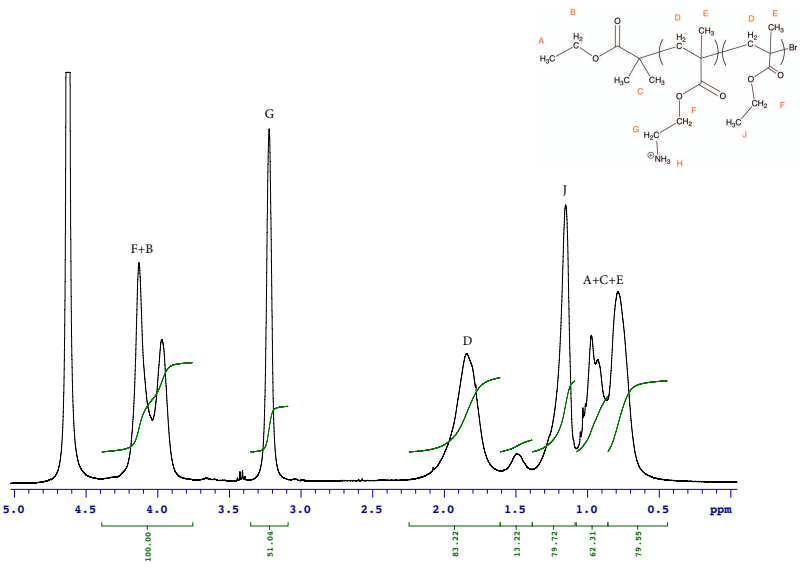

Figure B.67. ^{1}H NMR spectra of P_L9

P_S10

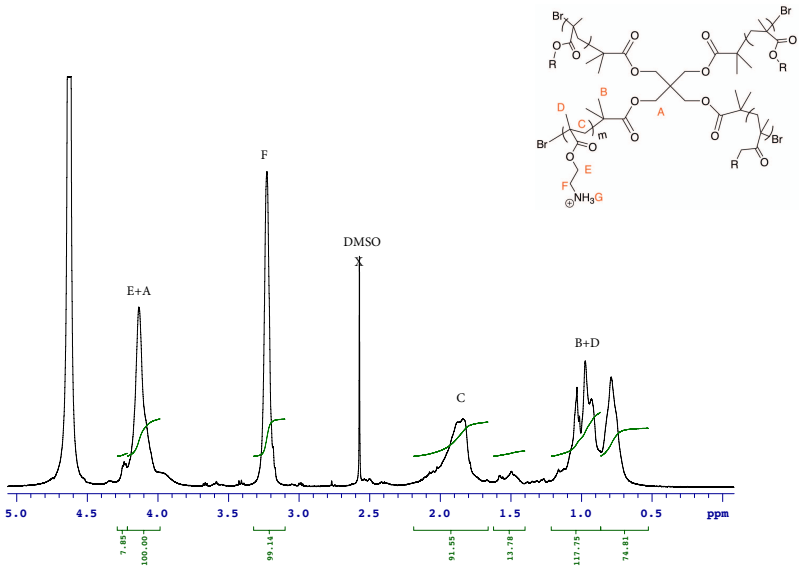

Figure B.68. ^{1}H NMR spectra of P_S10

P_S11

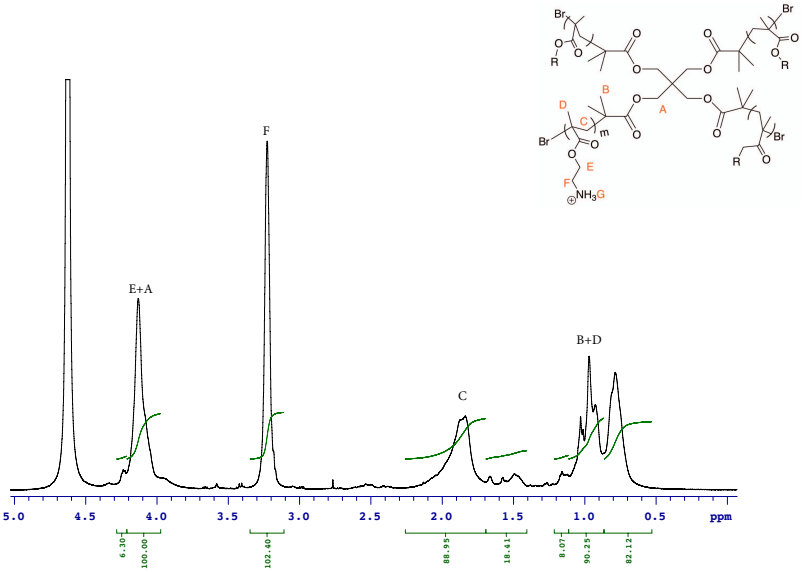

Figure B.69. ^{1}H NMR spectra of P_S11

P_S12

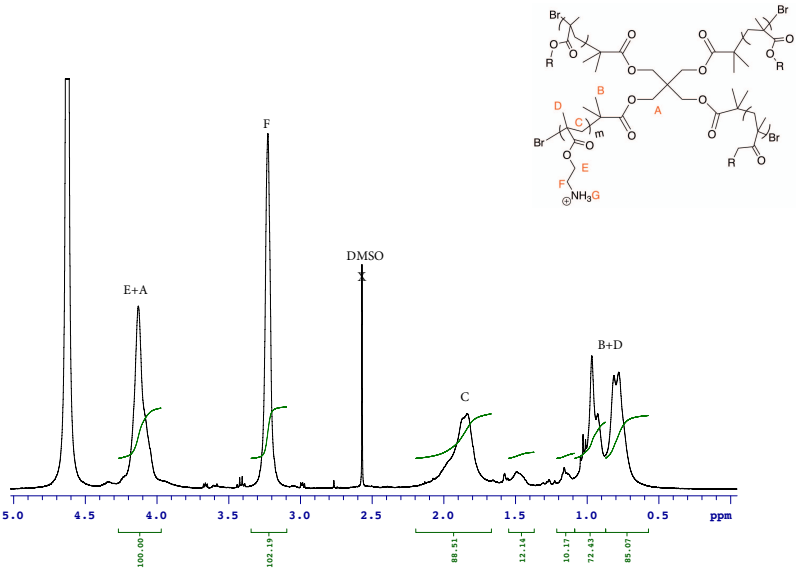

Figure B.70. ^{1}H NMR spectra of P_S12

P_S13

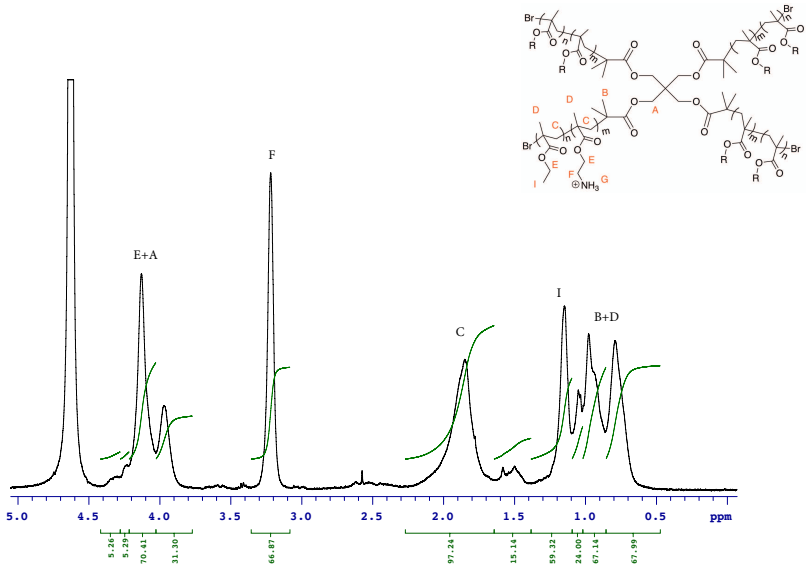

Figure B.71. ^{1}H NMR spectra of P_S13

P_S14

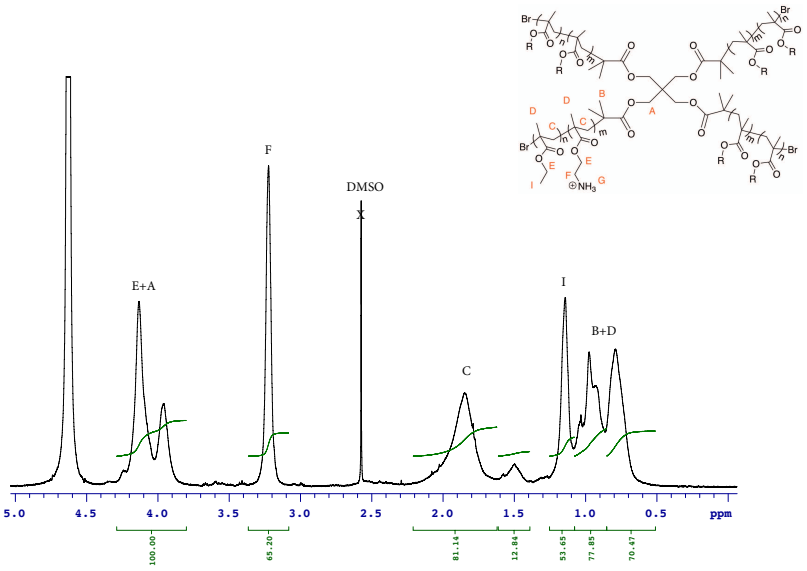

Figure B.72. ^{1}H NMR spectra of P_S14

P_S15

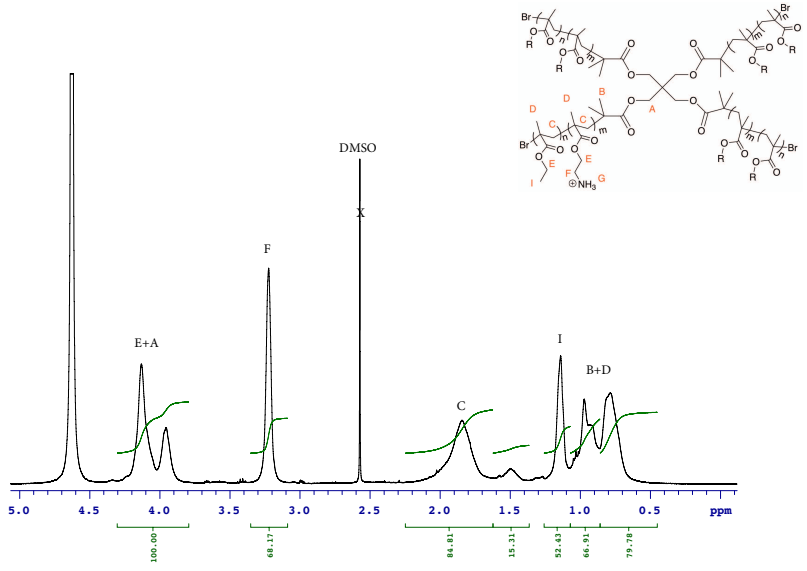

Figure B.73. ^{1}H NMR spectra of P_S15

P_S16

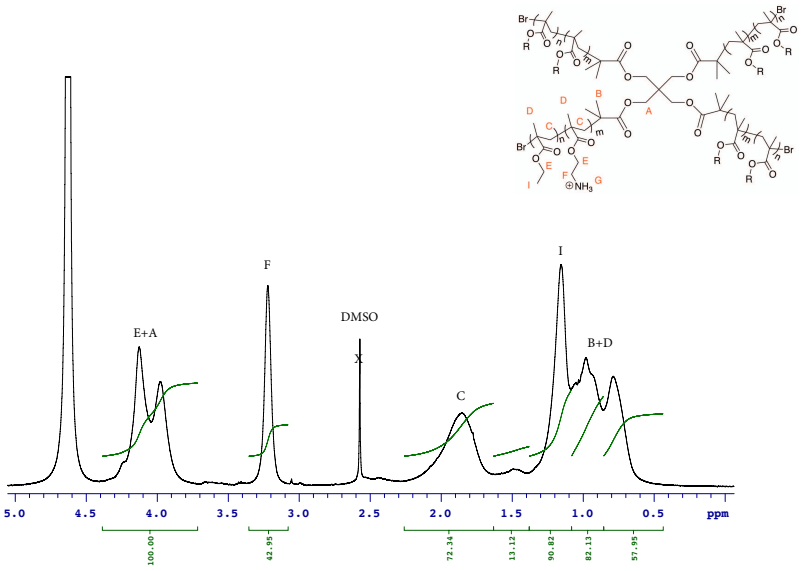

Figure B.74. ^{1}H NMR spectra of P_S16

P_S17

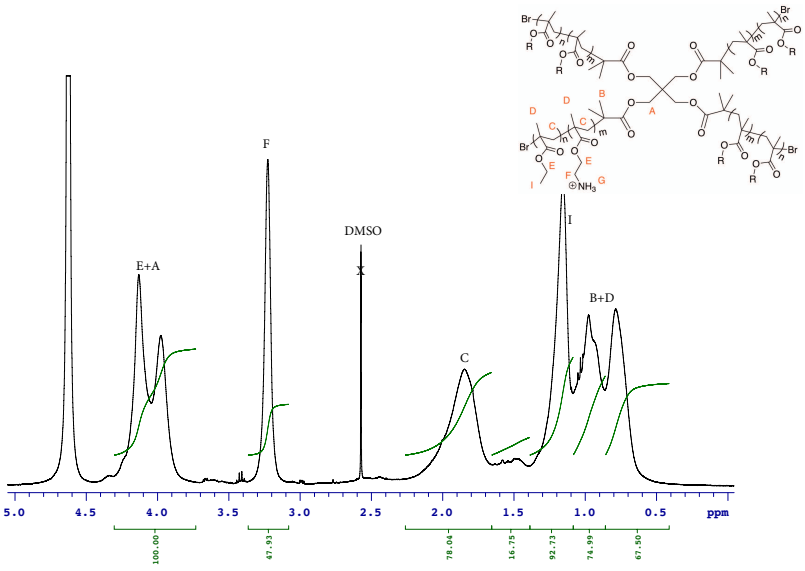

Figure B.75. ^{1}H NMR spectra of P_S17

P_S18

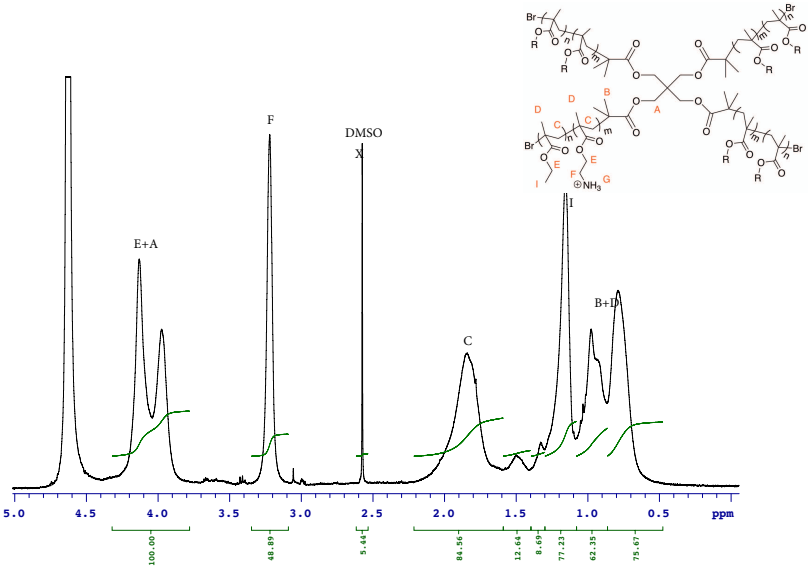

Figure B.76. ^{1}H NMR spectra of P_S18

Appendix C. Characterization of P-1 and P-2 polymers by ^{1}H NMR and GPC

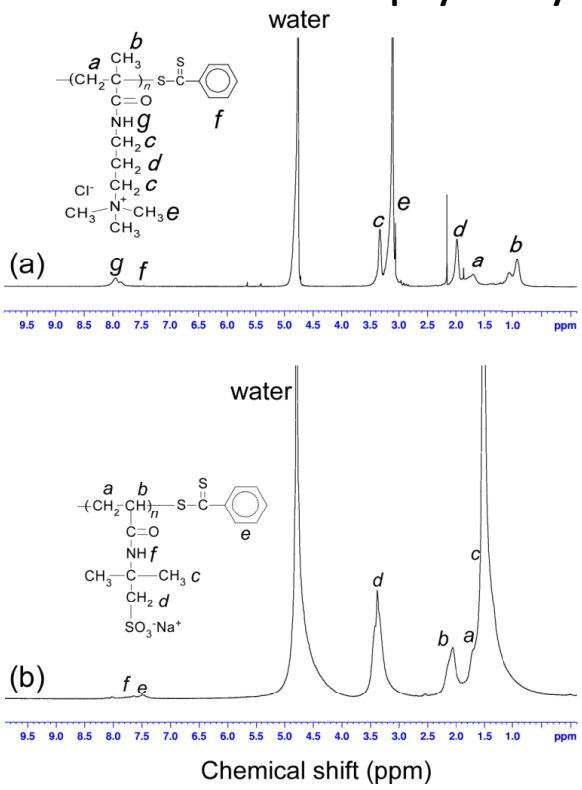

Figure C.77. ^{1}H NMR spectra for (a) P-1 and (b) P-2 in D_2O.

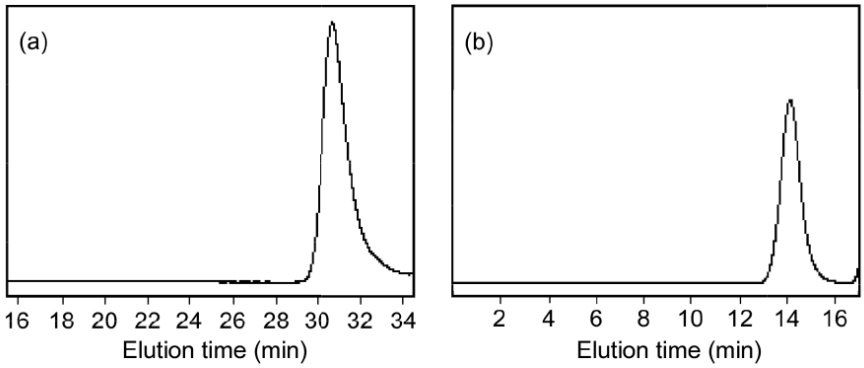

Figure C.78. GPC elution curves for (a) P-1 using two Shodex Ohpak SB-804 HQ columns and a 0.3 M Na_2SO_4 aqueous solution containing 0.5 M acetic acid as an eluent and (b) P-2 using a Shodex Asahipak GF-7M HQ column and a phosphate buffer (pH 9) containing 10 vol% acetonitrile as an eluent

Appendix D. Characterization of fluorescein labeled P-1 (F-P-1)

^{1}H NMR was measured with a Bruker DRX-500. Gel-permeation chromatography (GPC) was performed using a pump of Jasco PU-2080, refractive index (RI) detector of Jasco RI-2031 Plus and Shodex Ohpak SB-G guard column and 10 µm bead size SB-804 HQ column working at 40 °C under a flow rate of 0.6 mL/min. A 0.3 M Na_2SO_4 aqueous solution containing 0.5 M acetic acid was used as an eluent. The values of M_n and M_w/M_n were calibrated with standard poly(2-vinylpyridine) samples. UV-vis absorption spectra were obtained with a Jasco V-630 spectrometer using a quartz cell with an optical path length of 1.0 cm. Fluorescence measurements were performed using a Hitachi High Technologies F-2500 fluorescence spectrophotometer. Dynamic light scattering (DLS) measurements were performed using a Malvern Zetasizer nano ZS equipped with a He-Ne laser (4 mW at 632.8 nm) at 25 °C.

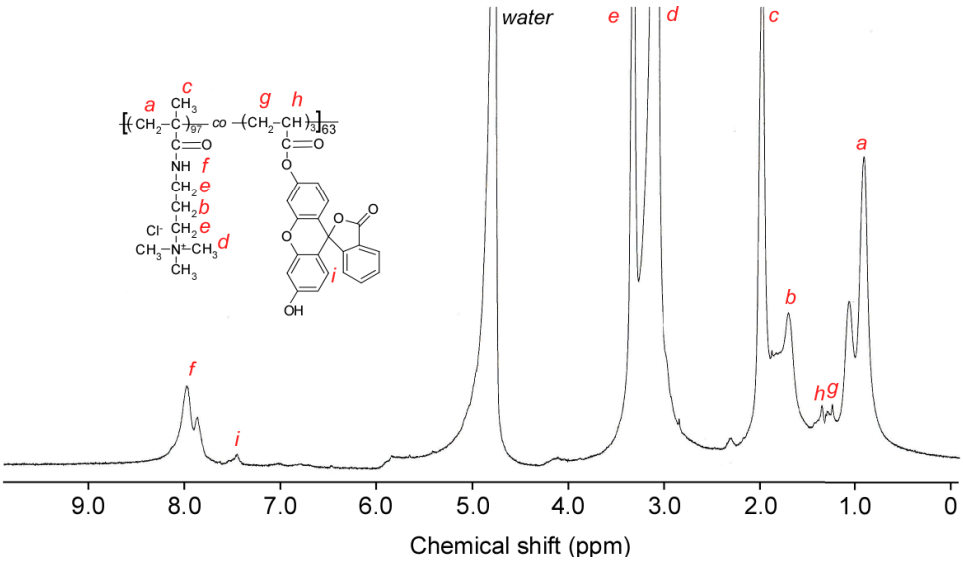

Figure D.79. ^{1}H NMR spectrum of F-P-1 in D_2O.

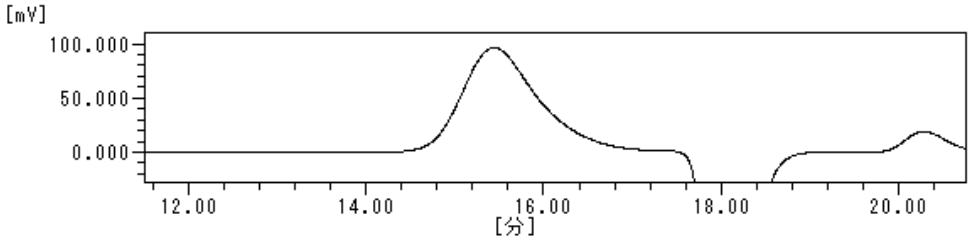

Figure D.80. GPC chart of F-P-1 using A 0.3 M Na_2SO_4 aqueous solution containing 0.5 M acetic acid as an eluent at 40 °C.

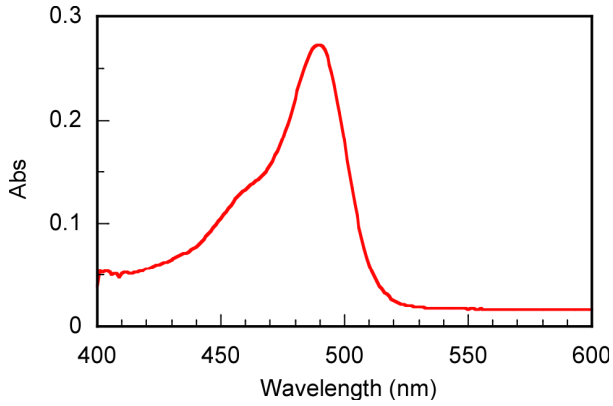

Figure D.81. UV-vis absorption spectrum of F-P-1in PBS at C_p = 0.05 g/L. F-P-1 was dissolved in PBS at polymer concentration (C_p) = 0.05 g/L. The maximum absorption can be observed at 489 nm. Fluorescence measurement was performed for F-P-1 in PBS at C_p = 0.05 g/L. The excitation wavelength was 489 nm. The slit widths of excitation and emission were 20 and 2.5 nm, respectively. The maximum fluorescence wavelength was 513 nm.

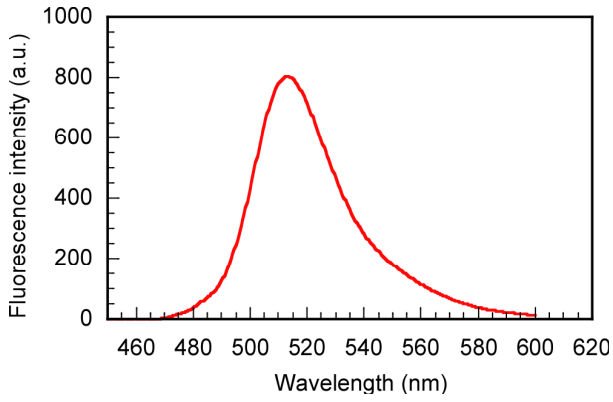

Figure D.82. Fluorescence emission spectrum for F-P-1in PBS at C_p = 0.05 g/L. F-P-1 was dissolved in PBS at C_p = 5.25 g/L. The solution was filtrated using membrane filter with 0.2 µm pore size. DLS measurement was performed at 25 °C (Figure 5). Bimodal hydrodynamic radius (R_h) distribution was observed.

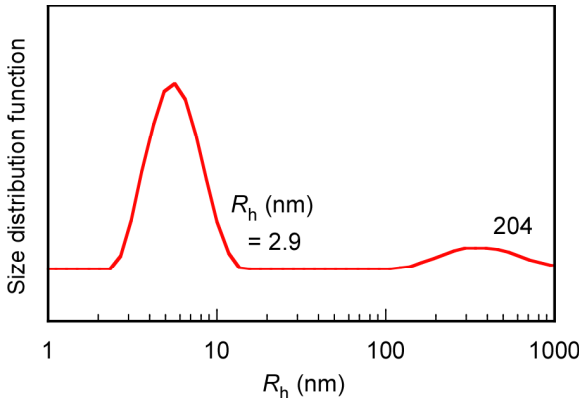

Figure D.83. Hydrodynamic radius (R_h) distribution for P(MAPTAC/AAcF$_3$)$_{63}$ in PBS at C_p = 5.25 g/L at 25 °C.

Bibliography

1. Fauci, A. S.; Touchette, N. A.; Folkers, G. K., Emerging infectious diseases: a 10-year perspective from the National Institute of Allergy and Infectious Diseases. *Emerg Infect Dis* **2005,** *11* (4), 519-525.
2. The World Health Report 2004 - Changing history. *J Adv Nurs* **2004,** *48* (5), 542-542.
3. Fleming, A., On the Antibacterial Action of Cultures of a Penicillium, with Special Reference to Their Use in the Isolation of B. Influenzae. *Brit J Exp Pathol* **1929,** *10* (3), 226-236.
4. Silver, L. L., Challenges of Antibacterial Discovery. *Clin Microbiol Rev* **2011,** *24* (1), 71-+.
5. Sciarretta, K.; Rottingen, J. A.; Opalska, A.; Van Hengel, A. J.; Larsen, J., Economic Incentives for Antibacterial Drug Development: Literature Review and Considerations From the Transatlantic Task Force on Antimicrobial Resistance. *Clin. Infect. Dis.* **2016,** *63* (11), 1470-1474.
6. Moellering, R. C., Linezolid: The first oxazolidinone antimicrobial. *Ann Intern Med* **2003,** *138* (2), 135-142.
7. Raja, A.; LaBonte, J.; Lebbos, J.; Kirkpatrick, P., Daptomycin. *Nat Rev Drug Discov* **2003,** *2* (12), 943-944.
8. Jacoby, G. A., History of Drug-Resistant Microbes. *Infect Dis* **2009**, 3-7.
9. Palumbi, S. R., Evolution - Humans as the world's greatest evolutionary force. *Science* **2001,** *293* (5536), 1786-1790.
10. Clatworthy, A. E.; Pierson, E.; Hung, D. T., Targeting virulence: a new paradigm for antimicrobial therapy. *Nat. Chem. Biol.* **2007,** *3* (9), 541-548.
11. McClure, N. S.; Day, T., A theoretical examination of the relative importance of evolution management and drug development for managing resistance. *P Roy Soc B-Biol Sci* **2014,** *281* (1797).
12. Awramik, S. M.; Schopf, J. W.; Walter, M. R., Filamentous Fossil Bacteria from the Archean of Western Australia. *Precambrian Res* **1983,** *20* (2-4), 357-374.
13. Munita, J. M.; Arias, C. A., Mechanisms of Antibiotic Resistance. *Microbiol Spectr* **2016,** *4* (2).
14. Neu, H. C., The Crisis in Antibiotic-Resistance. *Science* **1992,** *257* (5073), 1064-1073.
15. Jacoby, G. A., Mechanisms of resistance to quinolones. *Clin. Infect. Dis.* **2005,** *40*, S432-S438.
16. Pages, J. M.; James, C. E.; Winterhalter, M., The porin and the permeating antibiotic: a selective diffusion barrier in Gram-negative bacteria. *Nat. Rev. Microbiol.* **2008,** *6* (12), 893-903.
17. Blair, J. M. A.; Webber, M. A.; Baylay, A. J.; Ogbolu, D. O.; Piddock, L. J. V., Molecular mechanisms of antibiotic resistance. *Nat. Rev. Microbiol.* **2015,** *13* (1), 42-51.
18. Martinez, J. L., Antibiotics and antibiotic resistance genes in natural environments. *Science* **2008,** *321* (5887), 365-367.

19. Fajardo, A.; Martinez, J. L., Antibiotics as signals that trigger specific bacterial responses. *Curr Opin Microbiol* **2008,** *11* (2), 161-167.
20. Levy, S. B.; Marshall, B., Antibacterial resistance worldwide: causes, challenges and responses. *Nat Med* **2004,** *10* (12), S122-S129.
21. Nikaido, H., Multidrug Resistance in Bacteria. *Annu. Rev. Biochem* **2009,** *78*, 119-146.
22. Olsen, I., Biofilm-specific antibiotic tolerance and resistance. *Eur J Clin Microbiol* **2015,** *34* (5), 877-886.
23. Potera, C., Microbiology - Forging a link between biofilms and disease. *Science* **1999,** *283* (5409), 1837-+.
24. (NIH), N. I. o. H. Research on Microbial Biofilms. https://grants.nih.gov/grants/guide/pa-files/PA-03-047.html.
25. Mah, T. F. C.; O'Toole, G. A., Mechanisms of biofilm resistance to antimicrobial agents. *Trends Microbiol.* **2001,** *9* (1), 34-39.
26. Hoiby, N.; Bjarnsholt, T.; Givskov, M.; Molin, S.; Ciofu, O., Antibiotic resistance of bacterial biofilms. *Int. J. Antimicrob Ag.* **2010,** *35* (4), 322-332.
27. d'Angelo, I.; Conte, C.; La Rotonda, M. I.; Miro, A.; Quaglia, F.; Ungaro, F., Improving the efficacy of inhaled drugs in cystic fibrosis: Challenges and emerging drug delivery strategies. *Adv Drug Deliver Rev* **2014,** *75*, 92-111.
28. Walters, M. C.; Roe, F.; Bugnicourt, A.; Franklin, M. J.; Stewart, P. S., Contributions of antibiotic penetration, oxygen limitation, and low metabolic activity to tolerance of Pseudomonas aeruginosa biofilms to ciprofloxacin and tobramycin. *Antimicrob. Agents Chemother.* **2003,** *47* (1), 317-323.
29. Evans, D. J.; Allison, D. G.; Brown, M. R. W.; Gilbert, P., Susceptibility of Pseudomonas-Aeruginosa and Escherichia-Coli Biofilms Towards Ciprofloxacin - Effect of Specific Growth-Rate. *J. Antimicrob. Chemother.* **1991,** *27* (2), 177-184.
30. Flemming, H. C.; Neu, T. R.; Wozniak, D. J., The EPS matrix: The "House of Biofilm cells". *J. Bacteriol.* **2007,** *189* (22), 7945-7947.
31. Suci, P. A.; Mittelman, M. W.; Yu, F. P.; Geesey, G. G., Investigation of Ciprofloxacin Penetration into Pseudomonas-Aeruginosa Biofilms. *Antimicrob. Agents Chemother.* **1994,** *38* (9), 2125-2133.
32. Tseng, B. S.; Zhang, W.; Harrison, J. J.; Quach, T. P.; Song, J. L.; Penterman, J.; Singh, P. K.; Chopp, D. L.; Packman, A. I.; Parsek, M. R., The extracellular matrix protects Pseudomonas aeruginosa biofilms by limiting the penetration of tobramycin. *Environ. Microbiol.* **2013,** *15* (10), 2865-2878.
33. Hughes, D.; Andersson, D. I., Environmental and genetic modulation of the phenotypic expression of antibiotic resistance. *Fems Microbiology Reviews* **2017,** *41* (3), 374-391.
34. Dever, L. A.; Dermody, T. S., Mechanisms of Bacterial-Resistance to Antibiotics. *Arch Intern Med* **1991,** *151* (5), 886-895.
35. Davies, J.; Davies, D., Origins and Evolution of Antibiotic Resistance. *Microbiol Mol Biol R* **2010,** *74* (3), 417-+.
36. Evans, R. C.; Holmes, C. J., Effect of Vancomycin Hydrochloride on Staphylococcus-Epidermidis Biofilm Associated with Silicone Elastomer. *Antimicrob. Agents Chemother.* **1987,** *31* (6), 889-894.

37. Gristina, A. G.; Hobgood, C. D.; Webb, L. X.; Myrvik, Q. N., Adhesive Colonization of Biomaterials and Antibiotic-Resistance. *Biomaterials* **1987,** *8* (6), 423-426.
38. Nickel, J. C.; Ruseska, I.; Wright, J. B.; Costerton, J. W., Tobramycin Resistance of Pseudomonas-Aeruginosa Cells Growing as a Biofilm on Urinary Catheter Material. *Antimicrob. Agents Chemother.* **1985,** *27* (4), 619-624.
39. Ceri, H.; Olson, M. E.; Stremick, C.; Read, R. R.; Morck, D.; Buret, A., The Calgary Biofilm Device: New technology for rapid determination of antibiotic susceptibilities of bacterial biofilms. *J. Clin. Microbiol.* **1999,** *37* (6), 1771-1776.
40. Stewart, P. S., Mechanisms of antibiotic resistance in bacterial biofilms. *Int J Med Microbiol* **2002,** *292* (2), 107-113.
41. Zasloff, M., Antimicrobial peptides of multicellular organisms. *Nature* **2002,** *415* (6870), 389-395.
42. Hancock, R. E. W.; Lehrer, R., Cationic peptides: a new source of antibiotics. *Trends Biotechnol.* **1998,** *16* (2), 82-88.
43. Wang, G. S.; Li, X.; Wang, Z., APD3: the antimicrobial peptide database as a tool for research and education. *Nucleic Acids Res.* **2016,** *44* (D1), D1087-D1093.
44. Yeaman, M. R.; Yount, N. Y., Mechanisms of antimicrobial peptide action and resistance. *Pharmacol Rev* **2003,** *55* (1), 27-55.
45. Hancock, R. E. W.; Sahl, H. G., Antimicrobial and host-defense peptides as new anti-infective therapeutic strategies. *Nat. Biotechnol.* **2006,** *24* (12), 1551-1557.
46. Brogden, K. A., Antimicrobial peptides: Pore formers or metabolic inhibitors in bacteria? *Nat. Rev. Microbiol.* **2005,** *3* (3), 238-250.
47. Nguyen, L. T.; Haney, E. F.; Vogel, H. J., The expanding scope of antimicrobial peptide structures and their modes of action. *Trends Biotechnol.* **2011,** *29* (9), 464-472.
48. Hilchie, A. L.; Wuerth, K.; Hancock, R. E. W., Immune modulation by multifaceted cationic host defense (antimicrobial) peptides. *Nat. Chem. Biol.* **2013,** *9* (12), 761-768.
49. Zasloff, M., Magainins, a Class of Antimicrobial Peptides from Xenopus Skin - Isolation, Characterization of 2 Active Forms, and Partial Cdna Sequence of a Precursor. *P Natl Acad Sci USA* **1987,** *84* (15), 5449-5453.
50. Matsuzaki, K.; Harada, M.; Handa, T.; Funakoshi, S.; Fujii, N.; Yajima, H.; Miyajima, K., Magainin 1-Induced Leakage of Entrapped Calcein out of Negatively-Charged Lipid Vesicles. *Biochim. Biophys. Acta* **1989,** *981* (1), 130-134.
51. Eisenberg, D.; Schwarz, E.; Komaromy, M.; Wall, R., Analysis of Membrane and Surface Protein Sequences with the Hydrophobic Moment Plot. *J. Mol. Biol.* **1984,** *179* (1), 125-142.
52. Palermo, E. F.; Vemparala, S.; Kuroda, K., Antimicrobial Polymers: Molecular Design as Synthetic Mimics of Host-Defense Peptides. *Acs Sym Ser* **2013,** *1135*, 319-330.
53. Oren, Z.; Shai, Y., Mode of action of linear amphipathic alpha-helical antimicrobial peptides. *Biopolymers* **1998,** *47* (6), 451-463.
54. Shai, Y., Mode of action of membrane active antimicrobial peptides. *Biopolymers* **2002,** *66* (4), 236-248.
55. Sato, H.; Felix, J. B., Peptide-membrane interactions and mechanisms of membrane destruction by amphipathic alpha-helical antimicrobial peptides. *Bba-Biomembranes* **2006,** *1758* (9), 1245-1256.

56. Jenssen, H.; Hamill, P.; Hancock, R. E. W., Peptide antimicrobial agents. *Clin Microbiol Rev* **2006,** *19* (3), 491-+.
57. Wade, D.; Boman, A.; Wahlin, B.; Drain, C. M.; Andreu, D.; Boman, H. G.; Merrifield, R. B., All-D Amino Acid-Containing Channel-Forming Antibiotic Peptides. *P Natl Acad Sci USA* **1990,** *87* (12), 4761-4765.
58. Hamuro, Y.; Schneider, J. P.; DeGrado, W. F., De novo design of antibacterial beta-peptides. *JACS* **1999,** *121* (51), 12200-12201.
59. Patch, J. A.; Barron, A. E., Helical peptoid mimics of magainin-2 amide. *JACS* **2003,** *125* (40), 12092-12093.
60. Ong, Z. Y.; Wiradharma, N.; Yang, Y. Y., Strategies employed in the design and optimization of synthetic antimicrobial peptide amphiphiles with enhanced therapeutic potentials. *Adv Drug Deliver Rev* **2014,** *78*, 28-45.
61. Powell, W. A.; Catranis, C. M.; Maynard, C. A., Synthetic Antimicrobial Peptide Design. *Mol Plant Microbe In* **1995,** *8* (5), 792-794.
62. Tossi, A.; Tarantino, C.; Romeo, D., Design of synthetic antimicrobial peptides based on sequence analogy and amphipathicity. *Eur. J. Biochem.* **1997,** *250* (2), 549-558.
63. Gordon, Y. J.; Romanowski, E. G.; McDermott, A. M., A review of antimicrobial peptides and their therapeutic potential as anti-infective drugs. *Curr Eye Res* **2005,** *30* (7), 505-515.
64. Steckbeck, J. D.; Deslouches, B.; Montelaro, R. C., Antimicrobial peptides: new drugs for bad bugs? *Expert Opin Biol Th* **2014,** *14* (1), 11-14.
65. Marr, A. K.; Gooderham, W. J.; Hancock, R. E. W., Antibacterial peptides for therapeutic use: obstacles and realistic outlook. *Curr. Opin. Pharm.* **2006,** *6* (5), 468-472.
66. Tew, G. N.; Liu, D. H.; Chen, B.; Doerksen, R. J.; Kaplan, J.; Carroll, P. J.; Klein, M. L.; DeGrado, W. F., De novo design of biomimetic antimicrobial polymers. *P Natl Acad Sci USA* **2002,** *99* (8), 5110-5114.
67. Tew, G. N.; Scott, R. W.; Klein, M. L.; Degrado, W. F., De Novo Design of Antimicrobial Polymers, Foldamers, and Small Molecules: From Discovery to Practical Applications. *Acc. Chem. Res.* **2010,** *43* (1), 30-39.
68. Takahashi, H.; Palermo, E. F.; Yasuhara, K.; Caputo, G. A.; Kuroda, K., Molecular Design, Structures, and Activity of Antimicrobial Peptide-Mimetic Polymers. *Macromol. Biosci.* **2013,** *13* (10), 1285-1299.
69. Kuroda, K.; DeGrado, W. F., Amphiphilic polymethacrylate derivatives as antimicrobial agents. *JACS* **2005,** *127* (12), 4128-4129.
70. Kuroda, K.; Caputo, G. A.; DeGrado, W. F., The Role of Hydrophobicity in the Antimicrobial and Hemolytic Activities of Polymethacrylate Derivatives. *Chem-Eur J* **2009,** *15* (5), 1123-1133.
71. Palermo, E. F.; Kuroda, K., Chemical Structure of Cationic Groups in Amphiphilic Polymethacrylates Modulates the Antimicrobial and Hemolytic Activities. *Biomacromolecules* **2009,** *10* (6), 1416-1428.
72. Palermo, E. F.; Sovadinova, I.; Kuroda, K., Structural Determinants of Antimicrobial Activity and Biocompatibility in Membrane-Disrupting Methacrylamide Random Copolymers. *Biomacromolecules* **2009,** *10* (11), 3098-3107.
73. Palermo, E. F.; Kuroda, K., Structural determinants of antimicrobial activity in polymers which mimic host defense peptides. *Appl. Microbiol. Biotechnol.* **2010,** *87* (5), 1605-1615.

74. Palermo, E. F.; Lee, D. K.; Ramamoorthy, A.; Kuroda, K., Role of Cationic Group Structure in Membrane Binding and Disruption by Amphiphilic Copolymers. *J. Phys. Chem. B* **2011,** *115* (2), 366-375.
75. Sovadinova, I.; Palermo, E. F.; Urban, M.; Mpiga, P.; Caputo, G. A.; Kuroda, K., Activity and Mechanism of Antimicrobial Peptide-Mimetic Amphiphilic Polymethacrylate Derivatives. *Polymers-Basel* **2011,** *3* (3), 1512-1532.
76. Thoma, L. M.; Boles, B. R.; Kuroda, K., Cationic Methacrylate Polymers as Topical Antimicrobial Agents against Staphylococcus aureus Nasal Colonization. *Biomacromolecules* **2014,** *15* (8), 2933-2943.
77. Takahashi, H.; Nadres, E. T.; Kuroda, K., Cationic Amphiphilic Polymers with Antimicrobial Activity for Oral Care Applications: Eradication of S-mutans Biofilm. *Biomacromolecules* **2017,** *18* (1), 257-265.
78. Nadres, E. T.; Takahashi, H.; Kuroda, K., Radical-Medicated End-Group Transformation of Amphiphilic Methacrylate Random Copolymers for Modulation of Antimicrobial and Hemolytic Activities. *J. Polym. Sci. Pol. Chem.* **2017,** *55* (2), 304-312.
79. Hong, S.; Takahashi, H.; Nadres, E. T.; Mortazavian, H.; Caputo, G. A.; Younger, J. G.; Kuroda, K., A Cationic Amphiphilic Random Copolymer with pH-Responsive Activity against Methicillin-Resistant Staphylococcus aureus. *Plos One* **2017,** *12* (1).
80. Palermo, E. F.; Vemparala, S.; Kuroda, K., Cationic Spacer Arm Design Strategy for Control of Antimicrobial Activity and Conformation of Amphiphilic Methacrylate Random Copolymers. *Biomacromolecules* **2012,** *13* (5), 1632-1641.
81. Kuroda, K.; Caputo, G. A.; DeGrado, W. F., The Role of Hydrophobicity in the Antimicrobial and Hemolytic Activities of Polymethacrylate Derivatives. *Chem. Eur. J.* **2009,** *15* (5), 1123-1133.
82. Tam, J. P.; Lu, Y. A.; Yang, J. L., Antimicrobial dendrimeric peptides. *Eur. J. Biochem.* **2002,** *269* (3), 923-932.
83. Wiradharma, N.; Liu, S. Q.; Yang, Y. Y., Branched and 4-Arm Starlike alpha-Helical Peptide Structures with Enhanced Antimicrobial Potency and Selectivity. *Small* **2012,** *8* (3), 362-366.
84. Siedenbiedel, F.; Fuchs, A.; Moll, T.; Weide, M.; Breves, R.; Tiller, J. C., Star-Shaped Poly(styrene)-block-Poly(4-vinyl-N-methylpyridiniumiodide) for Semipermanent Antimicrobial Coatings. *Macromol. Biosci.* **2013,** *13* (10), 1447-1455.
85. Li, Y. M.; Yu, H. S.; Qian, Y. F.; Hu, J. M.; Liu, S. Y., Amphiphilic Star Copolymer-Based Bimodal Fluorogenic/Magnetic Resonance Probes for Concomitant Bacteria Detection and Inhibition. *Adv. Mater.* **2014,** *26* (39), 6734-6741.
86. Pasquier, N.; Keul, H.; Heine, E.; Moeller, M.; Angelov, B.; Linser, S.; Willumeit, R., Amphiphilic Branched Polymers as Antimicrobial Agents. *Macromol. Biosci.* **2008,** *8* (10), 903-915.
87. Francolini, I.; Donelli, G., Prevention and control of biofilm-based medical-device-related infections. *FEMS Immunol. Med. Microbiol.* **2010,** *59* (3), 227-238.
88. Pavithra, D.; Doble, M., Biofilm formation, bacterial adhesion and host response on polymeric implants - issues and prevention. *Biomed Mater* **2008,** *3* (3).
89. Simoes, M.; Simoes, L. C.; Vieira, M. J., A review of current and emergent biofilm control strategies. *Lwt-Food Sci Technol* **2010,** *43* (4), 573-583.

90. Brackman, G.; Cos, P.; Maes, L.; Nelis, H. J.; Coenye, T., Quorum Sensing Inhibitors Increase the Susceptibility of Bacterial Biofilms to Antibiotics In Vitro and In Vivo. *Antimicrob. Agents Chemother.* **2011,** *55* (6), 2655-2661.
91. Christensen, L. D.; van Gennip, M.; Jakobsen, T. H.; Alhede, M.; Hougen, H. P.; Hoiby, N.; Bjarnsholt, T.; Givskov, M., Synergistic antibacterial efficacy of early combination treatment with tobramycin and quorum-sensing inhibitors against Pseudomonas aeruginosa in an intraperitoneal foreign-body infection mouse model. *J. Antimicrob. Chemother.* **2012,** *67* (5), 1198-1206.
92. Alkawash, M. A.; Soothill, J. S.; Schiller, N. L., Alginate lyase enhances antibiotic killing of mucoid Pseudomonas aeruginosa in biofilms. *Apmis* **2006,** *114* (2), 131-138.
93. Kaplan, J. B., Therapeutic Potential of Biofilm-Dispersing Enzymes. *The International Journal of Artificial Organs* **2009,** *32* (9), 545-554.
94. Whitchurch, C. B.; Tolker-Nielsen, T.; Ragas, P. C.; Mattick, J. S., Extracellular DNA required for bacterial biofilm formation. *Science* **2002,** *295* (5559), 1487-1487.
95. Tolker-Nielsen, T.; Hoiby, N., Extracellular DNA and F-actin as targets in antibiofilm cystic fibrosis therapy. *Future Microbiol* **2009,** *4* (6), 645-647.
96. Lorite, G. S.; Rodrigues, C. M.; de Souza, A. A.; Kranz, C.; Mizaikoff, B.; Cotta, M. A., The role of conditioning film formation and surface chemical changes on Xylella fastidiosa adhesion and biofilm evolution. *J. Colloid Interface Sci.* **2011,** *359* (1), 289-295.
97. Oliveira, R., Influence of surface characteristics on the adhesion of Alcaligenes denitrificans to polymeric substrates AU - Teixeira, P. *J. Adhes. Sci. Technol.* **1999,** *13* (11), 1287-1294.
98. Oh, Y. J.; Lee, N. R.; Jo, W.; Jung, W. K.; Lim, J. S., Effects of substrates on biofilm formation observed by atomic force microscopy. *Ultramicroscopy* **2009,** *109* (8), 874-880.
99. Gubner, R.; Beech, I. B., The effect of extracellular polymeric substances on the attachment of Pseudomonas NCIMB 2021 to AISI 304 and 316 stainless steel. *Biofouling* **2000,** *15* (1-3), 25-36.
100. Petrova, O. E.; Sauer, K., Sticky Situations: Key Components That Control Bacterial Surface Attachment. *J. Bacteriol.* **2012,** *194* (10), 2413-2425.
101. Schierholz, J. M.; Beuth, J., Implant infections: a haven for opportunistic bacteria. *J Hosp Infect* **2001,** *49* (2), 87-93.
102. Habash, M.; Reid, G., Microbial biofilms: Their development and significance for medical device-related infections. *J Clin Pharmacol* **1999,** *39* (9), 887-898.
103. Kalasin, S.; Santore, M. M., Non-specific adhesion on biomaterial surfaces driven by small amounts of protein adsorption. *Colloid Surface B.* **2009,** *73* (2), 229-236.
104. Fuqua, W. C.; Winans, S. C.; Greenberg, E. P., Quorum Sensing in Bacteria - the Luxr-Luxi Family of Cell Density-Responsive Transcriptional Regulators. *J. Bacteriol.* **1994,** *176* (2), 269-275.
105. Limoli, D. H.; Jones, C. J.; Wozniak, D. J., Bacterial Extracellular Polysaccharides in Biofilm Formation and Function. *Microbiol Spectr* **2015,** *3* (3).
106. Klapper, I.; Rupp, C. J.; Cargo, R.; Purvedorj, B.; Stoodley, P., Viscoelastic fluid description of bacterial biofilm material properties. *Biotechnol. Bioeng.* **2002,** *80* (3), 289-296.

107. Stoodley, P.; Cargo, R.; Rupp, C. J.; Wilson, S.; Klapper, I., Biofilm material properties as related to shear-induced deformation and detachment phenomena. *J Ind Microbiol Biot* **2002,** *29* (6), 361-367.
108. Kaplan, J. B., Biofilm Dispersal: Mechanisms, Clinical Implications, and Potential Therapeutic Uses. *J Dent Res* **2010,** *89* (3), 205-218.
109. Siedenbiedel, F.; Tiller, J. C., Antimicrobial Polymers in Solution and on Surfaces: Overview and Functional Principles. *Polymers-Basel* **2012,** *4* (1), 46-71.
110. Lichter, J. A.; Van Vliet, K. J.; Rubner, M. F., Design of Antibacterial Surfaces and Interfaces: Polyelectrolyte Multilayers as a Multifunctional Platform. *Macromolecules* **2009,** *42* (22), 8573-8586.
111. Mi, L.; Jiang, S. Y., Integrated Antimicrobial and Nonfouling Zwitterionic Polymers. *Angew. Chem. Int. Edit.* **2014,** *53* (7), 1746-1754.
112. Goda, T.; Ishihara, K.; Miyahara, Y., Critical update on 2-methacryloyloxyethyl phosphorylcholine (MPC) polymer science. *J. Appl. Polym. Sci.* **2015,** *132* (16).
113. Nejadnik, M. R.; van der Mei, H. C.; Norde, W.; Busscher, H. J., Bacterial adhesion and growth on a polymer brush-coating. *Biomaterials* **2008,** *29* (30), 4117-4121.
114. Shukla, A.; Fleming, K. E.; Chuang, H. F.; Chau, T. M.; Loose, C. R.; Stephanopoulos, G. N.; Hammond, P. T., Controlling the release of peptide antimicrobial agents from surfaces. *Biomaterials* **2010,** *31* (8), 2348-2357.
115. Kumar, R.; Munstedt, H., Silver ion release from antimicrobial polyamide/silver composites. *Biomaterials* **2005,** *26* (14), 2081-2088.
116. Hetrick, E. M.; Schoenfisch, M. H., Reducing implant-related infections: active release strategies. *Chem. Soc. Rev.* **2006,** *35* (9), 780-789.
117. Tiller, J. C.; Liao, C. J.; Lewis, K.; Klibanov, A. M., Designing surfaces that kill bacteria on contact. *P Natl Acad Sci USA* **2001,** *98* (11), 5981-5985.
118. Lin, J.; Qiu, S. Y.; Lewis, K.; Klibanov, A. M., Bactericidal properties of flat surfaces and nanoparticles derivatized with alkylated polyethylenimines. *Biotechnol. Progr.* **2002,** *18* (5), 1082-1086.
119. Singh, A. V.; Vyas, V.; Patil, R.; Sharma, V.; Scopelliti, P. E.; Bongiorno, G.; Podesta, A.; Lenardi, C.; Gade, W. N.; Milani, P., Quantitative Characterization of the Influence of the Nanoscale Morphology of Nanostructured Surfaces on Bacterial Adhesion and Biofilm Formation. *Plos One* **2011,** *6* (9).
120. Carman, M. L.; Estes, T. G.; Feinberg, A. W.; Schumacher, J. F.; Wilkerson, W.; Wilson, L. H.; Callow, M. E.; Callow, J. A.; Brennan, A. B., Engineered antifouling microtopographies - correlating wettability with cell attachment. *Biofouling* **2006,** *22* (1), 11-21.
121. Gudipati, C. S.; Greenlief, C. M.; Johnson, J. A.; Prayongpan, P.; Wooley, K. L., Hyperbranched fluoropolymer and linear poly(ethylene glycol) based Amphiphilic crosslinked networks as efficient antifouling coatings: An insight into the surface compositions, topographies, and morphologies. *J. Polym. Sci. Pol. Chem.* **2004,** *42* (24), 6193-6208.
122. Cao, Z. Q.; Mi, L.; Mendiola, J.; Ella-Menye, J. R.; Zhang, L.; Xue, H.; Jiang, S. Y., Reversibly Switching the Function of a Surface between Attacking and Defending against Bacteria. *Angew. Chem. Int. Edit.* **2012,** *51* (11), 2602-2605.
123. Dorner, F.; Boschert, D.; Schneider, A.; Hartleb, W.; Al-Ahmad, A.; Lienkamp, K., Toward Self-Regenerating Antimicrobial Polymer Surfaces. *Acs Macro Lett.* **2015,** *4* (12), 1337-1340.

124. Sundaram, H. S.; Ella-Menye, J.-R.; Brault, N. D.; Shao, Q.; Jiang, S., Reversibly switchable polymer with cationic/zwitterionic/anionic behavior through synergistic protonation and deprotonation. *Chemical Science* **2014,** *5* (1), 200-205.
125. Edahiro, J.-i.; Sumaru, K.; Tada, Y.; Ohi, K.; Takagi, T.; Kameda, M.; Shinbo, T.; Kanamori, T.; Yoshimi, Y., In Situ Control of Cell Adhesion Using Photoresponsive Culture Surface. *Biomacromolecules* **2005,** *6* (2), 970-974.
126. Cole, M. A.; Voelcker, N. H.; Thissen, H., Electro-induced protein deposition on low-fouling surfaces. *Smart Materials & Structures* **2007,** *16* (6), 2222-2228.
127. Park, T. G.; Hoffman, A. S., Sodium Chloride-Induced Phase-Transition in Nonionic Poly(N-Isopropylacrylamide) Gel. *Macromolecules* **1993,** *26* (19), 5045-5048.
128. Klemm, P.; Vejborg, R. M.; Hancock, V., Prevention of bacterial adhesion. *Appl. Microbiol. Biotechnol.* **2010,** *88* (2), 451-459.
129. Cegelski, L.; Pinkner, J. S.; Hammer, N. D.; Cusumano, C. K.; Hung, C. S.; Chorell, E.; Aberg, V.; Walker, J. N.; Seed, P. C.; Almqvist, F.; Chapman, M. R.; Hultgren, S. J., Small-molecule inhibitors target Escherichia coli amyloid biogenesis and biofilm formation. *Nat. Chem. Biol.* **2009,** *5* (12), 913-919.
130. Aberg, V.; Almqvist, F., Pilicides - small molecules targeting bacterial virulence. *Org Biomol Chem* **2007,** *5* (12), 1827-1834.
131. Maresso, A. W.; Schneewind, O., Sortase as a target of anti-infective therapy. *Pharmacol Rev* **2008,** *60* (1), 128-141.
132. Okuda, K.; Hanada, N.; Usui, Y.; Takeuchi, H.; Koba, H.; Nakao, R.; Watanabe, H.; Senpuku, H., Inhibition of Streptococcus mutans adherence and biofilm formation using analogues of the SspB peptide. *Arch Oral Biol* **2010,** *55* (10), 754-762.
133. Ofek, I.; Hasy, D. L.; Sharon, N., Anti-adhesion therapy of bacterial diseases: prospects and problems. *FEMS Immunol. Med. Microbiol.* **2003,** *38* (3), 181-191.
134. Shoaf, K.; Mulvey, G. L.; Armstrong, G. D.; Hutkins, R. W., Prebiotic galactooligosaccharides reduce adherence of enteropathogenic Escherichia coli to tissue culture cells. *Infect Immun* **2006,** *74* (12), 6920-6928.
135. Jiang, X. H.; Abgottspon, D.; Kleeb, S.; Rabbani, S.; Scharenberg, M.; Wittwer, M.; Haug, M.; Schwardt, O.; Ernst, B., Antiadhesion Therapy for Urinary Tract Infections-A Balanced PK/PD Profile Proved To Be Key for Success. *J. Med. Chem.* **2012,** *55* (10), 4700-4713.
136. Barras, A.; Martin, F. A.; Bande, O.; Baumann, J. S.; Ghigo, J. M.; Boukherroub, R.; Beloin, C.; Siriwardena, A.; Szunerits, S., Glycan-functionalized diamond nanoparticles as potent E. coli anti-adhesives. *Nanoscale* **2013,** *5* (6), 2307-2316.
137. Branderhorst, H. M.; Liskamp, R. M. J.; Visser, G. M.; Pieters, R. J., Strong inhibition of cholera toxin binding by galactose dendrimers. *Chem. Commun.* **2007,** (47), 5043-5045.
138. Thompson, J. P.; Schengrund, C. L., Inhibition of the adherence of cholera toxin and the heat-labile enterotoxin of Escherichia coli to cell-surface GM1 by oligosaccharide-derivatized dendrimers. *Biochem. Pharmacol.* **1998,** *56* (5), 591-597.
139. Signoretto, C.; Canepari, P.; Stauder, M.; Vezzulli, L.; Pruzzo, C., Functional foods and strategies contrasting bacterial adhesion. *Curr. Opin. Biotechnol.* **2012,** *23* (2), 160-167.
140. Brown, M. R. W.; Allison, D. G.; Gilbert, P., Resistance of Bacterial Biofilms to Antibiotics - a Growth-Rate Related Effect. *J. Antimicrob. Chemother.* **1988,** *22* (6), 777-780.

141. Fisher, R. A.; Gollan, B.; Helaine, S., Persistent bacterial infections and persister cells. *Nat. Rev. Microbiol.* **2017,** *15* (8), 453-464.
142. Lewis, K., Persister cells, dormancy and infectious disease. *Nat. Rev. Microbiol.* **2007,** *5* (1), 48-56.
143. Kohanski, M. A.; DePristo, M. A.; Collins, J. J., Sublethal Antibiotic Treatment Leads to Multidrug Resistance via Radical-Induced Mutagenesis. *Mol Cell* **2010,** *37* (3), 311-320.
144. Andersson, D. I.; Hughes, D., Microbiological effects of sublethal levels of antibiotics. *Nat. Rev. Microbiol.* **2014,** *12* (7), 465-478.
145. Aloush, V.; Navon-Venezia, S.; Seigman-Igra, Y.; Cabili, S.; Carmeli, Y., Multidrug-resistant Pseudomonas aeruginosa: Risk factors and clinical impact. *Antimicrob. Agents Chemother.* **2006,** *50* (1), 43-48.
146. Cosgrove, S. E.; Qi, Y. L.; Kaye, K. S.; Harbarth, S.; Karchmer, A. W.; Carmeli, Y., The impact of methicillin-resistance in Staphylococcus aureus bacteremia on patient outcomes: Mortality, length of stay, and hospital charges. *Infect Cont Hosp Ep* **2005,** *26* (2), 166-174.
147. Engemann, J. J.; Carmeli, Y.; Cosgrove, S. E.; Fowler, V. G.; Bronstein, M. Z.; Trivette, S. L.; Briggs, J. P.; Sexton, D. J.; Kaye, K. S., Adverse clinical and economic outcomes attributable to methicillin resistance among patients with Staphylococcus aureus surgical site infection. *Clin. Infect. Dis.* **2003,** *36* (5), 592-598.
148. Harrison, J. J.; Ceri, H.; Badry, E. A.; Roper, N. J.; Tomlin, K. L.; Turner, R. J., Effects of the twin-arginine translocase on the structure and antimicrobial susceptibility of Escherichia coli biofilms. *Can. J. Microbiol.* **2005,** *51* (8), 671-683.
149. Wood, T. K.; Knabel, S. J.; Kwan, B. W., Bacterial Persister Cell Formation and Dormancy. *Appl Environ Microb* **2013,** *79* (23), 7116-7121.
150. Choudhary, G. S.; Yao, X. Y.; Wang, J.; Peng, B.; Bader, R. A.; Ren, D. C., Human Granulocyte Macrophage Colony-Stimulating Factor Enhances Antibiotic Susceptibility of Pseudomonas aeruginosa Persister Cells. *Sci Rep-Uk* **2015,** *5*.
151. Barraud, N.; Buson, A.; Jarolimek, W.; Rice, S. A., Mannitol Enhances Antibiotic Sensitivity of Persister Bacteria in Pseudomonas aeruginosa Biofilms. *Plos One* **2013,** *8* (12).
152. Fjell, C. D.; Hiss, J. A.; Hancock, R. E. W.; Schneider, G., Designing antimicrobial peptides: form follows function. *Nat Rev Drug Discov* **2012,** *11* (1), 37-51.
153. Xue, Y.; Xiao, H. N.; Zhang, Y., Antimicrobial Polymeric Materials with Quaternary Ammonium and Phosphonium Salts. *Int J Mol Sci* **2015,** *16* (2), 3626-3655.
154. Yu, G. Z.; Baeder, D. Y.; Regoes, R. R.; Rolff, J., Predicting drug resistance evolution: insights from antimicrobial peptides and antibiotics. *P Roy Soc B-Biol Sci* **2018,** *285* (1874).
155. Kenawy, E. R.; Worley, S. D.; Broughton, R., The chemistry and applications of antimicrobial polymers: A state-of-the-art review. *Biomacromolecules* **2007,** *8* (5), 1359-1384.
156. Timofeeva, L.; Kleshcheva, N., Antimicrobial polymers: mechanism of action, factors of activity, and applications. *Applied Microbiology and Biotechnology* **2011,** *89* (3), 475-492.
157. Engler, A. C.; Wiradharma, N.; Ong, Z. Y.; Coady, D. J.; Hedrick, J. L.; Yang, Y. Y., Emerging trends in macromolecular antimicrobials to fight multi-drug-resistant infections. *Nano Today* **2012,** *7* (3), 201-222.
158. Ganewatta, M. S.; Tang, C. B., Controlling macromolecular structures towards effective antimicrobial polymers. *Polymer* **2015,** *63*, A1-A29.

159. Krumm, C.; Tiller, J. C., Chapter 15 Antimicrobial Polymers and Surfaces - Natural Mimics or Surpassing Nature? In *Bio-inspired Polymers*, The Royal Society of Chemistry: 2017; pp 490-522.
160. Zubris, D. L.; Minbiole, K. P. C.; Wuest, W. M., Polymeric Quaternary Ammonium Compounds: Versatile Antimicrobial Materials. *Curr. Top. Med. Chem.* **2017,** *17* (3), 305-318.
161. Ergene, C.; Yasuhara, K.; Palermo, E. F., Biomimetic antimicrobial polymers: recent advances in molecular design. *Polymer Chemistry* **2018,** *9* (18), 2407-2427.
162. Uppu, D. S. S. M.; Samaddar, S.; Hoque, J.; Konai, M. M.; Krishnamoorthy, P.; Shome, B. R.; Haldar, J., Side Chain Degradable Cationic–Amphiphilic Polymers with Tunable Hydrophobicity Show in Vivo Activity. *Biomacromolecules* **2016,** *17* (9), 3094-3102.
163. Coady, D. J.; Ong, Z. Y.; Lee, P. S.; Venkataraman, S.; Chin, W.; Engler, A. C.; Yang, Y. Y.; Hedrick, J. L., Enhancement of Cationic Antimicrobial Materials via Cholesterol Incorporation. *Advanced Healthcare Materials* **2014,** *3* (6), 882-889.
164. Locock, K. E. S.; Michl, T. D.; Stevens, N.; Hayball, J. D.; Vasilev, K.; Postma, A.; Griesser, H. J.; Meagher, L.; Haeussler, M., Antimicrobial Polymethacrylates Synthesized as Mimics of Tryptophan-Rich Cationic Peptides. *Acs Macro Lett.* **2014,** *3* (4), 319-323.
165. Tew, G. N.; Scott, R. W.; Klein, M. L.; Degrado, W. F., De Novo Design of Antimicrobial Polymers, Foldamers, and Small Molecules: From Discovery to Practical Applications. *Acc. Chem. Res.* **2009,** *43* (1), 30-39.
166. Ludtke, S. J.; He, K.; Heller, W. T.; Harroun, T. A.; Yang, L.; Huang, H. W., Membrane pores induced by magainin. *Biochemistry-Us* **1996,** *35* (43), 13723-13728.
167. Hall, J. E.; Vodyanoy, I.; Balasubramanian, T. M.; Marshall, G. R., Alamethicin - a Rich Model for Channel Behavior. *Biophys. J.* **1984,** *45* (1), 233-247.
168. Oda, Y.; Kanaoka, S.; Sato, T.; Aoshima, S.; Kuroda, K., Block versus Random Amphiphilic Copolymers as Antibacterial Agents. *Biomacromolecules* **2011,** *12* (10), 3581-3591.
169. Hancock, R. E. W. Hancock Laboratory Methods. http://cmdr.ubc.ca/bobh/methods.htm.
170. Giacometti, A.; Cirioni, O.; Barchiesi, F.; Del Prete, M. S.; Fortuna, M.; Caselli, F.; Scalise, G., In vitro susceptibility tests for cationic peptides: Comparison of broth microdilution methods for bacteria that grow aerobically. *Antimicrob. Agents Chemother.* **2000,** *44* (6), 1694-1696.
171. Sanda, F.; Koyama, E.; Endo, T., Synthesis and reactions of a poly(methacrylate) from an optically active amino alcohol. *J. Polym. Sci. Pol. Chem.* **1998,** *36* (12), 1981-1986.
172. Ilker, M. F.; Nusslein, K.; Tew, G. N.; Coughlin, E. B., Tuning the hemolytic and antibacterial activities of amphiphilic polynorbornene derivatives. *JACS* **2004,** *126* (48), 15870-15875.
173. Mowery, B. P.; Lee, S. E.; Kissounko, D. A.; Epand, R. F.; Epand, R. M.; Weisblum, B.; Stahl, S. S.; Gellman, S. H., Mimicry of antimicrobial host-defense peptides by random copolymers. *JACS* **2007,** *129* (50), 15474-+.
174. Bush, K.; Courvalin, P.; Dantas, G.; Davies, J.; Eisenstein, B.; Huovinen, P.; Jacoby, G. A.; Kishony, R.; Kreiswirth, B. N.; Kutter, E.; Lerner, S. A.; Levy, S.; Lewis, K.; Lomovskaya, O.; Miller, J. H.; Mobashery, S.; Piddock, L. J. V.; Projan, S.; Thomas, C. M.; Tomasz, A.; Tulkens, P. M.; Walsh, T. R.; Watson, J. D.; Witkowski, J.; Witte, W.; Wright, G.; Yeh, P.; Zgurskaya, H. I., Tackling antibiotic resistance. *Nature Reviews Microbiology* **2011,** *9* (12), 894-896.

175. Fernandes, P., Antibacterial discovery and development - the failure of success? *Nat. Biotechnol.* **2006,** *24* (12), 1497-1503.
176. Dufresne, M. H.; Leroux, J. C., Study of the micellization behavior of different order amino block copolymers with heparin. *Pharm. Res.* **2004,** *21* (1), 160-169.
177. Teschler, J. K.; Zamorano-Sanchez, D.; Utada, A. S.; Warner, C. J. A.; Wong, G. C. L.; Linington, R. G.; Yildiz, F. H., Living in the matrix: assembly and control of Vibrio cholerae biofilms. *Nat. Rev. Microbiol.* **2015,** *13* (5), 255-268.
178. Vlamakis, H.; Chai, Y. R.; Beauregard, P.; Losick, R.; Kolter, R., Sticking together: building a biofilm the Bacillus subtilis way. *Nat. Rev. Microbiol.* **2013,** *11* (3), 157-168.
179. Joo, H. S.; Otto, M., Molecular Basis of In Vivo Biofilm Formation by Bacterial Pathogens. *Chem. Biol.* **2012,** *19* (12), 1503-1513.
180. Costerton, J. W.; Stewart, P. S.; Greenberg, E. P., Bacterial biofilms: A common cause of persistent infections. *Science* **1999,** *284* (5418), 1318-1322.
181. Bryers, J. D.; Ratner, B. D., Bioinspired implant materials befuddle bacteria. *Asm News* **2004,** *70* (5), 232-237.
182. Bryers, J. D., Medical Biofilms. *Biotechnol. Bioeng.* **2008,** *100* (1), 1-18.
183. Macia, M. D.; Rojo-Molinero, E.; Oliver, A., Antimicrobial susceptibility testing in biofilm-growing bacteria. *Clin Microbiol Infec* **2014,** *20* (10), 981-990.
184. Rybtke, M.; Hultqvist, L. D.; Givskov, M.; Tolker-Nielsen, T., Pseudomonas aeruginosa Biofilm Infections: Community Structure, Antimicrobial Tolerance and Immune Response. *J. Mol. Biol.* **2015,** *427* (23), 3628-3645.
185. Martinez-Solano, L.; Macia, M. D.; Fajardo, A.; Oliver, A.; Martinez, J. L., Chronic Pseudomonas aeruginosa Infection in Chronic Obstructive Pulmonary Disease. *Clin. Infect. Dis.* **2008,** *47* (12), 1526-1533.
186. Oliver, A.; Canton, R.; Campo, P.; Baquero, F.; Blazquez, J., High frequency of hypermutable Pseudomonas aeruginosa in cystic fibrosis lung infection. *Science* **2000,** *288* (5469), 1251-1253.
187. Pasparakis, G.; Cockayne, A.; Alexander, C., Control of bacterial aggregation by thermoresponsive glycopolymers. *JACS* **2007,** *129* (36), 11014-+.
188. Mintzer, M. A.; Dane, E. L.; O'Toole, G. A.; Grinstaff, M. W., Exploiting Dendrimer Multivalency To Combat Emerging and Re-Emerging Infectious Diseases. *Mol. Pharmaceut.* **2012,** *9* (3), 342-354.
189. Bertrand, N.; Gauthier, M. A.; Bouvet, C.; Moreau, P.; Petitjean, A.; Leroux, J. C.; Leblond, J., New pharmaceutical applications for macromolecular binders. *J. Controlled Release* **2011,** *155* (2), 200-210.
190. Bossier, P.; Verstraete, W., Triggers for microbial aggregation in activated sludge? *Appl. Microbiol. Biotechnol.* **1996,** *45* (1-2), 1-6.
191. Edzwald, J. K., Coagulation in Drinking-Water Treatment - Particles, Organics and Coagulants. *Water Sci. Technol.* **1993,** *27* (11), 21-35.
192. Wickramasinghe, S. R.; Leong, Y. K.; Mondal, S.; Liow, J. L., Influence of cationic flocculant properties on the flocculation of yeast suspensions. *Adv. Powder Technol.* **2010,** *21* (4), 374-379.

193. Schwarz-Linek, J.; Winkler, A.; Wilson, L. G.; Pham, N. T.; Schilling, T.; Poon, W. C. K., Polymer-induced phase separation in Escherichia coli suspensions. *Soft Matter* **2010,** *6* (18), 4540-4549.
194. Dorken, G.; Ferguson, G. P.; French, C. E.; Poon, W. C. K., Aggregation by depletion attraction in cultures of bacteria producing exopolysaccharide. *J. R. Soc. Interface* **2012,** *9* (77), 3490-3502.
195. Lee, C. S.; Robinson, J.; Chong, M. F., A review on application of flocculants in wastewater treatment. *Process Saf. Environ.* **2014,** *92* (6), 489-508.
196. Lui, L. T.; Xue, X.; Sui, C.; Brown, A.; Pritchard, D. I.; Halliday, N.; Winzer, K.; Howdle, S. M.; Fernandez-Trillo, F.; Krasnogor, N.; Alexander, C., Bacteria clustering by polymers induces the expression of quorum-sensing-controlled phenotypes. *Nat. Chem.* **2013,** *5* (12), 1058-1065.
197. Zhang, P.; Lu, H.; Chen, H.; Zhang, J.; Liu, L.; Lv, F.; Wang, S., Cationic Conjugated Polymers-Induced Quorum Sensing of Bacteria Cells. *Anal. Chem.* **2016,** *88* (6), 2985-2988.
198. Kostakioti, M.; Hadjifrangiskou, M.; Hultgren, S. J., Bacterial Biofilms: Development, Dispersal, and Therapeutic Strategies in the Dawn of the Postantibiotic Era. *Csh. Perspect. Med.* **2013,** *3* (4).
199. Donlan, R. M., Biofilm formation: A clinically relevant microbiological process. *Clin. Infect. Dis.* **2001,** *33* (8), 1387-1392.
200. Cook, G. S.; Costerton, J. W.; Lamont, R. J., Biofilm formation by Porphyromonas gingivalis and Streptococcus gordonii. *J Periodontal Res* **1998,** *33* (6), 323-327.
201. BioSciences, I. *Biofilm Protocol Optimization For Pseudomonas aeruginosa: Culture Media, Incubation Time, and Biofilm Measurement*; 2016.
202. Harrison-Balestra, C.; Cazzaniga, A. L.; Davis, S. C.; Mertz, P. M., A wound-isolated Pseudomonas aeruginosa grows a biofilm in vitro within 10 hours and is visualized by light microscopy. *Dermatol Surg* **2003,** *29* (6), 631-635.
203. Tomasiewicz, D. M.; Hotchkiss, D. K.; Reinbold, G. W.; Read, R. B.; Hartman, P. A., The Most Suitable Number of Colonies on Plates for Counting. *J. Food Prot.* **1980,** *43* (4), 282-286.
204. Gregory, J., Rates of Flocculation of Latex Particles by Cationic Polymers. *J. Colloid Interface Sci.* **1973,** *42* (2), 448-456.
205. Gregory, J., Flocculation of Polystyrene Particles with Cationic Polyelectrolytes. *T. Faraday Soc.* **1969,** *65* (560p), 2260-&.
206. Rivas, B. L.; Pereira, E. D.; Mondaca, M. A., Biostatic behavior of side chain charged-polycations and polymer-Ag complexes. *Polym. Bull.* **2003,** *50* (5-6), 327-333.
207. Morgan, H. C.; Meier, J. F.; Merker, R. L. Method of creating a biostatic agent using interpenetrating network polymers. 2000.
208. Melrose, G. J. H.; Kleppe, C. M.; Langley, J. W.; Stewart, J. M.; Van Dyk, J. Biostatic and biocidal compositions. 1988.
209. Yang, R.; Li, H. J.; Huang, M.; Yang, H.; Li, A. M., A review on chitosan-based flocculants and their applications in water treatment. *Water Res.* **2016,** *95*, 59-89.
210. Schleheck, D.; Barraud, N.; Klebensberger, J.; Webb, J. S.; McDougald, D.; Rice, S. A.; Kjelleberg, S., Pseudomonas aeruginosa PAO1 Preferentially Grows as Aggregates in Liquid Batch Cultures and Disperses upon Starvation. *Plos One* **2009,** *4* (5).

211. Kragh, K. N.; Hutchison, J. B.; Melaugh, G.; Rodesney, C.; Roberts, A. E. L.; Irie, Y.; Jensen, P. O.; Diggle, S. P.; Allen, R. J.; Gordon, V.; Bjarnsholt, T., Role of Multicellular Aggregates in Biofilm Formation. *Mbio* **2016,** *7* (2).
212. Christensen, G. D.; Simpson, W. A.; Younger, J. J.; Baddour, L. M.; Barrett, F. F.; Melton, D. M.; Beachey, E. H., Adherence of Coagulase-Negative Staphylococci to Plastic Tissue-Culture Plates - a Quantitative Model for the Adherence of Staphylococci to Medical Devices. *J. Clin. Microbiol.* **1985,** *22* (6), 996-1006.
213. O'Toole, G. A., Microtiter Dish Biofilm Formation Assay. *Jove-J. Vis. Exp.* **2011,** (47).
214. Melaugh, G.; Hutchison, J.; Kragh, K. N.; Irie, Y.; Roberts, A.; Bjarnsholt, T., Shaping the Growth Behaviour of Biofilms Initiated from Bacterial Aggregates (vol 11, e0149683, 2016). *Plos One* **2016,** *11* (4).
215. Aparna, M. S. P. B. D.; Yadav, S., Biofilms: Microbes and Disease. *Braz J Infect Dis* **2008,** *12* (6), 526-530.
216. Moreau-Marquis, S.; Stanton, B. A.; O'Toole, G. A., Pseudomonas aeruginosa biofilm formation in the cystic fibrosis airway. *Pulm Pharmacol Ther* **2008,** *21* (4), 595-599.
217. Herrmann, G.; Yang, L. A.; Wu, H.; Song, Z. J.; Wang, H. Z.; Hoiby, N.; Ulrich, M.; Molin, S.; Riethmuller, J.; Doring, G., Colistin-Tobramycin Combinations Are Superior to Monotherapy Concerning the Killing of Biofilm Pseudomonas aeruginosa. *J Infect Dis* **2010,** *202* (10), 1585-1592.
218. Trapnell, B. C.; Rolfe, M.; McColley, S.; Montgomery, A. B.; Moorehead, L.; Geller, D., Fosfomycin/Tobramycin for Inhalation (Fti): Efficacy Results of a Phase 2 Placebo-Controlled Trial in Patients with Cystic Fibrosis and Pseudomonas Aeruginosa. *Pediatr Pulm* **2010**, 302-302.
219. Anwar, H.; Costerton, J. W., Enhanced Activity of Combination of Tobramycin and Piperacillin for Eradication of Sessile Biofilm Cells of Pseudomonas-Aeruginosa. *Antimicrob. Agents Chemother.* **1990,** *34* (9), 1666-1671.
220. Smyth, A. R.; Cifelli, P. M.; Ortori, C. A.; Righetti, K.; Lewis, S.; Erskine, P.; Holland, E. D.; Givskov, M.; Williams, P.; Camara, M.; Barrett, D. A.; Knox, A., Garlic as an Inhibitor of Pseudomonas aeruginosa Quorum Sensing in Cystic Fibrosis-A Pilot Randomized Controlled Trial. *Pediatr Pulm* **2010,** *45* (4), 356-362.
221. Hentzer, M.; Wu, H.; Andersen, J. B.; Riedel, K.; Rasmussen, T. B.; Bagge, N.; Kumar, N.; Schembri, M. A.; Song, Z. J.; Kristoffersen, P.; Manefield, M.; Costerton, J. W.; Molin, S.; Eberl, L.; Steinberg, P.; Kjelleberg, S.; Hoiby, N.; Givskov, M., Attenuation of Pseudomonas aeruginosa virulence by quorum sensing inhibitors. *EMBO J.* **2003,** *22* (15), 3803-3815.
222. Bjarnsholt, T.; Jensen, P. O.; Burmolle, M.; Hentzer, M.; Haagensen, J. A. J.; Hougen, H. P.; Calum, H.; Madsen, K. G.; Moser, C.; Molin, S.; Hoiby, N.; Givskov, M., Pseudomonas aeruginosa tolerance to tobramycin, hydrogen peroxide and polymorphonuclear leukocytes is quorum-sensing dependent. *Microbiol.-Sgm* **2005,** *151*, 373-383.
223. Oliver, J. D., The viable but nonculturable state in bacteria. *J Microbiol* **2005,** *43*, 93-100.
224. Kaprelyants, A. S.; Gottschal, J. C.; Kell, D. B., Dormancy in Non-Sporulating Bacteria. *FEMS Microbiol. Lett.* **1993,** *104* (3-4), 271-286.
225. Gilbert, P.; Collier, P. J.; Brown, M. R. W., Influence of Growth-Rate on Susceptibility to Antimicrobial Agents - Biofilms, Cell-Cycle, Dormancy, and Stringent Response. *Antimicrob. Agents Chemother.* **1990,** *34* (10), 1865-1868.

226. Nguyen, D.; Joshi-Datar, A.; Lepine, F.; Bauerle, E.; Olakanmi, O.; Beer, K.; McKay, G.; Siehnel, R.; Schafhauser, J.; Wang, Y.; Britigan, B. E.; Singh, P. K., Active Starvation Responses Mediate Antibiotic Tolerance in Biofilms and Nutrient-Limited Bacteria. *Science* **2011,** *334* (6058), 982-986.
227. Taber, H. W.; Mueller, J. P.; Miller, P. F.; Arrow, A. S., Bacterial Uptake of Aminoglycoside Antibiotics. *Microbiol Rev* **1987,** *51* (4), 439-457.
228. MacLeod, D. L.; Velayudhan, J.; Kenney, T. F.; Therrien, J. H.; Sutherland, J. L.; Barker, L. M.; Baker, W. R., Fosfomycin Enhances the Active Transport of Tobramycin in Pseudomonas aeruginosa. *Antimicrob. Agents Chemother.* **2012,** *56* (3), 1529-1538.
229. Defraine, V.; Fauvart, M.; Michiels, J., Fighting bacterial persistence: Current and emerging anti-persister strategies and therapeutics. *Drug Resist Update* **2018,** *38*, 12-26.
230. Meylan, S.; Porter, C. B. M.; Yang, J. H.; Belenky, P.; Gutierrez, A.; Lobritz, M. A.; Park, J.; Kim, S. H.; Moskowitz, S. M.; Collins, J. J., Carbon Sources Tune Antibiotic Susceptibility in Pseudomonas aeruginosa via Tricarboxylic Acid Cycle Control. *Cell Chem Biol* **2017,** *24* (2), 195-206.
231. Marques, C. N. H.; Morozov, A.; Planzos, P.; Zelaya, H. M., The Fatty Acid Signaling Molecule cis-2-Decenoic Acid Increases Metabolic Activity and Reverts Persister Cells to an Antimicrobial-Susceptible State. *Appl Environ Microb* **2014,** *80* (22), 6976-6991.
232. Mohamed, M. F.; Brezden, A.; Mohammad, H.; Chmielewski, J.; Seleem, M. N., Targeting biofilms and persisters of ESKAPE pathogens with P14KanS, a kanamycin peptide conjugate. *Bba-Gen Subjects* **2017,** *1861* (4), 848-859.
233. Mitsukami, Y.; Donovan, M. S.; Lowe, A. B.; McCormick, C. L., Water-soluble polymers. 81. Direct synthesis of hydrophilic styrenic-based homopolymers and block copolymers in aqueous solution via RAFT. *Macromolecules* **2001,** *34* (7), 2248-2256.
234. Bryan, L. E.; Nicas, T.; Holloway, B. W.; Crowther, C., Aminoglycoside-Resistant Mutation of Pseudomonas-Aeruginosa Defective in Cytochrome-C552 and Nitrate Reductase. *Antimicrob. Agents Chemother.* **1980,** *17* (1), 71-79.
235. Chambless, J. D.; Hunt, S. M.; Stewart, P. S., A three-dimensional computer model of four hypothetical mechanisms protecting biofilms from antimicrobials. *Appl Environ Microb* **2006,** *72* (3), 2005-2013.
236. Li, X. Z.; Nikaido, H.; Poole, K., Role of Mexa-Mexb-Oprm in Antibiotic Efflux in Pseudomonas-Aeruginosa. *Antimicrob. Agents Chemother.* **1995,** *39* (9), 1948-1953.
237. De Kievit, T. R.; Parkins, M. D.; Gillis, R. J.; Srikumar, R.; Ceri, H.; Poole, K.; Iglewski, B. H.; Storey, D. G., Multidrug efflux pumps: Expression patterns and contribution to antibiotic resistance in Pseudomonas aeruginosa biofilms. *Antimicrob. Agents Chemother.* **2001,** *45* (6), 1761-1770.
238. Whiteley, M.; Bangera, M. G.; Bumgarner, R. E.; Parsek, M. R.; Teitzel, G. M.; Lory, S.; Greenberg, E. P., Gene expression in Pseudomonas aeruginosa biofilms. *Nature* **2001,** *413* (6858), 860-864.
239. Lewis, K., Persister cells: molecular mechanisms related to antibiotic tolerance. In *Antibiotic resistance*, Springer: 2012; pp 121-133.
240. Hassett, D. J.; Cuppoletti, J.; Trapnell, B.; Lymar, S. V.; Rowe, J. J.; Yoon, S. S.; Hilliard, G. M.; Parvatiyar, K.; Kamani, M. C.; Wozniak, D. J.; Hwang, S. H.; McDermott, T. R.; Ochsner, U. A., Anaerobic metabolism and quorum sensing by Pseudomonas aeruginosa biofilms in chronically

infected cystic fibrosis airways: rethinking antibiotic treatment strategies and drug targets. *Adv Drug Deliver Rev* **2002,** *54* (11), 1425-1443.
241. Soto, S. M., Role of efflux pumps in the antibiotic resistance of bacteria embedded in a biofilm. *Virulence* **2013,** *4* (3), 223-229.
242. Lambert, P. A., Mechanisms of antibiotic resistance in Pseudomonas aeruginosa. *J Roy Soc Med* **2002,** *95*, 22-26.
243. Aeschlimann, J. R., The Role of Multidrug Efflux Pumps in the Antibiotic Resistance of Pseudomonas aeruginosa and Other Gram-Negative Bacteria. *Pharmacotherapy: The Journal of Human Pharmacology and Drug Therapy* **2003,** *23* (7), 916-924.
244. Wu, H. F.; Niu, Y. H.; Padhee, S.; Wang, R. S. E.; Li, Y. Q.; Qiao, Q.; Bai, G.; Cao, C. H.; Cai, J. F., Design and synthesis of unprecedented cyclic gamma-AApeptides for antimicrobial development. *Chemical Science* **2012,** *3* (8), 2570-2575.
245. Huang, M. L.; Shin, S. B. Y.; Benson, M. A.; Torres, V. J.; Kirshenbaum, K., A Comparison of Linear and Cyclic Peptoid Oligomers as Potent Antimicrobial Agents. *Chemmedchem* **2012,** *7* (1), 114-122.
246. Oren, Z.; Shai, Y., Cyclization of a cytolytic amphipathic alpha-helical peptide and its diastereomer: Effect on structure, interaction with model membranes, and biological function. *Biochemistry-Us* **2000,** *39* (20), 6103-6114.
247. Unger, T.; Oren, Z.; Shai, Y., The effect of cyclization of magainin 2 and melittin analogues on structure, function, and model membrane interactions: Implication to their mode of action. *Biochemistry-Us* **2001,** *40* (21), 6388-6397.
248. Fischer, D.; Li, Y. X.; Ahlemeyer, B.; Krieglstein, J.; Kissel, T., In vitro cytotoxicity testing of polycations: influence of polymer structure on cell viability and hemolysis. *Biomaterials* **2003,** *24* (7), 1121-1131.